

**BAW-2241NP-A**

**Revision 2**

# **Fluence and Uncertainty Methodologies**

NRC Acceptance

Revision 2 - April, 2006

Revision 1 - April, 2000

Original - February, 1999

**AREVA NP Inc.**

(An AREVA and Siemens Company)

**AREVA NP Inc.**

This document, including the information contained herein, is the property of AREVA NP Inc., an AREVA and Siemens company.

This document is designated to be non-proprietary (NP).

**AREVA NP Inc.**

(An AREVA and Siemens Company)

**BAW-2241NP-A**

**Revision 2**

Submitted

Regulatory Affairs

June, 2003

Submitted

March, 2005

**NRC Acceptance Letter**

**April, 2006**

**&**

**Safety Evaluation Report**

**Fluence and Uncertainty Methodologies**

**BWR Benchmarks & Uncertainties**

**AREVA NP Inc.**

(An AREVA and Siemens Company)



UNITED STATES  
NUCLEAR REGULATORY COMMISSION  
WASHINGTON, D.C. 20555-0001

April 28, 2006

Mr. Ronnie L. Gardner, Manager  
Site Operations and Regulatory Affairs  
AREVA NP Inc.  
3315 Old Forest Road  
Lynchburg, VA 24501

SUBJECT: FINAL SAFETY EVALUATION FOR REVISION 1 OF APPENDIX G TO  
BAW-2241(P) REVISION 2, "FLUENCE AND UNCERTAINTY  
METHODOLOGIES" (TAC NO. MC6631)

Dear Mr. Gardner:

By letter dated March 31, 2005, and its supplement dated November 8, 2005, Framatome ANP (FANP), now known as AREVA NP (AREVA), submitted Topical Report (TR) Revision 1 of Appendix G to BAW-2241(P) Revision 2, "Fluence and Uncertainty Methodologies," to the U.S. Nuclear Regulatory Commission (NRC) staff for review and approval. By letter dated March 20, 2006, an NRC draft safety evaluation (SE) regarding our approval of Revision 1 of Appendix G to BAW-2241(P) Revision 2, was provided for your review and comments. By letter dated March 30, 2006, AREVA commented on the draft SE. These comments were discussed in a teleconference between AREVA and the NRC staff on April 18, 2006. The NRC staff's disposition of AREVA's comments on the draft SE are discussed in the attachment to the final SE enclosed with this letter.

The NRC staff has found that Revision 1 of Appendix G to BAW-2241(P) Revision 2, is acceptable for referencing in licensing applications to the extent specified and under the limitations delineated in the TR and in the enclosed final SE. The final SE defines the basis for our acceptance of the TR.

Our acceptance applies only to material provided in the subject TR. We do not intend to repeat our review of the acceptable material described in the TR. When the TR appears as a reference in license applications, our review will ensure that the material presented applies to the specific plant involved. License amendment requests that deviate from this TR will be subject to a plant-specific review in accordance with applicable review standards.

In accordance with the guidance provided on the NRC website, we request that AREVA publish accepted proprietary and non-proprietary versions of this TR within three months of receipt of this letter. The accepted versions shall incorporate this letter and the enclosed final SE after the title page. Also, they must contain historical review information, including NRC requests for additional information and your responses. The accepted versions shall include an "-A" (designating accepted) following the TR identification symbol.

R. Gardner

- 2 -

If future changes to the NRC's regulatory requirements affect the acceptability of this TR, AREVA and/or licensees referencing it will be expected to revise the TR appropriately, or justify its continued applicability for subsequent referencing.

Sincerely,

A handwritten signature in black ink, appearing to read 'H. Nieh', written in a cursive style.

Ho K. Nieh, Deputy Director  
Division of Policy and Rulemaking  
Office of Nuclear Reactor Regulation

Project No. 728

Enclosure: Final SE



UNITED STATES  
NUCLEAR REGULATORY COMMISSION  
WASHINGTON, D.C. 20555-0001

FINAL SAFETY EVALUATION BY THE OFFICE OF NUCLEAR REACTOR REGULATION

REVISION 1 OF APPENDIX G TO BAW-2241(P) REVISION 2.

"FLUENCE AND UNCERTAINTY METHODOLOGIES"

AREVA NP

PROJECT NO. 728

1.0 INTRODUCTION AND BACKGROUND

By letter dated March 31, 2005, and its supplement dated November 8, 2005, Framatome ANP (FANP), now known as AREVA NP, submitted Revision 1 of Appendix G to BAW-2241(P) Revision 2, "Fluence and Uncertainty Methodologies," to the U.S. Nuclear Regulatory Commission (NRC) staff for review and approval (Ref. 1). The proposed methodology is intended for application to boiling water reactors (BWRs). Appendix G constitutes an extension of the BAW-2241(P) pressurized water reactor (PWR) pressure vessel fluence methods and uncertainties to account for the differences introduced by its application to BWRs. The Appendix G approach for BWRs is semi-analytic using the most recent fluence calculational methods and nuclear data sets. In the proposed methodology, the vessel fluence is determined by a transport calculation in which the core neutron source is explicitly represented and the neutron flux is propagated from the core through the downcomer to the vessel (rather than by an extrapolation of the measurements). The dosimeter measurements are only used to determine the calculational bias and uncertainty.

Appendix G provides a description of the extension of the BAW-2241-P PWR calculational methodology for application to BWRs. This includes the treatment of the BWR jet pump/riser geometrical configuration in the numerical transport calculation, determination of the core water number densities (void fractions) and the accuracy assessment for BWRs. BAW-2241(P) and Appendix G to BAW-2241(P) adhere to General Design Criteria (GDC) 30, 31, and the guidance in Regulatory Guide (RG) 1.190 (Ref. 2). As part of the qualification for BWR application, Appendix G presents benchmark comparisons for the Pool Critical Assembly (PCA) dosimetry experiment (Ref. 3), the BNL BWR (BNL-6115) calculational benchmark problem (Ref. 4), and a Browns Ferry-2 (BF-2) surveillance capsule dosimetry measurement (Ref. 5). The Appendix G fluence calculation and uncertainty methodology is summarized in Section 2 of this safety evaluation (SE). The evaluation of the important technical issues raised during this review is presented in Section 3 and the Summary and limitations are in Section 4 of this SE.

2.0 SUMMARY OF THE APPENDIX G FLUENCE CALCULATIONAL METHODS AND BENCHMARKING COMPARISONS

2.1 Semi-Analytic Fluence Calculational Methodology

The basic FANP methodology for calculating BWR fluence is the same semi-analytic methodology used for PWRs. The fluence methodology is the result of a series of updates and improvements to the BAW-1485 methodology developed for the 177-fuel assembly plants

described in References 6 and 7. These updates were made to improve the accuracy of the fluence prediction and to further quantify the calculational uncertainty. The improvements include the implementation of the BUGLE-93 cross sections, based on the evaluated nuclear data file B-VI (ENDF/B-VI) multi-group nuclear data set (Ref. 8). The fluence calculations are performed with the DORT discrete ordinates transport code (Ref. 9). As in the case of PWRs, the BWR core neutron source term is determined using core-follow data which has been matched to in-core measurements of the three-dimensional power distribution. The prediction of the best-estimate fluence is based on a direct calculation rather than a measurement extrapolated to the vessel inner-wall. The BAW-2241(P) approach incorporates the provisions of RG 1.190 for predicting both the vessel fluence and the dosimeter response.

The extension of the semi-analytic method for BWR applications includes a detailed modeling of the neutron transport through the jet pumps. The Appendix G procedure for constructing the DORT model provides a fine  $(r, \theta)$  planar mesh for representing the BWR jet pump cylindrical geometry. Using analytic expressions for the model region thickness and area, a detailed description of both (a) the flux attenuation through the jet pump structures and (b) the neutron collision densities in the jet pump material regions is provided.

The calculation of the BWR vessel fluence is further complicated (compared to the PWR analysis) by the coolant voiding in the fuel bundles. The reduced water density in the fuel bundles reduces the neutron flux radial attenuation and increases the leakage from the core. The FANP calculational method includes a special treatment of the increased core leakage due to fuel bundle coolant voiding. The FANP method is based on an accurate matching of the DORT transport calculations and the core-follow calculations of the core leakage in the presence of reduced coolant density in the fuel bundles. The core-follow calculations provide an accurate simulation of the core operating power history.

In the FANP semi-analytic method for PWRs, axial synthesis is used to determine the vessel three-dimensional fluence distribution. However, FANP has extended this method for application to BWRs to account for the increased number of axial shapes due to control rod insertion and non-uniform axial voiding. This extension allows for an increased number and a non-uniform distribution of axial planes in the synthesis. The detailed input for the synthesis and multi-channel planar model calculations is provided by time-dependent three-dimensional core-follow calculations.

## 2.2 Fluence Measurement and Calculational Benchmarks

Appendix G provides an extensive description of the benchmarking of the FANP vessel fluence calculational methodology. The Appendix G benchmarks include: (a) the Oak Ridge National Laboratory PCA Benchmark Experiment, (b) the Brookhaven National Laboratory BWR pressure vessel benchmark calculation (BNL-6115) and (c) BF-2 pressure vessel surveillance capsule dosimetry measurement. The ratio of the FANP calculation-to-benchmark result provides a quantitative indication of the FANP calculation uncertainty.

The PCA is a well documented vessel mock-up experiment including high accuracy dosimetry measurements. The PCA core includes twenty-five Material Test Reactor curved-plate type fuel elements and the simulator geometry includes a thermal shield, pressure vessel and void box outside the vessel. The PCA dosimetry measurements were made at positions in front and

behind the thermal shield, at locations in front and behind the vessel and at vessel internal locations. The PCA dosimetry measurements include the Np-237(n, f), U-238(n, f), In-115(n, n'), Ni-58(n, p) and Al-27(n,  $\alpha$ ) reactions. Detailed comparisons presented for both the thermal shield and vessel locations indicate good agreement with the dosimetry measurements.

NUREG/CR-6115, "Pressure Vessel Fluence Calculation Benchmark Problems and Solutions," (Ref. 4) provides the detailed specification and corresponding numerical solutions for a BWR pressure vessel fluence benchmark problem. The benchmark problem provides a reference calculation for a configuration typical of an operating BWR including downcomer and vessel fluences and the dosimeter response at an in-vessel surveillance capsule. The surveillance capsule dosimetry includes the Np-237(n, f), U-238(n, f), Ni-58(n, p), Fe-54(n, p), Ti-46(n, p) and Cu-63(n,  $\alpha$ ) reaction rates. The FANP model provides a detailed representation of an octant of the problem geometry and includes a radial region which extends from the center of the core out to the outer surface of the vessel. Detailed FANP/BNL-6115 comparisons are presented for both (a) the azimuthal fluence through the vessel and (b) the dosimetry reaction rates. The vessel fluence and surveillance capsule dosimetry comparisons indicate good agreement.

The BF-2 capsule dosimetry measurement provides a benchmark that includes the full as-built BWR material/geometry configuration and an operational core neutron source. The BF-2 capsule ( $E > 1.0$  MeV) flux was determined by General Electric Nuclear Energy (GENE) using the measured iron, nickel and copper reaction rates. The FANP prediction of the BF-2 capsule flux measurement indicated that the fluence calculations are accurate and consistent with the random uncertainty of the FANP data base.

### 3.0 TECHNICAL EVALUATION

Appendix G of the topical report BAW-2241(P) provides the FANP methodology for performing BWR pressure vessel fluence calculations and determining the associated calculational uncertainty. The review of the FANP methodology focused on: (1) the details of the fluence calculation methods and (2) the conservatism in the estimated calculational uncertainty. As a result of the review of the methodology, several important technical issues were identified which required additional information and clarification from FANP. The request for Additional Information (RAI) was transmitted in Reference 10. The information requested was provided by FANP in the responses included in Reference 11. This evaluation is based on the material presented in the topical report and in Reference 11. The evaluation of the major issues raised during the review is summarized below.

#### 3.1 Semi-Analytic Fluence Calculational Methodology

The FANP semi-analytic calculational methodology is used to determine the pressure vessel fluence, predict the surveillance capsule fluence, determine dosimeter response for the benchmark experiments and perform fluence sensitivity analyses. The neutron transport calculation, selection and processing of the nuclear data, and analysis of the benchmark measurements generally follow the approach described in the RG 1.190.



RG 1.190 notes that as fuel burnup increases the number of plutonium fissions increases, resulting in an increase in the number of neutrons per fission and a hardening of the neutron spectrum. Neglect of either of these effects results in a nonconservative prediction of the vessel fluence. In Response 8 of Reference 11, FANP describes the method used to incorporate these effects in the methodology. It is indicated that the uranium and plutonium isotopic inventory is tracked for each fuel assembly and the uranium and plutonium neutron emission rates are determined for the individual isotopes. The fuel inventory is determined for each depletion time-step and is tracked in three dimensions using a program that is benchmarked to the incore detector data. In Response 8, FANP evaluates the approximation used to determine the burnup-dependent core neutron spectrum. This evaluation indicates that the effect of the spectrum approximation used in the methodology is negligible.

Because of the strong exponential fluence attenuation, the calculation of the fluence is especially sensitive to both the distance separating the core and the vessel and the barrel thickness. In order to insure an accurate prediction of BWR vessel fluence, consistent with the uncertainty analysis of Appendix G, a reliable estimate of the vessel diameter and barrel thickness are required for input to the DORT transport calculation. To insure the vessel internals geometry is accurately represented, FANP has indicated (Response 5, Reference 11) that a quality assurance review of the drawings is performed as part of the determination of the dimensions used in the DORT transport models.

The fluence analysis of the Davis-Besse benchmark experiment is presented in Section 3 of the BAW-2241(P) topical report to illustrate the application of the semi-analytical methodology. In this analysis, a 45-degree sector of the configuration geometry determined by the symmetry of the PWR fuel loading pattern is modeled. In BWR fluence calculations, the configuration geometry also includes the jet-pumps, risers and surveillance dosimetry which must also be considered in the determination of the azimuthal sector to be modeled. In Response 2 of Reference 11, FANP has indicated that, if the BWR plant core/vessel/dosimetry geometry does not have sufficient symmetry to allow the use of a 45-degree sector, the model will be expanded to an appropriate angular representation (e.g., as a 90-degree sector).

In applications of earlier versions of the semi-analytic methodology, benchmark calculations were performed in the cavity region for the nozzles and seal plate. The calculational modeling in this region, several hundred centimeters above the beltline, was limited and resulted in negative neutron fluxes. The negative fluxes are of concern since they are unphysical and indicate large per cent errors in the calculation. FANP has indicated in Response 1 of Reference 11, that the negative fluxes were due to the large spatial and angular mesh used in the earlier models due to limited computer memory. Because of advances in computer technology which allow fine mesh spatial representations, negative fluxes have not been obtained using the current DORT fluence calculational models.

In the semi-analytic methodology, the fluence accumulated at the vessel at end-of-life (EOL) is determined in two steps. The current fluence is determined first based on the actual operating power history of the plant. The additional fluence accumulated during the remaining plant life (i.e., at EOL) is determined based on a projected core power history. The PWR power history projection and resulting fluence uncertainty are described in Section 7 of BAW-2241(P). In Response 6 of Reference 11, FANP has indicated that the BWR power projection uncertainty has been determined and the BWR EOL fluence standard deviation is less than twenty percent.

The MELLLA<sup>+</sup> expansion of the operating range has been implemented at several BWR plants. This expansion can result in a change in the thermal-hydraulic conditions in the downcomer that can affect the attenuation of the neutron flux. In response to RAI-7, FANP has indicated in Reference 11 that the downcomer water properties determined by the core-follow calculations are exactly duplicated in the DORT fluence calculations.

The reduced water density in the fuel bundles (compared to PWRs) introduces an additional complication in the determination of the BWR vessel fluence. The reduced water density (i.e., coolant voiding) reduces the radial attenuation of the neutron flux and increases the leakage from the core. The extension of the semi-analytical method for BWR application includes a new method described by Equation-G.7 of Section G.3. No quantitative validation or verification has been provided to justify the application of this new method in either Appendix G or in Responses 9, 10, 11, 13 and 16. In view of the many approximations implicit in this method and the lack of supporting qualification, this method is not acceptable to be used in applications of the FANP fluence methodology.

### 3.2 Fluence Measurement and Calculational Benchmarks

The comparison of the semi-analytic fluence predictions with measurement and calculational benchmarks is a necessary and critical part of the qualification of the FANP methodology. The calculation and measurement benchmarks provide an independent assessment of the accuracy of the Appendix G fluence predictions. The calculation-to-measurement (C/M) values resulting from the measurement benchmarking are used to determine the calculation bias and uncertainty (i.e., standard deviation).

In the measurement benchmarks, the methods used to convert the dosimeter response to fluence are complex typically involving adjustments for power history, reaction product half-lives, photo-fission contributions to the fission dosimeters, local perturbation factors for the surveillance capsule and/or instrumentation and dosimeter impurities. In addition, to ensure an accurate prediction of the dosimeter response, a detailed spatial representation of the dosimeter holder tube/surveillance capsule geometry must be included in the DORT model. In Response 3 of Reference 11, FANP has indicated that the differences in the dosimetry introduced by the BWR application (viz., dosimetry wires/foils, holder tubes, encapsulation, etc.) are treated explicitly rather than by modeling approximations. FANP states further in Response 4 of Reference 11 that the procedures for determining the fluence from the dosimeter response conform to the applicable ASTM standards.

The FANP calculational procedure includes the application of a bias removal function to the calculated ( $E > 1.0$  MeV) fluence. The bias removal function is based on PWR data taken as part of the Davis Besse Unit-1 Cavity Dosimetry Measurement Program. No BWR data has been provided to justify application of the function in BWR applications. Since this correction can result in a nonconservative reduction in the ( $E > 1.0$  MeV) fluence, the bias removal function is not acceptable to be used in BWR applications.

The uncertainty in the vessel fluence calculation depends on the plant-to-plant variation in the as-built core/internals/vessel geometry, core power and exposure distributions, and the plant power history. Because of the limited number of BWR operating reactor measurement

benchmarks included in Appendix G and to insure a reliable assessment of the fluence calculational uncertainty, additional measurement qualification must be provided in plant-specific applications of the fluence methodology. In the initial four (4) applications of the FANP BWR methodology, the fluence predictions of the Appendix G methodology must be compared with surveillance capsule or cavity fluence measurements for the vessel being analyzed. If the results of the C/M comparisons for these measurements are not consistent with the BAW-2241(P) uncertainty analysis (recognizing the uncertainty of a limited sample size), the uncertainty analysis must be updated or the deviations explained. In addition, after the initial four applications of the fluence methodology, the uncertainty analysis must be updated with at least four (4) additional BWR dosimetry measurement comparisons to confirm, and update if necessary, the Appendix G fluence calculational bias and uncertainty. As required by RG 1.190, this confirmation/update must also be performed as subsequent measurements become available.

#### 4.0 CONCLUSION, LIMITATIONS AND CONDITIONS

Appendix G of the Topical Report BAW-2241(P), "Fluence and Uncertainty Methodologies," and the supporting documentation provided in Reference 11 have been reviewed in detail. Based on this review, it is concluded that the proposed methodology is acceptable for determining the pressure vessel fluence of BWRs under the following conditions:

1. In view of the many approximations in the method described by Equation-G.7 of Section G.3 and the lack of supporting qualification, this method is not acceptable to be used in applications of the FANP fluence methodology. However, in conjunction with Condition No. 3 below, if additional BWR benchmark comparisons show biases that are directly related to calculations without Equation-G.7, then the Equation-G.7 results would be acceptable for a single plant-specific application. For each and every plant-specific application, the NRC staff must be notified and the dosimetry benchmark results, with and without Equation-G.7, presented in either the surveillance report or some other appropriate report. If the results from the eight (8) additional dosimetry benchmark comparisons to measurements required by Condition No. 3 below validate Equation-G.7, then FANP may submit the combined data to the NRC staff and request a revision of this condition.
2. The bias correction is based on PWR data and no qualification data is available for justifying BWR application. Since this correction can result in a nonconservative reduction in the > 1-MeV fluence, the bias removal function is not acceptable to be used in BWR applications. However, in conjunction with Condition No. 3 below, if additional BWR benchmark comparisons confirm that BWR dosimeter biases are the same as the FANP benchmark database biases, then the bias removal function would be acceptable for a single plant-specific application. For each and every plant-specific application, the NRC staff must be notified and the dosimetry benchmark results, with and without the application of the bias removal function, presented in either the surveillance report or some other appropriate report. If the results from the eight (8) additional dosimetry benchmark comparisons to measurements required by Condition No. 3 below validate the bias removal function for BWRs, then FANP may submit the combined data to the NRC staff and request a revision of this condition.

3. Because of the limited number of BWR benchmark calculations to operating data, an additional qualification must be provided in plant-specific applications of the Appendix G fluence methodology. When measured data is available, this must include: (1) in the initial four (4) applications, a comparison of the Appendix G fluence prediction with measurements for the vessel being analyzed and an update of the uncertainty analysis if necessary and (2) after the four initial applications of the methodology, the uncertainty analysis must be updated with at least four (4) additional BWR dosimetry measurement comparisons to confirm, and update if necessary, the Appendix G fluence calculational bias and uncertainty. As required by RG 1.190, this confirmation/update must also be performed as subsequent measurements become available. When measured data is not available, the plant-specific application must include an analytic sensitivity evaluation of the calculational uncertainties between the plant without measured data and a comparable plant that has an appropriate benchmark of the calculations to dosimetry measurements. The plant-specific evaluation, without an appropriate calculational benchmark, must incorporate a larger uncertainty and a positive bias in the fluence predictions for the structural materials.

#### 5 0 REFERENCES

1. Letter from Jerald S. Holm, Framatome ANP to Document Control Desk (NRC), "Request for Review and Approval of Revision-1 of Appendix G to BAW-2241(P), Revision 2, 'Fluence and Uncertainty Methodologies'," dated March 31, 2005.
2. Office of Nuclear Regulatory Research, "Calculational and Dosimetry Methods for Determining Pressure Vessel Neutron Fluence," Regulatory Guide 1.190, U.S. Nuclear Regulatory Commission, March 2001.
3. W.N. McElroy, Editor, "LWR Pressure Vessel Surveillance Dosimetry Improvement Program: PCA Experiments and Blind Test," NUREG/CR-1861 (Hanford Engineering Development Laboratory, HEDL-TME 80-87), July 1981.
4. J. F. Carew, K. Hu, A. Aronson, A. Prince, and G. Zamonsky, "Pressure Vessel Fluence Calculation Benchmark Problems and Solutions," NUREG/CR-6115, BNL-NUREG-52395, September 2001.
5. L. J. Tilly, B. D. Frew, B. J. Branlund, "Pressure-Temperature Curves for TVA Browns Ferry Unit 3," GE Nuclear Energy, GE-NE-0000-0013-3193-02a-R1, Revision 1, August 2003.
6. King, S. Q., et al., "Pressure Vessel Fluence Analysis for 177-FA Reactors," BAW-1485P, Rev. 1, April 1998.
7. Whitmarsh, C. L., "Pressure Vessel Fluence Analysis for 177-FA Reactors," BAW-1485, June 1978.

8. Radiation Shielding Information Center (RSIC), Oak Ridge National Laboratory (ORNL), "BUGLE-93: Coupled 47 Neutron, 20 Gamma-Ray Group Cross Section Library Derived from ENDF/B-VI for LWR Shielding and Pressure Vessel Dosimetry Applications," DLC-175, April 1994.
9. Mark A. Rutherford, et. al., "DORT, Two Dimensional Discrete Ordinates Transport Code, (BWNT Version of RISC/ORNL Code DORT)," FANP Document # BWNT-TM-107, May 1995.
10. "Request for Additional Information for Appendix G of Topical Report BAW-2241-P," E-Mail, Michelle C. Honcharik (NRC) to Gayle Elliot (FANP), dated September 8, 2005.
11. "Response to a Request for Additional Information Regarding BAW-2241(P), Appendix G, 'Fluence and Uncertainty Methodologies'," Letter, Ronnie L. Gardner to Document Control Desk, U. S. Nuclear Regulatory Commission, dated November 8, 2005.

Principal Contributor: L. Lois

Date: April 28, 2006

**BAW-2241NP-A**

**Revision 1**

Submitted  
April, 1999

**NRC Acceptance Letter**

**April, 2000**

**&**

**Safety Evaluation Report**

**Fluence and Uncertainty Methodologies**

**Generic PWR Uncertainties**

**AREVA NP Inc.**

(An AREVA and Siemens Company)



UNITED STATES  
NUCLEAR REGULATORY COMMISSION

WASHINGTON, D.C. 20555-0001

April 5, 2000

Mr. J. J. Kelly, Manager  
B&W Owners Group Services  
3315 Old Forest Road  
P.O. Box 10935  
Lynchburg, VA 24506-3663

SUBJECT: ACCEPTANCE FOR REFERENCING OF LICENSING TOPICAL REPORT  
BAW-2241P, REVISION 1, "FLUENCE AND UNCERTAINTY METHODOLOGIES"  
(TAC NO. M98962)

Dear Mr. Kelly:

The U.S. Nuclear Regulatory Commission (NRC) staff has completed its review of the subject topical report, which was submitted by the Babcock and Wilcox Owners Group (B&WOG) by letter dated April 30, 1999. The report was prepared by Framatome Technologies, Inc. (FTI), acting on behalf of the B&WOG. The staff has found that this report is acceptable for referencing in licensing applications to the extent specified and under the limitations delineated in the report and the associated NRC safety evaluation, which is enclosed. The evaluation defines the bases for acceptance of the report. The staff will not repeat its review of the matters described in the BAW-2241P, Revision 1, when the report appears as a reference in license applications, except to ensure that the material presented applies to the specific plant involved.

In accordance with procedures established in NUREG-0390, the NRC requests that the B&WOG publish accepted versions of the submittal, proprietary and non-proprietary, within three months of receipt of this letter. The accepted versions shall incorporate this letter and the enclosed safety evaluation between the title page and the abstract, and an -A (designating accepted) following the report identification symbol. The staff's requests for additional information (RAIs) and the B&WOG responses to RAIs during the review cycle shall be included as an appendix in the approved version of the topical report.

Pursuant to 10 CFR 2.790, the staff has determined that the enclosed safety evaluation does not contain proprietary information. However, the staff will delay placing the safety evaluation in the public document room for 10 calendar days from the date of this letter to allow you the opportunity to comment on the proprietary aspects only. If, after that time, you do not request that all or portions of the safety evaluation be withheld from public disclosure in accordance with 10 CFR 2.790, the safety evaluation will be placed in the NRC Public Document Room.

Mr. J. J. Kelly

- 2 -

April 5, 2000

If the NRC's criteria or regulations change so that its conclusion that the submittal is acceptable is invalidated, the B&WOG and/or the applicant referencing the topical report will be expected to revise and resubmit its respective documentation, or submit justification for the continued applicability of the topical report without revision of the respective documentation.

Should you have any questions or wish further clarification, please call Stewart Bailey at (301) 415-1321 or Lambros Lois at (301) 415-3233.

Sincerely

A handwritten signature in black ink, appearing to read "S. A. Richards", with a large, stylized flourish at the end.

Stuart A. Richards, Director  
Project Directorate IV & Decommissioning  
Division of Licensing and Project Management  
Office of Nuclear Reactor Regulation

Project No. 693

Enclosure: Safety Evaluation

cc w/encl: See next page



cc:

Mr. Guy G. Campbell, Chairman  
B&WOG Executive Committee  
Vice President - Nuclear  
FirstEnergy Nuclear Operating Company  
Davis-Besse Nuclear Power Station  
5501 North State Rt. 2  
Oak Harbor, OH 43449

Ms. Sherry L. Bernhoff, Chairman  
B&WOG Steering Committee  
Florida Power Corporation  
Crystal River Energy Complex  
15760 West Power Line St.  
Crystal River, FL 34428-6708

Mr. J. J. Kelly, Manager  
B&W Owners Group Services  
Framatome Technologies, Inc.  
P.O. Box 10935  
Lynchburg, VA 24506-0935

Mr. F. McPhatter, Manager  
Framatome Cogema Fuels  
3315 Old Forest Road  
P.O. Box 10935  
Lynchburg, VA 24506-0935

Mr. R. Schomaker, Manager  
Framatome Cogema Fuels  
3315 Old Forest Road  
P.O. Box 10935  
Lynchburg, VA 24506-0935

Mr. Michael Schoppman  
Licensing Manager  
Framatome Technologies, Inc.  
1700 Rockville Pike, Suite 525  
Rockville, MD 20852-1631



UNITED STATES  
NUCLEAR REGULATORY COMMISSION  
WASHINGTON, D.C. 20555-0001

SAFETY EVALUATION BY THE OFFICE OF NUCLEAR REACTOR REGULATION

TOPICAL REPORT BAW-2241P, REVISION 1

"FLUENCE AND UNCERTAINTY METHODOLOGIES"

BABCOCK AND WILCOX OWNERS GROUP

1.0 INTRODUCTION

By letter dated May 14, 1997, the Babcock and Wilcox Owners Group (B&WOG) submitted Topical Report BAW-2241P, regarding a methodology for determining the pressure vessel fluence and associated uncertainties for NRC review (Reference 1). The submittal was prepared by Framatome Technologies, Inc. (FTI) on behalf of the B&WOG. The proposed methodology was intended for application to PWR plants and included numerous updates and improvements to the methods described in References 2 and 3. The approach used in BAW-2241-P is semi-analytic using the most recent fluence calculational methods and nuclear data sets. In the proposed methodology, the vessel fluence is determined by a transport calculation in which the core neutron source is explicitly represented and the neutron flux is propagated from the core through the downcomer to the vessel. The dosimeter measurements are only used to determine the calculational bias and uncertainty. The staff evaluation was completed on February 28, 1998, and found the proposed methodology acceptable for application to Babcock and Wilcox (B&W) plants. The B&WOG subsequently submitted additional information to demonstrate the applicability of the methodology to Westinghouse (W) and Combustion Engineering (CE) plants.

On April 30, 1999, the B&WOG submitted BAW-2241P, Revision 1, which consists of BAW-2241P, with added Appendix E (Reference 4). Review of BAW-2241P, Revision 1, has been completed and is the subject of this safety evaluation. The review and the evaluation were conducted in accordance with the provisions of Draft Regulatory Guide DG-1053 on neutron dosimetry, and BAW-2241P is found to be generally consistent with DG-1053.

The topical report provides a detailed description of the application of the proposed methodology to the calculation of the recent Davis-Besse cavity dosimetry experiment (References 7-9). This includes a description of both the discrete ordinates transport calculation and the techniques used to interpret the in-vessel and cavity dosimeter response. The Davis-Besse measurements have been included in the FTI benchmark data-base and are used to determine the measurement biases and uncertainties. The fluence calculation and uncertainty methodology presented in BAW-2241P, Revision 1, is summarized in Section 2. The evaluation of the important technical issues raised during this review is presented in Section 3, and the summary and limitations are in Section 4.

## 2.0 SUMMARY OF THE TOPICAL REPORT

### 2.1 Semi-Analytic Computational Methodology

The FTI semi-analytic fluence calculational methodology is the result of a series of updates and improvements to the BAW-1485 methodology developed for the 177-fuel assembly plants, described in References 2 and 3. These updates were made to improve the accuracy of the fluence prediction and to further quantify the calculational uncertainty. The improvements include the implementation of the BUGLE-93 ENDF/B-VI multi-group nuclear data set (Reference 9). The fluence calculations are performed with the DOT discrete ordinates transport code (Reference 10). The prediction of the best-estimate fluence is based on a direct calculation and includes an energy-dependent adjustment based on measurement. The BAW-2241P, Revision 1, approach incorporates most of the provisions of DG-1053 for predicting both the vessel fluence and the dosimeter response.

Predictions of the dosimeter response measurements are required to determine the calculation-to-measurement (C/M) data base. The FTI methodology includes dosimeter response adjustments for the half-lives of the reaction products, photo-fission contributions to the fission dosimeters, and dosimeter impurities. The predictions are made for both in-vessel and cavity dosimetry using the same methods used to determine the vessel fluence. In order to ensure an accurate prediction of the dosimeter response, a detailed spatial representation of the dosimeter holder tube/surveillance capsule geometry is included in the DOT model. Perturbation factors which account for the effect of the support beams and the instrumentation were calculated and applied to the predicted dosimeter responses. Energy-dependent axial synthesis factors are included to account for the axial dependence of the fluence.

### 2.2 Davis-Besse Cavity Dosimetry Benchmark Experiment

BAW-2241P, Revision 1, provides an extensive description of the Davis-Besse, Unit-1, Cycle-6, cavity dosimetry benchmark program. The program included both in-vessel and cavity experiments and provides a demonstration of the FTI dosimetry measurement methodology. The Davis-Besse dosimetry included an extensive set of activation foils, fission foils and cavity stainless steel chain segments. The in-vessel dosimetry consisted of standard dosimeter sets with energy thresholds down to 0.5 MeV. The in-vessel capsules were located at the azimuthal peak fluence location while the cavity holders were distributed azimuthally. The cavity chains extended from the concrete floor up to the seal plate (spanning the active core height) and were used to determine the axial fluence distribution. The measurement program included eighty dosimetry sets which were installed prior to Cycle 6 and removed in February 1990, after a full cycle (380 effective full power days) of irradiation.

The Davis-Besse dosimetry set included Cu-63 (n, $\alpha$ ), Ti-46 (n,p), Ni-58 (n,p), Fe-54 (n,p), U238 (n,f) and Np-237 (n,f) threshold dosimeters. In addition, solid state track recorders (SSTRs) and helium accumulation fluence monitors (HAFMs) were included in the dosimetry set. The fissionable dosimeters were counted using two techniques: (1) the foils and wires were counted directly, and (2) the oxide powders were dissolved and diluted prior to counting. The detector was calibrated using a NIST-traceable mixed gamma standard source. The dosimeter measurements were corrected for dosimeter/detector geometry, self-absorption and photo-fission induced activity. When the foil or dosimeter thickness was large and/or the distance to

the detector was small, the geometry correction was determined with the NIOBIUM special purpose Monte Carlo program.

The measurement technique used for the non-fissionable dosimeters and chain dosimeters was essentially the same as that used for the fissionable dosimeters, although no dissolution was required. A NIST-traceable mixed gamma standard source was used for calibrating the detector and corrections for self-absorption and geometry were included. The Fe-54 (n,p) and Co-59 (n, $\gamma$ ) activities were used to determine the axial fluence shapes from the chain measurements.

### 2.3 Calculation-to-Measurement (C/M) Data Base and Uncertainty Analysis

FTI uses the comparisons of the calculated and measured dosimeter responses to benchmark and qualify the fluence methodology. Specifically, the data-base of calculation-to-measurement (C/M) values is used to determine the calculation bias and uncertainty (i.e., standard deviation). The data-base is large including a full set of dosimeter types and both in-vessel and cavity measurements. The data-base includes 35 capsule analyses (including two from the PCA benchmark experiment), three standard cavity measurements and the Davis-Besse cavity benchmark experiment.

The measured data is evaluated by material and dosimeter type and is adjusted to account for the dependence on power history and decay since shutdown. The statistical analysis of the C/M data indicates that the calculational model can predict: (1) the measured dosimeter response to within a standard deviation of seven percent or less, and (2) the end-of-life vessel fluence to within a standard deviation of less than twenty percent.

## 3.0 SUMMARY OF THE TECHNICAL EVALUATION

Topical Report BAW-2241P, Revision 1, provides the FTI methodology for performing pressure vessel fluence calculations and the determination of the associated calculational uncertainty. The review of the FTI methodology focused on: (1) the details of the fluence calculation methods, and (2) the conservatism in the estimated calculational uncertainty. As a result of the review of the methodology, several important technical issues were identified which required additional information and clarification from FTI. The request for additional information (RAI) was transmitted in References 11 to 13 and was discussed with FTI in a meeting at NRC Headquarters on August 5 and 6, 1998. The information requested was provided by FTI in the responses included in References 14 to 16. This evaluation is based on the material presented in the topical report and in References 14 to 16. The evaluation of the major issues raised during the review are summarized in the following subsections.

### 3.1 Semi-Analytic Calculational Methodology

The FTI semi-analytic calculational methodology is used to determine the pressure vessel fluence, predict the surveillance capsule fluence, determine dosimeter response for the benchmark experiments and perform fluence sensitivity analyses. The neutron transport calculation, selection and processing of the nuclear data and analysis of the Davis-Besse benchmark experiment generally follows the approach described in DG-1053.

DG-1053 notes that as fuel burnup increases the number of plutonium fissions increases, resulting in an increase in the number of neutrons per fission and a hardening of the neutron spectrum. Neglect of either of these effects results in a nonconservative prediction of the vessel fluence. In Responses 1-3 and 1-10 of Reference 14, FTI describes the method used to incorporate these effects in the methodology. It is indicated that the uranium and plutonium isotopic inventory is tracked for each fuel assembly and the uranium and plutonium neutron emission rates are determined for the individual isotopes. The fuel inventory is determined for each depletion time-step and is tracked in three dimensions using a program that is benchmarked to in-core detector data. In Response 1-10 (Reference 14), FTI evaluates the approximation used to determine the burnup-dependent core neutron spectrum. This evaluation indicates that the effect of the spectrum approximation used in the methodology is negligible.

Typically, PWR internals include steel former plates for additional support between the core shroud and barrel. These plates provide additional core-to-vessel fluence attenuation and can have a significant effect on the surveillance capsule dosimeters and the neutron fluence at the vessel. In Response 1-4 (Reference 14), FTI stated that several designs include core shroud former plates and that these plates have been included in the data-base fluence transport analyses. In addition, FTI has provided DOT calculated fluence profiles which quantify the fluence reduction introduced by the former plates.

### 3.2 Measurement Methodology

The FTI vessel fluence methodology includes an extensive set of plant surveillance capsule fluence measurements as well as the Davis-Besse benchmark measurements. These measurements are important since they are used to determine the calculational uncertainty and bias. In response to RAI 1-16, FTI has stated in Reference 13 that the dosimeter measurements conform to the applicable ASTM standards. In addition, in conformance with DG-1053, FTI performed a reference field measurement validation, which has been provided to the NRC in Reference 15.

The dosimeter reaction rate is determined by measuring the activity due to a specific reaction product. Before the reaction rate can be determined the effect of interfering reactions must be removed. Typically, this will involve the interference from: (1) the fission products resulting from plutonium buildup in the U-238 dosimeters, (2) the fission products resulting from U-235 impurities, (3) the fission products resulting from photo-fission reactions in the U-238 dosimeters, and (4) impurities having decay energies close to the reaction product being measured. FTI has stated in Response 1-16 (Reference 14) that these effects have been evaluated and, when they were significant, have been accounted for in determining the dosimeter response.

The determination of the photo-fission correction for the U-238 (n,f) dosimeters requires a coupled gamma/neutron transport calculation (which is not required for the analysis of the (n,p) dosimeters). This calculation is sensitive to both the neutron and photon cross sections. To ensure the accuracy of these calculations, FTI has stated in Response 1-14 (Reference 14) that photo-fission corrections determined using an alternate neutron/photon cross section library agree (to within a percent) with the corrections used in the BAW-2241P, Revision 1, analysis.

The FTI data-base includes two distinct types of U-238 fission dosimeters. The statistical analysis of the C/M data-base is made without any recognition of the difference between these two sets of dosimetry data. In Response 1-12 (Reference 14), FTI has evaluated the two sets of U-238 data in order to identify any significant difference in either the uncertainty or bias inferred from this data. The evaluation showed no significant difference between the two U-238 data sets.

### 3.3 Calculation-to-Measurement (C/M) Data Base and Uncertainty Analysis

DG-1053 requires that the vessel fluence calculational methodology be benchmarked against reactor surveillance dosimetry data. The FTI topical report includes an extensive set of calculation-to-measurement benchmark comparisons. FTI has evaluated the C/M data statistically in order to estimate the uncertainty in the fluence predictions and determine the calculational bias.

The plant-to-plant variation in the as-built core/internals/vessel geometry, core power and exposure distributions, and the plant power history are major contributors to the uncertainty in the vessel fluence calculation. The contribution of these uncertainty components can be minimized by selecting the C/M data from only a few plants. In fact, as part of the integrated vessel material surveillance program (BAW-1543A), several of the FTI data sets were taken at a single host plant. FTI has identified the specific data sets and host plant in Response 2-13 (Reference 16). In order to ensure that these data sets have not resulted in an erroneous reduction in the data-base calculation uncertainty, the uncertainty for these plants has been evaluated separately. This evaluation indicated a larger uncertainty for the C/M data taken at the surrogate plants and that use of the surrogate data was not resulting in a non-conservative calculational uncertainty.

The C/M data-base includes a relatively complete set of Np-237(n,f) dosimeters. However, while the calculation-to-measurement agreement is generally good for most dosimeter types, the agreement for the Np-237 dosimeters is poor. In Response 2-18 (Reference 16), FTI has indicated that it is presently evaluating the calculation-to-measurement discrepancies for Np-237. It is important to note, however, that the BAW-2241-P fluence methodology does not include the Np-237(n,f) dosimeter data in the determination of the calculation uncertainty and bias.

The BAW-2241-P analysis includes a detailed evaluation of the measurement uncertainty. This evaluation is based on estimates of the various uncertainties that affect the measurement process and analytic calculations of the sensitivity of the measurement process to these uncertainty components (Reference 16). The calculational uncertainty is determined using the overall data-base C/M variance and the estimated measurement uncertainty. In order to ensure a conservative estimate of the calculational uncertainty, FTI has increased the estimated calculational uncertainty by about 50 percent.

The FTI calculational procedure includes the application of a group-wise multiplicative bias to the calculated > 1-MeV fluence. This bias is based on comparisons of calculation and measurement for both in-vessel capsules and cavity dosimetry and is to be applied to determine the best-estimate fluence. The application of the bias is conservative and results in a relatively small, but positive, increase in the calculated > 1-MeV fluence.

### 3.4 Application to Westinghouse and Combustion Engineering Plants

The BAW-2241P, Revision 1, methodology is intended for application to W and CE plants, as well as B&W plants. As justification for the application to W and CE plants, FTI has included both W and CE plant dosimetry data in the C/M data-base. In response to request for additional information (RAI) number 1 (RAI-1 in Reference 17) concerning the consistency of the C/M data, FTI has stated that the dosimetry measurements and calculations for the W and CE plants were performed with the same methods used to determine the C/M data for the B&W plants (i.e., the methods described in BAW-2241P, Revision 1). In addition, in response to RAI-2 (Reference 17), it is stated that no W or CE C/M data has been eliminated from the comparisons.

The review of the C/M data-base indicated that the standard deviation between the calculations and measurements is smaller for the CE plants than for the W and B&W plants. It is therefore conservative to apply the larger overall data-base uncertainty to the CE plants. However, the inclusion of the C/M data for the CE plants in the FTI data-base may result in an erroneous reduction in the uncertainty applied to the W and B&W plants. In Response 7 of Reference 17, FTI has evaluated the increase in calculational uncertainty when the C/M data for the CE plants is excluded from the FTI data-base. The resulting increase in calculational uncertainty is found to be very small compared to: (1) the conservatism included in the estimated calculational uncertainty, and (2) the uncertainty requirements of DG-1053.

### 4.0 SUMMARY AND LIMITATIONS

Topical Report BAW 2241P, Revision 1, "Fluence and Uncertainty Methodologies," and its supporting documentation provided in References 14 and 16 have been reviewed in detail. Based on this review, it is concluded that the proposed methodology is acceptable for referencing in licensing applications for determining the pressure vessel fluence of W, CE and B&W designed reactors.

The following limitations apply:

1. The FTI dosimetry C/M data-base includes an extensive set of PWR core/internals/vessel configurations. However, the dosimetry set is not complete and there are certain designs that are not included in the data-base (e.g., cores including partial-length fuel assembly designs). FTI has indicated (Response-9 of Reference-17) that in the case where the BAW-2241P, Revision 1, methodology is applied to a plant including a feature not included in the FTI data-base, an additional evaluation will be performed. This will include an evaluation of the effect on the dosimetry measurements, calculation-to-measurement ratios and the analytical uncertainties. FTI has stated that the fluence calculational uncertainty will be increased if this evaluation indicates that the uncertainties given in BAW-2241P, Revision 1, are not adequate.
2. Should there be changes in the input cross section of this methodology, the licensee will evaluate the changes for their impact and , if necessary, will modify the methodology accordingly.
3. The licensee will provide the staff with a record of future modifications of the methodology.

The NRC staff will require licensees referencing this topical report in licensing applications to document how these conditions are met.

## 5.0 REFERENCES

1. "B&WOG Topical Report BAW 2241-P, 'Fluence and Uncertainty Methodologies'," Letter, from J. H. Taylor (B&WOG) to US NRC, dated May 14, 1997.
2. BAW-1485P, Revision 1, "Pressure Vessel Fluence Analysis for 177-FA Reactors," S. Q. King, et al., Framatome Technologies, Inc., April 1998.
3. BAW-1485, "Pressure Vessel Fluence Analysis for 177-FA Reactors," C.L. Whitmarsh, Babcock and Wilcox Corporation, June 1978.
4. BAW-2241P, Revision 1, "Fluence and Uncertainty Methodologies," R. J. Worsham III, Framatome Technologies, Inc., April 1999.
5. Draft Regulatory Guide DG-1053, "Calculational and Dosimetry Methods for Determining Pressure Vessel Neutron Fluence," Office of Nuclear Regulatory Research, U.S. Nuclear Regulatory Commission, June 1996.
6. BAW-1875-A, "The B&W Owners Group Cavity Dosimetry Program," S. Q. King, Babcock and Wilcox Corporation, July 1986.
7. Coor, Jimmy L., "Analysis of B&W Owner's Group Davis-Besse Cavity Dosimetry Benchmark Experiment" Volumes I, II and III, B&W Nuclear Environmental Services, Inc. (NESI), NESI # 93:136112:02, May 1993, FTI Doc. # 38-1210656-00, Released May 30, 1995.
8. BAW-2205-00, "B&WOG Cavity Dosimetry Benchmark Program Summary Report," J. R. Worsham III, et al., Framatome Technologies, Inc., December 1994.
9. "BUGLE-93: Coupled 47 Neutron, 20 Gamma-Ray Group Cross Section Library Derived from ENDF/B-VI for LWR Shielding and Pressure Vessel Dosimetry Applications," Radiation Shielding Information Center (RSIC), Oak Ridge National Laboratory (ORNL), DLC-175, April 1994.
10. "DOT4.3: Two Dimensional Discrete Ordinates Transport Code," Hassler, L. A., et al., (B&W Version of RSIC/ORNL Code DOT4.3), FTI Doc. # NPD-TM-24, July 1986.
11. "Request for Additional Information for Topical Report BAW-2241-P," Letter, Joseph L. Birmingham (NRC) to J. J. Kelley (B&WOG), dated January 30, 1998.
12. "Request for Additional Information for Topical Report BAW-2241-P," Letter, Joseph L. Birmingham (NRC) to J. J. Kelley (B&WOG), dated April 8, 1998.
13. "Request for Additional Information for Topical Report BAW-2241-P," Letter, S. Bailey (NRC) to J. J. Kelley (B&WOG), dated October 26, 1999.



14. "Response to NRC Request for Additional Information for Topical Report BAW-2241-P, 'Fluence and Uncertainty Methodologies'," Letter, OG-1708, R. W. Clark (BWOG) to J. L. Birmingham (NRC), dated May 29, 1998.
15. Letter from R.W. Clark, B&WOG to US NRC, and attached report, "Standard and Reference Field Validation," by T. Worsham and Q. King dated May 19, 1999.
16. "Response to NRC's April 8, 1998 Request for Additional Information for Topical Report BAW-2241-P, 'Fluence and Uncertainty Methodologies'," Letter, OG-1726, R. W. Clark (BWOG) to J. L. Birmingham (NRC), dated October 30, 1998.
17. "Response to NRC's October 26, 1999, Request for Additional Information - Framatome Topical Report BAW-2241-P, Revision 1, 'Fluence and Uncertainty Methodologies'," Letter, FTI-99-3850, J. R. Worsham III (FTI) to S. Bailey (NRC), dated November 30, 1999.

Principal Contributor: L. Lois

Date: April 5, 2000

**BAW-2241NP-A**

**Original**

Submitted

May, 1997

**NRC Acceptance Letter**

**February, 1999**

**&**

**Safety Evaluation Report**

**&**

**Technical Evaluation Report**

**Fluence and Uncertainty Methodologies**

**B & W Owners Group**

**AREVA NP Inc.**

(An AREVA and Siemens Company)



UNITED STATES  
NUCLEAR REGULATORY COMMISSION  
WASHINGTON, D.C. 20555-0001

Mr. J.J. Kelley  
B&W Owners Group Services  
Framatome Technologies, Incorporated  
P.O. Box 10935  
Lynchburg, VA 24506-0935

SUBJECT: ACCEPTANCE FOR REFERENCING OF LICENSING TOPICAL REPORT  
BAW-2241 P, "FLUENCE AND UNCERTAINTY METHODOLOGIES,"  
(TAC NO. M98962)

Dear Mr. Kelley:

The NRC staff has completed its review of the subject topical report which was submitted by the B&W Owners Group by letter dated May 14, 1997. The report was prepared by Framatome Technologies Incorporated acting on behalf of the B&W Owners Group. The staff has found that this report is acceptable for referencing in licensing applications to the extent specified and under the limitations delineated in the report and the associated NRC safety evaluation, which is enclosed. The evaluation defines the bases for acceptance of the report. The staff will not repeat its review of the matters described in the BAW-2241P, when the report appears as a reference in license applications, except to ensure that the material presented applies to the specific plant involved.

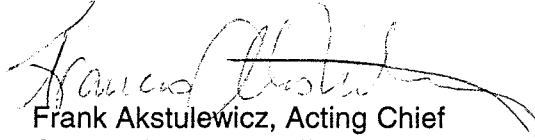
In accordance with procedures established in NUREG-0390, the NRC requests that the B&W Owners Group publish accepted versions of the submittal, proprietary and non-proprietary, within 3 months of receipt of this letter. The accepted versions shall incorporate this letter and the enclosed safety evaluation between the title page and the abstract and an -A (designating accepted) following the report identification symbol. The staff's requests for additional information (RAIs) and the B&W Owners Group responses to RAIs during the review cycle shall be included as an appendix in the approved version of the topical report. In addition, the B&W Owners Group must incorporate into both the NP and P versions of BAW-2241 the statement: "The use of this methodology is subject to the three conditions in the staff's safety evaluation dated February 18, 1999."

Pursuant to 10 CFR 2.790, the staff has determined that the enclosed safety evaluation does not contain proprietary information. However, the staff will delay placing the safety evaluation in the public document room for 30 calendar days from the date of this letter to allow you the opportunity to comment on the proprietary aspects only. If, after that time, you do not request that all or portions of the safety evaluation be withheld from public disclosure in accordance with 10 CFR 2.790, the safety evaluation will be placed in the NRC Public Document Room.

If the NRC's criteria or regulations change so that its conclusion that the submittal is acceptable are invalidated, the B&W Owners Group and/or the applicant referencing the topical report will be expected to revise and resubmit its respective documentation, or submit justification for the continued applicability of the topical report without revision of the respective documentation.

The staff was assisted in this evaluation by Dr. John Carew of BNL as a contractor (Under Contract No. JCN L-2589 Task 16). The contractor's Technical Evaluation Report (TER) is in Enclosure 2. Should you have any questions or wish further clarification, please call me at (301) 415-1136, or Lambros Lois at (301) 415-3233.

Sincerely



Frank Akstulewicz, Acting Chief  
Generic Issues and Environmental Projects  
Division of Regulatory Improvement Programs  
Office of Nuclear Reactor Regulation

Enclosure 1: Topical Report BAW-2241-P, Safety Evaluation  
Enclosure 2: Topical Report BAW-2241-P, Technical Evaluation Report

B&W Owners Group

Project No. 693

cc: Mr. M. Shoppman, Manager  
Rockville Licensing Operations  
Framatome Technologies, Inc.  
1700 Rockville Pike, Suite 525  
Rockville, MD 20852-1631

SAFETY EVALUATION BY THE OFFICE OF NUCLEAR REACTOR REGULATION  
BAW-2421P "FLUENCE AND UNCERTAINTY METHODOLOGIES"  
FRAMATOME TECHNOLOGIES INCORPORATED

## 1 INTRODUCTION AND BACKGROUND

By letter dated May 14, 1997, the B&W Owners Group (B&WOG) submitted information regarding a methodology for determining the pressure vessel fluence and associated calculational uncertainties for NRC review (Reference 1). The submittal was prepared by Framatome Technologies Incorporated on behalf of the B&W Owners Group. The proposed methodology is intended for application to B&W plants and includes numerous updates and improvements to the B&W methods described in References 2 and 3. The approach used in BAW-2241-P is semi-analytic using the most recent fluence calculational methods and nuclear data sets. In the proposed methodology, the vessel fluence is determined by a transport calculation in which the core neutron source is explicitly represented and the neutron flux is propagated from the core through the core barrel the baffle and the downcomer to the vessel (rather than by an extrapolation of the measurements). The dosimeter measurements are only used to determine the calculational bias and uncertainty. While the uncertainty analysis used in BAW 2241-P differs from the approach of Draft Regulatory Guide DG-1053 (Reference-4), the method proposed for predicting the dosimeter response and the vessel inner-wall fluence is generally consistent with DG-1053.

BAW-2241-P provides the FTI methodology for performing pressure vessel fluence calculations and the determination of the associated calculational uncertainty. The review of the FTI methodology focused on: (1) the details of the fluence calculation methods and (2) the conservatism in the estimated calculational uncertainty. As a result of the review of the methodology, several important technical issues were identified which required additional information and clarification from FTI. This information was requested in References-10 and 11 and was discussed with FTI in a meeting at NRC Headquarters on August 5 and 6, 1998. The information requested was provided by FTI in the responses included in References 12 and 13. This evaluation is based on the material presented in the topical report and in References 12 and 13.

The topical report provides a detailed description of the application of the proposed methodology to the calculation of the recent Davis Besse Cavity Dosimetry Experiment (References 5-7). This includes a description of both the discrete ordinates transport calculation and the techniques used to interpret the in-vessel and cavity dosimeter response. The Davis Besse measurements have been included in the FTI benchmark data-base and are used to determine the measurement biases and uncertainties. The BAW-2241-P fluence calculation and uncertainty methodology is summarized in Section 2. The evaluation of the important technical issues raised during this review is presented in Section 3 and the applicable restrictions and the Technical Position is given in the "Summary and Limitations" Section 4.

## 2 SUMMARY OF THE "FLUENCE AND UNCERTAINTY METHODOLOGIES"

### 2.1 Semi-Analytic Computational Methodology

The FTI semi-analytic fluence calculational methodology is the result of a series of updates and improvements to the BAW-1485 methodology developed for the 177 fuel assembly plants described in References 2 and 3. These updates were made to improve the accuracy of the fluence prediction and to further quantify the calculational uncertainty. The improvements include the implementation of the BUGLE-93 ENDF/B-VI multi-group nuclear data set (Reference 8). The fluence calculations are performed with the DOT discrete ordinates transport code (Reference 9). The prediction of the best-estimate fluence is based on a direct calculation and does not include a normalization or adjustment based on measurement, as recommended in DG-1053. The BAW-2241-P approach incorporates most of the provisions of the Draft Regulatory Guide DG-1053 for predicting both the vessel fluence and the dosimeter response.

Predictions and corresponding measurements of the dosimeter response are required to determine the calculation-to-measurement (C/M) data base. The FTI methodology includes dosimeter response adjustments for the half-lives of the reaction products, photo-fission contributions to the fission dosimeters and impurities. The predictions are made for both in-vessel and cavity dosimetry using the same methods used to determine the vessel fluence. In order to ensure an accurate prediction of the dosimeter response, a detailed spatial representation of the dosimeter holder tube/surveillance capsule geometry is included in the DOT model. Perturbation factors which account for the effect of the support beams and the instrumentation were calculated

and applied to the predicted dosimeter responses. Energy-dependent axial synthesis factors are included to account for the axial dependence of the fluence.

## 2.2 Davis Besse Cavity Dosimetry Benchmark Experiment

The BAW-2241-P Topical Report provides an extensive description of the Davis Besse Unit-1, Cycle-6 Cavity Dosimetry Benchmark Program. The program included both in-vessel and cavity experiments and provides a demonstration of the FTI dosimetry measurement methodology. The Davis Besse dosimetry experiment included an extensive set of activation foils, fission foils and cavity stainless steel chain segments. The in-vessel dosimetry consisted of standard dosimeter sets with energy thresholds down to 0.5 MeV. The in-vessel capsules were located at the azimuthal peak fluence location while the cavity holders were distributed azimuthally. The cavity chains extended from the concrete floor up to the seal plate (spanning the active core height) and were used to determine the axial fluence distribution. The measurement program included eighty dosimetry sets which were installed prior to Cycle-6 and removed in February 1990 after a full cycle (380 EFPDs) of irradiation.

The Davis Besse dosimetry set included Cu-63 (n, $\alpha$ ) Co-60, Ti-46 (n,p) Sc-46, Ni-58 (n,p) Co-58, Fe-54 (n,p) Mn-54, U238 (n,f) and Np-237 (n,f) threshold dosimeters. In addition, Solid State Track Recorders (SSTRs) and Helium Accumulation Fluence Monitors (HAFMs) were included in the dosimetry set. The fissionable dosimeters were counted using two techniques; (1) the foils and wires were counted directly and (2) the oxide powders were dissolved and diluted prior to counting. The detector was calibrated using a NIST-traceable mixed gamma standard source. The dosimeter measurements were corrected for dosimeter/detector geometry, self-absorption and for photo-fission induced activity. When the foil or dosimeter thickness was large and/or the distance to the detector was small, the geometry correction was determined with the NIOBIUM special purpose Monte Carlo program.

The measurement technique used for the non-fissionable dosimeters and chain dosimeters was essentially the same as that used for the fissionable dosimeters, although no dissolution was required. A NIST-traceable mixed gamma standard source was used for calibrating the detector and corrections for self-absorption and geometry were included. The Fe-54 (n,p) Mn-54 and Co-59 (n, $\gamma$ ) Co-60 activities were used to determine the axial fluence shapes from the chain measurements.

### 2.3 Calculation-to-Measurement (C/M) Data Base and Uncertainty Analysis

FTI uses the comparisons of the calculated and measured dosimeter responses to benchmark and qualify the fluence methodology. Specifically, the data-base of C/M values is used to determine the calculation bias and uncertainty (i.e., standard deviation). The data-base is large including a full set of dosimeter types, C/M data for the B&WOG plants and both in-vessel and cavity measurements. The data-base includes thirty-five capsule analyses (including two from the PCA Benchmark Experiment), three standard cavity measurements and the Davis Besse Cavity Benchmark Experiment.

The measured data is evaluated by material and dosimeter type and is adjusted to account for the dependence on power history and decay since shutdown. The quality of the C/M data is evaluated and data that is considered unreliable is removed from the analysis. The statistical analysis of the C/M data indicates that the calculational model can predict (1) the measured dosimeter response to within a standard deviation of seven percent or less and (2) the end-of-life vessel fluence to within a standard deviation of less than twenty percent.

## 3 SUMMARY OF THE TECHNICAL EVALUATION

### 3.1 Semi-Analytic Calculational Methodology

The FTI semi-analytic calculational methodology is used to determine the pressure vessel fluence, predict the surveillance capsules fluence, determine dosimeter response for the benchmark experiments and perform fluence sensitivity analyses. The neutron transport calculation, selection and processing of the nuclear data and analysis of the Davis Besse benchmark experiment generally follows the approach described in the Draft Regulatory Guide-1053.

The Draft Guide notes that as fuel burnup increases the number of plutonium fissions increases, resulting in an increase in the number of neutrons per fission and a hardening of the neutron spectrum. Neglect of either of these effects results in a nonconservative prediction of the vessel fluence. In Responses 1-3 and 1-10 of Reference-12, FTI describes the method used to incorporate these effects in the methodology. It is indicated that the uranium and plutonium isotopic inventory is tracked for each fuel assembly and the uranium and plutonium neutron emission rates are determined for the individual isotopes. The fuel inventory is determined for each depletion time-step and is tracked in three dimensions using a program that is benchmarked



to incore detector data. In Response 1-10 (Reference-12), FTI evaluates the approximation used to determine the burnup-dependent core neutron spectrum. This evaluation indicates that the effect of the spectrum approximation used in the methodology is negligible.

Typically, PWR internals include steel former plates for additional support between the core shroud and barrel. These plates provide additional core-to-vessel fluence attenuation and can have a significant effect on the surveillance capsule dosimeters and the neutron fluence at the vessel. In Response 1-4 (Reference-12), FTI has indicated that the B&W design includes core shroud former plates and that these plates have been included in the fluence transport analyses. In addition, FTI has provided DOT calculated fluence profiles indicating the fluence reduction introduced by the former plates.

### 3.2 Measurement Methodology

The FTI vessel fluence methodology includes an extensive set of B&W plant surveillance capsule fluence measurements as well as the Davis Besse benchmark measurements. These measurements are important since they are used to determine the calculational uncertainty and bias. In response to RAI 1-16, FTI has indicated in Reference-12 that the dosimeter measurements conform to the applicable ASTM standards. In addition, in conformance with DG-1053, FTI is presently performing a reference field measurement validation which will be provided to the NRC upon completion (expected 1999).

The dosimeter reaction rate is determined by measuring the activity due to a specific reaction product. Before the reaction rate can be determined the effect of interfering reactions must be removed. Typically, this will involve: (1) the interference from the fission products resulting from plutonium buildup in the U-238 dosimeters (2) the interference from the fission products resulting from U-235 impurities (3) the interference from the fission products resulting from photo-fission reactions in the U-238 dosimeters and (4) interference from impurities having decay energies close to the reaction product being measured. FTI has indicated in Response 1-16 (Reference 12) that these effects have been evaluated and when they were significant have been accounted for in determining the dosimeter response.

The determination of the photo-fission correction for the U-238 (n,f) dosimeters requires a coupled gamma/neutron transport calculation throughout the problem geometry. This calculation is not required for the analysis of typical (n,p) dosimeters and is sensitive to both the neutron and photon

cross sections. To insure the accuracy of these calculations, FTI has indicated in Response 1-14 (Reference 12) that photo-fission corrections determined using an alternate neutron/photon cross section library agree (to within a percent) with the corrections used in the BAW 2241-P analysis.

The FTI data-base includes two distinct types of U-238 fission dosimeters based on their physical characteristics. The statistical analysis of the C/M data-base is made without any recognition of the difference between these two sets of dosimetry data. In Response 1-12 (Reference 12), FTI has evaluated the two sets of U-238 data in order to identify any significant difference in either the uncertainty or bias inferred from this data. The evaluation indicated no significant difference between the two U-238 data sets.

### 3.3 Calculation-to-Measurement (C/M) Data Base and Uncertainty Analysis

The Draft Regulatory Guide DG-1053 (Reference-4) requires that the vessel fluence calculational methodology be benchmarked against reactor surveillance dosimetry data. The FTI topical report includes an extensive set of C/M benchmark comparisons for B&W designed reactors. FTI has evaluated the C/M data statistically in order to estimate the uncertainty in the fluence predictions and determine the calculational bias.

The plant-to-plant variation in the as-built core/internals/vessel geometry, core power and exposure distributions, and the plant power history are major contributors to the uncertainty in the vessel fluence calculation. A number of surveillance capsules were obtained from the integrated vessel material surveillance plan. About 40% of the capsules in the data base were partially or totally irradiated in one or the other of two host plants. FTI has identified the specific data sets and host plant in Response 2-13 (Reference-13). In order to insure that these data sets have not incorrectly reduced the data-base calculation uncertainty, the uncertainty for these plants has been evaluated separately. This evaluation indicated a larger uncertainty for the C/M data taken at the surrogate plants and that use of the surrogate data was not resulting in a nonconservative calculational uncertainty.

The C/M data-base includes a relatively complete set of Np-237(n,f) dosimeters. However, while the calculation-to-measurement agreement is generally good for most dosimeter types, the agreement for the Np-237 dosimeters is poor. In Response 2-18 (Reference-13), FTI has indicated that it is presently evaluating the calculation-to-measurement discrepancies for Np-237.

It is important to note, however, that the BAW-2241-P fluence methodology does not include the Np-237(n,f) dosimeter data in the determination of the calculation uncertainty and bias.

The BAW-2241-P analysis includes a detailed evaluation of the measurement uncertainty. This evaluation is based on estimates of the various uncertainties that affect the measurement process and analytic calculations of the sensitivity of the measurement process to these uncertainty components (Reference-13). The calculational uncertainty is determined using the overall data-base C/M variance and the estimated measurement uncertainty. In order to insure a conservative estimate of the calculational uncertainty, FTI has increased the estimated calculational uncertainty by ~ 50%.

The FTI calculational procedure includes the application of a group-wise multiplicative bias to the calculated  $E > 1$ -MeV fluence. This bias is based on comparisons of calculation and measurement for both in-vessel capsules and cavity dosimetry and is to be applied to determine the best-estimate fluence. The application of the bias is conservative and results in a relatively small, but positive, increase in the calculated  $E > 1$ -MeV fluence.

#### 4 SUMMARY AND LIMITATIONS

The Topical Report BAW 2241-P, "Fluence and Uncertainty Methodologies," and supporting documentation provided in References 12 and 13 have been reviewed in detail. Based on this review, it is concluded that the proposed methodology is acceptable for determining the pressure vessel fluence of B&W designed reactors and to be referenced in B&W designed reactor licensing actions.

The following limitations will apply:

- 1 The methodology is applicable only to B&W designed reactors,
- 2 Should there be changes in the input cross section of this methodology the licensee will evaluate the changes for their impact and if necessary will modify the methodology accordingly, and
- 3 The licensee will provide the staff with a record of future modifications of the methodology.

The NRC staff will require licensees referencing this topical report in licensing applications to document how these conditions are met.

## 5 REFERENCES

1. "B&WOG Topical Report BAW 2241-P, 'Fluence and Uncertainty Methodologies,'" Letter, J. H. Taylor (B&WOG) to US NRC, dated May 22, 1997.
2. King, S. Q., et al., "Pressure Vessel Fluence Analysis for 177-FA Reactors," BAW-1485P, Rev. 1, April 1998.
3. Whitmarsh, C. L., "Pressure Vessel Fluence Analysis for 177-FA Reactors," BAW-1485, June 1978.
4. Office of Nuclear Regulatory Research, "Calculational and Dosimetry Methods for Determining Pressure Vessel Neutron Fluence," Draft Regulatory Guide DG-1053, U.S. Nuclear Regulatory Commission, June 1996.
5. King, S. Q., "The B&W Owners Group Cavity Dosimetry Program," BAW-1875-A, July 1986.
6. Coor, Jimmy L., "Analysis of B&W Owner's Group Davis Besse Cavity Dosimetry Benchmark Experiment," Volumes I, II and III, B&W Nuclear Environmental Services, Inc. (NESI), NESI # 93:136112:02, May 1993, FTI Doc. # 38-1210656-00, Released May 30, 1995.
7. "B&WOG Cavity Dosimetry Benchmark Program Summary Report," J. R. Worsham III, et al., BAW-2205-00, December 1994.
8. Radiation Shielding Information Center (RSIC), Oak Ridge National Laboratory (ORNL), "BUGLE-93: Coupled 47 Neutron, 20 Gamma-Ray Group Cross Section Library Derived from ENDF/B-VI for LWR Shielding and Pressure Vessel Dosimetry Applications," DLC-175, April 1994.
9. Hassler, L. A., et al., "DOT4.3: Two Dimensional Discrete Ordinates Transport Code," (B&W Version of RSIC/ORNL Code DOT4.3), FTI Doc. # NPD-TM-24, July 1986.
10. "Request for Additional Information for Topical BAW-2241-P," Letter, Joseph L. Birmingham (NRC) to J. J. Kelley (BWOOG), dated January 30, 1998.
11. "Request for Additional Information for Topical BAW-2241-P," Letter, Joseph L. Birmingham (NRC) to J. J. Kelley (BWOOG), dated April 8, 1998.
12. "Response to NRC Request for Additional Information for Topical Report BAW-2241-P, 'Fluence and Uncertainty Methodologies,'" Letter, OG-1708, R. W. Clark (BWOOG) to J. L. Birmingham (NRC), dated May 29, 1998.
13. "Response to NRC's April 8, 1998 Request for Additional Information for Topical Report BAW-2241-P, 'Fluence and Uncertainty Methodologies,'" Letter, OG-1726, R. W. Clark (BWOOG) to J. L. Birmingham (NRC), dated October 30, 1998.

## TECHNICAL EVALUATION REPORT

**Report Title:** Fluence and Uncertainty Methodologies

**Report Number:** BAW-2241P

**Report Date:** April 1997

**Originating Organization:** Framatome Technologies Inc.

### 1.0 INTRODUCTION

In Reference-1, Framatome Technologies Inc. (FTI) has submitted the proposed methodology for determining the pressure vessel fluence and associated calculational uncertainties for NRC review and approval. The proposed methodology is intended for application to B&W plants and includes numerous updates and improvements to the B&W methods described in References 2 and 3. The approach used in BAW-2241-P is semi-analytic using the most recent fluence calculational methods and nuclear data sets. In the proposed methodology, the vessel fluence is determined by a transport calculation in which the core neutron source is explicitly represented and the neutron flux is propagated from the core through the downcomer to the vessel (rather than by an extrapolation of the measurements). The dosimeter measurements are only used to determine the calculational bias and uncertainty. While the uncertainty analysis used in BAW 2241-P differs from the approach of Draft Regulatory Guide DG-1053 (Reference-4), the method proposed for predicting the dosimeter response and the vessel inner-wall fluence is generally consistent with DG-1053.

The topical report provides a detailed description of the application of the proposed methodology to the calculation of the recent Davis Besse Cavity Dosimetry Experiment (References 5-7). This includes a description of both the discrete ordinates transport calculation and the techniques used to interpret the in-vessel and cavity dosimeter response. The Davis Besse measurements have been included in the FTI benchmark data-base and are used to determine the measurement biases and uncertainties. The BAW-2241-P fluence calculation and uncertainty methodology is summarized in Section 2. The evaluation

of the important technical issues raised during this review is presented in Section 3 and the Technical Position is given in Section 4.

## **2.0 SUMMARY OF THE FTI FLUENCE AND UNCERTAINTY METHODOLOGIES**

### **2.1 Semi-Analytic Computational Methodology**

The FTI semi-analytic fluence calculational methodology is the result of a series of updates and improvements to the BAW-1485 methodology developed for the 177 fuel assembly plants described in References 2 and 3. These updates were made to improve the accuracy of the fluence prediction and to further quantify the calculational uncertainty. The improvements include the implementation of the BUGLE-93 ENDF/B-VI multi-group nuclear data set (Reference-8). The fluence calculations are performed with the DOT discrete ordinates transport code (Reference- 9). The prediction of the best-estimate fluence is based on a direct calculation and does not include a normalization or adjustment based on measurement, as recommended in DG-1053. The BAW-2241-P approach incorporates most of the provisions of the Draft Regulatory Guide DG-1053 for predicting both the vessel fluence and the dosimeter response.

Predictions of the dosimeter response measurements are required to determine the calculation-to-measurement (C/M) data base. The FTI methodology includes dosimeter response adjustments for the half-lives of the reaction products, photo-fission contributions to the fission dosimeters and impurities. The predictions are made for both in-vessel and cavity dosimetry using the same methods used to determine the vessel fluence. In order to insure an accurate prediction of the dosimeter response, a detailed spatial representation of the dosimeter holder tube/surveillance capsule geometry is included in the DOT model. Perturbation factors which account for the effect of the support beams and the instrumentation were calculated and applied to the predicted dosimeter responses. Energy-dependent axial synthesis factors are included to account for the axial dependence of the fluence.

### **2.2 Davis Besse Cavity Dosimetry Benchmark Experiment**

The BAW-2241-P Topical Report provides an extensive description of the Davis Besse Unit-1 Cycle-6 Cavity Dosimetry Benchmark Program. The program included both in-vessel and cavity experiments and provides a demonstration of the FTI dosimetry measurement methodology. The Davis Besse dosimetry included an extensive set of activation foils, fission foils and cavity stainless steel chain

segments. The in-vessel dosimetry consisted of standard dosimeter sets with energy thresholds down to 0.5 MeV. The in-vessel capsules were located at the azimuthal peak fluence location while the cavity holders were distributed azimuthally. The cavity chains extended from the concrete floor up to the seal plate (spanning the active core height) and were used to determine the axial fluence distribution. The measurement program included eighty dosimetry sets which were installed prior to Cycle-6 and removed in February 1990 after a full cycle (380 EFPD) of irradiation.

The Davis Besse dosimetry set included Cu-63 (n, $\alpha$ ), Ti-46 (n,p), Ni-58 (n,p), Fe-54 (n,p), U238 (n,f) and Np-237 (n,f) threshold dosimeters. In addition, Solid State Track Recorders (SSTRs) and Helium Accumulation Fluence Monitors (HAFMs) were included in the dosimetry set. The fissionable dosimeters were counted using two techniques; (1) the foils and wires were counted directly and (2) the oxide powders were dissolved and diluted prior to counting. The detector was calibrated using a NIST-traceable mixed gamma standard source. The dosimeter measurements were corrected for dosimeter/detector geometry, self-absorption and for photo-fission induced activity. When the foil or dosimeter thickness was large and/or the distance to the detector was small, the geometry correction was determined with the NIOBIUM special purpose Monte Carlo program.

The measurement technique used for the non-fissionable dosimeters and chain dosimeters was essentially the same as that used for the fissionable dosimeters, although no dissolution was required. A NIST-traceable mixed gamma standard source was used for calibrating the detector and corrections for self-absorption and geometry were included. The Fe-54 (n,p) and Co-59 (n, $\gamma$ ) activity were used to determine the axial fluence shapes from the chain measurements.

### **2.3 Calculation-to-Measurement (C/M) Data Base and Uncertainty Analysis**

FTI uses the comparisons of the calculated and measured dosimeter responses to benchmark and qualify the fluence methodology. Specifically, the data-base of calculation-to-measurement (C/M) values is used to determine the calculation bias and uncertainty (i.e., standard deviation). The data-base is large including a full set of dosimeter types, C/M data for several B&W designed plants and both in-vessel and cavity measurements. The data-base includes thirty-five capsule analyses (including two from the PCA Benchmark Experiment), three standard cavity measurements and the Davis Besse Cavity Benchmark Experiment.

The measured data is evaluated by material and dosimeter type and is adjusted to account for the dependence on power history and decay since shutdown. The quality of the C/M data is evaluated and data that is considered unreliable is removed from the analysis. The statistical analysis of the C/M data indicates that the calculational model can predict (1) the measured dosimeter response to within a standard deviation of seven percent or less and (2) the end-of-life vessel fluence to within a standard deviation of less than twenty percent.

### **3.0 SUMMARY OF THE TECHNICAL EVALUATION**

The Topical Report BAW-2241-P provides the FTI methodology for performing pressure vessel fluence calculations and the determination of the associated calculational uncertainty. The review of the FTI methodology focused on: (1) the details of the fluence calculation methods and (2) the conservatism in the estimated calculational uncertainty. As a result of the review of the methodology, several important technical issues were identified which required additional information and clarification from FTI. This information was requested in References-10 and 11 and was discussed with FTI in a meeting at NRC Headquarters on August 5 and 6, 1998. The information requested was provided by FTI in the responses included in References 12 and 13. This evaluation is based on the material presented in the topical report and in References 12 and 13. The evaluation of the major issues raised during the review are summarized in the following.

#### **3.1 Semi-Analytic Calculational Methodology**

The FTI semi-analytic calculational methodology is used to determine the pressure vessel fluence, predict the surveillance capsules fluence, determine dosimeter response for the benchmark experiments and perform fluence sensitivity analyses. The neutron transport calculation, selection and processing of the nuclear data and analysis of the Davis Besse benchmark experiment generally follows the approach described in the Draft Regulatory Guide-1053.

The Draft Guide notes that as fuel burnup increases the number of plutonium fissions increases, resulting in an increase in the number of neutrons per fission and a hardening of the neutron spectrum. Neglect of either of these effects results in a nonconservative prediction of the vessel fluence. In Responses 1-3 and 1-10 of Reference-12, FTI describes the method used to incorporate these effects in the methodology. It is indicated that the uranium and plutonium isotopic inventory is tracked for each fuel



assembly and the uranium and plutonium neutron emission rates are determined for the individual isotopes. The fuel inventory is determined for each depletion time-step and is tracked in three dimensions using a program that is benchmarked to incore detector data. In Response 1-10 (Reference-12), FTI evaluates the approximation used to determine the burnup-dependent core neutron spectrum. This evaluation indicates that the effect of the spectrum approximation used in the methodology is negligible.

Typically, PWR internals include steel former plates for additional support between the core shroud and barrel. These plates provide additional core-to-vessel fluence attenuation and can have a significant effect on the surveillance capsule dosimeters and the neutron fluence at the vessel. In Response 1-4 (Reference-12), FTI has indicated that the B&W design includes core shroud former plates and that these plates have been included in the fluence transport analyses. In addition, FTI has provided DOT calculated fluence profiles indicating the fluence reduction introduced by the former plates.

### **3.2 Measurement Methodology**

The FTI vessel fluence methodology includes an extensive set of B&W plant surveillance capsule fluence measurements as well as the Davis Besse benchmark measurements. These measurements are important since they are used to determine the calculational uncertainty and bias. In response to RAI 1-16, FTI has indicated in Reference-12 that the dosimeter measurements conform to the applicable ASTM standards. In addition, in conformance with DG-1053, FTI is presently performing a reference field measurement validation which will be provided to the NRC upon completion (expected 1999).

The dosimeter reaction rate is determined by measuring the activity due to a specific reaction product. Before the reaction rate can be determined the effect of interfering reactions must be removed. Typically, this will involve: (1) the interference from the fission products resulting from plutonium buildup in the U-238 dosimeters (2) the interference from the fission products resulting from U-235 impurities (3) the interference from the fission products resulting from photo-fission reactions in the U-238 dosimeters and (4) interference from impurities having decay energies close to the reaction product being measured. FTI has indicated in Response 1-16 (Reference-12) that these effects have been evaluated and when they were significant have been accounted for in determining the dosimeter response.

The determination of the photo-fission correction for the U-238 (n,f) dosimeters requires a coupled gamma/neutron transport calculation throughout the problem geometry. This calculation is not required for the analysis of typical (n,p) dosimeters and is sensitive to both the neutron and photon cross sections. To insure the accuracy of these calculations, FTI has indicated in Response 1-14 (Reference-12) that photo-fission corrections determined using an alternate neutron/photon cross section library agree (to within a percent) with the corrections used in the BAW 2241-P analysis.

The FTI data-base includes two distinct types of U-238 fission dosimeters. The statistical analysis of the C/M data-base is made without any recognition of the difference between these two sets of dosimetry data. In Response 1-12 (Reference-12), FTI has evaluated the two sets of U-238 data in order to identify any significant difference in either the uncertainty or bias inferred from this data. The evaluation indicated no significant difference between the two U-238 data sets.

### **3.3 Calculation-to-Measurement (C/M) Data Base and Uncertainty Analysis**

The Draft Regulatory Guide DG-1053 (Reference-4) requires that the vessel fluence calculational methodology be benchmarked against reactor surveillance dosimetry data. The FTI topical report includes an extensive set of calculation-to-measurement benchmark comparisons for B&W designed reactors. FTI has evaluated the C/M data statistically in order to estimate the uncertainty in the fluence predictions and determine the calculational bias.

The plant-to-plant variation in the as-built core/internals/vessel geometry, core power and exposure distributions, and the plant power history are major contributors to the uncertainty in the vessel fluence calculation. The contribution of these uncertainty components can be minimized by selecting the C/M data from only a few plants. In fact, as part of the Integrated Vessel Material Surveillance Program (BAW-1543A), several of the FTI data sets were taken at a single host plant. FTI has identified the specific data sets and host plant in Response 2-13 (Reference-13). In order to insure that these data sets have not incorrectly reduced the data-base calculation uncertainty, the uncertainty for these plants has been evaluated separately. This evaluation indicated a larger uncertainty for the C/M data taken at the surrogate plants and that use of the surrogate data was not resulting in a nonconservative calculational uncertainty.

The C/M data-base includes a relatively complete set of Np-237(n,f) dosimeters. However, while the calculation-to-measurement agreement is generally good for most dosimeter types, the agreement for the Np-237 dosimeters is poor. In Response 2-18 (Reference-13), FTI has indicated that it is presently evaluating the calculation-to-measurement discrepancies for Np-237. It is important to note, however, that the BAW-2241-P fluence methodology does not include the Np-237(n,f) dosimeter data in the determination of the calculation uncertainty and bias.

The BAW-2241-P analysis includes a detailed evaluation of the measurement uncertainty. This evaluation is based on estimates of the various uncertainties that affect the measurement process and analytic calculations of the sensitivity of the measurement process to these uncertainty components (Reference-13). The calculational uncertainty is determined using the overall data-base C/M variance and the estimated measurement uncertainty. In order to insure a conservative estimate of the calculational uncertainty, FTI has increased the estimated calculational uncertainty by ~ 50%.

The FTI calculational procedure includes the application of a group-wise multiplicative bias to the calculated > 1-MeV fluence. This bias is based on comparisons of calculation and measurement for both in-vessel capsules and cavity dosimetry and is to be applied to determine the best-estimate fluence. The application of the bias is conservative and results in a relatively small, but positive, increase in the calculated > 1-MeV fluence.

#### **4.0 TECHNICAL POSITION**

The Topical Report BAW 2241-P, "Fluence and Uncertainty Methodologies," and supporting documentation provided in References 12 and 13 have been reviewed in detail. Based on this review, it is concluded that the proposed methodology is acceptable for determining the pressure vessel fluence of B&W designed reactors.

## REFERENCES

1. "B&WOG Topical Report BAW 2241-P, 'Fluence and Uncertainty Methodologies,'" Letter, J. H. Taylor (B&WOG) to US NRC, dated May 22, 1997.
2. King, S. Q., et al., "Pressure Vessel Fluence Analysis for 177-FA Reactors," BAW-1485P, Rev. 1, April 1998.
3. Whitmarsh, C. L., "Pressure Vessel Fluence Analysis for 177-FA Reactors," BAW-1485, June 1978.
4. Office of Nuclear Regulatory Research, "Calculational and Dosimetry Methods for Determining Pressure Vessel Neutron Fluence," Draft Regulatory Guide DG-1053, U.S. Nuclear Regulatory Commission, June 1996.
5. King, S. Q., "The B&W Owners Group Cavity Dosimetry Program," BAW-1875-A, July 1986.
6. Coor, Jimmy L., "Analysis of B&W Owner's Group Davis Besse Cavity Dosimetry Benchmark Experiment," Volumes I, II and III, B&W Nuclear Environmental Services, Inc. (NESI), NESI # 93:136112:02, May 1993, FTI Doc. # 38-1210656-00, Released May 30, 1995.
7. "B&WOG Cavity Dosimetry Benchmark Program Summary Report," J. R. Worsham III, et al., BAW-2205-00, December 1994.
8. Radiation Shielding Information Center (RSIC), Oak Ridge National Laboratory (ORNL), "BUGLE-93: Coupled 47 Neutron, 20 Gamma-Ray Group Cross Section Library Derived from ENDF/B-VI for LWR Shielding and Pressure Vessel Dosimetry Applications," DLC-175, April 1994.
9. Hassler, L. A., et al., "DOT4.3: Two Dimensional Discrete Ordinates Transport Code," (B&W Version of RSIC/ORNL Code DOT4.3), FTI Doc. # NPD-TM-24, July 1986.
10. "Request for Additional Information for Topical BAW-2241-P," Letter, Joseph L. Birmingham (NRC) to J. J. Kelley (B&WOG), dated January 30, 1998.
11. "Request for Additional Information for Topical BAW-2241-P," Letter, Joseph L. Birmingham (NRC) to J. J. Kelley (B&WOG), dated April 8, 1998.

12. "Response to NRC Request for Additional Information for Topical Report BAW-2241-P, 'Fluence and Uncertainty Methodologies'," Letter, OG-1708, R. W. Clark (BWOG) to J. L. Birmingham (NRC), dated May 29, 1998.
13. "Response to NRC's April 8, 1998 Request for Additional Information for Topical Report BAW-2241-P, 'Fluence and Uncertainty Methodologies'," Letter, OG-1726, R. W. Clark (BWOG) to J. L. Birmingham (NRC), dated October 30, 1998.

**AREVA NP Inc.**

Lynchburg, Va, 24506

**Topical Report BAW-2241**

Revision 2

**Fluence and Uncertainty Methodologies**

J. R. Worsham, III

**Abstract**

The results presented in this topical demonstrate AREVA NP's exceptional accuracy in its completely unbiased, best – estimate fluence calculations, and they show that there is a high degree of confidence in the very small random uncertainties, beginning with a standard deviation of seven percent in the measurements. As confirmed by the Nuclear Regulatory Commission's acceptance letters, the methodologies in this topical are applicable to any LWR with the results showing the same accuracy and consistent uncertainties.

The fluence and uncertainty methodologies discussed in the topical are used in calculations of the neutron and gamma radiation throughout the reactor system, including the internal structures and vessel. The topical information highlights the numerous improvements that AREVA NP made between 1988 and 2006. These improvements began with the B & W Owners Group Cavity Dosimetry Benchmark Experiment. The National Institute of Standards and Technology's evaluation of the experiment provided an update of the measurement biases and uncertainties for the entire AREVA NP dosimetry database. The improvements continued with generic biases and random uncertainties in the calculations of BWRs and PWRs. The AREVA NP databases of BWR and PWR dosimetry provide a high level of confidence in the exceptional accuracy of the calculations.

**AREVA NP Inc.**

(An AREVA and Siemens Company)

**RECORD OF REVISIONS**

<u>Rev. No.</u>	<u>Section or Paragraph Change</u>	<u>Description of Change</u>
0	Original Document	Submitted 1997
0	<i>Appendix D</i>	RAIs Accepted 1999
1	<i>Appendix E</i>	Generic PWR Uncertainties Submitted 1999
1	<i>Appendix F</i>	RAIs Accepted 2000
2	<i>Appendix G</i> Regulatory Affairs	Updated Methods for BWRs Submitted 2003
2	<i>Appendix G</i>	BWR Benchmarks & Uncertainties Submitted 2005
2	<i>Appendix H</i>	RAIs Accepted 2006

**AREVA NP Inc.**  
(An AREVA and Siemens Company)

**Table of Contents**

<u>Section</u>	<u>Page</u>
<b>NRC Acceptance Letters</b>	
<b>Safety Evaluation Reports</b>	1
<b>Technical Evaluation Report (Original Only)</b>	11
<b>Abstract</b>	i
<b>Record of Revisions</b>	ii
<b>1.0 Introduction</b>	1 - 1
<b>2.0 Background</b>	2 - 1
<b>3.0 Semi - Analytical (Calculational) Methodology</b>	3 - 1
<b>4.0 Experimental Setup for Davis Besse Cavity Dosimetry</b>	4 - 1
<b>5.0 Measurement Methodology</b>	5 - 1
<b>6.0 Measurement to Calculational Ratios of Dosimeter Responses</b>	6 - 1
<b>7.0 Uncertainty Methodology</b>	7 - 1

- CONTINUED -

**AREVA NP Inc.**  
(An AREVA and Siemens Company)



**Table of Contents - CONTINUED -**

<u>Section</u>	<u>Page</u>
7.1 Dosimetry Measurement Biases and Standard Deviations	7 - 7
7.2 Dosimetry Computational Biases and Standard Deviations	7 - 23
7.3 Vessel Fluence Standard Deviations	7 - 36
<b>8.0 References</b>	8 - 1
<b><i>Appendix A</i> AREVA NP's Dosimetry Data-Base</b>	A - 1
<b><i>Appendix B</i> Measured Dosimetry Results</b>	B - 1
<b><i>Appendix C</i> Computational Perturbation Factors for Dosimetry</b>	C - 1
<b><i>Appendix D</i> FANP Responses to the Request for Additional Information for Topical BAW-2241P</b>	D - 1
<b><i>Appendix E</i> Generic PWR Uncertainties</b>	E - 1
<b><i>Appendix F</i> FANP Responses to the Request for Additional Information for Topical BAW-2241P, Revision 1</b>	F - 1
<b><i>Appendix G</i> BWR Benchmarks &amp; Uncertainties</b>	G - 1
<b><i>Appendix H</i> AREVA NP Responses to the Request for Additional Information for Topical BAW-2241P, Revision 2</b>	H - 1

## 1.0 Introduction

This topical report was developed in three separate stages. The first stage focused on the B & W Owners Group “Cavity Dosimetry Program”. This program was developed to address the Nuclear Regulatory Commission (NRC) issues concerning dosimetry measurements. The initial NRC issues arose in 1977 with the “Dosimetry Improvement Program” and were followed by the NRC’s “Blind Test” in 1981.<sup>37</sup> The NRC focused the issues on a comprehensive validation of the uncertainties in the measurements. Finally, in the NRC’s regulatory guide, “Calculational And Dosimetry Methods For Determining Pressure Vessel Neutron Fluence”, developed as a proposed draft in 1988, and published in 2001,<sup>G3</sup> the requirement to have the measurement uncertainties validated in a standard – reference field was specified. Even though the various laboratories used National Institute of Standards and Technology benchmark standards as the basis for their measurements, the NRC wanted each laboratory’s measurement uncertainties to be independently validated by the National Institute of Standards and Technology using a standard – reference field. In 1986, the B & W owners contracted the National Institute of Standards and Technology to validate the AREVA NP laboratory’s dosimetry measurement uncertainties.

As noted in the first three topical report sections containing (1) the “NRC Acceptance Letters,” (2) the “Safety Evaluation Reports,” and (3) the “Technical Evaluation Report,” the NRC accepted the original report, BAW-2241P-A, in February of 1999. This report contained eight sections, including Reference Section 8, and appendices *A* through *D*.

The second stage of development for this report began immediately following the Safety Evaluation Report for the first stage. The first stage contained numerous dosimetry measurements from Westinghouse and Combustion Engineering reactors. However, the NRC noted that while AREVA NP's "Fluence and Uncertainty Methodologies" are applicable to any PWR, there are industry uncertainty issues that need to be addressed. One company that performs a significant number of non - B & W fluence analyses using the measurement based FERRET – SAND unfolding methodology consistently produces biases, with uncertainties between 10 and 25 percent. AREVA NP's best-estimate fluence methodology produces no biases in the results and has an uncertainty of 9.9 percent. However, the NRC noted that the FTI database is weighted with 69 percent B & W reactors. Thus, they requested that the Westinghouse and Combustion Engineering analyses be specifically evaluated as a function of plant type to determine if consistent biases or large random uncertainties are evident.

As noted in the April, 2000 "NRC Acceptance Letters," and the "Safety Evaluation Reports," the NRC accepted the "Generic PWR Uncertainties" in Revision 1 of BAW-2241P-A. While other fluence analysts have large unexplained biases with uncertainties as large as 25 percent, Revision 1 appendices *E* and *F* show AREVA NP has no biases and an uncertainty no greater than 9.9 percent.

The third stage of development for this report began in 2001 when AREVA NP acquired BWR technology by forming a joint venture with Siemens. The joint venture provided the means of validating the PWR fluence methods for BWR designs. While the "BWR Benchmarks & Uncertainties" in *Appendix G* of the topical report was prepared in 2002,

AREVA NP Inc.  
(An AREVA and Siemens Company)

interaction between AREVA NP's Regulatory Affairs group and the NRC delayed the Revision 2 formal review.

As noted in the "NRC Acceptance Letters," and the "Safety Evaluation Reports," the NRC accepted Revision 2 of BAW-2241P-A in April of 2006. The "B W R Benchmarks & Uncertainties" in Revision 2 added appendices *G* and *H* to the topical.

The following introductory discussion is related to the original NRC submittal of the topical. The introductory section for Revision 1, "Generic P W R Uncertainties" begins in *Appendix E*. The introductory section for Revision 2, "B W R Benchmarks & Uncertainties" begins in *Appendix G*.

In 1997 the utilities that own and operate Babcock and Wilcox (B & W) reactors entered a new phase of monitoring and evaluating the neutron fluence to determine its effects on the degradation of the mechanical properties of their reactor vessel steels and welds. This new phase represents significant technological improvements over the previous methods used to determine vessel fluences:

1. The vessel fluences are predicted using calculated results from an analytical methodology.
2. Cavity dosimetry has been installed in each operating plant.<sup>1</sup>
3. The uncertainty in the dosimetry measurements has been reevaluated and verified to be unbiased and has a standard deviation of 7.0 percent or less.

NON-PROPRIETARY

---

4. The uncertainty in benchmark comparisons of calculated to measured dosimetry results has been updated to include 35 capsule analyses, including 2 from the PCA "Blind Test", a comprehensive cavity benchmark experiment, and 3 standard cavity analyses.
5. The calculated capsule specimen fluence uncertainty is unbiased and has a standard deviation of 7.0 percent or less. The calculated vessel fluence uncertainty at an extrapolated end of life has a standard deviation that is less than 20.0 percent with appropriate monitoring.

These improvements are derived from the results of the B & W Owners Group (B&WOG) Cavity Dosimetry Program. The dosimetry program had three objectives:

1. Develop a methodology to accurately monitor the neutron fluence throughout the reactor core, internals, vessel, and cavity shield and support structure using neutron transport calculations validated by benchmarks to cavity dosimetry measurements.
2. Develop an uncertainty methodology consistent with the fluence methodology that provides appropriate estimates of the systematic and random deviations.
3. Evaluate the dosimeter types that could be utilized in the vessel cavity regions to provide adequate measurements for benchmarking the calculations.

The program was completed in 1992, but two issues were raised by the United States Nuclear Regulatory Commission (NRC) in their preliminary review of the results. The

AREVA NP Inc.  
(An AREVA and Siemens Company)

first was that the NRC's previously recommended cross section library, BUGLE-80<sup>2</sup>, was biased (which was clearly confirmed by the results from the "Benchmark Experiment" part of the "Cavity Dosimetry Program"). The second issue was that the NRC was concerned with the vessel fluence uncertainties being consistent with the Pressurized Thermal Shock Safety Analysis<sup>3,4,5</sup> and screening criteria<sup>6</sup> without an analytical modeling of the uncertainties. The B&WOG decided to update the cavity dosimetry program before submitting a fluence topical to the NRC. The update consisted of (1) a reanalysis of the Benchmark Experiment using the NRC's latest recommended library, BUGLE-93<sup>7</sup>, and (2) a new uncertainty evaluation that integrated (a) an analytical vessel fluence uncertainty, (b) cavity and capsule benchmarks, and (c) the Cavity Dosimetry Program reevaluation of the measurement uncertainty.

In 1993, before the updates to the Cavity Dosimetry Program could be completed, the NRC issued Draft Regulatory Guide DG-1025, "Calculational And Dosimetry Methods For Determining Pressure Vessel Neutron Fluence",<sup>8</sup> which outlined the requirements for comprehensive analytical, benchmark, and measurement fluence uncertainties. The draft guide contains more requirements than those outlined by the NRC for the Cavity Dosimetry Program, and in June of 1996, the draft guide was reissued for comments (as DG-1053).<sup>19</sup> As discussed in Sections 2.4.3 and 3.0, the fluence methodology has been changed to a Semi – Analytical method, with BUGLE-93 cross sections. In this method, the fluence results are absolute, best-estimate calculations, with no plant - specific adjustments.

The B & W Owners and FTI will evaluate the draft guide requirements when they become part of a Regulatory Guide. In the interim period however, before the draft guide

NON-PROPRIETARY

---

is finalized, most of the owners will be updating their reactor coolant system pressure-temperature limits for heat-ups and cool-downs. In addition, most owners will be revalidating the analytical monitoring of their vessels by performing vessel fluence analyses that include absolute calculations of the fluence and benchmark comparisons of the calculations to cavity dosimetry measurements. Since the methodology for validating the calculations with benchmark comparisons to cavity dosimetry measurements represents a significant technological improvement over the previous methodology,<sup>9</sup> and the Benchmark Experiment provides an update of the measurement uncertainty as well as an update of the benchmark uncertainty, the B&WOG has funded the preparation of this topical report.

This report describes five significant technological improvements. These improvements incorporate the requirements noted in the draft guide, such as the requirement that the vessel fluence predictions be determined completely from calculations without any adjustments or normalization to each plant specific measurement. However, some of the new draft guide requirements, such as the comprehensive evaluation of an analytical uncertainty model to estimate the vessel fluence uncertainty and the comprehensive statistical evaluations of benchmarks to determine the calculational bias may not be as comprehensive as intended by the NRC. The B & W Owners do not believe that it is cost effective to modify the evaluations at this time. The analytical uncertainty model is based on an update of the previous evaluations,<sup>9, 10, 11, 12</sup> and the benchmarks are based on an update of the greater than 0.1 MeV (million electron Volts, Mega-Volts) weighted fluence response functions. When the draft guide is issued in final form, the uncertainty evaluations will be reassessed to determine if they comply with the guide, and if a revised topical report is needed.

AREVA NP Inc.  
(An AREVA and Siemens Company)

## **2.0 Background**

The purpose of this topical report is to (a) describe the Framatome Technologies, Inc. (FTI) improved methodology for predicting the fluence throughout the reactor and vessel cavity structure, and (b) describe the corresponding uncertainty methodology for estimating the bias and standard deviation in the fluence predictions. The methodologies that will be discussed follow a history of nearly thirty years of technological improvements. This is the fifth in the series of topicals describing the improvements.<sup>9,12,13,14</sup> The reasons for the earlier improvements were to increase the accuracy and to reduce the uncertainty in the fluence predictions for the vessel and weld material specimens. These most recent improvements are to increase the accuracy of the fluence predictions and verify the fluence uncertainty for the actual vessel material and welds, rather than that of the capsule specimens of vessel and weld materials.

### **2.1 Irradiation Embrittlement 1950's - 1977**

Accuracy and precision in the predictions of the vessel fluence are important in order to accurately and precisely determine the neutron irradiation effects upon vessel materials. Since the late 1950's it has been known that relatively low levels of neutron irradiation could degrade the mechanical properties of the steels and welds used in the fabrication of reactor vessels. The degradation appeared to be the result of an increase in embrittlement. However, the phenomenon was difficult to understand because it varied significantly from one type of steel to another, one heat treatment to another and one weld to another. Research and development programs were initiated to better understand the irradiation embrittlement phenomenon. In 1961, the American Society for Testing and Materials established a standard for reactor vessel surveillance programs (ASTM E 185-61, "Standard Practice for Conducting Surveillance Tests for Light-Water Cooled Nuclear Power Reactor Vessels"). FTI (formerly Babcock and Wilcox) developed a



## **FTI Non-Proprietary**

surveillance program to monitor the changes in the mechanical properties of vessel material test specimens for each reactor that was in accordance with the ASTM standard.

By the late 1960's, the Naval Research Laboratory had discovered that copper and phosphorus were the elements that most significantly affected the irradiation embrittlement process. However, the accuracy and reliability of the empirical techniques used to evaluate the irradiation damage to vessel materials were poor. In 1973, the NRC implemented 10 CFR 50, Appendix G, "Fracture Toughness Requirements" and 10 CFR 50 Appendix H, "Reactor Vessel Material Surveillance Program Requirements" to improve the quality of predictions of irradiation damage by relying on the theoretical concepts of fracture mechanics rather than on empirical techniques.

### **2.2 Dosimetry Improvement 1977 - 1992**

When Charpy specimens from the surveillance programs in operating reactors began to be available in sufficient quantity, correlations of the data resulted in large uncertainties in the predictions of embrittlement ( $\Delta RT_{NDT}$ ). The uncertainties in the correlated predictions were due in part to the uncertainties in the predictions of the integral of the neutron fluence ( $\phi t$ ) over time, where  $\phi$  is the neutron flux with an energy greater than 1.0 MeV and  $t$  is the total time of neutron irradiation. FTI recognized that the industry needed an accurate and consistent methodology for predicting Charpy specimen fluences. Therefore, in concert with the "Light Water Reactor Pressure Vessel Surveillance Dosimetry Improvement Program" that the NRC initiated in 1977 to improve dosimetry measurement predictions, FTI developed the most technologically advanced methods for performing dosimetry measurements and fluence analyses. The accuracy and consistency of the FTI methods were independently confirmed by R.L. Simons, E.P. Lippincott, et alia, from the Westinghouse Hanford Company.<sup>15</sup>

**Framatome Technologies Inc.**

Table 2-1 shows the standard deviations in the adjustments that Simons made to have the industry predictions of capsule fluence values be consistent.

Table 2-1

Standard Deviations In The Fluence Adjustments<sup>15</sup> For Reg. Guide 1.99, Rev. 2

<u>Capsule</u>	<u>Standard Deviation (%)</u>
Westinghouse	29.7
CE	24.2
B & W	5.6

Clearly, the FTI methodology produced very precise fluence predictions. The precision in the FTI results, and Simons' adjustment of the other capsule fluences, provided fracture mechanics analysts with the means of analyzing reactor vessel materials to ensure (1) sufficient margin for nonbrittle behavior, and (2) minimal probability of a rapidly propagating fracture.<sup>17</sup> The FTI fluence analysis methodology has satisfied the basic requirements of 10 CFR 50, Appendices G and H, with respect to vessel material test specimens. However, the NRC and some industry experts have expressed reservations about the fluence methodologies used by various analysts in the industry.

The reservations have focused on the requirements for vessel evaluations rather than specimen evaluations. The basic vessel uncertainty requirements are defined by the Pressurized Thermal Shock (PTS) Safety Analyses.<sup>3, 4, 5</sup> The PTS Safety Analyses are based on probabilistic evaluations of overcooling transients. The results of these analyses are defined in terms of a 95 percent probability that the mean frequency of PTS events causing vessels to crack is within 10 percent of  $5 \times 10^{-6}$  per reactor year, if  $RT_{PTS}$  is not

## **FTI Non-Proprietary**

greater than the 10 CFR 50.61<sup>6</sup> screening criteria. The fluence uncertainty associated with the safety analyses is assumed to be that estimated by Simons<sup>15</sup> for the embrittlement to fluence correlation.<sup>16,17</sup> The root mean square standard deviation of Simons measured fluences is 21 percent. The NRC has defined acceptable values of the fluence uncertainty to be 20 percent<sup>8</sup> or less to maintain consistency with the PTS screening criteria<sup>6</sup> and the Regulatory Guide 1.99, Revision 2 embrittlement correlation.<sup>17</sup>

Reviewing Table 2-1 clearly shows why the NRC and some industry experts have expressed reservations about the fluence uncertainty. Fluence predictions for Westinghouse and CE capsules have adjustments with standard deviations that are larger than the acceptable uncertainty. For Westinghouse capsules, more than 55 percent of the original fluence predictions required a greater than 20 percent adjustment to be consistent with the industry. While the NRC's acceptable uncertainty for the industry may be no more than 20 percent, the average value in Table 2-1 is clearly lowered by the FTI results. If embrittlement correlations for safety analysis are based on a 20 percent standard deviation, there is clearly a concern that industry analyses of Westinghouse and CE capsules are not within the 20 percent criteria. However, the B & W standard deviation of 5.6 percent indicates that the FTI fluence predictions are very accurate, and much smaller than the 20 percent criterion.

As noted above, the accuracy and reliability of the FTI fluence methodology was established in concert with the NRC's "LWR Pressure Vessel Surveillance Dosimetry Improvement Program." When this program was initiated in 1977, the NRC needed to know the uncertainties in the capsule fluence predictions in order to develop an industry embrittlement correlation suitable for safety analyses. With the limited data available, FTI found that the only uncertainties that could be estimated with any confidence were bounding values. Therefore, FTI provided the NRC and its contractors with capsule

## **FTI Non-Proprietary**

specimen embrittlement data, fluence predictions, and the bounding capsule fluence uncertainties derived from measured dosimetry activities and response functions. The bounding uncertainty value for the capsule measurements is 15 percent as shown in Reference 12. The bounding values of the fluence uncertainties subsequently became the FTI standard set. This set was accepted by the NRC as referenced in the "Integrated Reactor Vessel Material Surveillance Program".<sup>10</sup>

### **2.3 Licensing Basis 1977 - Present (1997)**

The NRC Safety Evaluation of the integrated surveillance program states:<sup>10</sup>

*Uncertainties in neutron fluence estimates were discussed by the staff in its review of the B & W owners group request for exemptions to the requirements of Appendix H, 10 CFR 50. The dosimetry methodology and vessel fluence analysis have been reviewed and accepted by the staff in a memorandum dated December 5, 1984 from L.S. Rubenstein to W.V. Johnston, "Review of Response to the Request for Additional Information on Capsule RSI-B for Rancho Seco, Reported in BAW-1702.*

*In the staff's review of BAW-1702 it was reported that this methodology resulted in a maximum uncertainty in end-of-life vessel fluence of 34 percent. This uncertainty may be reduced for vessels not containing in-vessel dosimetry by inclusion of dosimetry devices in the reactor cavity. The B & W Owners Group has indicated that they have begun testing of these types of dosimeter devices. However, until these devices are installed, plants without dosimetry in the reactor vessel will have to rely on the methods of neutron fluence analysis documented in BAW 1702.*

**Framatome Technologies Inc.**

The NRC Evaluation of BAW-1702 provided the following table:<sup>11</sup>

Table 2-2

FLUENCE CALCULATION UNCERTAINTY

<u>Calculation</u>	<u>Uncertainty %</u>	
	<u>Without Capsule Rotation</u>	<u>With Capsule Rotation</u>
<i>Capsule (derived from measured activity)</i>	$\pm 14$	$\pm 15$
<i>Pressure vessel (maximum location for capsule irradiation time interval)</i>	$\pm 20$	$\pm 21$
<i>Pressure vessel (maximum location, long term extrapolation)</i>	$\pm 22$	$\pm 23$
<i>Pressure vessel welds</i>	$\pm 33$	$\pm 34$

**CONCLUSION**

*We have reviewed the Sacramento Municipal Utility District response dated September 27, 1984 regarding Rancho Seco surveillance capsule dosimetry. Due to the capsule rotation the computational uncertainty of the flux as applied to the maximum location of the pressure weld should be increased by a small amount i.e., from  $\pm 33.0\%$  to  $\pm 34.0\%$ .*

## **FTI Non-Proprietary**

FTI's standard uncertainties in Table 2-2 are based on bounding values that were first documented in 1978.<sup>12</sup> Since 1978, the NRC and its contractors have performed (1) a least squares adjustment of the capsule fluence values to obtain an industry consistent set,<sup>15</sup> (2) a least squares correlation of capsule embrittlement measurements to the industry consistent capsule fluence values,<sup>16</sup> and (3) generic pressurized thermal shock (PTS) safety analysis of Westinghouse,<sup>5</sup> CE,<sup>4</sup> and B & W<sup>3</sup> reactors using probabilistic fracture mechanics analyses of the effects of rapid overcooling transients. In each of the three analyses performed for the NRC (fluence adjustments, embrittlement correlations and generic safety analyses), fluence uncertainties were estimated and appropriately treated. However, the uncertainties were not estimated in terms of bounding values, but rather as standard deviations. Therefore, there is a confidence factor difference between the bounding FTI standard fluence uncertainties and the value that the NRC assumed for PTS evaluations and coolant system pressure - temperature embrittlement evaluations.

A confidence factor with a value of 2.0 is used in the PTS safety analysis. This confidence factor provides a 95 percent probability that the risk of vessel failure due to PTS events is acceptable for any plant as long as the value of  $RT_{PTS}$  is below the PTS screening criteria.<sup>6</sup> A confidence factor of 2 is also used in the Regulatory Guide 1.99<sup>17</sup> "Margin" term. Therefore, the bounding fluence uncertainties that are consistent with the PTS screening criteria,<sup>6</sup> Regulatory Guide 1.99<sup>17</sup>, and the FTI standard set, would be less than or equal to 40 percent. This is the value that is assumed for NRC evaluations and approval of the FTI set of standard uncertainties in Table 2-2.

### **2.3.1 Reference Fluence Methodology**

Prior to 1973, the FTI fluence methodology was based on one-dimensional diffusion theory for spatial neutron transport with multigroup removal cross sections corrected for anisotropic effects.<sup>14</sup> By 1973, when the NRC added Appendices G and H to the Federal Register (10 CFR 50), FTI had expanded their analytical capabilities by adding the ANISN and DOT computer codes to the fluence methodology.<sup>13</sup> The cross section library had also been updated to the CASK data set.<sup>18</sup> This data provided anisotropic scattering cross sections with a  $P_3$  Legendre expansion of the energy - angular variables.

The analysis of capsule dosimetry and the predictions of material specimen fluences began in 1976. At that time, the "Reference Fluence Methodology" included DOT - II W, with radial ( $r$ ) and theta ( $\theta$ ) coordinates modeling the radial plane of the reactor,  $S_6$  quadrature for the angular flux expansion, and CASK cross sections with a  $P_1$  expansion of the angular scattering. The  $P_1$  DOT results were modified by the ratio of  $P_3$  to  $P_1$  ANISN results. The source of neutrons was represented by a two-dimensional distribution of fission rates in each fuel pin integrated over the appropriate operational period with a U-235 fission spectrum. The synthesis of the  $r, \theta$  DOT results to three - dimensions ( $r, \theta, z$ ) was accomplished with the results from a three-dimensional nodal diffusion theory computer code that explicitly modeled the peripheral fuel assemblies throughout the operational period. The normalized shape of the fission power in the axial ( $z$ ) direction provided the functional distribution of the time-averaged flux from the core periphery to the vessel.

The capsule analysis utilized cell theory to treat the geometrical modeling in an independent DOT calculation of an azimuthal segment with rectangular coordinates. The time-averaged flux spectrum for the dosimetry and material specimens was found to be

## **FTI Non-Proprietary**

sufficiently representative of the spectrum at the center of the capsule. Therefore, comparisons of measured dosimeter activities to calculated activities were based on integrated averages at the center of the capsule. The integration of time dependent functions, such as fission rates, and isotopic production and decay, included the appropriate dependencies such that comparisons of measurements and calculations were functionally equivalent in time.

This model is described in the Reference 12 topical report. It was the basis for the capsule fluences using appropriate weighting of the dosimetry measurements. The uncertainties in the measured activities were determined to be unbiased, but in attempting to define the standard deviation, there were too few independent capsule measurements (only six) to confirm that the distribution in the deviations was sufficiently normal. Therefore, bounding values of the uncertainties were estimated. The bounding values,<sup>12</sup> and those in Table 2-2 are essentially the same.

The comparisons of calculated activities to measured values averaged less than 10 percent in the energy range around 1.0 MeV. With the bounding uncertainty in the measured activities being estimated as 15 percent or less, it was not possible to identify any separate biases in the calculations. Therefore, the calculated and measured fluences with an energy greater than 1.0 MeV at the capsule were the same values. The capsule fluences were defined as measured values for application to embrittlement analyses. The bounding uncertainty (2 standard deviations) in the capsule fluences was estimated as the statistically combined uncertainties for the measured activities (15 percent) and the activation cross sections (11 percent). Thus, the "measured" fluence at the capsule, with energies greater than 1.0 MeV, was defined to have an uncertainty of 19 percent or less.

**Framatome Technologies Inc.**



## FTI Non-Proprietary

The vessel fluence was determined using a modification to the DOT calculational methodology just described. The modification utilized a cylindrical  $(r, z)$  geometrical model with the appropriate source of neutrons from the three - dimensional fission rates. The cylindrical coordinates provided a symmetrical three - dimensional model of the vessel beltline region. Asymmetries in the fission source distribution and core former region were evaluated from the planar  $(r, \theta)$  DOT results. Since the capsule calculations of the dosimetry indicated agreement between the calculations and measurements within the measurement uncertainty, the vessel fluences were defined as measured values with combined measurement and analytical uncertainties.

### 2.3.2 Methodology Validation

In 1977, when the NRC established their "Light Water Reactor Pressure Vessel Surveillance Dosimetry Improvement Program", one part of this program was to test the industry to evaluate the overall bias and uncertainty in the fluence predictions. To ensure that the evaluation actually represented the bias and uncertainty from each participant, the test was developed to be a "blind test". This meant that the participants would not know the measurement results before everyone had submitted their calculational results. The Pool Critical Assembly (PCA) blind test was supervised by the Oak Ridge National Laboratory (ORNL).<sup>37</sup> FTI and the other industry participants modeled the PCA reactor and predicted dosimetry activations in the vessel and internals structure. FTI submitted their calculations to ORNL, and ORNL compared FTI's calculations ( $C$ ) to their measurements ( $M$ ) and sent FTI the  $C/M$  results along with the assessment of their measurement uncertainty. The  $C/M$  results indicated a mean deviation of 6.7 percent. The ORNL measurement uncertainty was between 6.0 percent and 10.0 percent. These uncertainty results were the best of all participants, including Oak Ridge and the Brookhaven National Laboratory, who already knew the measured results.<sup>37</sup>

## **FTI Non-Proprietary**

Since 1976, there have been six revisions, or modifications, to update the fluence methodology. This topical report describes the fifth and sixth revisions in detail. Sections 2.3.3 through 2.3.6 briefly outline the first two revisions and the first two modifications. The four previous methodologies are:

- 1) Semi - Empirical
- 2) Semi - Empirical BUGLE-80
- 3) Measurement - Based
- 4) Hand - Adjoint

The fifth and sixth updated methodologies are:

- 5) Semi - Analytical BUGLE-80
- 6) Semi - Analytical BUGLE-93

Only the Reference (Section 2.3.1, page 2 - 8), Semi - Empirical and Semi - Empirical BUGLE-80 methodologies are consistent with the uncertainties reviewed in this topical and described in Table 2-2.

### **2.3.3 Semi - Empirical**

The methods, procedures, and computer modeling that comprise the Semi - Empirical methodology are described in Reference 9. This methodology was completed by 1980 and was used for the PCA blind test calculations. The significant differences from the "Reference Methodology" are: (1) updates of the DOT code, (2)  $P_3$  scattering and an  $S_8$  quadrature directly in the DOT model, (3) corrections for short half-lives, photofissions and fissile impurities associated with the dosimetry comparisons, (4) the synthesis of the vessel beltline fluence used the axial distribution of the three-dimensional fission rate, (5) the combination of activities to determine the greater than 1.0 MeV measured fluence applied equal weighting to the U-238, Np-237, Ni-58 and Fe-54

dosimeters, and (6) the  $M/C$  ratio of activities for the four dosimeters responding above 1.0 MeV provided a normalization to convert calculated fluences to measured ones. The  $M/C$  normalization was applied to calculated capsule fluences to represent measured fluences even though the  $C/M$  ratios never indicated a bias in the calculations. The  $M/C$  ratios were only applied to predictions of vessel fluences if the ratio was greater than one (1.0). This methodology was used until 1990 when it was phased out and replaced by the Semi - Empirical BUGLE-80 methodology.

#### **2.3.4 Measurement - Based**

In 1983, the Semi - Empirical methodology was simplified and reduced to the Measurement - Based methodology. The development of the Measurement - Based methodology involved averaging the calculational results from the Semi - Empirical methodology and treating them as constants. The two key constants were the dosimeter activation response functions and the vessel lead factors. The lead factors represented the ratio of the greater than 1.0 MeV flux at the capsule to the vessel flux at weld and other important locations.<sup>9</sup> If the spectral and spatial distribution of the neutrons from the fission source remained constant, then this methodology would be equivalent to the Semi - Empirical and notably simpler. However, the (reactor) core fuel management changed dramatically in the ensuing years to the Framatome Cogema Fuel Company's invention of the low leakage fuel loading scheme. Consequently, the spectral and spatial distribution of the neutrons changed significantly and the uncertainties in the results of the Measurement - Based methodology were unknown. In Reference 9, an estimate of 50 percent uncertainty was judged to be appropriate.

This methodology was discontinued in 1986 after the analyses of six capsules. These capsules are not included in the fluence uncertainty database.

### 2.3.5 Semi - Empirical BUGLE-80

By 1990, the calculations of the B & W Owners Group Cavity Dosimetry Benchmark Program had begun. The program incorporated two calculational analyses of the dosimetry. The two calculational methods, procedures, and computer models were identical with the exception that one analysis used the CASK library<sup>18</sup> and the other used the BUGLE-80 library<sup>2</sup>. The results of the *C/M* benchmark comparisons for the capsules indicated that no independent bias could be determined with BUGLE-80 and that the standard deviation in the BUGLE-80 calculations was equivalent to the standard deviation in the CASK calculations.

The results of *C/M* benchmark comparisons for the cavity dosimetry indicated that the BUGLE-80 library resulted in a large bias in the calculations. However, since the capsule calculations had no bias and had a standard deviation comparable to previous results, the Semi - Empirical BUGLE-80 methodology was used for fluence predictions of capsules and the vessel inside surface. The uncertainties were within FTI's standard set of values in Table 2-2.

### 2.3.6 Hand - Adjoint

In 1990, the B & W Owners Group had FTI develop the Hand - Adjoint methodology for predicting changes in the fluence due to fuel management changes. This methodology was designed to quickly update the predicted reactor vessel fluence at the end of life (EOL) whenever a new fuel cycle design was implemented that differed from the reference design used to predict the fluences at EOL. The methodology is based on using adjoint calculations with the Semi - Empirical (CASK) methodology to define constant factors that relate peripheral assembly fission rates to specific vessel locations. The methodology has no defined uncertainty because it is not intended for predicting the

fluence. The methodology simply provides a means of estimating the effect of fuel management changes on vessel fluence. Since the Hand-Adjoint methodology is not intended for fluence predictions, no benchmark comparisons of calculations to measurements in the FTI database utilize this methodology.

## **2.4 NRC Issues**

The five improvements to the fifth and sixth FTI fluence methodologies and associated uncertainties (page 1 - 1) that are presented in this topical report address the following outstanding issues that FTI and the NRC have discussed since 1985:

- 1) Vessel Surveillance
- 2) Measurement Uncertainties
- 3) Calculated Fluences
- 4) Update of Benchmarks

There is a fifth outstanding issue concerning additional uncertainty evaluations discussed in Draft Regulatory Guide DG-1053.<sup>19</sup> As noted previously, FTI and the B & W Owners view most of the provisions in the draft as improvements to plant safety. Therefore, the intention is to incorporate these provisions into the fluence and fluence uncertainty methodologies. However, because the draft is in the review process, and this topical report needs to address the B & W Owners update of their pressure - temperature limits for heat-up and cool-down, this report does not address the additional draft regulatory guide uncertainty evaluations. The four NRC issues are briefly reviewed in the following subsections.

### **2.4.1 Vessel Surveillance**

In 1976, several owners of B & W reactors found that the surveillance capsule holder tubes had been damaged during operation. The damage necessitated the removal of the

holder tubes. While replacement of the holder tubes was an option, it was a poor one in comparison with the Integrated Reactor Vessel Material Surveillance Program.<sup>10</sup> The integrated program utilized similar reactors with holder tubes to irradiate vessel material specimens from reactors without them. In addition, the NRC granted the reactors without holder tubes an exemption from Appendix H requirements for a period of five years. During this period, a cavity dosimetry program was developed with vessel monitoring conducted by calculational evaluations.

The Cavity Dosimetry Program was presented to the NRC in a topical report in 1986.<sup>20</sup> By 1990, all B & W Owners had installed dosimeters in the cavities of their reactors. While these dosimeters cannot provide an active role in surveillance (because the fluxes that reach the cavity have different spectra and lower levels than the key locations at the surface and one-quarter thickness of the vessel), these dosimeters provide results for benchmarking the calculations. Calculational evaluations of vessel fluences continue to provide the monitoring required for vessel surveillance. Periodic vessel surveillance updates include benchmarks to dosimetry to verify that the accuracy and uncertainty in the calculations continues to be within the reference values noted in Section 7.0 .

The vessel surveillance program, to ensure appropriate monitoring for extrapolated projections of the fluence for the reactor coolant system pressure - temperature curves and the end of life PTS criteria, is not addressed in this topical.

#### **2.4.2 Measurement Uncertainties**

When FTI provided the NRC with the topical report describing the "Integrated Reactor Vessel Material Surveillance Program" in 1985,<sup>10</sup> uncertainties in the neutron fluence estimates were discussed with the staff. The NRC approved the values provided in Table 2-2. However, in 1988, when FTI submitted Revision 1 of the topical , "Pressure

## **FTI Non-Proprietary**

Vessel Fluence Analysis for 177-FA Reactors",<sup>9</sup> the NRC questioned the measured fluence uncertainties. The documentation referencing the laboratory uncertainties could not be independently verified. Therefore, the NRC's question concerning the measured fluence uncertainties remained an open issue even though the uncertainty values noted in Table 2-2 remained as the basis for safety and licensing analyses using FTI fluence predictions.

The B & W Owners Group Cavity Dosimetry Program included a reevaluation of the measurement uncertainties (Section 7.1). Not only was each step of the experimental process reviewed to estimate the uncertainties in the equipment and procedures, but each step was independently reviewed by W. N. (Bill) McElroy and R. (Ray) Gold as noted in their "Written Comments and Recommendations Related to the Review of the B&WOG (B & W Owners Group) Davis-Besse Cavity Dosimetry Benchmark Program".<sup>21</sup> The Quality Assurance verification of the experimental methodology and the independent review by the consultants indicated that the values in Table 2-2 are greater than the measurement standard deviation by a confidence factor of 2.0. This implies that there is a 95 percent probability that the measurement uncertainties in Table 2-2 bound the uncertainties for any plant specific evaluation.

### **2.4.3 Calculated Fluences**

In February of 1993, the NRC had a meeting with industry representatives. At the meeting, the NRC explained that various experts have expressed concerns that the uncertainty in the fluence predictions may be inconsistent with the Pressurized Thermal Shock (PTS) Safety Analyses.<sup>22</sup> By September of 1993, the NRC had released Draft Regulatory Guide DG-1025 which explained that the current technology for determining reactor vessel fluences based on dosimetry measurements needed updating. A key feature of the draft guide is that vessel fluence predictions must be based on calculations. Extrapolations of measured fluences are not acceptable.

## **FTI Non-Proprietary**

FTI evaluated the fluence treatment in the generic PTS Safety Analyses<sup>22</sup> and found that the probabilistic analyses of overcooling transients, embrittlement uncertainties, and fluence uncertainties are a concern with respect to measurement based fluence predictions. The concern is that the PTS analyses are based on a 95 percent probability that the mean frequency for through-wall crack penetration is less than  $5 \times 10^{-6}$  per reactor year. Consequently, the measured vessel fluences must have an uncertainty that is consistent with the 95 percent probability. However, there are no vessel fluence measurements. Without such data, it is difficult to ensure that the "measured" vessel fluences are within 95 percent tolerance limits of the true predictions. Therefore, it is also difficult to ensure that vessel embrittlement predictions are consistent with the PTS Safety Analyses.

To enhance the safety of vessel embrittlement evaluations, FTI is changing the fluence methodology from the Semi - Empirical measurement based technology to the Semi - Analytical calculational based technology. As discussed in Section 2.3.3, the Semi - Empirical methodology has no bias between the calculations and measurements, therefore the calculated fluence with energies greater than 1.0 MeV equaled the measured fluence. The calculated fluences for each plant specific analysis were normalized to the measurements. The measured fluence uncertainties could thereby be estimated in terms of the uncertainties in the experimental methodology and the uncertainties in the dosimeter response functions.

The change from the Semi - Empirical, measurement based methodology to the Semi - Analytical, calculational based methodology is the principal topic described in this report. The effects on previous capsule and vessel fluence predictions are negligible in terms of any net bias (although some vessel fluence values may be too high). The effects on embrittlement correlations should be examined. The principle effects will be in the uncertainty methodology to estimate the standard deviation in the calculated fluence. The

**Framatome Technologies Inc.**



uncertainty methodology will be different from that previously used to estimate the bounding values in Table 2-2 (see Section 7.0).

#### **2.4.4 Update of Benchmarks**

When FTI submitted Revision 1 of the "Pressure Vessel Fluence Analysis for 177-FA Reactors" topical report to the NRC in 1988, the NRC wanted to see the entire database of capsule dosimetry to verify the uncertainty in the calculational benchmark to measurements. Because the topical never resolved the issue of measurement uncertainties, the entire database was never sent to the NRC. Again in 1995, the NRC was reviewing FTI fluence uncertainties associated with embrittlement predictions of Entergy Operations' Waterford reactor vessel and wanted to review the entire database. However, when Entergy reduced the period for their pressure - temperature technical specification limits for heat-up and cool-down from 20 effective full power years to 15, the NRC dropped their request for the database.

This topical report contains an update of the entire FTI database of capsule and cavity dosimetry measurements and calculations as shown in Table A-1. The capsule and cavity *C/M* benchmark results are summarized in Table A-2.

**3.0 Semi - Analytical (Calculational) Methodology**

**3.1 DOT Transport Calculations**

**Figure 3-1**

**Global Outline**

**3.1.1 Geometric Models**

**3.1.1.1  $r, \theta$  Modeling**

**Figure 3-2**  
**R - Theta DOT**

**FTI Non-Proprietary**



**FTI Non-Proprietary**

**3.1.1.2  $r,z$  Modeling**

**Figure 3-3**  
**R - Z DOT**

**3.1.2 Distributed Source**

**(3.1)**

(3.2)

**3.1.3 Cross Section Sets**

**3.1.4 Execution of DOT Runs**

**3.2 DOT**



**Figure 3-4**

**FTI Non-Proprietary**

**Figure 3-5**

**Figure 3-6**

**Figure 3-7**

**Figure 3-8**

**Figure 3-9**

1. Holders A and R are located near the seal plate.
2. Holders B and C are located near the outlet nozzle level.
3. Holders D and E are located near the top of the active fuel.
4. Holders F, G, H, N, P, and Q are located near the midplane.



**3.3 Calculated Dosimeter Response**

**3.3.1 Three - Dimensional Synthesis of Results**

Three - dimensional discrete ordinates (TORT) calculations of the vessel flux have not been shown to have sufficient accuracy, and neither have three - dimensional Monte Carlo calculations. The most accurate three - dimensional method is the synthesis of two, two - dimensional DOT calculations. The macroscopic cross sections and fission sources can be appropriately weighted for the reactor core and adjacent reflector regions. Beyond these regions, the reactor internals, vessel and support structure are sufficiently cylindrical for an  $r, z$  cylindrical model to provide very accurate results.

$\phi_g^{3D}(r, \theta, z)$  is the three - dimensional flux in energy group  $g$  at the spatial point defined by its cylindrical coordinates,  $r$ ,  $\theta$ , and  $z$ .

(3.3)

$$\phi_g^{3D}(r, \theta, z) = H_g(r, z) \phi_g^{R\theta}(r, \theta, z = \bar{z}) \quad (3.4)$$

(3.5)

and

(3.6)

These equations can be combined as follows:

(3.7)

(3.8)

Rearranging the terms:

(3.9)

(3.10)

where

(3.11)

(3.12)

$$\frac{1}{H} \int_H \phi_g^{3D}(r, \theta, z) dz = \phi_g^{R\theta}(r, \theta, z = \bar{z}) \quad (3.13)$$

(3.14)

(3.15)

(3.16)

A special computer program has been developed to read the DOT output files and process the two - dimensional fluxes into three - dimensional fluxes.

### 3.3.2 Fraction of Saturation

The modeling of the dosimeter response functions in the DOT input, results in calculations of saturated specific activities. The measured specific activities, on the other hand, correspond to the specific activities that built up in each dosimeter over the actual irradiation history. In order to have meaningful comparisons of measurements to calculations, the calculated results must be corrected by a power - history dependent factor, called the fraction of saturation,  $S_d$ , which is given by Equation 3.17.

$$S_d = \sum_j F_j \left[ 1 - e^{-\lambda_d t_j} \right] e^{-\lambda_d (T - \tau_j)} \quad (3.17)$$

where:

- $S_d$  is the fraction of saturation for dosimeter type "d" at shutdown.
- $F_j$  is the fraction of full power during the  $j$ 'th time interval.
- $\lambda_d$  is the decay constant for product isotope of dosimeter "d",  $\text{sec}^{-1}$ .
- $t_j$  is the time interval for irradiation period "j", sec.
- $T$  is the total calendar time from startup to shutdown, sec.
- $\tau_j$  is the time interval from startup to end of  $j$ 'th irradiation period.

Application of this factor to the appropriate DOT calculations of each dosimeter, results in a specific activity that corresponds to the dosimeter activity at shutdown. Since the measured activities are all adjusted from the time of counting to the time of shutdown, the two specific activities, measured and calculated, represent the same quantity, and are therefore directly comparable.

### **3.3.3 Calculated Dosimeter Activities**

The calculations ( $C$ ) of the dosimeter activities using the DOT results and the fraction of saturation (Equation 3.17) are expressed by Equation 3.18. These calculated activities are directly comparable with measurements.

(3.18)

where:



The response functions  $R_{d,g}$  are simply obtained from the cross-sections:

$$R_{d,g} = B_d \sigma_{d,g} \quad (3.19)$$

where  $B_d$  is constant for a specific dosimeter type, and  $\sigma_{d,g}$  is the microscopic cross section for the reaction of dosimeter  $d$  in energy group  $g$ . A computer program has been developed to calculate  $R_{d,g}$  for all dosimeter types at all spatial locations.

#### **4.0 General Arrangement of Experiment**

The Cavity Dosimetry Benchmark Experiment, also known as the In-Out Experiment, was a full-scale test conducted in the Davis-Besse Unit 1 B & W - designed 177 fuel assembly reactor, using both in-vessel and out-of-vessel dosimetry measurements. The measurements consisted of more than 650 dosimeters. Of these 650 dosimeters, most were radiometric monitors (RMs), 499. The RMs consisted of 243 activation foils, wires - et cetera, 47 fission foils - et cetera, and 209 flux mapping stainless steel chain segments - et cetera. In addition, there were 76 SSTRs (solid state track recorders), 22 ultra-high purity niobium dosimeters, and 44 HAFMS (helium accumulation fluence monitors) evenly split between beryllium and lithium. There were also 9 LiF (lithium fluoride) detector chips. The LiF chips are gamma fluence detectors and were specially developed by the National Institute of Standards and Technology (NIST) for this specific application. They provide accurate results at the high - gamma fluence exposure levels expected in the experiment. The dosimetry described above was provided by six program contributors - the B & W Owners Group; Hanford Engineering Development Laboratory (HEDL); Center for the Study of Nuclear Energy, Mol, Belgium (CEN/SCK); NIST; Rockwell International; and the Arkansas Technical University.

The in-vessel dosimetry consisted of two standard unirradiated TMI-2 surveillance capsules installed in the surveillance capsule holder tube at the peak flux (11°) location. (Throughout this document, unless otherwise stated, azimuthal positions are referenced to one of the four "major axes.") These capsules contained six standard B & W RM dosimeter sets covering incident neutron threshold energies from 0.5 eV to 2.5 MeV.

The cavity dosimetry consisted of sixteen specially fabricated aluminum dosimetry holders, each containing five sets of dosimeters. A detailed sketch of the cavity dosimetry holder is given in Figure 4-1, showing the numerical designation for each position of the canisters containing a set of dosimeters. Cable assemblies containing these holders were then designed in a manner that allowed for accurately known measurements of the dosimeter locations, maintaining the dosimetry in a known direction either facing towards or away from the core, and each installation and removal. Five cable assemblies containing the dosimeter holders at various axial positions were installed in the cavity at specific azimuthal positions. The azimuthal locations were chosen to avoid possible areas of large flux gradients, which are difficult to predict analytically. Figure 4-2 shows the general arrangement of the cavity dosimetry holders. The assemblies at 6°, 11°, and 11.5° were located in the region of maximum flux, while the holder at 42.5° was in the minimum flux region. Table 4-1 details the dosimetry loaded in the holders by canister position. Note that dosimeters loaded in positions 1 and 2 were placed in aluminum cans and are unshielded, while dosimeters loaded in positions 3, 4, and 5 were placed in gadolinium<sup>25</sup> cans to shield them from the thermal flux.

Four 50 ft-long beaded stainless steel chains were also placed in the cavity region to achieve accurate axial flux profiles at the azimuthal positions of interest. The chain assemblies were mounted beneath Nuclear Instrumentation boxes in four of the open source check tube penetrations, one in each quadrant of the cavity. The chains were anchored with a heavy weight at the containment floor to limit lateral movement during plant operation. An additional 35 ft-long University of Arkansas stainless steel chain was suspended from the 11° train.

All 80 sets of dosimetry, stainless steel chains, and surveillance capsules were installed for one cycle of operation in the Davis-Besse Unit 1 plant and removed at the completion of Cycle 6 in February 1990. The coordinate location dimensions of the cavity dosimetry holders are listed in Table 4-2, with the reference coordinate system presented in Figure 4-3. A plan view, Figure 4-4, is included showing the relative positions of the temporary cavity dosimetry assemblies, the permanent cavity dosimetry holder, the stainless steel chains, and the in-vessel standard surveillance capsules.

Table 4-1 Loading Plan of Cavity Dosimetry Holders

Holder and Location	Unshielded Positions 1, 2 (Aluminum Cases)	Shielded Positions 3, 4, 5 (Gadolinium Cases)
<p style="text-align: center;">A</p> <p>11.5° Seal Plate Elevation</p>	<p>1 - B&amp;W RMs Fe Co</p> <p>2 - B&amp;W RMs Fe Co</p>	<p>3 - LiF</p> <p>4 - B&amp;W RMs Fe Co HAFM 3 Be Li</p> <p>5 - B&amp;W RMs Fe Ni 3 Cu Co</p>
<p style="text-align: center;">B</p> <p>11.5° Nozzle Elevation</p>	<p>1 - HEDL RM</p> <p>2 - B&amp;W RMs Fe Co</p> <p>B&amp;W SSTR (2B)</p>	<p>3 - LiF</p> <p>4 - HEDL RM HEDL SSTR (23H)</p> <p>5 - B&amp;W SSTR (2C2) B&amp;W RMs Fe Ni 2 Cu Co</p>

Table 4-1 Loading Plan of Cavity Dosimetry Holders (Cont'd)

Holder and Location	Unshielded Positions 1, 2 (Aluminum Cases)	Shielded Positions 3, 4, 5 (Gadolinium Cases)
<p style="text-align: center;">C</p> <p>11.5° Nozzle Elevation</p>	<p>1 - B&amp;W RMs Fe Co</p> <p>2 - B&amp;W RMs Fe Co</p>	<p>3 - SS Chain #1</p> <p>4 - B&amp;W RMs Fe Ni 2 Cu Co Nb (ToyoSoda) HAFM 3 Be Li</p>
<p style="text-align: center;">D</p> <p>11.5° Upper Active Fuel Elevation</p>	<p>1 - HEDL RM</p> <p>2 - B&amp;W RMs Fe Co B&amp;W SSTR (EB)</p>	<p>3 - LiF</p> <p>4 - B&amp;W RMs Fe Ni Cu Co</p> <p>5 - B&amp;W SSTRs (3C, B&amp;W-17) HEDL SSTR (Z2H) HEDL RM</p>

Table 4-1 Loading Plan of Cavity Dosimetry Holders (Cont'd)

Holder and Location	Unshielded Positions 1, 2 (Aluminum Cases)	Shielded Positions 3, 4, 5 (Gadolinium Cases)
<p style="text-align: center;"><b>E</b></p> <p>11.5° Upper Active Fuel Elevation</p>	<p>1 - B&amp;W RMs Fe Co</p> <p>2 - SS Chain #2</p>	<p>3 - SS Chain #3</p> <p>4 - B&amp;W RMs Fe Co Nb HAFM 3 Be 1 Li</p> <p>5 - B&amp;W RMs</p>
<p style="text-align: center;"><b>F</b></p> <p>11.5° Core Midplane Evaluation</p>	<p>1 - B&amp;W RMs Fe Co PUD</p> <p>2 - B&amp;W SSTR (4B) HEDL SSTR (A2H)</p>	<p>3 - B&amp;W RMs Fe Ni Cu Co Nb (ToyoSoda) HAFM 3 Be Li Nb (MOL)</p> <p>4 - B&amp;W SSTRs (4C, B&amp;W-18) HEDL SSTR (A2H)</p> <p>5 - MOL RM</p>

Table 4-1 Loading Plan of Cavity Dosimetry Holders (Cont'd)

Holder and Location	Unshielded Positions 1, 2 (Aluminum Cases)	Shielded Positions 3, 4, 5 (Gadolinium Cases)
<p style="text-align: center;"><b>G</b></p> <p>11.5° Core Midplane Elevation</p>	<p>1 - HEDL RM PUD</p> <p>2 - B&amp;W RMs Fe Co Co-Al Wire Fe Wire PUD</p>	<p>3 - LiF</p> <p>4 - LiF</p> <p>5 - HEDL RM B&amp;W RMs Ni Wire Co-Al Wire Np-Al Wire U-Al Wire</p>
<p style="text-align: center;"><b>H</b></p> <p>42.5° Core Midplane Elevation</p>	<p>1 - B&amp;W RMs Fe Co</p> <p>2 - SS Chain #4</p>	<p>3 - LiF</p> <p>4 - B&amp;W RMs Fe Co Nb (ToyoSoda) HAFM 3 Be Li</p> <p>5 - SS Chain #5 U-238 Powder Np-237 Powder</p>
<p style="text-align: center;">No I Holder</p>		



Table 4-1 Loading Plan of Cavity Dosimetry Holders (Cont'd)

Holder and Location	Unshielded Positions 1, 2 (Aluminum Cases)	Shielded Positions 3, 4, 5 (Gadolinium Cases)
<p style="text-align: center;">J</p> <p>11.0° Core Midplane Elevation</p>	<p>1 - B&amp;W RMs Fe Co Co-Al Wire Fe Wire</p> <p>2 - SS Chain #6</p>	<p>3 - B&amp;W RMs Fe Co Nb (ToyoSoda) Nb (MOL) HAFM 3 Be Li</p> <p>4 - B&amp;W RMs Fe Co</p> <p>5 - Co-Al Wire Ni Wire Np-Al Wire U-AL Wire</p>
<p style="text-align: center;">K</p> <p>11.0° Core Midplane Elevation</p>	<p>1 - U of A RM</p> <p>2 - B&amp;W RMs Fe Co SS Chain #7</p>	<p>3 - U of A RM</p> <p>4 - U of A RM</p> <p>5 - B&amp;W RMs Fe Co</p>

Table 4-1 Loading Plan of Cavity Dosimetry Holders (Cont'd)

Holder and Location	Unshielded Positions 1, 2 (Aluminum Cases)	Shielded Positions 3, 4, 5 (Gadolinium Cases)
<p style="text-align: center;">L</p> <p>6° Core Midplane Elevation</p>	<p>1 - HEDL RM B&amp;W RMs Co-Al Wire Fe Wire</p> <p>2 - B&amp;W RMs 2 Fe 2 Co Co-Al Wire Fe Wire</p>	<p>3 - HEDL RM B&amp;W RMs Co-Al Wire Ni Wire Np-Al Wire U-Al Wire</p> <p>4 - B&amp;W RMs Fe Ni Cu Co Co-Al Wire Ni Wire Np Wire U-Al Wire</p> <p>5 - B&amp;W RMs Fe Co</p>
<p style="text-align: center;">N</p> <p>42.5° Core Midplane Elevation</p>	<p>1 - B&amp;W SSTR (33B)</p> <p>2 - B&amp;W RM Fe Co Co-Al Wire Fe Wire</p>	<p>3 - B&amp;W RMs Fe Ni Cu Co</p> <p>4 - Co-Al Wire Ni Wire Np Wire U-Al Wire B&amp;W SSTR (33C)</p> <p>5 - 2 Np-237 Powder</p>

Table 4-1 Loading Plan of Cavity Dosimetry Holders (Cont'd)

Holder and Location	Unshielded Positions 1, 2 (Aluminum Cases)	Shielded Positions 3, 4, 5 (Gadolinium Cases)
No M Holder		
No O Holder		
<p>P</p> <p>26.5° Core Midplane Elevation</p>	<p>1 - 2 Co-Al Wire 2 Fe Wire</p> <p>2 - B&amp;W RMs Fe Co Co-Al Wire Fe Wire</p>	<p>3 - LiF</p> <p>4 - 2 Co-Al Wire 2 Ni Wire 2 Np Wire 2 U-Al Wire</p> <p>5 - U-Al Wire Np Wire Co-Al Wire Ni Wire</p>
<p>Q</p> <p>26.5° Core Midplane Elevation</p>	<p>1 - B&amp;W RMs Fe Co</p> <p>2 - B&amp;W RMs Fe Co</p>	<p>3 - B&amp;W RMs Fe Ni Cu Co Nb (ToyoSoda) HAFM 3 Be Li</p> <p>4 - B&amp;W RMs Fe Co</p> <p>5 - HAFM 3 Be Li Nb (MOL) 2 Nb (ToyoSoda)</p>

Table 4-1 Loading Plan of Cavity Dosimetry Holders (Cont'd)

Holder and Location	Unshielded Positions 1, 2 (Aluminum Cases)	Shielded Positions 3, 4, 5 (Gadolinium Cases)
<p style="text-align: center;">R</p> <p>11.5° Seal Plate Elevation</p>	<p>1 - Bechtel RMs Fe Co</p> <p>2 - Bechtel SSTR (B&amp;W-1) B&amp;W SSTR (1B)</p>	<p>3 - LiF</p> <p>4 - Bechtel RMs Fe Ni 3 Cu Co B&amp;W SSTR (1C)</p> <p>5 - Bechtel SSTR (B&amp;W-3) Bechtel SSTR (B&amp;W-2)</p>
<p style="text-align: center;">S</p> <p>11.5° Core Midplane Elevation Source Tube "A"</p>	<p>1 - B&amp;W RMs Fe Co</p> <p>2 - B&amp;W SSTRs (5B, 6B)</p>	<p>3 - R&amp;W RMs Fe Ni Cu Co</p> <p>4 - Nb (ToyoSoda) B&amp;W SSTRs (6C, 5C, B&amp;W-15, B&amp;W-16)</p> <p>5 - MOL RM</p>

Table 4-1 Loading Plan of Cavity Dosimetry Holders (Cont'd)

Holder and Location	Unshielded Positions 1, 2 (Aluminum Cases)	Shielded Positions 3, 4, 5 (Gadolinium Cases)
<p style="text-align: center;">T</p> <p>11.5° Core Midplane Elevation</p> <p>Source Tube "B"</p>	<p>1 - HEDL RM</p> <p>2 - B&amp;W RMs Fe Co</p>	<p>3 - LiF</p> <p>4 - HEDL RM Bechtel SSTR (B&amp;W-6)</p> <p>5 - HAFM 3 Be 1 Li HAFM 3 Be 1 Li 2 Nb (MOL) 2 ToyoSoda Nb B&amp;W RMs Fe Ni Cu Co</p>

Table 4-1 Loading Plan of Cavity Dosimetry Holders (Cont'd)

Holder and Location	Unshielded Positions 1, 2 (Aluminum Cases)	Shielded Positions 3, 4, 5 (Gadolinium Cases)
<p style="text-align: center;">U</p> <p>11.5° Core Midplane Elevation</p> <p>Source Tube "Connector"</p>		<p>4 - B&amp;W RMs Fe Ni Cu Co B&amp;W SSTR (B&amp;W-7 = 8C)</p>

Notes:

- 1) LiF detector chips are in shielded locations, but are in aluminum cases.
- 2) MOL RMs use aluminum cases with internal Cd shielding.

Key:

- B&W = BWNS supplied dosimetry
- HEDL = Hanford Engineering Development Laboratory supplied dosimetry package
- MOL = Center for the Study of Nuclear Energy, MOL Belgium supplied dosimetry package
- PUD = Paired Uranium Detector
- RM = Radiometric Monitor
- SSTR = Solid State Track Recorder
- HAFM = Helium Accumulative Fluence Monitor
- U of A = University of Arkansas supplied dosimetry package (now property of Arkansas Tech University)
- LiF = Lithium Fluoride detector

Table 4-2 Coordinate Location of Dosimetry

Holder I.D.	Azimuth (deg)	Radial (in)	Axial (in)
11 1/2 Degrees			
A	191.5	114.625"	- 17.459"
R	191.5	114.625"	- 26.147"
B	191.5	115.375"	- 79.959"
C	191.5	115.375"	- 88.647"
D	191.5	115.375"	-133.959"
E	191.5	115.375"	-142.616"
F	191.5	115.375"	-205.866"
G	191.5	115.375"	-214.459"
26 1/2 Degrees			
Q	206.5	119.297"	-206.238"
P	206.5	119.297"	-213.762"
42 1/2 Degrees			
H	222.5	115.982"	-206.238"
N	222.5	115.982"	-213.762"
11 Degrees			
J	349.0	115.375"	-205.428"
K	349.0	115.375"	-214.490"
6 Degrees			
M	6.0	115.185"	-210.603"
L	6.0	115.185"	-219.166"
Permanent (11 1/2°)			
S	191.8	128.812"	-201.625*
T	191.8	128.812"	-220.875*

\* Elevation dimensions for the Permanent dosimetry capsules are taken to the center line of the center capsule lid closure bolts for both the upper and lower capsules.

Figure 4.1 Cavity Dosimetry Holder



Figure 4.2 General Arrangement of Cavity Dosimetry Benchmark Experiment

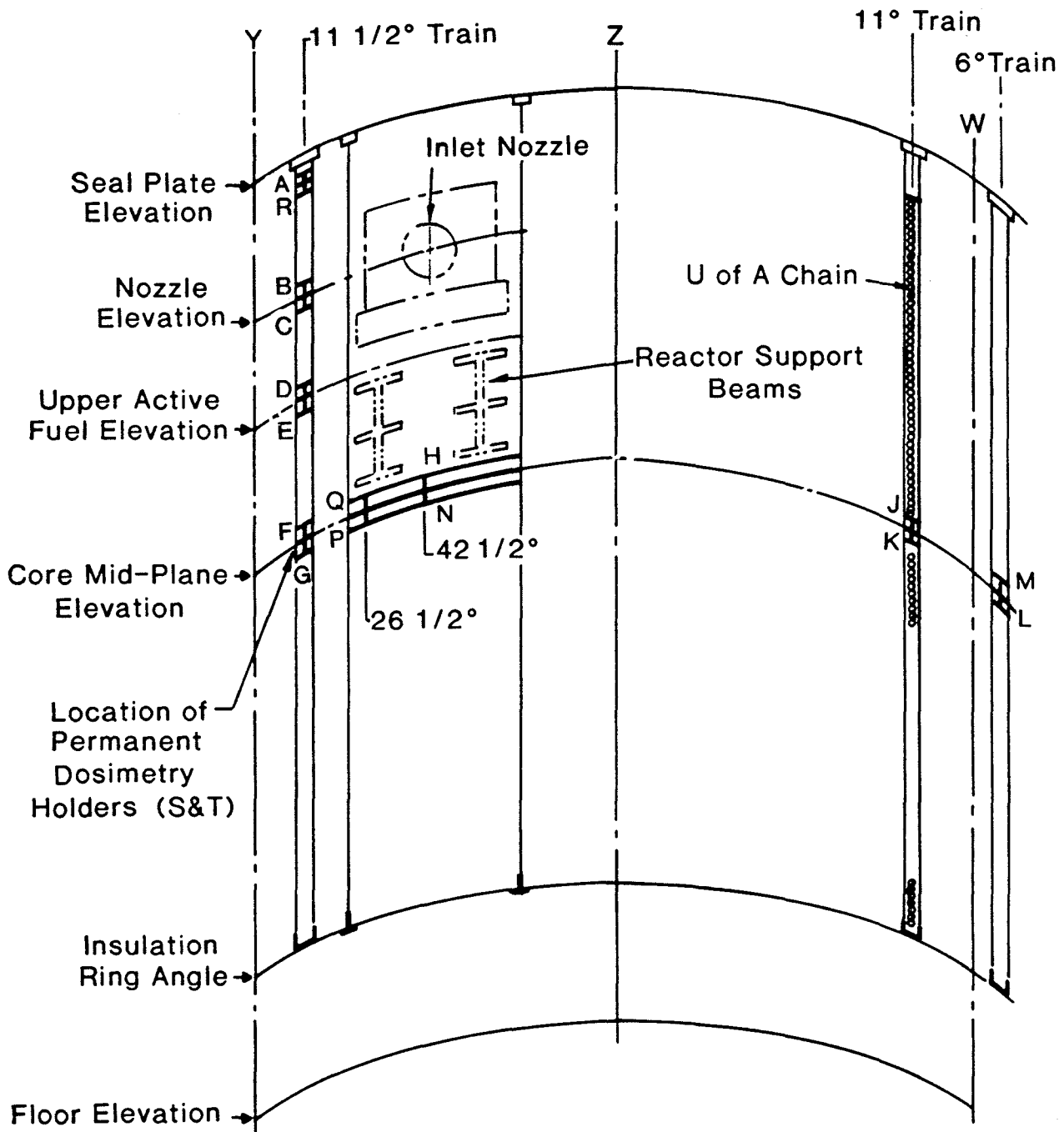


Figure 4.3 Reference RV Coordinate System

Figure 4.4 Cavity Dosimetry Experiment Plan View

## **5.0 Measurement Methodology**

There were three categories of neutron dosimeters irradiated in the experiment:

1. Radiometric Dosimeters: fissionable, activation, niobium, and stainless-steel chains (Section 5.1),
2. Solid State Track Recorders (Section 5.2), and
3. Helium Accumulation Fluence Monitors (Section 5.3).

For each of these three categories of neutron detectors, the indicated subsection provides a discussion of the measurement techniques, the corrections required to determine specific activity from counting data, and the measurement results.

### **5.1 Radiometric Dosimeters**

The radiometric dosimeters, including stainless steel chains, were analyzed by B&W Nuclear Environmental Services (NES) at its Lynchburg Research Center. The measurement techniques, corrections, and measured results are reported in References 24 and 25. A summary of the measurement techniques, corrections, and results, however, is included in this section.

#### **5.1.1 Fissionable Radiometric Dosimeters (U-235, U-238, Np-237)**

Forty-seven fissionable radiometric dosimeters were irradiated in Davis-Besse Cycle 6 at locations described in Section 4 and the capsule.

##### **5.1.1.1 Measurement Techniques**

One measurement technique was used for the wires, foils, and vanadium encapsulated oxide

## FTI Non-Proprietary

wires while another was used for the powder dosimeters. Each wire, foil, and encapsulated dosimeter was washed and dried. Its diameter or thickness was measured with a micrometer and it was weighed on an analytical balance. Each dosimeter was then mounted on a PetriSlide™ with double-sided tape and a preliminary 300 second count was taken on the 31% Princeton Gamma-Tech (PGT) gamma spectrometer to select the best distance from dosimeter to detector to be used in the final count. The target for the final count was 10,000 counts in the photo-peak of interest while keeping the counter dead time below 15%.

The  $^{137}\text{Cs}$  662 keV gamma was counted and analyzed for all of the fissionable radiometric dosimeters. In addition, the  $^{233}\text{Pa}$  312 keV gamma was counted for some  $^{237}\text{Np}$  dosimeters, the  $^{235}\text{U}$  186 keV gamma for the  $^{235}\text{U}$  dosimeter and the  $^{234\text{m}}\text{Pa}$  1001 keV gamma for some  $^{238}\text{U}$  dosimeters. The counting data was taken and processed with a computer-based multichannel analyzer using the shutdown date of January 26, 1990 as the reference date for decay corrections. The detector was calibrated for the foil, wire and encapsulated dosimeters with a NIST-traceable mixed gamma "point source" standard. The source was actually a thin spot a few millimeters in diameter. The mounting of the dosimeters was such that the side of the dosimeter closest to the detector was in the same plane as the standard source. A correction was therefore required in most cases for the fact that the effective distance from the dosimeter to the detector differed slightly from the standard to detector distance. This is discussed below with other corrections.

The data is reported in micro-Curies per gram of target ( $\mu\text{Ci/gm}$ ) where the target is the first named isotope in the designation of each reaction. The fraction of the dosimeter mass that corresponds to the mass of each fissionable isotope was therefore required. It was determined from information on the fraction of the aluminum alloy mass that was  $^{238}\text{U}$  or  $^{237}\text{Np}$ , the fraction of the oxide mass that was  $^{238}\text{U}$ ,  $^{235}\text{U}$  or  $^{237}\text{Np}$ , and the fraction of the mass of encapsulated dosimeters that was vanadium.

A different measurement technique was used for the fissionable oxide powders. The uranium oxide dosimeters were dissolved in HNO<sub>3</sub> and diluted to 20 mL in a scintillation vial. The neptunium oxide dosimeters were digested in 6N HCl/16N HF with addition of 30% H<sub>2</sub>O<sub>2</sub> until dissolved and were also diluted to 20 ml in a scintillation vial. The activity for each was determined by counting the <sup>137</sup>Cs 662 keV gamma with the PGT gamma spectrometer and decay correcting to January 26, 1990. A NIST-traceable mixed gamma standard was counted in an identical geometry, therefore, no corrections for geometry or attenuation were required for the dissolved dosimeters. The mass of uranium was determined by inductively coupled plasma atomic emission spectroscopy and the mass of neptunium was determined from the measured <sup>233</sup>Pa content using the 312 keV gamma.

#### **5.1.1.2 Corrections**

As stated above, the data for the wires, foils and encapsulated wires were corrected for the difference between the effective distance from dosimeter to detector and the standard to detector distance. In the standard correction contained in the NES spread sheets, the dosimeters are partitioned into four slabs parallel to the face of the detector. A correction factor is determined for each slab assuming that the response varies as the reciprocal of the distance to the detector squared. The geometry factor for the dosimeter is then obtained from a weighted average of the slab factors using the cross-sectional area of each slab as the weight.

The dosimeter results are also corrected for self-absorption of the 662 keV gamma used to measure the <sup>137</sup>Cs activity. In the standard correction in the NES spread sheets the narrow angle formula by W. R. Dixon<sup>26</sup> is used for foils and a formula by Evans and Evans<sup>27</sup> is used for cylindrical wires. The equation for foils is

$$I_o = I \frac{\mu t}{1 - e^{-\mu t}} \quad (5.1)$$

where

- $\mu$  =  $\rho \mu_o$  a linear attenuation coefficient,  $\text{cm}^{-1}$
- $\rho$  = density,  $\text{gm}/\text{cm}^3$
- $\mu_o$  = mass attenuation coefficient,  $\text{cm}^2/\text{gm}$
- $t$  = foil thickness,  $\text{cm}$
- $I$  = measured intensity with self absorption
- $I_o$  = corrected intensity

The equation for wires is similar in principle but has many more terms. The correction is a function of the linear attenuation coefficient, the radius of the wire, and the distance from wire to detector. Values for the mass attenuation coefficients were interpolated from the Storm and Israel tables.<sup>28</sup> Linear attenuation coefficients for alloys and oxides were obtained from the mass coefficient for each constituent and combined as a mixture.

The corrections for all the fissionable radiometric dosimeters were first made using the standard corrections contained in the NES spread sheets. The results in Reference 24 are based on these corrections. The approximations contained in these corrections are valid when the wire diameter or foil thickness is small and when the distance from the dosimeter to the detector is large. Most of the fissionable radiometric dosimeters, however, did not meet this criteria. For this reason, a Monte Carlo method was used to calculate the correction factors for the fissionable dosimeters except for the thin foil and powders. The foils met the criteria, and the powdered dosimeters did not require corrections.

The Monte Carlo method is the same as used for niobium and described in Section 5.1.3. The code, named NIOBIUM, was used with input appropriate for the 662 keV <sup>137</sup>Cs gamma

## **FTI Non-Proprietary**

rather than the 16.6 keV X-ray used for niobium in Section 5.1.3. In this code, gammas are started isotropically with a uniform distribution throughout the dosimeter. A hit is recorded for all gammas that both escape the dosimeter and travel in a direction to hit the detector. A sufficient number of histories are used to record at least 10,000 hits at the detector. Three cases were calculated:

1. Source of gammas distributed in actual dosimeter geometry and actual attenuation coefficient.
2. Source of gammas distributed in actual dosimeter geometry and a vanishingly small attenuation coefficient.
3. Source of gammas distributed in point source geometry and with a very small attenuation coefficient.

A total correction factor may be obtained from the ratio of Case 3 to Case 1. The geometry factor is the ratio of Case 2 to Case 3 and the self-absorption factor is the ratio of Case 2 to Case 1. The ratio of the total correction calculated with the Monte Carlo method to the total correction calculated using the standard method is included with the results.

The diameter of each vanadium encapsulated wire was estimated using measured dosimeter mass and vendor supplied data on mass and composition of the encapsulated wire. The Monte Carlo method was used to calculate the geometry and self-absorption factors assuming that the wire was at the center of the dosimeter. In addition, a correction factor of 1.008 was applied to account for the transmission through the vanadium wall. This corresponds to an effective wall thickness of 0.0075 inch.

The concentration of  $^{235}\text{U}$  in most of the  $^{238}\text{U}$  dosimeters is approximately 12 ppm. The one exception to this is the uranium aluminum alloy where the concentration is 350 ppm. This level is high enough to require a correction to the uranium alloy data. The K4 location in



**FTI Non-Proprietary**

the cavity contained both a  $^{235}\text{U}$  and  $^{238}\text{U}$  gadolinium covered dosimeter. A correction factor of 0.9074 was derived from the measured data. Similarly calculated data for  $^{235}\text{U}$  and  $^{238}\text{U}$  in a surveillance capsule inside the reactor leads to a correction factor of 0.952.

Corrections were also made for photofissions in  $^{238}\text{U}$  and  $^{237}\text{Np}$ , in both the surveillance capsules and the cavity. Calculated correction factors based on cross sections in the upper three energy gamma groups in the CASK group structure are as follows:

	$^{238}\text{U}$	$^{237}\text{Np}$
Surveillance Capsule	0.950	0.980
Cavity	0.968	0.994

**5.1.1.3 Measured Results**

The measured activities per gram of target nuclide is listed in Appendix B, (1) Table B-1.1-1 for the  $^{238}\text{U}$  radiometric dosimeters, (2) Table B-1.1-2 for the  $^{237}\text{Np}$  radiometric dosimeters, and (3) Table B-1.1-3 for the one  $^{235}\text{U}$  radiometric dosimeter. The correction factors used for photofissions and  $^{235}\text{U}$  and  $^{238}\text{U}$  are listed as well as factors to correct the Monte Carlo method of calculating the geometry and self-absorption factors.

**5.1.2 Non-Fissionable Radiometric Dosimeters**

Two-hundred and forty-three non-fissionable radiometric dosimeters were irradiated in Davis-Besse Cycle 6. In addition, four stainless steel beaded chains were divided into

segments and counted as discussed in Section 5.1.4. The distribution by type and general location is given in Table 5.1.2-1.

#### **5.1.2.1 Measurement Techniques**

The measurement technique is basically the same as described in Section 5.1.1 for fissionable wires and foils. The dosimeters were washed, dried, measured, weighed, and each dosimeter was mounted on a PetriSlide™ with double-sided tape. A preliminary 300 second count was taken on the 31% PGT gamma spectrometer to select the best distance from dosimeter to detector to be used in the final count. The target for the final count was 10,000 counts in the photopack of interest while keeping the counter dead time below 15%.

The photopeaks used to determine the activity for each dosimeter are listed in Table 5.1.2-2. The detector was calibrated with a NIST-traceable mixed gamma "point source". The dosimeter data was processed with a computer-based multichannel analyzer using the shutdown date of January 26, 1990 as the reference date for decay corrections. The data is reported in micro-Curies per gram of target isotope. The fraction of the dosimeter mass corresponding to the target isotope mass is, therefore, required. This was obtained from the weight fraction of the element in the alloys and/or the weight fraction of the target in the element. The weight fraction for all of the dosimeters is summarized in Table 5.1.2-3. The impurities in the dosimeters were sufficiently low such that they did not affect the target weight.

#### **5.1.2.2 Corrections**

Two corrections were made to the non-fissionable radiometric data. One was the geometry correction which accounts for the slight difference in effective distance from the dosimeter

to the detector and the distance from standard to detector. The other was the self-absorption correction. The corrections for wires and foils for non-fissionable radiometric dosimeters are identical to the standard corrections for fissionable radiometric wires and foils described in Section 5.1.1.

#### **5.1.2.3 Measured Results**

The measured results for the activity per gram of target are listed in Appendix B, Tables B-1.2-4 through B-1.2-11. The geometry and self-absorption correction factors are also listed. The conventional treatment of the two factors is such that the uncorrected data is divided by the geometry factor and multiplied by the self-absorption factor to yield the corrected data.

#### **5.1.3 Niobium Dosimeters**

Twenty-two high purity niobium dosimeters were exposed in the cavity in Davis-Besse during Cycle 6. Twenty of these were near midplane, one was at the upper active fuel elevation and one was at the nozzle elevation. Of the twenty-one, which were compared, four were part of the MOL dosimeters, two were part of the AT4 dosimeters, and fifteen were part of the B&W dosimeters. The fifteen B&W niobium dosimeters include ten low Ta dosimeters obtained from Toyo Soda and five obtained from MOL.

##### **5.1.3.1 Measurement Techniques**

**FTI Non-Proprietary**

(5.2)

where:

**5.1.3.2 Corrections**

### 5.1.3.3 Measured Results

The measured activity of  $^{93m}\text{Nb}$  per gram of  $^{93}\text{Nb}$  is listed in Appendix B, Table B-1.3-1 for each of the 22 Nb dosimeters. The activity due to fluorescence caused by  $^{182}\text{Ta}$  and  $^{94}\text{Nb}$  is also listed. In all cases, the correction for fluorescence was very low. This is due to a combination of low tantalum and a long wait time from the end of the irradiation to the time that the dosimeter activities were measured. The correction for  $^{94}\text{Nb}$  fluorescence ranged from 0.16% to 0.38% for all dosimeters other than the one in location C4 which was 1.3%. The correction for  $^{182}\text{Ta}$  fluorescence was less than 0.1% for all dosimeters except (a) the foil in location K3 which was 3.2%, (b) the wire in K3 which was 0.45%, and (c) the four MOL dosimeters in F5 and S5 which averaged 2.3%.

### 5.1.4 Stainless Steel Chains

Four B&WOG stainless steel chains located as shown in Figure 4.4 were irradiated during Cycle 6. The chains consisted of thin wall hollow spherical beads connected together with short wire links. The beads are 0.468 cm in diameter and weigh approximately 0.21 gm per bead with four beads per inch of chain length. The chains extended from near the seal plate to the concrete floor. Samples were cut from the chains and analyzed for both the  $^{54}\text{Fe}(n,p)^{54}\text{Mn}$  and  $^{59}\text{Co}(n,\gamma)^{60}\text{Co}$  reactions to provide axial flux distribution information.

Nine one-inch long chain segments were also loaded in "pill boxes" for comparison with the conventional radiometric dosimeters.

#### **5.1.4.1 Measurement Techniques**

The measurement technique for the chain segments was similar to that for the other radiometric dosimeters. However, because of the significant difference in geometry, the corrections were determined in a different way. After cleaning, the chains were cut as required and each measurement segment was weighed and mounted on a PetriSlide™ using a double-sided tape and spiraling the chain segments around the center of the slide. Measurement segments were cut every six inches over the height of the fuel, near the upper concrete lip, and near the nozzle elevation. Otherwise, segments were cut every 12 inches. The measurement segments were two-inches long (eight beads) from 30 inches above the fuel to 36 inches below the fuel and the remainder of the segments were four-inches long (16 beads).

The 834 keV photo-peak from  $^{54}\text{Mn}$  was used to analyze the  $^{54}\text{Mn}$  reaction and the 1332 keV photopeak from  $^{60}\text{Co}$  was used to analyze the  $^{59}\text{Co} (n,\gamma)^{60}\text{Co}$  reaction. The detector was calibrated with a NIST traceable mixed gamma "point source" and the data was processed with a computer-based multichannel analyzer using the shutdown date of January 26, 1990 as the reference date for decay corrections.

The fraction of the mass of the chain segments corresponding to  $^{54}\text{Fe}$  and to  $^{59}\text{Co}$  is required to express the activity in microcuries per gram of target isotope. Unirradiated samples of the chains were dissolved in  $\text{HCl}/\text{HNO}_3$  acid and were analyzed by inductively coupled plasma atomic emission spectrometry. The elemental weight fraction was determined to be 0.6693 for Fe and 0.0037 for Co. After combining with the isotopic weight fractions, the fraction of the chain mass that is  $^{54}\text{Fe}$  was determined to be 0.0382 and the fraction that is  $^{59}\text{Co}$  is 0.0037.

#### 5.1.4.2 Corrections

Two corrections were made to the chain data. One was a geometric correction which accounts for the difference in effective distance from the chain segment to the detector and the distance from the "point source" standard to the detector. The other was a correction for the absorption within the chain systems of the 834 keV gammas in the  $^{54}\text{Mn}$  case and the 1332 keV gammas in the  $^{60}\text{Co}$  case. The standard method of correcting for self-absorption could not be applied to the chain segments because of the difference in geometry from either foils or wires. The standard wire geometric formula, however, gives a good approximation for the geometry factor. In this case, the standard wire formula yields a geometric factor of 0.9402. This is for a diameter of 0.46778 cm and a shelf-to-detector distance of 7.387 cm. The Monte Carlo method was used to confirm that this is also an appropriate value for chain segment at the same shelf distance.

A measured total correction factor was obtained for the  $^{60}\text{Co}$  measurements.

After the chain segments were analyzed on the PetriSlides™, selected segments were dissolved in 1 = 1 HCl/HNO<sub>3</sub> acid and diluted to 500 mL in a Marinelli beaker. The  $^{60}\text{Co}$  activity was then measured with the gamma spectrometer calibrated for the Marinelli geometry using a NIST traceable standard. Since no corrections are required for the dissolved Marinelli geometry case, the total correction factor for the chain segment on the PetriSlide™ could be determined by comparing the two measurements. The  $^{60}\text{Co}$  data are very consistent and yield an average total correction factor of  $1.102 \pm 0.009$ . The total correction factor is:

$$F_{\text{Total}} = F_A/F_G$$



**FTI Non-Proprietary**

where  $F_A$  is the self-absorption factor and  $F_G$  is the geometry factor. Using the geometry factor from above gives the following correction factors for the chain segment  $^{60}\text{Co}$  data.

$$\begin{aligned} F_{\text{TOTAL}} &= 1.102 \\ F_G &= .9402 \\ F_A &= 1.036 \end{aligned}$$

An attempt was made to measure the total correction factor for  $^{54}\text{Mn}$  in the same way; however, for some unknown reason, the data was very inconsistent. The correction factors for  $^{54}\text{Mn}$  were, therefore, determined from the  $^{60}\text{Co}$  data. The geometry factor for  $^{54}\text{Mn}$  is the same as for  $^{60}\text{Co}$ . The only unknown factor is then the self-absorption factor for  $^{54}\text{Mn}$ . This was obtained by estimating the difference in self-absorption for the  $^{54}\text{Mn}$  834 keV gamma versus the  $^{60}\text{Co}$  1332 keV gamma in a chain segment. The linear attenuation coefficient for the two gammas in stainless steel was determined using the NIST program XGAM as:

E	$\mu$
1332 keV	0.408 $\text{cm}^{-1}$
834 keV	0.516 $\text{cm}^{-1}$

An effective foil thickness then determines the  $^{60}\text{Co}$  self-absorption factor of 1.036 using the standard foil equation and  $\mu = 0.408 \text{ cm}^{-1}$ . The same formula yields a self-absorption factor of 1.046 using the same thickness and  $\mu = 0.516 \text{ cm}^{-1}$ . It was assumed that the fractional change would be the same for the chain segments, therefore, for  $^{54}\text{Mn}$ ,

$$F_G = 0.9402$$

$$F_A = 1.046$$

$$F_T = 1.113$$

#### 5.1.4.3 Measured Results

The measured  $^{54}\text{Mn}$  activities per gram of  $^{54}\text{Fe}$  and the  $^{60}\text{Co}$  activities per gram of  $^{59}\text{Co}$  are listed in Appendix B, Tables B-1.4-1 through B-1.4-4. The last part of each sample ID is a distance in inches from the top of each chain hanger to the center of each sample. This coordinate will be designated as  $Z^1$  and will be a positive number. Two other axial coordinates are used.  $Z$  is an axial coordinate in inches with origin at the seal plate level. A negative value of  $Z$  then indicates a point below the seal plate. The top of each chain hanger was 13.5 inches below the seal plate, therefore,

$$Z = Z^1 - 13.5$$

$Y$  designates another axial coordinate which is the distance in cm above the bottom of the lower grid. The relation between  $Y$  and  $Z$  is:

$$Y = (295.375 + Z) \times 2.54 \quad (5.3)$$

The bottom of the active fuel is at  $Z^1 = 268.5$  in. Nominal midplane is at 196.5 in. and top of fuel at 124.5 in. based on 144 in. of fuel height. The actual fuel height is approximately 142.5 in. making the top of the fuel at  $Z^1 = 126$  in. and midplane at  $Z^1 = 197.25$  in.

Activity measurements for the chain segments irradiated in the "pill boxes" are listed in

Table B-1.4-5 of Appendix B.

## 5.2 Solid State Track Recorders (SSTRs)

Solid State Track Recorders (SSTR) neutron dosimeters were prepared at the Hanford Engineering Development Laboratory (HEDL) and the Westinghouse Science & Technology Center (STC) under contract to the B&W Nuclear Service Company for exposure at Davis Besse Unit 1 during operating cycle 6. A total of eighty-five ultra low-mass fissionable deposits of  $^{235}\text{U}$ ,  $^{239}\text{Pu}$ ,  $^{237}\text{Np}$ , and  $^{238}\text{U}$  with mica SSTRs were assembled into thirty-three dosimetry packets. The as-built information for the dosimeters is contained in References 30 and 31. Following irradiation of the dosimeters in the reactor cavity of Davis-Besse during cycle 6, the dosimeters were retrieved and shipped to Westinghouse STC for analysis.

### 5.2.1 Measurement Techniques

All 85 SSTRs were etched in 49% HF at 22.0°C for a minimum of one hour. Deposit uniformities were consistent with previous experience in most cases and presented no difficulties for track scanning.

Most SSTRs were scanned with the Westinghouse Automated Track Scanner, but in selected cases some were manually scanned. Ten of the cases occurred when the track density exceeded the capabilities of the automated scanner and a manual estimating procedure was used. In all cases, at least two independent scans were performed and replicate agreement between the two scans was required. The minimum and maximum track counts obtained were 3599 and  $7 \times 10^5$ , respectively, with 60 of the 85 SSTRs having less than 100,000 tracks.

### 5.2.2 Measured Results

The measurements, in Fissions/Atom for each SSTR, are noted in Reference 32. The first column contains the alphanumeric dosimeter holder identifier and the numeric position number. Positions 1 and 2 have no thermal neutron shielding, positions 3 through 5 have a gadolinium covering. The SSTRs did not have sufficient unbiased standards to serve as valid measurements, therefore no results are included.

### 5.3 Helium Accumulation Fluence Monitors (HAFMs)

HAFMs are neutron dosimeters that use the accumulation of helium gas as the measurable quantity that is related to neutron fluence.<sup>25</sup> The helium is generated through  $(n, \alpha)$  reactions in the target material and remains, unchanged, in the detector material for several years after formation. The amount of helium is measured by high-sensitivity gas mass spectrometry.

Eleven aluminum-wrapped beryllium HAFM packages and eleven individual Al-Li wire HAFMs, were fabricated for the B & W Owners Group at Rockwell and were processed by Rockwell for helium analysis. Each beryllium package contained three beryllium pieces weighing from  $\sim 1.5$  to 4 mg each. The beryllium is from Rockwell Lot 7. Beryllium purity is 99.99%. Measured boron impurity in the beryllium is 8.9 wt. ppm.

The Al-Li alloy HAFMs were in the form of bare wires, 0.5 mm in diameter and  $\sim 6$  mm long. The Al-Li alloy came from Rockwell Lot 5 material, which was originally fabricated by the Central Bureau for Nuclear Measurements (CBNM) at Geel, Belgium. The composition of the Al-Li is Al-0.73  $\pm$  0.01 wt. % Al, with a  ${}^6\text{Li}$  content of 95.7  $\pm$  0.1 at. %.

### 5.3.1 Measurement Techniques

#### 5.3.1.1 Beryllium HAFMs

Following identification by package number, each beryllium package was carefully unwrapped and the individual beryllium samples removed. Each beryllium sample was then examined under a low power optical microscope to verify sample integrity. In addition, the beryllium samples were weighed to compare their post-irradiation mass with that obtained during sample fabrication at Rockwell. In each case, no significant mass change was observed.

After identification and inspection, two of the individual beryllium HAFMs in each package were prepared for duplicate helium analysis. This preparation involved first etching the sample to remove  $\sim 0.05$  mm off the surface, followed by weighing to determine the etched sample mass. The purpose of the etching step was to remove surface material which could have been affected by  $\alpha$  - recoil either into or out of the samples during irradiation.

Duplicate helium analyses are performed routinely to give an indication of the analysis reproducibility and also to give an indication of the gross helium homogeneity within each sample.

#### 5.3.1.2 Al-Li Alloy HAFMs

As was done for the beryllium samples, the Al-Li wire HAFMs were first etched to remove  $\sim 0.05$  mm of surface material which could have been affected by  $\alpha$  - recoil either into or out of the samples. The Al-Li samples were then subdivided into three approximately equal mass specimens. Two of the specimens were subsequently analyzed for their helium content.

The helium content of each specimen was determined by isotope-dilution mass spectrometry following vaporization of each in a resistance-heated tungsten-wire crucible in one of the mass spectrometer system's high-temperature vacuum furnaces. The absolute amount of  $^4\text{He}$  released was measured relative to a known quantity of added  $^3\text{He}$  "spike."

The  $^3\text{He}$  spikes were obtained by expanding and partitioning a known quantity of gas through a succession of calibrated volumes. The mass spectrometer was calibrated for mass sensitivity during each series of runs by analyzing known mixtures of  $^3\text{He}$  and  $^4\text{He}$ .

### **5.3.2 Measured Results**

The results of the helium measurements are given in Appendix B, Tables B-4.2-1 and B-4.2-2, and are listed as total atoms of helium released, and as helium concentrations in atomic parts per million ( $10^{-6}$  atom fraction) or in atomic parts per billion ( $10^{-9}$  atom fraction).<sup>25</sup> Helium concentrations are relative to the total number of Be or  $^6\text{Li}$  atoms in each Be or Al-Li specimen, respectively. Conversion from total helium to helium concentration was based on a calculated number of atoms per gram of  $6.682 \times 10^{22}$  for the beryllium, and  $0.06942 \times 10^{22}$  for the Al-Li alloy.

For the beryllium results in Table B-4.2-1, the concentration values listed in Column 5 have been corrected for small amounts of helium previously measured at Rockwell in unirradiated beryllium material from the same Rockwell lot. These measurements indicated an initial helium concentration level in the beryllium of 0.05 appb. The Column 5 data have also been corrected for helium generation from the small boron impurity (8.9 wt. ppm) in the Lot 7 beryllium. This latter correction was calculated from the helium concentrations measured in the Al-Li HAFMs at the same reactor locations (assuming a  $^{10}\text{B}/^6\text{Li}$  thermal neutron cross section ratio of 4.08), and amounted to only  $\sim 0.3\%$  of the total helium generation.

Table 5.1.2-1. Non-Fissionable Radiometric Dosimeters

Type	Midplane and Upper Active Fuel	In-Vessel Capsules	Nozzle and Seal Plate Level	Total
Fe	50	8	14	72
Ni	23	8	5	36
Cu	15		11	26
Ti	9		2	11
Ag/Al	7		2	9
Co/Al	27	16	2	45
Co	31		12	43
Sc	1			1
	163	32	48	243

Table 5.1.2-2. Photopeak Analyzed for Each Reaction

Reaction	Gamma Ray
$^{54}\text{Fe}(n,p) ^{54}\text{Mn}$	834 kev
$^{58}\text{Ni}(n,p) ^{58}\text{Co}$	811 kev
$^{63}\text{Cu}(n, ) ^{60}\text{Co}$	1332 kev
$^{46}\text{Ti}(n,p) ^{46}\text{Sc}$	1121 kev
$^{109}\text{Ag}(n, ) ^{110\text{m}}\text{Ag}$	658 kev
$^{59}\text{Co}(n, ) ^{60}\text{Co}$	1332 kev

Table 5.1.2-3. Isotopic Fractions and Weight Fractions of Target Nuclides

Dosimeter	Target Nuclide	Isotopic Fraction of Target	Weight Fraction of Target Element
Cobalt	$^{59}\text{Co}$	1.0000	ALL - 1.0000
Cobalt/Aluminum	$^{59}\text{Co}$	1.0000	BWOG - 0.0066 ATU - 0.0054 HEDL - 0.00117 HEDL - 0.00496 MOL - 0.01
Silver/Aluminum	$^{109}\text{Ag}$	0.48624	ATU - 0.0465 HEDL - 0.00147
Iron	$^{54}\text{Fe}$	0.057	ALL - 1.0000
Nickel	$^{58}\text{Ni}$	0.6739	ALL - 1.0000
Copper	$^{63}\text{Cu}$	0.6850	ALL - 1.0000
Scandium	$^{45}\text{Sc}$	1.0000	ALL - 1.0000
Titanium	$^{46}\text{Ti}$	0.0768	ALL - 1.0000
Uranium	$^{235}\text{U}$ $^{238}\text{U}$ $^{238}\text{U}/\text{Al}$ $^{238}\text{U}$ V encap	1.0000 1.0000 1.0000 1.0000	ATU - 0.4431 BWOG - ICP HEDL - 1.0000 BWOG - 0.1032 ATU - 0.39432 MOL - 0.13746 MOL - 0.14475
Neptunium	$^{237}\text{Np}$ $^{237}\text{Np}/\text{Al}$ $^{237}\text{Np}$ V encap	1.0000 1.0000 1.0000	BWOG - $^{233}\text{Pa}$ BWOG - 0.0144 ATU - 0.11472 ATU - 0.11348 MOL - 0.21316
Niobium	$^{93}\text{Nb}$	1.0000	ALL - Monte Carlo
Stainless Steel Chains	$^{54}\text{Fe}$ $^{59}\text{Co}$	0.057 1.0000	BWOG - 0.6702 (ICP) BWOG - 0.0037 (ICP)



**6.0 Comparison of Measured-To-Calculated Dosimeter Responses**

One of the goals of the Cavity Dosimetry Program was to develop a calculation-based methodology which can be used to accurately determine the flux. This methodology has been developed and was outlined in Section 3.0 . This section presents the traditional *M/C* ratios from the benchmark experiment part of the dosimetry program.

**6.1 In-Vessel *M/C*s**

Two standard unirradiated surveillance capsules were loaded in the Davis - Besse reactor at the 11<sup>0</sup> azimuthal position, one on top of the other. These two capsules, TMI2-C and TMI2-E, were irradiated for the duration of cycle 6 and removed after shutdown, which occurred on January 26, 1990, following 380.3 effective full power days of operation.

Each capsule contained a set of 24 radiometric wire dosimeters, defined below:

Dosimeter	Quantity (Per Capsule)	Covered (Y/N)
U238	4	Y
Np237	4	Y
Ni	4	Y
Co	4	Y
Fe	4	N
Co	4	N

Following removal, the dosimetry was shipped to the B & W laboratory for removal from the capsule and counting. The measurement procedures previously described

(Sections 5.5.1 and 5.1.2) apply for the in-vessel dosimetry as well as the cavity dosimetry. The measured activities were decay-adjusted to the time of shutdown.

The previously described DOT analysis (Section 3.3) determined the "calculated responses" for all dosimeters, both in-vessel and ex-vessel, corrected for all known biases.

As discussed below, the in-capsule calculated activities were determined in a slightly different way than the ex-vessel calculated activities were determined.

Accurate determination of the flux in the capsule is possible only if the perturbing effects of the capsule wall and the surveillance specimens are properly accounted for. Since it is not possible to properly account for those effects using  $r, z$  geometry, the basis for the in-capsule flux and dosimeter response calculations must be the  $r, \theta$  DOT calculations.

The fluxes calculated by the  $r, \theta$  DOT analysis are axially averaged fluxes, and thus they must be corrected to determine the flux at the actual axial dosimeter position. To that end, specific axial synthesis factors,  $A_z$ , have been derived.

The three - dimensional flux for any in-vessel capsule dosimeter response calculation is then defined as:

$$\phi_g^{3D} = A_z \phi_g^{R\theta}(r, \theta) \quad (6.1)$$

where  $g$  is an energy group index, and  $\phi_g^{R\theta}(r, \theta)$  is the flux calculated by the two - dimensional DOT  $r, \theta$  run at the point defined by its cylindrical coordinates  $r$  and  $\theta$ .

The calculated dosimeter response is then given by:

$$C_d = S_d \sum_g R_{d,g} \phi_g^{3D} \quad (6.2)$$

where  $S_d$  is the fraction of saturation of dosimeter  $d$  for the irradiation period of interest (see Section 3.3.2), and  $R_{d,g}$  is the response function for dosimeter  $d$  with incident energy in group  $g$ .

Table 6-1 shows the average  $M/C$  by dosimeter type together with the number of dosimeters for each type, and the root mean square standard deviation from Equation 6.3 .

Table 6-1 In-Vessel Average M/Cs

Dosimeter Type	No. of Dosimeters	M/C	Deviation (%)
Fe 54	8	0.942	4.0
Ni 58	8	0.968	5.1
Np 237 Rm covered	8	1.176	7.2
U 238 RM covered	8	1.099	4.6
Co-Al covered	8	0.767	3.4
Co-Al bare	5	1.059	7.5

## 6.2 Ex-Vessel M/Cs

Several dosimeters of various types were installed at numerous locations in the Davis - Besse cavity. Each individual dosimeter response was analytically calculated, and

compared with its corresponding measured value. The large amount of data can be analyzed in various ways. The following analysis simply compares the  $M/C$  averages of the first and second moments by material type and reaction type. The first moment average of the  $M/C$  values is listed in Table 6-2 along with the number of dosimeters for each material - reaction type.

The statistical quality of the various  $M/C$  ratios is obtained by calculating the root mean square standard deviation from the mean variance of the second moment.

$$\text{variance} = \frac{\sum_d \left\{ \left( \frac{M}{C} \right)_d - \left( \frac{M}{C} \right) \right\}^2}{N_d - 1} \tag{6.3}$$

$$\text{standard deviation} = + \sqrt{\text{variance}}$$

The standard deviations are listed in Table 6-3 for each dosimeter type.

Summarizing:

- No location bias is observed.
- There is a strong bias by dosimeter type. Thermal dosimeters have large deviations, Np dosimeters appear to have special problems, and all other dosimeters show consistently good results.
- The statistical quality of non-thermal dosimeters is very good and shows no obvious aberrations.

Table 6-2 Ex-Vessel Average M/C by Type

Dosimeter	Reaction Type	M/C	No. of Dosimeter
Fe54	A	0.954	50
Ni58	C	0.947	23
Cu63	T	0.971	15
Ti46	I	0.994	8
Ag109	V	0.612	2
Co59 (Al)	A	0.562	15
Co59	T	0.275	16
	I		
	O		
	N		
	(covered)		
Nb		1.076	21
Be	HAFM	0.961	8
Np237	F	1.406	14
U238	I	1.087	15
U235	S	0.646	1
	S		
	I		
	O		
	N		
	A		
	B		
	L		
	E		
	(covered)		

Table 6-2 Ex-Vessel Average M/C by Type (Continued)

Dosimeter	Reaction Type	M/C	No. of Dosimeter
Ag109	A	0.652	5
Co59 (Al)	C	0.829	12
Co59	T	0.663	15
	I		
	V		
	A		
	T		
	I		
	O		
	N		
	(bare)		

Table 6-3 Measured-to-Calculated Ratios and Standard Deviations for Cavity Dosimetry

Dosimeter	Reaction Type	M/C	# of Dosimeter	Deviation (%)
Fe54	Activation	0.954	50	4.3
Ni58	(covered)	0.947	23	3.5
Cu63	"	0.971	15	3.3
Ti46	"	0.994	8	5.7
Ag109	"	0.612	2	1.8
Co59 (Al)	"	0.562	15	8.8
Co59	"	0.275	16	2.7
Nb		1.076	21	5.9
Be	HAFM	0.961	8	3.4
Np237	Fissionable	1.406	14	19.5
U238	(covered)	1.087	15	6.6
U235	"	0.646	1	---
U235	SSTR (bare)	---	5	---
Pu239	"	---	4	---
Ag109	Activation	0.652	5	10.0
Co59 (Al)	(bare)	0.829	12	13.6
Co59	"	0.663	15	11.0

**7.0 Uncertainty Methodology**



**FTI Non-Proprietary**

**FTI Non-Proprietary**

**Figure 7-1 Uncertainty Schematic**

**FTI Non-Proprietary**

**FTI Non-Proprietary**

**7.1 Dosimetry Measurement Biases and Standard Deviations**

**FTI Non-Proprietary**

**7.1.1 Biases**



**7.1.2 Standard Deviations**

**FTI Non-Proprietary**

**Table 7-1 Bases of Measurement Errors**

**Radiometric Dosimeters**

**Helium Accumulation Detectors**

\*cm represents centimeters  
mg represents milligrams, and  
appb represents atomic parts per billion

**FTI Non-Proprietary**

**FTI Non-Proprietary**

(7.1)

(7.2)

(7.3)

(7.4)

**FTI Non-Proprietary**

**(7.5)**

**Table 7-2**  
**Cavity Dosimeter Uncertainties**

Dosimeter	Qty	Type	Uncertainty % Range	Uncertainty % Average
Np-237	3 3	Wire Powder		
U-235	1	Wire		
Ti-46	11	Foil		
Cu-63	21 5	Foil Wire		
Fe-54	56 8	Foil Wire		
Ag-109/A1	8 1	Wire Foil		
Co-59	43	Wire		
Sc-45	1	Foil		
Ni-58	20 8	Foil Wire		
Co-59/A1	26 3	Wire Foil		
Nb-93	21 1	Foil Wire		
U-238	4 1 3	Powder Foil Wire		
Np-237/A1	8	Wire		
U-238/A1	8	Wire		
HAFM	11	Chunk		

**Table 7-3**  
**Capsule Dosimeter Uncertainties**

Dosimeter	Qty	Type	Uncertainty % Range	Uncertainty % Average
Fe-54	8	Wire		
Ni-58	8	Wire		
Co-59/A1	16	Wire		
Np-237/A1	8	Wire		
U-238/A1	8	Wire		



**Table 7-4**  
**Dosimeter Uncertainties By Material Type**

<u>Cavity Dosimeter (#)</u>	<u>Reaction Type</u>	<u>Mean Relative Standard Deviation %</u>
U-238	$(n, f)$ Cs-137	
Np-237	$(n, f)$ Cs-137	
Fe-54	$(n, p)$ Mn-54	
Ni-58	$(n, p)$ Co-58	
Ti-46	$(n, p)$ Sc-46	
Cu-63	$(n, \alpha)$ Co-60	
<sup>a</sup> Be-9 HAFM	$(n, \alpha)$ $\beta^-$ , Li-6	
Nb-93	$(n, n')$ Nb-93m	

<sup>a</sup>The beryllium helium accumulation fluence monitors (HAFMs) are exceptional dosimeters with a very high degree of precision and very low uncertainty.

**FTI Non-Proprietary**

**Table 7-5**  
**Dosimeter Uncertainties By Material Type**

<u>Capsule Dosimeter (#)</u>	<u>Reaction Type</u>	<u>Mean Relative Standard Deviation %</u>
U-238	( <i>n, f</i> ) Cs-137	
Np-237	( <i>n, f</i> ) Cs-137	
Fe-54	( <i>n, p</i> ) Mn-54	
Ni-58	( <i>n, p</i> ) Co-58	

$$\sigma_M = \quad (7.6)$$

where

$Mean\ Measurement\ Uncertainty \leq$
---------------------------------------

 (7.7)

**FTI Non-Proprietary**

**7.2 Dosimetry Computational Biases and Standard Deviations**

## FTI Non-Proprietary

The 95 percent confidence level provides the basis for performing sensitivity calculations to determine changes in the vessel fluences and dosimeter activities to biases and standard deviations in the independent variables in the calculations. The DOT discrete ordinates solution of the multigroup transport equation can be used to identify all independent variable types affecting the fluence uncertainty. The most general grouping of independent variables in the transport equation is composed of two types, the macroscopic cross sections and the eigenfunction source. These two variable types are dependent upon the multigroup energy ( $g$ ), the geometric position ( $r$ ), time ( $t$ ), the angular emission ( $\Omega_n$ ), and the directional scattering  $\{P_l(\Omega_n \cdot \Omega'_n)\}$ . Therefore, the two primary variable types are subdivided into four additional macroscopic cross section variables and three additional source variables. (The angular emission ( $\Omega_n$ ) of the fission source is symmetric, thus there is no uncertainty about the angular emission distribution.) This gives seven types of independent variables. In addition to time being an independent variable for the macroscopic cross sections and source, time is an independent variable type directly affecting the fluence uncertainty. Time is further divided into a dependent function of the geometric position ( $r$ ). This increases the types of independent variables to nine. The last three types of independent variables that are part of the DOT solution are the spatial mesh size ( $\Delta r$ ), the number ( $n$ ) of discrete angular segments ( $\Omega_n$ ), and the solution convergence. These variables represent uncertainties in the procedures used to determine the numerical solution. This brings the total number of independent variable types to twelve.

While many of the variable types represent a single uncertainty, the variable types that are functions of the geometric position and energy group represent multiple uncertainties. For example, the uncertainties in the macroscopic cross sections as a function of position include the isotopic concentrations. The uncertainties in the isotopic concentrations and

the confidence levels associated with these uncertainties are different for the pressure vessel steel, thermal shield steel, barrel steel, and the baffle plate steel. This also applies to the downcomer water (between the barrel and vessel), former region water (between the baffle and barrel), and the fuel region water. Thus, the uncertainties in the macroscopic cross sections as a function of position would include seven independent uncertainties for the steel and water isotopic concentrations.

The "Response Function Matrix" step above the "Embrittlement Confidence Level" step in Figure 7-1 represents the sensitivity calculations of vessel fluence and dosimeter activity responses to the uncertainties in the independent variables. The product of (a) the "Transport Model" response functions, and (b) the reactor and neutronic uncertainties defines the biases ( $B_\phi$ ) and standard deviations ( $\sigma_\phi$ ) in the greater than 0.1 MeV and 1.0 MeV calculated fluxes for the vessel and dosimeter activities. The reactor and neutronic uncertainties are determined from the design and fabrication specifications and procedures.

The biases and standard deviations calculated using the DOT Semi - Analytical methodology described in Section 3.0 form the bases for the calculational biases ( $B_C$ ) and standard deviations ( $\sigma_C$ ).



(7.8)

(7.9)

**7.2.1 Biases**

$$B_C = \quad (7.10)$$

$B_C = 0.0$	(7.11)
-------------	--------

**FTI Non-Proprietary**

(7.12)

**FTI Non-Proprietary**

(7.13)

*Dosimeter Activity ( $E \geq .1 \text{ MeV}$ ) =*

(7.14)

7.2.2 Standard Deviations

$$\overline{\sigma_{C/M}} = \quad (7.15)$$

$$\overline{\sigma_{C/M}} =$$

(7.16)

(7.17)

(7.18)



$$\sigma_C (\textit{Activity}) =$$

(7.19)

(7.20)

$$\sigma_C (\text{Dosimetry Fluence}) \leq \quad (7.21)$$

### 7.3 Vessel Fluence Standard Deviations

(7.22)

$$\sigma_C^2 (Vessel) = \quad (7.23)$$

$$\sigma_C (\text{Vessel Fluence}) \leq$$

(7.24)

**Table 7-6**  
**Calculational Fluence Uncertainties**

<u>Type of Calculation</u>	<u>Uncertainty %</u>	
	<u><math>\sigma</math></u>	<u><math>\approx \pm 2 \sigma</math></u>
Capsule (derived from benchmark to measurements)	Standard Deviation	95 % / 95 % Confidence
Pressure Vessel (maximum location, with appropriate benchmark)		
Pressure Vessel (maximum location, long term extrapolation)		

(7.25)

$$\sigma_C \text{ (EOL Vessel Fluence)} \leq$$

(7.26)

**FTI Non-Proprietary**





## 8.0 References

1. David B. Matthews, Project Director, Office of Nuclear Reactor Regulation, United States Nuclear Regulatory Commission, "Cavity Dosimetry Program - Oconee Nuclear Station Units 1, 2, and 3", December 5, 1988, letter to H.B. Tucker Vice President, Duke Power Company.
2. Radiation Shielding Information Center (RSIC), Oak Ridge National Laboratory (ORNL), "BUGLE-80: Coupled 47 Neutron, 20 Gamma-Ray, P<sub>3</sub>, Cross-Section Library for LWR Shielding Calculations", DLC-075, August, 1980.
3. T.J. Burns, et alia, Oak Ridge National Laboratory, "Preliminary Development of an Integrated Approach to the Evaluation of Pressurized Thermal Shock Risk as Applied to the Oconee Unit 1 Nuclear Power Plant", NUREG/CR-3770 (ORNL/TM-9176), May, 1986.
4. D.L. Selby, et alia, Oak Ridge National Laboratory, "Pressurized Thermal Shock Evaluation of the Calvert Cliffs Unit 1 Nuclear Power Plant", NUREG/CR-4022 (ORNL/TM-9408), November, 1985.
5. D.L. Selby, et alia, Oak Ridge National Laboratory, "Pressurized Thermal Shock Evaluation of the H.B. Robinson Unit 2 Nuclear Power Plant", NUREG/CR-4183 (ORNL/TM-9567), November, 1985.
6. Title 10 of the Code of Federal Regulations (CFR), Part 50, Section 50-61, "Fracture Toughness Requirements for Protection Against Pressurized Thermal Shock Events", 10 CFR 50.61, June 30, 1993.
7. Radiation Shielding Information Center (RSIC), Oak Ridge National Laboratory (ORNL), "BUGLE-93: Coupled 47 Neutron, 20 Gamma-Ray Group Cross Section Library Derived from ENDF/B-VI for LWR Shielding and Pressure Vessel Dosimetry Applications", DLC-175, April, 1994.
8. Office of Nuclear Regulatory Research, "Calculational and Dosimetry Methods For Determining Pressure Vessel Neutron Fluence", Draft Regulatory Guide DG-1025, U.S. Nuclear Regulatory Commission, September, 1993.
9. S.Q. King, et alia, "Pressure Vessel Fluence Analysis for 177-FA Reactors", BAW-1485P, Rev. 1, April, 1988.

## FTI Non-Proprietary

10. A.L. Lowe, Jr., K.E. Moore and J.D. Aadland, "Integrated Reactor Vessel Material Surveillance Program", BAW-1543A, Rev. 2, May, 1985.
11. A.L. Lowe, Jr., W.A. Pavinich, W.L. Redd, J.K. Schmotzer and C.L. Whitmarsh, "Analysis of Capsule RS1-B, Sacramento Municipal Utility District, Rancho Seco Unit 1", BAW-1702, February, 1982.
12. C.L. Whitmarsh, "Pressure Vessel Fluence Analysis For 177-FA Reactors", BAW-1485, June, 1978.
13. H.S. Palme, G.S. Carter and C.L. Whitmarsh, "Reactor Vessel Material Surveillance Program, Compliance With 10 CFR 50, Appendix H, For Oconee Class Reactors", BAW-10100A, February, 1975.
14. G.T. Snyder and L.H. Bohn, "Reactor Vessel Material Surveillance Program", BAW-10006, June, 1969.
15. R.L. Simons, L.S. Kellogg, E.P. Lippincott, W.N. McElroy and D.L. Oberg, "Re-Evaluation Of The Dosimetry For Reactor Pressure Vessel Surveillance Capsules", NUREG/CP-0029, Volume 2, Proceedings of the Fourth ASTM-EURATOM Symposium on Reactor Dosimetry, National Bureau of Standards, Gaithersburg, Maryland, March 22-26, 1982.
16. G.L. Guthrie, "Charpy Trend Curves Based On 177 PWR Data Points", NUREG/CR-3391, HEDL-TME 83-22, Volume 2, Hanford Engineering Development Laboratory, LWR Pressure Vessel Surveillance Dosimetry Improvement Program, Progress Report, April 1983 - June 1983.
17. Office of Nuclear Regulatory Research, "Radiation Embrittlement Of Reactor Vessel Materials", Regulatory Guide 1.99, Revision 2, U.S. Nuclear Regulatory Commission, May, 1988.
18. Radiation Shielding Information Center (RSIC), Oak Ridge National Laboratory, "CASK 40 Group Coupled Neutron and Gamma Ray Cross Section Data", DLC-23.
19. Office of Nuclear Regulatory Research, "Calculational And Dosimetry Methods For Determining Pressure Vessel Neutron Fluence", Draft Regulatory Guide DG-1053, U.S. Nuclear Regulatory Commission, June, 1996.

20. S.Q. King, "The B & W Owners Group Cavity Dosimetry Program", BAW-1875-A, July, 1986.
21. R. Gold (MC<sup>2</sup>) and W.N. McElroy (CTS), "Written Comments and Recommendations Related to the Review of the B&WOG (B & W Owners Group) Davis-Besse Cavity Dosimetry Benchmark Program", October, 1992.
22. Office of Nuclear Regulatory Research, "Format And Content Of Plant-Specific Pressurized Thermal Shock Safety Analysis Reports For Pressurized Water Reactors", Regulatory Guide 1.154, U.S. Nuclear Regulatory Commission, January, 1987. (See References 3, 4 and 5 for specific results.)
23. L.A. Hassler, et alia, "DOT4.3, Two Dimensional Discrete Ordinates Transport Code", (B & W Version of RISC/ORNL Code DOT4.3), July, 1986.
24. Jimmy L. Coor, "Analysis of B&W Owner's Group Davis Besse Cavity Dosimetry Benchmark Experiment", Volumes I, II and III, B & W Nuclear Environmental Services, Inc. (NESI), May, 1993.
25. Brian M. Oliver, "Helium Analyses of Al-Li and Beryllium HAFMs", B & W Contract, Rockwell International Corporation, January 23, 1992.
26. W.R. Dixon, "Self-Absorption Corrections for Larger Gamma Ray Sources", NUCLEONICS, Volume 8, Number 4, Page 69, April, 1951.
27. R.D. Evans and R.O. Evans, "Studies of Self-Absorption in Gamma-Ray Sources", Reviews of Modern Physics, 20, Pages 305-326, January, 1948.
28. E. Storm and H.I. Israel, "Photon Cross-Sections from .001 to 1.00 MeV for Elements 1 through 100", Los Alamos Scientific Laboratory, Los Alamos, NM, LA-3753, UC-34, PHYSICS, TID-4500, June, 1967.
29. T.G. Williamson and A.C. Chubb, "Niobium Foil, Counting and Correction for Niobium X-rays from Trace Isotopes", UVA/532886/NEEP 90/102, Department of Nuclear Engineering and Engineering Physics, University of Virginia, Charlottesville, Virginia, August, 1989.

## FTI Non-Proprietary

30. \* F.H. Ruddy and J.G. Seidel, "As-Built Data for Westinghouse R&D Supplied Babcock & Wilcox Solid State Track Recorder Neutron Dosimeters", Westinghouse R&D Report 88-2S31-SSTRB-R4, July 28, 1988.
31. \* F.H. Ruddy, "Updated Mass Tables for Babcock & Wilcox Ultra Low-Mass Solid State Track Recorder Fissionable Deposits", Westinghouse R&D Report 88-2S31-SSTRB-R3, August 24, 1988.
32. \* F.H. Ruddy, et alia, "Neutron Dosimetry Results for Solid State Track Recorders Irradiated in the B&WOG Cavity Dosimetry Benchmark Experiment", STC Report 93-2TD1-BWSCN-R1, Westinghouse STC, March, 1993.
33. Jimmy L. Coor, "Uncertainty Assessment And Results of Niobium Analysis for Davis-Besse Cavity Dosimetry Benchmark Experiment", Volumes I, II and III, B & W Nuclear Environmental Services, Inc. (NESI), July, 1993.
34. P.N. Randall, "Basis for Revision 2 of the U.S. Nuclear Regulatory Commission's Regulatory Guide 1.99", Radiation Embrittlement of Nuclear Reactor Pressure Vessel Steels: An International Review (Second Volume), ASTM STP 909, American Society for Testing and Materials, Philadelphia, 1986.
35. H.A. Hassan, et alia, "Power Peaking Nuclear Reliability Factors", BAW-10119P-A, February, 1979.
36. A.B. Copsey, et alia, "Statistical Core Design For B & W Designed 177 FA Plants", BAW-10187P-A, March, 1994.
37. W.N. McElroy, "LWR Pressure Vessel Surveillance Dosimetry Improvement Program: PCA Experiments And Blind Test", Hanford Engineering Development Laboratory, NUREG/CR-1861 (HEDL-TME 80-87), July, 1981.

\*Only for information, the SSTR results are not qualified measurements.

**Appendix A FTI's Dosimetry Database**

This appendix contains two tables with FTI's database of dosimeter measurements, calculations, and benchmarks. It also contains an independent reference section identifying the appropriate sources of the measurements and calculations.

Table A-1 lists the 728 dosimeter measurements and calculations that have been qualified with uncertainty evaluations. The table is organized alphabetically by the plant name and capsule first, and then alphabetically by the plant name and cavity. The numerical reference (Ref.) for the data is noted. Each dosimeter position and target material is also noted. The measured and calculated results are defined in terms of micro-Curies per gram of the target material except for the beryllium - helium accumulation monitors (HAFMs) which are defined in terms of helium atom-parts per billion atoms of beryllium.

Table A-2 lists the  $C / M$  ratios for the 39 capsule and cavity dosimetry data-sets that represent the greater than 0.1 MeV reactions. These ratios are determined from Equations 7.12 and 7.13 as discussed in Section 7.2 . In addition, the mean random deviation ( $\Delta_{C/M}$ ) for each data-set is listed. The standard deviations are determined from Equations 7.10, 7.11 and 7.15, which are also discussed in Section 7.2 . The results indicate that there is no benchmark bias in the database, and the root mean square standard deviation is

**Table A-1 FTI Benchmark Database**

**Table A-2 Benchmark Comparison of *C/M***



**Table A-2 (Continued)**

***Appendix A* References**

- [1] BAW-1698, "Analysis of Capsule ANI-B, Arkansas Power & Light Company, Arkansas Nuclear One, Unit 1", A. L. Lowe, et. al., November 1981
  
- [2] BAW-2075, Rev. 1, "Analysis of Capsule AN1-C, Arkansas Power & Light Company, Arkansas Nuclear One, Unit 1", A.L. Lowe, Jr., L. Petrusha, et. al., October, 1989.
  
- [3] BAW-1440, "Analysis of Capsule AN1-E from Arkansas Power and Light Company, Arkansas Nuclear One Unit 1", A. L. Lowe, et al., April, 1977
  
- [4] BAW-2199, "Analysis of Capsule 97° Baltimore Gas & Calvert Cliffs Nuclear Power Plant Unit No. 2.," A.L. Lowe, Jr., D.J. Skulina, et. al., February 1994.
  
- [5] BAW-2049, "Analysis of Capsule CR3-F Florida Power Corporation Crystal River Unit-3," A.L. Lowe, Jr., L.B Wimmer, et. al., September 1988.
  
- [6] BAW-1910P, "Analysis of CR3-LG1", A. L. Lowe, et al., August, 1986.
  
- [7] BAW-2254P, "Test Results of Capsule CR3-LG2, B&W Owners Group", M. J. Devan, et al., October, 1995
  
- [8] BAW-2205-00, "B&WOG Cavity Dosimetry Benchmark Program Summary Report," J.R. Worsham III, et. al., December 1994.
  
- [9] BAW-2208, "Fracture Toughness Test Results from Capsule TE1-D The Toledo Edison Company Davis-Besse Nuclear Power Station Unit 1," A.L. Lowe Jr., et. al., October 1993.
  
- [10] BAW-1719, "Fracture Toughness Test Results from Capsule TE1-F The Toledo Edison Company Davis-Besse Nuclear Power Station Unit 1," A.L. Lowe Jr., et. al., March 1982.

- [11] BAW-1920P, "Analysis of Capsule DB1-LG1", A. L. Lowe, et al., October, 1986
  
- [12] BAW-2142, "Analysis of Capsule W-104 Northeast Nuclear Energy Company Millstone Nuclear Power Station, Unit No. 2," A.L. Lowe Jr., et. al., November 1991
  
- [13] Same as Reference [12]
  
- [14] BAW-2277, "Test Results of Capsule W, Northern States Power Company, Monticello Nuclear Generating Plant, (Irradiated at Prairie Island Unit 1)", M.J. DeVan and D.J. Skulina, June, 1996.
  
- [15] BAW-1638, "Analysis of Capsule V Virginia Electric & Power Company North Anna Unit No. 1," A.L. Lowe Jr., et. al., May 1981.
  
- [16] Baw-1794, "Analysis of Capsule V Virginia Electric & Power Company North Anna Unit No. 2," A.L. Lowe Jr., et. al., May 1981.
  
- [17] BAW-2050, "Analysis of Capsule OC1-C Duke Power Company Oconee Nuclear Station Unit-1," A.L. Lowe Jr., S.Q. King, et. al., October 1988.
  
- [18] BAW-1436, "Analysis of Capsule OC1-E Duke Power Company Oconee Nuclear Station 1," A.L. Lowe Jr., et. al., September 1977.
  
- [19] BAW-1699, "Analysis of Capsule OCII-A From Duke Power Company's Oconee Nuclear Station Unit 2," A.L. Lowe Jr., J.W. Ewing, et. al., December 1981.
  
- [20] BAW-1437, "Analysis of Capsule OCII-C From Duke Power Company Oconee Nuclear Station Unit 2," A.C. Cone Jr., ET Chulick, et. al., May 1977.
  
- [21] BAW-2051, "Analysis of Capsule OCII-E Duke Power Company Oconee Nuclear Station Unit-2," A.L. Lowe, Jr., L. Petrusa, et al., October, 1988.

## FTI Non-Proprietary

- [22] BAW-1438, "Analysis of Capsule OCIII-A From Duke Power Company Oconee Nuclear Station Unit 3," A.L. Lowe Jr., E. T. Chulick, et. al., July 1977.
- [23] BAW-1697, "Analysis of Capsule OCIII-B From Duke Power Company Oconee Nuclear Station, Unit 3," A.L. Lowe Jr., J.W. Ewing, et. al., October 1981.
- [24] BAW-2128, Rev. 1, "Analysis of Capsule OCIII-D, Duke Power Company, Oconee Nuclear Station, Unit-3", A.L. Lowe Jr., M.A. Rutherford, et. al., May, 1992.
- [25] NUREG/CR-1861, "LWR Pressure Vessel Surveillance Dosimetry Improvement Program: PCA Experiments and Blind Test," W.N. McElroy, Hanford Engineering Development Laboratory, HEDL-TME 80-87, July 1981.
- [26] BAW-1702, "Analysis of Capsule RS1-B Sacramento Municipal Utility District Rancho Seco Unit 1," A.L. Lowe, W. A. Pavinich, et. al., February 1982.
- [27] BAW-1792, "Analysis of RS1-D Sacramento Municipal Utility District Rancho Seco Unit 1," A.L. Lowe, L.L. Collins, et. al., October 1983.
- [28] BAW-2074, "Analysis of Capsule RS1-F Sacramento Municipal Utility District Rancho Seco Unit 1," A.L. Lowe, J.D. Aadland, et. al., April 1989.
- [29] BAW-2083, "Analysis of Capsule U Carolina Power & Light Company Shearon Harris Unit No. 1," A.L. Lowe Jr., J.D. Aadland, et. al., August 1989.
- [30] BAW-1880, "Analysis of Capsule W-83 Florida Power & Light Company St. Lucie Plant Unit No. 2," A.L. Lowe Jr., L. L. Collins, et. al., September 1985.
- [31] BAW-1439, "Analysis of Capsule TMI-1E From Metropolitan Edison Company Three Mile Island Nuclear Station-Unit 1," A.L. Lowe Jr., E.T. Chulick, et. al., January, 1977.

**FTI Non-Proprietary**

- [32] BAW-2253P, "Test Results of Capsule TMI2-LG1, B&W Owners Group", M. J. DeVan, et al., October, 1995.
- [33] BAW-2177, "Analysis of Capsule W-97, Waterford Generating Station, Unit 3", A. L. Lowe, et al., November, 1992.
- [34] BAW-2082, "Analysis of Capsule Y, Zion Nuclear Plant Unit 1", A. L. Lowe, et al., March, 1990.
- [35] "ANO-PT Fluence Results", (Cycles 10,11,12), S.Q. King, released July 17,1996.

***Appendix B* Measured Dosimetry Results**

The measured dosimetry results that have been discussed in Section 5 are presented in this appendix.

Table B-1.1-1  $^{238}\text{U}$  ( $n, f$ )  $^{137}\text{Cs}$  Activities

Location	Form	Measured Activity $\mu\text{Ci/gm}$	Correction Factors			Corrected Measured Activity $\mu\text{Ci/gm}$
			Photofission	U-235	Geom. and Self Abs. <sup>(a)</sup>	
G5	Foil	8.574-03	0.9680	1.000	1.000	8.300-03
K4	V-Encap.	1.190-02	0.9680	1.000	0.7948	9.155-03
F5	V-Encap.	1.060-02	0.9680	1.000	0.9073	9.310-03
S5	V-Encap.	8.274-03	0.9680	1.000	0.9077	7.270-03
H5	Powder	8.402-03	0.9680	1.000	1.000	8.133-03
L4	Powder	8.253-03	0.9680	1.000	1.000	7.989-03
L4	Powder	8.543-03	0.9680	1.000	1.000	8.270-03
L1	Powder	8.998-03	0.9680	1.000	1.000	8.710-03
G5	U/Al	1.096-02	0.9680	0.9074	0.9198	8.855-03
J5	U/Al	1.144-02	0.9680	0.9074	0.9184	9.228-03
M3	U/Al	1.093-02	0.9680	0.9074	0.9168	8.802-03
M4	U/Al	1.167-02	0.9680	0.9074	0.9170	9.400-03
N4	U/Al	1.017-02	0.9680	0.9074	0.9182	8.203-03
P4	U/Al	9.306-03	0.9680	0.9074	0.9158	7.485-03
P4	U/Al	1.026-02	0.9680	0.9074	0.9188	8.280-03
P5	U/Al	9.474-03	0.9680	0.9074	0.9196	7.653-03
CD1	U/Al	3.743	0.9500	0.9520	0.9576	3.242

(a) Ratio of total correction factor using Monte Carlo method-to-total factor using standard method.

Table B-1.1-1 (Cont'd)  $^{238}\text{U}$  ( $n, f$ )  $^{137}\text{Cs}$  Activities

Location	Form	Measured Activity $\mu\text{Ci/gm}$	Correction Factors			Corrected Measured Activity $\mu\text{Ci/gm}$
			Photofission	U-235	Geom. and Self Abs. <sup>(a)</sup>	
CD1	U/AI	3.743	0.9500	0.9520	0.9576	3.242
CD2	U/AI	1.987	0.9500	0.9520	0.9586	1.723
CD3	U/AI	3.052	0.9500	0.9520	0.9573	2.642
CD4	U/AI	2.936	0.9500	0.9520	0.9610	2.552
ED1	U/AI	2.147	0.9500	0.9520	0.9667	1.877
ED2	U/AI	3.995	0.9500	0.9520	0.9600	3.469
ED3	U/AI	3.081	0.9500	0.9520	0.9595	2.674
ED4	U/AI	3.021	0.9500	0.9520	0.9564	2.613

(b) Ratio of total correction factor using Monte Carlo method-to-total factor using standard method.



Table B-1.1-2  $^{237}\text{Np}$  ( $n, f$ )  $^{137}\text{Cs}$  Activities

Location	Form	Measured Activity $\mu\text{Ci/gm}$	Correction Factor Photofission	Correction for Geom. & Self Absorp. Factors <sup>(a)</sup>	Corrected Measured Activity $\mu\text{Ci/gm}$
F5	V-Encap.	1.505-01	0.994	0.9527	1.425-01
K4	V-Encap.	1.402-01	0.994	0.9527	1.328-01
S5	V-Encap.	1.196-01	0.994	0.9527	1.133-01
H5	Oxide Powder	1.523-01	0.994	1.000	1.514-01
N5	Oxide Powder	1.714-01	0.994	1.000	1.704-01
N5	Oxide Powder	1.984-01	0.994	1.000	1.972-01
G5	Np/Al Wire	1.620-01	0.994	0.9074	1.461-01
J5	Np/Al Wire	1.414-01	0.994	0.9186	1.291-01
M3	Np/Al Wire	1.629-01	0.994	0.9262	1.500-01
M4	Np/Al Wire	1.666-01	0.994	0.9263	1.534-01
N4	Np/Al Wire	1.356-01	0.994	0.9634	1.299-01
P4	Np/Al Wire	1.494-01	0.994	0.9702	1.441-01
P4	Np/Al Wire	1.473-01	0.994	0.9262	1.356-01
P5	Np/Al Wire	1.520-01	0.994	0.9279	1.402-01

(a) Ratio of total correction factor using Monte Carlo method-to-total factor using standard method.

Table B-1.1-2 (Cont'd)  $^{237}\text{Np}$  ( $n, f$ )  $^{137}\text{Cs}$  Activities

Location	Form	Measured Activity $\mu\text{Ci/gm}$	Correction Factor Photofission	Correction for Geom. & Self Absorp. Factors <sup>(a)</sup>	Corrected Measured Activity $\mu\text{Ci/gm}$
CD1	Np/Al Wire	2.180+01	0.980	0.9642	2.060+01
CD2	Np/Al Wire	1.247+01	0.980	0.9629	1.177+01
CD3	Np/Al Wire	1.702+01	0.980	0.9617	1.604+01
CD4	Np/Al Wire	1.660+01	0.980	0.9686	1.576+01
ED1	Np/Al Wire	1.319+01	0.980	0.9678	1.251+01
ED2	Np/Al Wire	2.180+01	0.980	0.9649	2.061+01
ED3	Np/Al Wire	1.764+01	0.980	0.9668	1.671+01
ED4	Np/Al Wire	1.455+01	0.980	0.9683	1.381+01

(a) Ratio of total correction factor using Monte Carlo method-to-total factor using standard method.

Table B-1.1-3  $^{235}\text{U}$  ( $n, f$ )  $^{137}\text{Cs}$  Activities

Location	Form	Measured Activity $\mu\text{Ci/gm}$	Correction for Geom. and Self Absorp. Factor <sup>(a)</sup>	Corrected Measured Act. $\mu\text{Ci/gm}$
K4	Vanadium Encap.	2.998	0.8896	2.667

<sup>(a)</sup> Ratio of total factor using Monte Carlo method-to-total factor using standard method.

Table B-1.2-4  $^{54}\text{Fe} (n, p) ^{54}\text{Mn}$  Activities

Location	Form	Foil Thickness or Wire Diam. cm	Post Irrad. Mass gm	Geometry Factor	Self Absorp. Factor	Activity $\mu\text{Ci}/\text{gram Target}$
A1	Foil	0.0127	0.14325	0.9913	1.0033	6.042-03
A2	Foil	0.0127	0.13813	0.9913	1.0033	6.179-03
A4	Foil	0.0127	0.14265	0.9913	1.0033	7.821-03
A5	Foil	0.0127	0.14175	0.9913	1.0033	8.252-03
B1	Foil	0.0787	0.78719	0.9431	1.0204	5.130-02
B2	Foil	0.0127	0.14115	0.9913	1.0033	5.316-02
B4	Foil	0.1270	1.22253	0.9189	1.0330	5.440-02
B5	Foil	0.0127	0.14058	0.9913	1.0033	5.645-02
C1	Foil	0.0127	0.14097	0.9913	1.0033	8.116-02
C2	Foil	0.0127	0.13646	0.9913	1.0033	7.980-02
C4	Foil	0.0127	0.14345	0.9913	1.0033	7.002-02
C5	Foil	0.0127	0.14171	0.9913	1.0033	6.999-02
D1	Foil	0.0787	0.79610	0.9481	1.0204	8.443-01
D2	Foil	0.0127	0.14241	0.9913	1.0033	8.734-01
D4	Foil	0.0127	0.14036	0.9913	1.0033	9.927-01
D5	Foil	0.1270	1.21763	0.9480	1.0330	9.957-01
E1	Foil	0.0127	0.13976	0.9913	1.0033	1.495+00
E4	Foil	0.0127	0.14265	0.9913	1.0033	1.295+00
E5	Foil	0.0127	0.14042	0.9913	1.0033	1.256+00

Table B-1.2-4 (Cont'd)  $^{54}\text{Fe} (n, p) ^{54}\text{Mn}$  Activities

Location	Form	Foil Thickness or Wire Diam. cm	Post Irrad. Mass gm	Geometry Factor	Self Absorp. Factor	Activity $\mu\text{Ci/gram Target}$
F1	Foil	0.0127	0.14339	0.9945	1.0033	2.782+00
F3	Foil	0.0127	0.13879	0.9945	1.0033	2.733+00
F5	Foil	0.0100	0.06435	0.9957	1.0026	2.737+00
G1	Foil	0.0787	0.79179	0.9895	1.0204	2.662+00
G2	Foil	0.0127	0.14382	0.9945	1.0033	2.793+00
G5	Foil	0.0787	0.79280	0.9671	1.0204	2.673+00
H1	Foil	0.0127	0.13649	0.9945	1.0033	2.440+00
H4	Foil	0.0127	0.14139	0.9945	1.0033	2.471
J1	Foil	0.0127	0.14065	0.9945	1.0033	2.871
J3	Foil	0.0127	0.14139	0.9945	1.0033	2.828
J4	Foil	0.0127	0.14178	0.9945	1.0033	2.847
K2	Foil	0.0127	0.13949	0.9945	1.0033	2.875
K3	Foil	0.0152	0.11777	0.9935	1.0039	2.744
K5	Foil	0.0127	0.14324	0.9945	1.0033	2.748
M1	Foil	0.0787	0.79210	0.9895	1.0204	2.812
M2	Foil	0.0127	0.14172	0.9945	1.0033	2.951
M2	Foil	0.0127	0.14285	0.9945	1.0033	2.972
M3	Foil	0.0787	0.79605	0.9671	1.0204	2.823
M4	Foil	0.0127	0.13842	0.9945	1.0033	2.921
M5	Foil	0.0127	0.13748	0.9945	1.0033	2.898

Table B-1.2-4 (Cont'd)  $^{54}\text{Fe} (n, p) ^{54}\text{Mn}$  Activities

Location	Form	Foil Thickness or Wire Diam. cm	Post Irrad. Mass gm	Geometry Factor	Self Absorp. Factor	Activity $\mu\text{Ci}/\text{gram}$ Target
N2	Foil	0.0127	0.13930	0.9945	1.0033	2.490
N3	Foil	0.0127	0.14212	0.9945	1.0033	2.505
P2	Foil	0.0127	0.13991	0.9945	1.0033	2.411
Q1	Foil	0.0127	0.14314	0.9945	1.0033	2.240
Q2	Foil	0.0127	0.14132	0.9945	1.0033	2.234
Q3	Foil	0.0127	0.14183	0.9945	1.0033	2.308
Q4	Foil	0.0127	0.13992	0.9945	1.0033	2.316
R1	Foil	0.0127	0.13771	0.9913	1.0033	1.439-02
R4	Foil	0.0127	0.14442	0.9913	1.0033	5.967-03
S1	Foil	0.0127	0.14320	0.9945	1.0033	2.168
S3	Foil	0.0127	0.13941	0.9945	1.0033	2.149
S5	Foil	0.0100	0.06403	0.9957	1.0026	2.189
T1	Foil	0.1270	1.23099	0.9831	1.0330	2.013
T2	Foil	0.0127	0.13932	0.9945	1.0033	2.161
T4	Foil	0.1270	1.22934	0.9480	1.0330	2.113
T5	Foil	0.0127	0.14131	0.9945	1.0033	2.065
U4	Foil	0.0127	0.14429	0.9945	1.0033	2.046
G2	Wire	0.1000	0.15818	0.9585	1.0215	2.789
J1	Wire	0.1000	0.16197	0.9585	1.0215	2.895

Table B-1.2-4 (Cont'd)  $^{54}\text{Fe} (n, p) ^{54}\text{Mn}$  Activities

Location	Form	Foil Thickness or Wire Diam. cm	Post Irrad. Mass gm	Geometry Factor	Self Absorp. Factor	Activity $\mu\text{Ci/gram Target}$
M1	Wire	0.1000	0.18389	0.9585	1.0215	2.949
M2	Wire	0.1000	0.21186	0.9585	1.0215	2.956
N2	Wire	0.1000	0.18805	0.9585	1.0215	2.582
P1	Wire	0.1000	0.18140	0.9585	1.0215	2.536
P1	Wire	0.1000	0.18563	0.9585	1.0215	2.435
P2	Wire	0.1000	0.18198	0.9585	1.0215	2.468
CD1	Wire	0.1022	0.15049	0.9965	1.0224	1.151+03
CD2	Wire	0.0991	0.15723	0.9966	1.0218	6.636+02
CD3	Wire	0.1015	0.15161	0.9965	1.0223	9.745+02
CD4	Wire	0.0995	0.15122	0.9966	1.0218	9.676+02
ED1	Wire	0.0991	0.15266	0.9966	1.0218	7.204+02
ED2	Wire	0.0986	0.15217	0.9966	1.0217	1.279+03
ED3	Wire	0.0998	0.14954	0.9966	1.0219	1.002+03
ED4	Wire	0.0991	0.14503	0.9966	1.0218	1.001+03

Table B-1.2-5  $^{58}\text{Ni}$  ( $n, p$ )  $^{58}\text{Co}$  Activities

Location	Form	Foil Thickness or Wire Diam. cm	Post Irrad. Mass gm	Geometry Factor	Self Absorp. Factor	Activity $\mu\text{Ci/gm}$ Target
A5	Foil	0.0254	0.28640	0.9892	1.0078	1.904-02
B4	Foil	0.0254	0.29551	0.9892	1.0078	1.233-01
B5	Foil	0.0254	0.28837	0.9892	1.0078	1.293-01
C4	Foil	0.0254	0.28646	0.9892	1.0078	1.671-01
D4	Foil	0.0254	0.28743	0.9892	1.0078	2.230
D5	Foil	0.0254	0.29485	0.9892	1.0078	2.281
F3	Foil	0.0254	0.28497	0.9966	1.0078	5.934
F5	Foil	0.0100	0.06733	0.9957	1.0030	6.048
G5	Foil	0.0254	0.28600	0.9892	1.0078	5.984
K1	Foil	0.0254	0.28579	0.9892	1.0078	6.179
M3	Foil	0.0254	0.29453	0.9892	1.0078	6.319
M4	Foil	0.0254	0.28607	0.9892	1.0078	6.342
N3	Foil	0.0254	0.28891	0.9892	1.0078	5.400
Q3	Foil	0.0252	0.28534	0.9892	1.0077	5.096
R4	Foil	0.0254	0.28535	0.9892	1.0078	2.277-02
S3	Foil	0.0254	0.28707	0.9892	1.0078	4.749
S5	Foil	0.0100	0.06725	0.9957	1.0030	4.772
T4	Foil	0.0254	0.29587	0.9892	1.0078	4.525
T5	Foil	0.0254	0.28789	0.9892	1.0078	4.566
U4	Foil	0.0252	0.28680	0.9892	1.0077	4.547



Table B-1.2-5 (Cont'd)  $^{58}\text{Ni} (n, p) ^{58}\text{Co}$  Activities

Location	Form	Foil Thickness or Wire Diam. cm	Post Irrad. Mass gm	Geometry Factor	Self Absorp. Factor	Activity $\mu\text{Ci/gm}$ Target
G5	Wire	0.1000	0.16340	0.9585	1.0255	5.818
J5	Wire	0.1000	0.17211	0.9585	1.0255	6.361
M3	Wire	0.1000	0.15196	0.9585	1.0255	6.313
M4	Wire	0.1000	0.16498	0.9585	1.0255	6.349
N4	Wire	0.1000	0.18124	0.9585	1.0255	5.492
P4	Wire	0.1000	0.14984	0.9585	1.0255	5.329
P4	Wire	0.1000	0.15580	0.9585	1.0255	5.376
P5	Wire	0.1000	0.16184	0.9585	1.0255	5.415
CD1	Wire	0.1007	0.13366	0.9965	1.0262	2.417+03
CD2	Wire	0.1002	0.12979	0.9966	1.0261	1.418+03
CD3	Wire	0.1003	0.12543	0.9965	1.0261	2.129+03
CD4	Wire	0.0991	0.11901	0.9966	1.0258	2.087+03
ED1	Wire	0.0991	0.13555	0.9966	1.0258	1.575+03
ED2	Wire	0.1001	0.12927	0.9966	1.0261	2.762+03
ED3	Wire	0.1002	0.12784	0.9965	1.0261	2.138+03
ED4	Wire	0.0992	0.13288	0.9966	1.0258	2.161+03

Table B-1.2-6  $^{63}\text{Cu} (n, \alpha) ^{60}\text{Co}$  Activities

Location	Form	Foil Thickness or Wire Diam. cm	Post Irrad. Mass gm	Geometry Factor	Self Absorp. Factor	Activity $\mu\text{Ci/gm}$ Target
A5	Foil	0.0254	0.28902	0.9827	1.0058	2.747-05
A5	Foil	0.0254	0.28974	0.9827	1.0058	1.683-05
A5	Foil	0.0254	0.28935	0.9827	1.0058	4.019-05
B5	Foil	0.0254	0.28888	0.9827	1.0058	8.772-05
B5	Foil	0.0254	0.29017	0.9827	1.0058	9.480-05
C4	Foil	0.0254	0.28958	0.9827	1.0058	1.269-04
C4	Foil	0.0254	0.28938	0.9827	1.0058	1.256-04
D4	Foil	0.0254	0.28951	0.9827	1.0058	2.595-03
F3	Foil	0.0254	0.28925	0.9827	1.0058	7.552-03
F5	Foil	0.0100	0.07052	0.9931	1.0023	7.339-03
K3	Foil	0.0254	0.27214	0.9827	1.0058	7.698-03
M4	Foil	0.0254	0.28933	0.9827	1.0058	8.098-03
N3	Foil	0.0254	0.28909	0.9827	1.0058	6.709-03
Q3	Foil	0.0254	0.28951	0.9827	1.0058	6.549-03
R4	Foil	0.0254	0.28938	0.9827	1.0058	5.416-05
R4	Foil	0.0254	0.28933	0.9827	1.0058	2.526-05
R4	Foil	0.0254	0.28937	0.9827	1.0058	2.312-05
S3	Foil	0.0254	0.28922	0.9827	1.0058	5.848-03
S5	Foil	0.0100	0.06988	0.9931	1.0023	5.817-03
T5	Foil	0.0254	0.28950	0.9827	1.0058	5.662-03

Table B-1.2-6 (Cont'd)  $^{63}\text{Cu} (n, \alpha) ^{60}\text{Co}$  Activities

Location	Form	Foil Thickness or Wire Diam. cm	Post Irrad. Mass gm	Geometry Factor	Self Absorp. Factor	Activity $\mu\text{Ci/gm}$ Target
U4	Foil	0.0254	0.28947	0.9827	1.0058	5.585-03
B4	Wire	0.0508	0.36395	0.9659	1.0096	8.087-05
D5	Wire	0.0508	0.36293	0.9659	1.0096	2.671-03
G5	Wire	0.0508	0.33822	0.9659	1.0096	7.557-03
M3	Wire	0.0508	0.34589	0.9659	1.0096	7.923-03
T4	Wire	0.0508	0.38800	0.9659	1.0096	5.573-03

Table B-1.2-7  $^{46}\text{Ti} (n, p) ^{46}\text{Sc}$  Activities

Location	Form	Foil Thickness cm	Post Irrad. Mass gm	Geometry Factor	Self Absorp. Factor	Activity $\mu\text{Ci/gm}$ Target
B4	Foil	0.0254	0.15712	0.9827	1.0032	1.409-02
B4	Foil	0.0254	0.15750	0.9827	1.0032	1.384-02
D5	Foil	0.0254	0.15703	0.9827	1.0032	3.946-01
D5	Foil	0.0254	0.15763	0.9986	1.0032	3.209-01*
F5	Foil	0.0127	0.04746	0.9913	1.0016	1.053
G5	Foil	0.0254	0.15748	0.9986	1.0032	1.028*
K1	Foil	0.0381	0.03567	0.9742	1.0048	1.062
M3	Foil	0.0254	0.15761	0.9986	1.0032	1.235*
S5	Foil	0.0127	0.04711	0.9913	1.0016	8.186-01
T4	Foil	0.0254	0.15799	0.9986	1.0032	8.835-01*
T4	Foil	0.0254	0.15765	0.9986	1.0032	9.119-01*

\* Low Counts: Therefore, high counting statistics error possible.

Table B-1.2-8  $^{109}\text{Ag} (n, \gamma) ^{110\text{m}}\text{Ag}$  Activities

Location	Form	Foil Thickness or Wire Diam. cm	Post Irrad. Mass gm	Geometry Factor	Self Absorp. Factor	Activity $\mu\text{Ci/gm Target}$
B1	Wire Alloy 0.147 wt% Ag	0.0508	0.09931	0.9785	1.0043	1.468+02
B4	Wire Alloy 0.147 wt% Ag	0.0508	0.10515	0.9785	1.0043	1.258+02
D1	Wire Alloy 0.147 wt% Ag	0.0508	0.10112	0.9785	1.0043	3.300+02
G1	Wire Alloy 0.147 wt% Ag	0.0508	0.07823	0.9785	1.0043	5.679+02
G5	Wire Alloy 0.147 wt% Ag	0.0508	0.09304	0.9785	1.0043	4.588+02
M1	Wire Alloy 0.147 wt% Ag	0.0508	0.08967	0.9785	1.0043	6.062+02
M3	Wire Alloy 0.147 wt% Ag	0.0508	0.09431	0.9785	1.0043	4.861+02
T1	Wire Alloy 0.147 wt% Ag	0.0508	0.10820	0.9785	1.0043	5.953+02
K1	Foil Alloy 4.65 wt% Ag	0.0127	0.04139	0.9983	1.0013	6.828+02

Table B-1.2-9 Cobalt/Aluminum  $^{59}\text{Co}$  ( $n, \gamma$ )  $^{60}\text{Co}$  Activities

Location	Form	Foil Thickness or Wire Diam. cm	Post Irrad. Mass gm	Geometry Factor	Self Absorp. Factor	Activity $\mu\text{Ci/gm}$ Target
B1	Wire 0.117 wt% Co	0.0508	0.10352	0.9785	1.0030	1.126+02
B4	Wire 0.496 wt% Co	0.0508	0.09817	0.9785	1.0030	6.187+01
D1	Wire 0.117 wt% Co	0.0508	0.10730	0.9785	1.0030	2.605+02
D5	Wire 0.496 wt% Co	0.0508	0.09804	0.9785	1.0030	1.452+02
G1	Wire 0.117 wt% Co	0.0508	0.08711	0.9785	1.0030	4.727+02
G2	Wire 0.66 wt% Co	0.0762	0.01562	0.9681	1.0045	4.652+02
G5	Wire 0.117 wt% Co	0.0508	0.10295	0.9785	1.0030	2.034+02
G5	Wire 0.66 wt% Co	0.0762	0.01848	0.9681	1.0045	1.957+02
J1	Wire 0.66 wt% Co	0.0762	0.01558	0.9681	1.0045	5.262+02
J5	Wire 0.66 wt% Co	0.0762	0.01950	0.9681	1.0045	2.076+02
M1	Wire 0.117 wt% Co	0.0508	0.10272	0.9785	1.0030	5.278+02
M1	Wire 0.66 wt% Co	0.0762	0.01529	0.9681	1.0045	5.218+02

Table B-1.2-9 (Cont'd) Cobalt/Aluminum  $^{59}\text{Co}$  ( $n, \gamma$ )  $^{60}\text{Co}$  Activities

Location	Form	Foil Thickness or Wire Diam. cm	Post Irrad. Mass gm	Geometry Factor	Self Absorp. Factor	Activity $\mu\text{Ci/gm}$ Target
M2	Wire 0.66 wt% Co	0.0762	0.01631	0.9681	1.0045	5.082+02
M3	Wire 0.117 wt% Co	0.0508	0.10284	0.9785	1.0030	2.093+02
M3	Wire 0.66 wt% Co	0.0762	0.01800	0.9681	1.0045	2.076+02
M4	Wire 0.66 wt% Co	0.0762	0.01932	0.9681	1.0045	1.998+02
N2	Wire 0.66 wt% Co	0.0762	0.01640	0.9681	1.0045	4.450+02
N4	Wire 0.66 wt% Co	0.0762	0.01877	0.9681	1.0045	1.956+02
P1	Wire 0.66 wt% Co	0.0762	0.01594	0.9681	1.0045	4.009+02
P1	Wire 0.66 wt% Co	0.0762	0.01524	0.9681	1.0045	3.993+02
P2	Wire 0.66 wt% Co	0.0762	0.01557	0.9681	1.0045	4.024+02
P4	Wire 0.66 wt% Co	0.0762	0.01792	0.9681	1.0045	1.849+02
P4	Wire 0.66 wt% Co	0.0762	0.01803	0.9681	1.0045	1.889+02
P5	Wire 0.66 wt% Co	0.0762	0.01838	0.9681	1.0045	1.889+02

Table B-1.2-9 (Cont'd) Cobalt/Aluminum  $^{59}\text{Co}$  ( $n, \gamma$ )  $^{60}\text{Co}$  Activities

Location	Form	Foil Thickness or Wire Diam. cm	Post Irrad. Mass gm	Geometry Factor	Self Absorp. Factor	Activity $\mu\text{Ci/gm}$ Target
T1	Wire 0.496 wt% Co	0.0508	0.10491	0.9785	1.0030	5.884+02
T4	Wire 0.496 wt% Co	0.0508	0.10682	0.9785	1.0030	2.250+02
F5	Foil 1.0 wt% Co	0.0100	0.02263	0.9957	1.0007	2.798+02
K3	Foil 0.54 wt% Co	0.0127	0.04395	0.9945	1.0009	2.029+02
S5	Foil 1.0 wt% Co	0.0100	0.02270	0.9957	1.0007	2.803+02



Table B-1.2-9 (Cont'd) Cobalt/Aluminum  $^{59}\text{Co}$  ( $n, \gamma$ )  $^{60}\text{Co}$  Activities

Location	Form	Foil Thickness or Wire Diam. cm	Post Irrad. Mass gm	Geometry Factor	Self Absorp. Factor	Activity $\mu\text{Ci/gm}$ Target
CD1	Bare Wire 0.66 wt% Co	0.0759	0.01674	0.9974	1.0046	1.972+05
CD2	Bare Wire 0.66 wt% Co	0.0765	0.01602	0.9974	1.0047	1.014+05
CD3	Bare Wire 0.66 wt% Co	0.0781	0.01544	0.9673	1.0046	3.985+01
CD4	Bare Wire 0.66 wt% Co	0.0759	0.01516	0.9974	1.0046	1.510+05
ED1	Bare Wire 0.66 wt% Co	0.0759	0.01538	0.9682	1.0045	2.407+01
ED2	Bare Wire 0.66 wt% Co	0.0759	0.01639	0.9974	1.0046	1.928+05
ED3	Bare Wire 0.66 wt% Co	0.0759	0.01634	0.9682	1.0045	3.653+01
ED4	Bare Wire 0.66 wt% Co	0.0762	0.01545	0.9974	1.0047	1.535+05

Table B-1.2-9 (Cont'd) Cobalt/Aluminum  $^{59}\text{Co}$  ( $n, \gamma$ )  $^{60}\text{Co}$  Activities

Location	Form	Foil Thickness or Wire Diam. cm	Post Irrad. Mass gm	Geometry Factor	Self Absorp. Factor	Activity $\mu\text{Ci/gm}$ Target
CD1	Shielded Wire 0.66 wt% Co	0.0758	0.01905	0.9974	1.0046	3.956+04
CD2	Shielded Wire 0.66 wt% Co	0.0764	0.02026	0.9974	1.0047	1.981+04
CD3	Shielded Wire 0.66 wt% Co	0.0743	0.01911	0.9974	1.0046	2.645+04
CD4	Shielded Wire 0.66 wt% Co	0.0752	0.01982	0.9974	1.0046	2.603+04
ED1	Shielded Wire 0.66 wt% Co	0.0747	0.01881	0.9974	1.0046	1.902+04
ED2	Shielded Wire 0.66 wt% Co	0.0745	0.01894	0.9974	1.0046	3.663+04
ED3	Shielded Wire 0.66 wt% Co	0.0759	0.02001	0.9974	1.0046	2.636+04
ED4	Shielded Wire 0.66 wt% Co	0.0773	0.01900	0.9973	1.0047	2.676+04

Table B-1.2-10 Cobalt Wires  $^{59}\text{Co}$  ( $n, \gamma$ )  $^{60}\text{Co}$  Activities

Location	Wire Diameter cm	Post Irrad. Mass gm	Geometry Factor	Self Absorp. Factor	Activity $\mu\text{Ci/gm}$ Target
A1	0.0381	0.01592	0.9949	1.0073	2.381+01
A2	0.0381	0.01557	0.9949	1.0073	2.447+01
A4	0.0381	0.01564	0.9949	1.0073	7.186
A5	0.381	0.01515	0.9838	1.0073	8.083
B2	0.0381	0.01068	0.9978	1.0073	8.926+01
B5	0.0381	0.01052	0.9838	1.0073	3.082+01
C1	0.0381	0.01055	0.9978	1.0073	1.113+02
C2	0.0381	0.01055	0.9978	1.0073	1.102+02
C4	0.0381	0.01045	0.9838	1.0073	3.131+01
C5	0.0381	0.01040	0.9949	1.0073	2.938+01
D2	0.0381	0.00529	0.9978	1.0073	2.132+02
D4	0.0381	0.00501	0.9838	1.0073	6.570+01
E1	0.0381	0.00552	0.9978	1.0073	2.504+02
E4	0.0381	0.00511	0.9949	1.0073	6.814+01
E5	0.0381	0.00517	0.9949	1.0073	7.027+01
F1	0.0381	0.00493	0.9978	1.0073	3.854+02
F3	0.0381	0.00557	0.9949	1.0073	1.045+02
G2	0.0381	0.00505	0.9978	1.0073	3.862+02
H1	0.0381	0.00533	0.9978	1.0073	3.578+02
H4	0.0381	0.00497	0.9978	1.0073	1.038+02
J1	0.0381	0.00555	0.9978	1.0073	4.518+02

Table B-1.2-10 (Cont'd) Cobalt Wires  $^{59}\text{Co}$  ( $n, \gamma$ )  $^{60}\text{Co}$  Activities

Location	Wire Diameter cm	Post Irrad. Mass gm	Geometry Factor	Self Absorp. Factor	Activity $\mu\text{Ci/gm}$ Target
J3	0.0381	0.00522	0.9978	1.0073	1.133+02
J4	0.00381	0.00504	0.9978	1.0073	1.112+02
K2	0.0381	0.00520	0.9978	1.0073	4.409+02
K5	0.0381	0.00507	0.9978	1.0073	1.109+02
M2	0.0381	0.00539	0.9978	1.0073	4.413+02
M2	0.0381	0.00515	0.9978	1.0073	4.444+02
M4	0.0381	0.00558	0.9949	1.0073	1.086+02
M5	0.0381	0.00531	0.9978	1.0073	1.137+02
N2	0.0381	0.00528	0.9978	1.0073	3.713+02
N3	0.0381	0.00514	0.9949	1.0073	1.084+02
P2	0.0381	0.00496	0.9978	1.0073	3.305+02
Q1	0.0381	0.00482	0.9978	1.0073	3.056+02
Q2	0.0381	0.00497	0.9978	1.0073	3.022+02
Q3	0.0381	0.00458	0.9949	1.0073	9.959+01
Q4	0.0381	0.00507	0.9978	1.0073	9.894+01
R1	0.0381	0.01583	0.9978	1.0073	4.330+01
R4	0.0381	0.01589	0.9949	1.0073	9.545
S1	0.0381	0.00476	0.9978	1.0073	4.477+02
S3	0.0381	0.00549	0.9949	1.0073	1.058+02
T2	0.0381	0.00498	0.9978	1.0073	4.229+02
T5	0.0381	0.00551	0.9949	1.0073	1.074+02
U4	0.0381	0.00502	0.9949	1.0073	1.088+02

Table B-1.2-11  $^{45}\text{Sc} (n, \gamma) ^{46}\text{Sc}$  Activities

Location	Form	Foil Thickness cm	Post Irrad. Mass gm	Geometry Factor	Self Absorp. Factor	Activity $\mu\text{Ci/gm}$ Target
K3	Foil	0.0152	0.01198	0.9991	1.0014	3.304+02

Table B-1.3-1  $^{93}\text{Nb}$  ( $n, n'$ )  $^{93\text{m}}\text{Nb}$  Activities

Location	Form	Niobium Source	Total Activity $\mu\text{Ci/gm}$ Target	Activity From $^{182}\text{Ta}$ Fluorescence $\mu\text{Ci/gm}$ Target	Activity From $^{94}\text{Nb}$ Fluorescence $\mu\text{Ci/gm}$ Target	Corrected Activity $\mu\text{Ci/gm}$ Target
C4	Foil	Toyo Soda	3.332-02	-----	4.412-04	3.288-02
E4	Foil	Toyo Soda	3.112-01	1.311-04	1.146-03	3.099-01
F3	Foil	MOL	5.752-01	-----	9.925-04	5.741-01
F3	Foil	Toyo Soda	5.917-01	2.120-04	1.821-03	5.897-01
H4	Foil	Toyo Soda	5.256-01	-----	1.817-03	5.238-01
J3	Foil	Toyo Soda	6.045-01	-----	1.841-03	6.027-01
K3	Foil	ATU	5.889-01	1.869-02	1.832-03	5.684-01
Q3	Foil	Toyo Soda	5.219-01	-----	1.763-03	5.201-01
Q5	Foil	MOL	5.364-01	-----	1.010-03	5.354-01
Q5	Foil	Toyo Soda	5.106-01	2.448-04	1.634-03	5.087-01
Q5	Foil	Toyo Soda	5.255-01	00000	1.663-03	5.239-01
S4	Foil	Toyo Soda	4.379-01	-----	1.658-03	4.361-01
T5	Foil	Toyo Soda	4.921-01	1.694-04	1.598-03	4.903-01
T5	Foil	Toyo Soda	4.488-01	-----	1.583-03	4.472-01

Table B-1.3-1 (Cont'd)  $^{93}\text{Nb}$  ( $n, n'$ )  $^{93\text{m}}\text{Nb}$  Activities

Location	Form	Niobium Source	Total Activity $\mu\text{Ci/gm}$ Target	Activity From $^{182}\text{Ta}$ Fluorescence $\mu\text{Ci/gm}$ Target	Activity From $^{94}\text{Nb}$ Fluorescence $\mu\text{Ci/gm}$ Target	Corrected Activity $\mu\text{Ci/gm}$ Target
T5	Foil	MOL	4.638-01	-----	7.993-04	4.630-01
T5	Foil	MOL	4.653-01	-----	8.947-04	4.644-01
J3	Foil	MOL	6.128-01	-----	1.007-03	6.118-01
F5	Foil	MOL	6.009-01	1.342-02	1.122-03	5.864-01
F5	Foil	MOL	6.130-01	1.288-02	1.110-03	5.990-01
S5	Foil	MOL	4.882-01	1.200-02	1.040-03	4.751-01
S5	Foil	MOL	4.780-01	1.188-02	1.049-03	4.651-01
K3	Wire	ATU	5.457-01	2.474-03	1.620-03	5.416-01

Table B-1.4-1 <sup>54</sup>Mn and <sup>60</sup>Co Activities for Chain in Octant WX

Sample ID	$\mu\text{Ci/gm Target Fe-54}$	$\mu\text{Ci/gm Target Co-59}$
CHN-WX3-1-4.5	Not Measured	Not Measured
CHN-WX3-2-10.5	Not Measured	Not Measured
CHNWX3-3-16.5	Not Measured	Not Measured
CHN-WX3-4-22.5	3.672E-02	7.125E+01
CHN-WX3-5-34.5	4.135E-02	4.898E+01
CHN-WX3-6-46.5	5.305E-02	5.547E+01
CHN-WX3-7-58.5	8.251E-02	6.722E+01
CHN-WX3-8-64.5	8.786E-02	7.402E+01
CHN-WX3-9-70.5	1.023E-01	8.042E+01
CHN-WX3-10-76.5	1.569E-01	8.838E+01
CHN-WX3-11-82.5	1.822E-01	9.824E+01
CHN-WX3-12-94.5	3.317E-01	1.263E+02
CHN-WX3-13-106.5	5.643E-01	1.470E+02
CHN-WX3-14-118.5	9.398E-01	1.787E+02
CHN-WX3-15-124.5	1.089E+00	1.959E+02
CHN-WX3-16-130.5	1.315E+00	2.149E+02
CHN-WX3-17-136.5	1.531E+00	2.302E+02
CHN-WX3-18-142.5	1.661E+00	2.432E+02
CHN-WX3-19-148.5	1.895E+00	2.501E+02
CHN-WX3-20-154.5	1.990E+00	2.599E+02
CHN-WX3-21-160.5	2.057E+00	2.761E+02
CHN-WX3-22-166.5	2.157E+00	2.909E+02



Table B-1.4-1 (Cont'd)  $^{54}\text{Mn}$  and  $^{60}\text{Co}$  Activities for Chain in Octant WX

Sample ID	$\mu\text{Ci/gm Target Fe-54}$	$\mu\text{Ci/gm Target Co-59}$
CHN-WX3-23-172.5	2.222E+00	3.049E+02
CHN-WX3-24-178.5	2.256E+00	3.243E+02
CHN-WX3-25-184.5	2.361E+00	3.191E+02
CHN-WX3-26-190.5	2.284E+00	3.178E+02
CHN-WX3-27-196.5	2.355E+00	3.289E+02
CHN-WX3-28-202.5	2.279E+00	3.339E+02
CHN-WX3-29-208.5	2.484E+00	3.379E+02
CHN-WX3-30-214.5	2.264E+00	3.241E+02
CHN-WX3-31-220.5	2.256E+00	3.016E+02
CHN-WX3-32-226.5	2.212E+00	2.860+02
CHN-WX3-33-232.5	2.058E+00	2.712E+02
CHN-WX3-34-238.5	1.934E+00	2.659E+02
CHN-WX3-35-244.5	1.933E+00	2.582E+02
CHN-WX3-36-250.5	1.675E+00	2.470E+02
CHN-WX3-37-256.5	1.512E+00	2.337E+02
CHN-WX3-38-262.5	1.280E+00	2.192E+02
CHN-WX3-39-268.5	1.082E+00	2.028E+02
CHN-WX3-40-280.5	7.149E-01	1.931E+02
CHN-WX3-41-292.5	4.431E-01	1.750E+02
CHN-WX3-42-304.5	2.811E-01	1.529E+02
CHN-WX3-43-316.5	2.067E-01	1.364E+02
CHN-WX3-44-328.5	1.477E-01	1.188E+02

Table B-1.4-1 (Cont'd) <sup>54</sup>Mn and <sup>60</sup>Co Activities for Chain in Octant WX

Sample ID	$\mu\text{Ci/gm Target Fe-54}$	$\mu\text{Ci/gm Target Co-59}$
CHN-WX3-45-340.5	1.154E-01	1.073E+02
CHN-WX3-46-352.5	9.559E-02	9.852E+01
CHN-WX3-47-364.5	8.357E-02	9.186E+01
CHN-WX3-48-376.5	6.267E-02	8.574E+01
CHN-WX3-49-388.5	4.402E-02	8.265E+01
CHN-WX3-50-400.5	4.107E-02	7.940E+01
CHN-WX3-51-412.5	3.817E-02	7.749E+01
CHN-WX3-52-424.5	4.622E-02	7.608E+01
CHN-WX3-53-436.5	2.060E-02	7.603E+01
CHN-WX3-54-448.5	Not Detected	7.629E+01
CHN-WX3-55-460.5	Not Measured	Not Measured
CHN-WX3-56-472.5	Not Measured	Not Measured

Table B-1.4-2 <sup>54</sup>Mn and <sup>60</sup>Co Activities for Chain in Octant XY

Sample ID	$\mu\text{Ci/gm Target Fe-54}$	$\mu\text{Ci/gm Target Co-59}$
CHN-XY4-1-4.5	Not Measured	Not Measured
CHN-XY4-2-10.5	Not Measured	Not Measured
CHN-XY4-3-16.5	Not Measured	Not Measured
CHN-XY4-4-22.5	Not Detected	4.064E+01
CHN-XY4-5-34.5	2.418E-02	2.938E+01
CHN-XY4-6-46.5	4.218E-02	3.374E+01
CHN-XY4-7-58.5	6.203E-02	4.373E+01
CHN-XY4-8-64.5	5.662E-02	5.065E+01
CHN-XY4-9-70.5	1.014E-01	6.088E+01
CHN-XY4-10-76.5	1.061E-01	7.178E+01
CHN-XY4-11-82.5	1.468E-01	8.515E+01
CHN-XY4-12-94.5	2.701E-01	1.163E+02
CHN-XY4-13-106.5	4.531E-01	1.446E+02
CHN-XY4-14-118.5	8.095E-01	1.743E+02
CHN-XY4-15-124.5	1.008E+00	1.936E+02
CHN-XY4-16-130.5	1.196E+00	2.103E+02
CHN-XY4-17-136.5	1.443E+00	2.264E+02
CHN-XY4-18-142.5	1.607E+00	2.370E+02
CHN-XY4-19-148.5	1.690E+00	2.429E+02
CHN-XY4-20-154.5	1.914E+00	2.451E+02
CHN-XY4-21-160.5	1.999E+00	2.454E+02
CHN-XY4-22-166.5	2.127E+00	2.347E+02

Table B-1.4-2 (Cont'd) <sup>54</sup>Mn and <sup>60</sup>Co Activities for Chain in Octant XY

Sample Id	$\mu\text{Ci/gm Target Fe-54}$	$\mu\text{Ci/gm Target Co-59}$
CHN-XY4-23-172.5	2.136E+00	2.398E+02
CHN-XY4-24-178.5	2.204E+00	2.473E+02
CHN-XY4-25-184.5	2.243E+00	2.482E+02
CHN-XY4-26-190.5	2.245E+00	2.468E+02
CHN-XY4-27-196.5	2.326E+00	2.516E+02
CHN-XY4-28-202.5	2.396E+00	2.517E+02
CHN-XY4-29-208.5	2.304E+00	2.490E+02
CHN-XY4-30-214.5	2.294E+00	2.462E+02
CHN-XY4-31-220.5	2.183E+00	2.440E+02
CHN-XY4-32-226.5	2.185E+00	2.397E+02
CHN-XY4-33-232.5	2.050E+00	2.529E+02
CHN-XY4-34-238.5	1.892E+00	2.595E+02
CHN-XY4-35-244.5	1.793E+00	2.590E+02
CHN-XY4-36-250.5	1.615E+00	2.529E+02
CHN-XY4-37-256.5	1.408E+00	2.426E+02
CHN-XY4-38-262.5	1.245E+00	2.280E+02
CHN-XY4-39-268.5	1.017E+00	2.115E+02
CHN-XY4-40-280.5	7.001E-01	1.953E+02
CHN-CY4-41-292.5	4.322E-01	1.752E+02
CHN-XY4-42-304.5	Not Measured	Not Detected
CHN-XY4-43-316.5	1.878E-01	1.316E+02
CHN-XY4-44-328.5	1.285E-01	1.148E+02

Table B-1.4-2 (Cont'd)  $^{54}\text{Mn}$  and  $^{60}\text{Co}$  Activities for Chain in Octant XY

Sample ID	$\mu\text{Ci/gm Target Fe-54}$	$\mu\text{Ci/gm Target Co-59}$
CHN-XY4-45-340.5	1.114E-01	1.026E+02
CHN-XY4-46-352.5	8.277E-02	9.324E+01
CHN-XY4-47-364.5	1.245E-02	8.536E+01
CHN-XY4-48-376.5	4.680E-02	7.980E+01
CHN-XY4-49-388.5	5.997E-02	7.509E+01
CHN-XY4-50-400.5	4.289E-02	6.847E+01
CHN-XY4-51-412.5	Not Detected	6.299E+01
CHN-XY4-52-424.5	3.312E-02	6.115E+01
CHN-XY4-53-436.5	Not Detected	6.083E+01
CHN-XY4-54-448.5	2.643E-02	6.105E+01
CHN-XY4-55-460.5	Not Measured	Not Measured
CHN-XY4-56-472.5	Not Measured	Not Measured

Table B-1.4-3 <sup>54</sup>Mn and <sup>60</sup>Co Activities for Chain in Octant YZ

Sample ID	$\mu\text{Ci/gm Target Fe-54}$	$\mu\text{Ci/gm Target Co-59}$
CHN-YZ1-1-4.5	Not Detected	3.675E+00
CHN-YZ1-2-10.5	Not Detected	1.417E+01
CHN-YZ1-3-16.5	9.152E-03	4.059E+01
CHN-YZ1-4-22.5	2.093E-02	6.655E+01
CHN-YZ1-5-34.5	3.452E-02	4.572E+01
CHN-YZ1-6-46.5	3.728E-02	5.002E+01
CHN-YZ1-7-58.5	6.686E-02	5.936E+01
CHN-YZ1-8-64.5	7.180E-02	6.373E+01
CHN-YZ1-9-70.5	8.069E-02	7.104E+01
CHN-YZ1-10-76.5	1.172E-01	7.871E+01
CHN-YZ1-11-82.5	1.486E-01	8.683E+01
CHN-YZ1-12-94.5	2.435E-01	1.092E+02
CHN-YZ1-13-106.5	4.304E-01	1.357E+02
CHN-YZ1-14-118.5	7.159E-01	1.650E+02
CHN-YZ1-15-124.5	8.683E-01	1.864E+02
CHN-YZ1-16-130.5	1.021E+00	2.036E+02
CHN-YZ1-17-136.5	1.183E+00	2.144E+02
CHN-YZ1-18-142.5	1.324E+00	2.294E+02
CHN-YZ1-19-148.5	1.043E+00	2.345E+02
CHN-YZ1-20-154.5	1.140E+00	2.565E+02
CHN-YZ1-21-160.5	1.247E+00	2.762E+02
CHN-YZ1-22-166.5	1.204E+00	2.764E+02

Table B-1.4-3 (Cont'd) <sup>54</sup>Mn and <sup>60</sup>Co Activities for Chain in Octant YZ

Sample ID	$\mu\text{Ci/gm Target Fe-54}$	$\mu\text{Ci/gm Target Co-59}$
CHN-YZ1-23-172.5	1.399E+00	3.042E+02
CHN-YZ1-24-178.5	1.402E+00	3.154E+02
CHN-YZ1-25-184.5	1.310E+00	2.955E+02
CHN-YZ1-26-190.5	1.450E+00	2.737E+02
CHN-YZ1-27-196.5	1.442E+00	2.868E+02
CHN-YZ1-28-202.5	1.362E+00	2.875E+02
CHN-YZ1-29-208.5	1.463E+00	3.025E+02
CHN-YZ1-30-214.5	1.508E+00	2.996E+02
CHN-YZ1-31-220.5	1.342E+00	2.822E+02
CHN-YZ1-32-226.5	1.416E+00	2.710E+02
CHN-YZ1-33-232.5	1.398E+00	2.561E+02
CHN-YZ1-34-238.5	1.327E+00	2.333E+02
CHN-YZ1-35-244.5	1.360E+00	2.328E+02
CHN-YZ1-36-250.5	1.491E+00	2.408E+02
CHN-YZ1-37-256.5	1.410E+00	2.412E+02
CHN-YZ1-38-262.5	1.270E+00	2.295E+02
CHN-YZ1-39-268.5	1.105E+00	2.161E+02
CHN-YZ1-40-280.5	7.383E-01	1.929E+02
CHN-YZ1-41-292.5	4.995E-01	1.725E+02
CHN-YZ1-42-304.5	3.278E-01	1.516E+02
CHN-YZ1-43-316.5	2.095E-01	1.330E+02
CHN-YZ1-44-328.5	1.650E-01	1.150E+02

Table B-1.4-3 (Cont'd)  $^{54}\text{Mn}$  and  $^{60}\text{Co}$  Activities for Chain in Octant YZ

Sample ID	$\mu\text{Ci/gm Target Fe-54}$	$\mu\text{Ci/gm Target Co-59}$
CHN-YZ1-45-340.5	1.22E-01	1.011E+02
CHN-YZ1-46-352.5	7.634E-02	9.250E+01
CHN-YZ1-47-364.5	7.326E-02	8.527E+01
CHN-YZ1-48-376.5	5.037E-02	7.879E+01
CHN-YZ1-49-388.5	4.719E-02	7.410E+01
CHN-YZ1-50-400.5	2.977E-02	7.022E+01
CHN-YZ1-51-412.5	Not Detected	6.791E+01
CHN-YZ1-52-424.5	3.099E-02	6.568E+01
CHN-YZ1-53-436.5	Not Detected	6.419E+01
CHN-YZ1-54-448.5	Not Measured	Not Measured
CHN-YZ1-55-460.5	1.838E-02	6.420E+01
CHN-YZ1-56-472.5	Not Measured	Not Measured



Table B-1.4-4 <sup>54</sup>Mn and <sup>60</sup>Co Activities for Chain in Octant ZW

Sample ID	$\mu\text{Ci/gm Target Fe-54}$	$\mu\text{Ci/gm Target Co-59}$
CHN-ZW2-1-4.5	Not Detected	2.887E+00
CHN-ZW2-2-10.5	1.326E-03	9.208E+00
CHN-ZW2-3-16.5	4.096E-03	2.731E+01
CHN-ZW2-4-22.5	1.405E-02	4.160E+01
CHN-ZW2-5-34.5	2.841E-02	3.040E+01
CHN-ZW2-6-46.5	4.377E-02	3.432E+01
CHN-ZW2-7-58.5	6.129E-02	4.450E+01
CHN-ZW2-8-64.5	7.787E-02	5.156E+01
CHN-ZW2-9-70.5	8.681E-02	6.096E+01
CHN-ZW2-10-76.5	1.108E-01	7.293E+01
CHN-ZW2-11-82.5	1.492E-01	8.667E+01
CHN-ZW2-12-94.5	2.661E-01	1.181E+02
CHN-ZW2-13-106.5	4.514E-01	1.476E+02
CHN-ZW2-14-118.5	8.068E-01	1.769E+02
CHN-ZW2-15-124.5	9.219E-01	1.962E+02
CHN-ZW2-16-130.5	1.188E+00	2.152E+02
CHN-ZW2-17-136.5	1.349E+00	2.288E+02
CHN-ZW2-18-142.5	1.571E+00	2.405E+02
CHN-ZW2-19-148.5	1.675E+00	2.458E+02
CHN-ZW2-20-154.5	1.896E+00	2.462E+02
CHN-ZW2-21-160.5	1.989E+00	2.475E+02
CHN-ZW2-22-166.5	2.052E+00	2.395E+02

Table B-1.4-4 (Cont'd) <sup>54</sup>Mn and <sup>60</sup>Co Activities for Chain in Octant ZW

Sample ID	$\mu\text{Ci/gm Target Fe-54}$	$\mu\text{Ci/gm Target Co-59}$
CHN-ZW2-23-172.5	2.208E+00	2.423E+02
CHN-ZW2-24-178.5	2.151E+00	2.492E+02
CHN-ZW2-25-184.5	2.276E+00	2.525E+02
CHN-ZW2-26-190.5	2.318E+00	2.473E+02
CHN-ZW2-27-196.5	2.255E+00	2.557E+02
CHN-ZW2-28-202.5	2.366E+00	2.578E+02
CHN-ZW2-29-208.5	2.296E+00	2.555E+02
CHN-ZW2-30-214.5	2.305E+00	2.502E+02
CHN-ZW2-31-220.5	2.291E+00	2.477E+02
CHN-ZW2-32-226.5	2.259E+00	2.369E+02
CHN-ZW2-33-232.5	2.101E+00	2.507E+02
CHN-ZW2-34-238.5	1.967E+00	2.597E+02
CHN-ZW2-35-244.5	1.847E+00	2.620E+02
CHN-ZW2-36-250.5	1.736E+00	2.555E+02
CHN-ZW2-37-256.5	1.500E+00	2.474E+02
CHN-ZW2-38-262.5	1.331E+00	2.354E+02
CHN-ZW2-39-268.5	1.090E+00	2.226E+02
CHN-ZW2-40-280.5	7.284E-01	2.022E+02
CHN-ZW2-41-292.5	4.871E-01	1.819E+02
CHN-ZW2-42-304.5	3.191E-01	1.591E+02
CHN-ZW2-43-316.5	2.257E-01	1.384E+02
CHN-ZW2-44-328.5	1.782E-01	1.209E+02

Table B-1.4-4 (Cont'd)  $^{54}\text{Mn}$  and  $^{60}\text{Co}$  Activities for Chain in Octant ZW

Sample ID	$\mu\text{Ci/gm Target Fe-54}$	$\mu\text{Ci/gm Target Co-59}$
CHN-ZW2-45-340.5	9.809E-02	1.096E+02
CHN-ZW2-46-352.5	9.543E-02	1.001E+02
CHN-ZW2-47-364.5	6.809E-02	9.224E+01
CHN-ZW2-48-376.5	4.997E-02	8.739E+01
CHN-ZW2-49-388.5	4.036E-02	8.362E+01
CHN-ZW2-50-400.5	2.808E-02	7.930E+01
CHN-ZW2-51-412.5	3.262E-02	7.763E+01
CHN-ZW2-52-424.5	2.823E-02	7.593E+01
CHN-ZW2-53-436.5	2.308E-02	7.549E+01
CHN-ZW2-54-448.5	2.248E-02	7.539E+01
CHN-ZW2-55-460.5	Not Measured	Not Measured
CHN-ZW2-56-472.5	Not Measured	Not Measured

Table B-1.4-5 Activity of Chain Segments Irradiated in "Pill Boxes"

Location	Shielded	$\mu\text{Ci } ^{54}\text{Mn}/\text{gram}$ $^{54}\text{Fe}$	$\mu\text{Ci } ^{60}\text{Co}/\text{gram}$ $^{59}\text{Co}$
C3	Yes	7.073E-02	3.646E+01
E2	No	1.401E+00	1.869E+02
E3	Yes	1.313E+00	8.232E+01
H2	No	2.352E+00	2.820E+02
H5	Yes	2.373E+00	1.212E+02
J2	No	2.826E+00	3.288E+02
K2	No	2.738E+00	3.281E+02
L1	No	2.984E+00	3.191E+02
L4	Yes	2.930E+00	1.239E+02

Table B-4.2-1 Helium Concentrations in Beryllium HAFMs  ${}^9\text{Be} (n, \alpha) {}^6\text{Li}$ 

Sample	Specimen Mass (mg)	Measured ${}^4\text{He}$ ( $10^{11}$ atoms)	Helium Concentration (appb) <sup>(a)</sup>		
			Measured	Corrected <sup>(b)</sup>	Average
DB-BEC-1/1 -1/3	2.71 3.52	1.582 2.008	0.8736 0.8537	0.820 0.800	0.81
DB-BEC-2/4 -2/5	1.89 2.50	2.056 2.705	1.628 1.619	1.57 1.56	1.57
DB-BEC-3/7 -3/9	3.02 2.21	2.730 2.063	1.353 1.397	1.30 1.34	1.32
DB-BEC-4/10 -4/12	2.68 2.86	0.222 0.264	0.124 0.138	0.072 0.086	0.08
DB-BEC-5/13 -5/15	3.35 2.66	2.979 2.419	1.331 1.361	1.28 1.31	1.30
DB-BEC-6/17 -6/18	2.69 2.53	3.181 2.947	1.770 1.743	1.71 1.69	1.70
DB-BEC-7/20 -7/21	2.73 2.26	2.731 2.261	1.497 1.497	1.44 1.44	1.44
DB-BEC-8/22 -8/23	1.82 1.66	2.312 2.015	1.901 1.817	1.85 1.76	1.81
DB-BEC-9/26 -9/27	2.14 1.77	0.175 0.098	0.122 0.083	0.072 0.033	0.05
DB-BEC-10/28 -10/30	1.77 2.06	1.815 2.105	1.535 1.529	1.48 1.47	1.48
DB-BEC-11/32 -11/33	1.72 1.95	2.145 2.349	1.866 1.803	1.81 1.75	1.78

<sup>(a)</sup> Helium concentration in atomic parts per billion ( $10^{-9}$  atom fraction) with respect to the number of beryllium atoms in the specimen.

<sup>(b)</sup> Corrected for measured helium concentration in unirradiated beryllium (0.05 appb), and from helium generation in boron impurity.

Framatome Technologies Inc.

Table B-4.2-2 Helium Concentrations in Al-Li HAFMS  ${}^6\text{Li} (n, \alpha) {}^3\text{H}$ 

Sample	Specimen Mass (mg)	Measured ${}^4\text{He}$ ( $10^{11}$ atoms)	Helium Concentration (appm) <sup>(a)</sup>	
			Measured	Average
DB-Li-1A -1B	0.723 0.609	4.534 3.765	0.9034 0.8906	0.897
DB-Li-2A -2B	0.798 0.609	1.484 1.147	0.2679 0.2713	0.270
DB-Li-3A -3B	0.753 0.583	5.218 4.135	0.9982 1.022	1.010
DB-Li-4A -4B	0.757 0.728	3.209 3.156	0.6106 0.6245	0.618
DB-Li-5A -5B	0.667 0.667	0.332 0.313	0.0717 0.0676	0.070
DB-Li-6A -6B	0.671 0.568	4.296 3.540	0.9223 0.8978	0.910
DB-Li-7B -7C	0.567 0.596	3.695 3.799	0.9387 0.9182	0.928
DB-Li-8A -8B	0.668 0.701	4.305 4.514	0.9284 0.9276	0.928
DB-Li-9A -9B	0.739 0.639	4.979 4.299	0.9705 0.9691	0.970
DB-Li-10A -10B	0.669 0.673	4.585 4.603	0.9870 0.9852	0.986
DB-Li-12A -12B	0.641 0.556	4.313 3.695	0.9693 0.9573	0.963

<sup>(a)</sup> Helium concentration in atomic parts per million ( $10^{-6}$  atom fraction) with respect to the number of  ${}^6\text{Li}$  atoms in the specimen.

***Appendix C* Calculational Perturbation Factors for Dosimetry**

The Semi - Empirical BUGLE-80 fluence methodology that FTI had developed in 1990 was used to determine calculational perturbation factors for the DORT models. This appendix list these factors. They are calculational factors used to appropriately modify the calculational results for the dosimetry activities. The procedures for determining the factors are discussed in Section 3.2.

Table C.1 **Perturbation Factors for  $^{54}\text{Fe} (n, p) ^{54}\text{Mn}$**



Table C.1 (Cont'd) **Perturbation Factors for  $^{54}\text{Fe} (n, p) ^{54}\text{Mn}$**

Table C.2 **Perturbation Factors for  $^{58}\text{Ni} (n, p) ^{58}\text{Co}$**

**Table C.3 Perturbation Factors for  $^{63}\text{Cu} (n, \alpha) ^{60}\text{Co}$**

Table C.4 Perturbation Factors for  $^{46}\text{Ti} (n, p) ^{46}\text{Sc}$

Table C.5 Perturbation Factors for  $^9\text{Be} (n, \alpha) - \text{Be HAFM}$

Table C.6 Perturbation Factors for  $^{238}\text{U} (n, f)$  Either  $^{137}\text{Cs}$  or SSTRs

Table C.7 Perturbation Factors for  $^{237}\text{Np}$  ( $n, f$ ) Either  $^{137}\text{Cs}$  or SSTRs

Table C.8 **Perturbation Factors for  $^{59}\text{Co} (n,\gamma) ^{60}\text{Co}$**

Table C.8 (Cont'd) **Perturbation Factors for  $^{59}\text{Co}$  ( $n,\gamma$ )  $^{60}\text{Co}$**



**Table C.9 Perturbation Factors for  $^{109}\text{Ag} (n, \gamma) ^{110\text{m}}\text{Ag}$**

**Table C.10 Perturbation Factors for  $^{235}\text{U} (n, f)$  Either  $^{137}\text{Cs}$  or SSTRs**

Table C.11 **Perturbation Factors for  $^{239}\text{Pu}$  ( $n, f$ ) SSTRs**

Table C.12 **Perturbation Factors for  $^{93}\text{Nb}$  ( $n, n'$ )  $^{93m}\text{Nb}$**

*Appendix D* FTI Responses to the -

**Request for Additional Information for  
Topical BAW-2241P *Fluence and Uncertainty Methodologies* \***

**Set 1 - Question 1**

The topical report states that the B&W owners will revalidate the analytical monitoring of the pressure vessel by performing vessel fluence analyses and benchmark comparisons to cavity measurements. How will the results of these analyses be used and will they be submitted in separate topical reports ?

Response

In the introductory section (1.0) of the Topical, on page 1 – 3, the following remarks were made as part of the discussion concerning why the B & W Owners were submitting a topical at this time.

In the interim period however, before the draft guide (DG-1053) is finalized, most of the owners will be updating their reactor coolant system pressure – temperature limits for heat-ups and cool-downs. In addition, most owners will be revalidating the analytical monitoring of their vessels by performing vessel fluence analyses that include absolute calculations of the fluence and benchmark comparisons of the calculations to cavity dosimetry measurements.

---

\*This *Appendix* contains its own Reference section. References D1 and D2 refer to the two sets of NRC requests for additional information.

The question concerns how the fluence results will be used for the updated pressure - temperature limits, and will they be submitted in a topical report. The results of the analyses from each B & W owner (a) revalidating the monitoring of their vessel (using best - estimate calculational results), and (b) performing a benchmark comparison of the calculations to cavity dosimetry measurements, will be used in reactor vessel embrittlement evaluations. The embrittlement evaluations are submitted to the NRC in updates to the plant Technical Specifications for revised pressure - temperature curves by each respective owner. The fluence values and uncertainties are referenced in the Technical Specification change submittal. They are not included in separate topical reports.

Embrittlement evaluations are based on the correlation of increasing fluence levels to increasing reference temperatures in the nil-ductility transition properties of specimens of the vessel materials. The embrittlement evaluations include a "Margin" term which is based on the uncertainties in the correlation.<sup>D3</sup> The NRC has suggested that the fluence uncertainties, forming part of the bases for the correlation uncertainties, can be represented by a standard deviation of 20 percent.<sup>D4</sup> The benchmark comparison of dosimetry calculations to measurements, for each B & W owner in their updated evaluation of reactor coolant system pressure - temperature limits for heat-ups and cool-downs, is used to determine if the calculations for each specific plant evaluation are consistent with the *Fluence and Uncertainty Methodologies* topical. Consistency between (a) the plant-specific uncertainties, and (b) the biases, standard deviations, and confidence levels in the topical, ensure that the plant-specific evaluations are consistent with the embrittlement correlations.

**Set 1 - Question 2**

**Provide a detailed description of the dosimeter, capsule and structural support geometry and how the modeling of this detail was validated.**

Response

The permanent dosimetry holder (capsule) consists of

as shown in

Figure D1 below.

Figure D1. Cross section of \_\_\_\_\_, \_\_\_\_\_ dosimetry holder, and dosimetry can.

Figure D2. Geometrical model of dosimetry holder and surrounding structures.

**Set 1 - Question 3**

**Describe how the effect of increased Pu in the high burnup fuel is included in the source calculation. Does this treatment allow for the cycle-specific variations ?**

Response

This question, concerning the effects of increased plutonium (Pu) concentrations in the high burnup fuel, and Question Set 1 - 9, concerning the dependence of the number of neutrons produced per fission on burnup, and Question Set 1 - 10, concerning the

**FTI Non-Proprietary**

neutron source spectra as a function isotopic production weighting, are all related. Therefore, in addition to the following explanation, the explanations for Question Sets 1 - 9 and 1 - 10 should also be reviewed.



**FTI Non-Proprietary**

**Set 1 – Question 4**

**Do the internals of the B&W plants include core shroud former plates and, if so, how is the effect of these plates included in the calculations ?**

Response

The B & W design includes core formers. The effects of the former plates are explicitly accounted for in the DORT analyses, as described below.

**Set 1 – Question 5**

**Are there differences between the calculation and measurement methods used for Davis Besse and the methods used for the other plants included in the Appendix-A data base? For example, were the methods used to determine the dosimeter corrections for the Appendix-A measurements the same as used for Davis Besse?**

Response

The first sentence of this question involves two questions, one concerning calculational methods, and the other concerning measurement methods. The differences between the measurement methods used for Davis Besse and the methods used for the other plants included in *Appendix A* will be addressed first.

The measurement methodology is described in Section 5 of the Topical. The measured results involve (1) a specific activity for the radiometric dosimeters described in Section 5.1, (2) the fissions per target atomic density for the solid state track recorders described in Section 5.2, and (3) helium concentrations in atomic parts per target concentration for the helium accumulation fluence monitors described in Section 5.3. The measurement methods used to obtain these results for the Davis Besse benchmark are the same as the methods used for the other plants referenced in *Appendix A*. This

**FTI Non-Proprietary**

includes the methods used to determine the dosimeter corrections for the *Appendix A* measurements.

**FTI Non-Proprietary**

**Framatome Technologies Inc.**

**Set 1 - Question 6**

**Will the BAW-2241-P methodology be applied to cores with partial length fuel assemblies and, if so, how will the  $(r, z)$  source of Section-3.1.2.2 be determined ?**

Response

The methodology can be applied to partial length fuel assembly poison inserts.

In general, the multi-planar  $r\theta$  sources and multi-channel  $rz$  sources are produced from the results of pin-by-pin, three-dimensional, time-averaged source distributions. The three-dimensional source distributions come from explicit three-dimensional fuel-cycle calculations, such as those from the NEMO or PDQ codes. The calculations of the sources are produced during core-follow benchmarks of the code results to measured power densities.

**Set 1 - Question 7**

**The Model-C  $(r, z)$  calculation results in negative fluxes and an unacceptable solution. Can this error in the Model-C calculation affect the results of the Model-B calculation ? For example, what is the sensitivity of the Model-B calculation to the albedo boundary conditions ?**

Response

The negative fluxes encountered in the  $r, z$  Model C DORT calculation occurred high up in the air cavity between the vessel and the concrete, and were determined to be the result of computer-memory-related inabilities to specify a large enough quadrature and/or small enough interval dimensions. Once that was ascertained, the Model C DORT run was abandoned, effectively reducing the size of the problem in the axial direction.

The cavity fluxes over the Model B elevation were determined by synthesis

**Set 1 - Question 8**

**Please Provide Reference 21.**

Response

It is enclosed in this submittal.

**Set 1 - Question 9**

**In view of the large variation in fuel burnup between assemblies and the dependence of the number of neutrons produced per fission ( $\nu$ ) on fuel burnup, what uncertainty is introduced by neglecting this dependence in Equation (4.1) ?**

**Response**

This question, concerning the dependence of the number of neutrons produced per fission on burnup, and Question Set 1 - 3, concerning the effects of increased plutonium (Pu) concentrations in the high burnup fuel, and Question Set 1 - 10, concerning the neutron source spectra as a function isotopic production weighting, are all related. Therefore, in addition to the following explanation, the explanations for Question Sets 1 - 3 and 1 - 10 should also be reviewed.

As explained when Question Set 1 - 3 was addressed above, the variation in fuel burnup between assemblies is modeled explicitly. This modeling includes, core - follow calculations which are compared to the measured core operational data, quasi-static time steps to appropriately treat time dependent behavior, explicit representation of the isotopics within the fuel assembly, and three-dimensional representation of the fuel pins and geometrical detail within the assembly. Thus, the dependence on the changing isotopics as a function of burnup, and the corresponding changes in the number of neutrons produced per fission in the fuel volume is not neglected. The burnup dependence of the neutrons produced per fission within a fuel assembly is included in the neutron source calculation.



The uncertainty in neutron production due to the uncertainty in the burnup of the fuel assemblies can be modeled with the uncertainty in the power distribution. The uncertainty in the power distribution is not normal when it is defined on a relative basis. However, an absolute deviation in the relative power distribution does represent a normal distribution. Using an upper bounding deviation with a 95 percent confidence level in the analytic sensitivity, indicated that the local uncertainty would be about 18 percent with a relative peripheral power of 0.50, and about 30 percent with a relative peripheral power of 0.30.

**Set 1 - Question 10**

**The core neutron source spectrum is determined by a neutron production weighting of the individual assembly neutron spectra. What uncertainty is introduced by the Equation (4.2) power weighting of the assembly spectra ?**

Response

This question, concerning the neutron source spectra as a function isotopic production weighting, and Question Set 1 - 3, concerning the effects of increased plutonium (Pu) concentrations in the high burnup fuel, and Question Set 1 - 9, concerning the dependence of the number of neutrons produced per fission on burnup, are all related. Therefore, in addition to the following explanation, the explanations for Question Sets 1 - 3 and 1 - 9 should also be reviewed.

As explained when Question Set 1 - 3 was addressed above, the neutron source spectrum is evaluated for each fuel assembly

In Equation 4.2 (now Equation 3.2), the assembly average fission emission spectrum is the result of the weighting from the isotopics, et cetera. The assembly fission emission spectrum is used in Equation 4.1 (now Equation 3.1) to define the neutron source spectrum for the core - fuel region. However, as noted by the spatial and spectral indices of the source term in Equation 4.1 (Equation 3.1), the source in the DOT models is not a constant spectrum as a function of space.

Thus, each finite mesh block in the DOT models of the fuel region within the core contains neutron source spectra that are unique to the fuel assembly region represented by the mesh block. Consequently, the core neutron source spectrum is not a single spectrum that has been weighted by the neutron productions throughout the core - fuel

region. The core source is represented by unique fuel assembly spectra appropriately applied to the respective mesh blocks within the fuel regions.

**Set 1 - Question 11**

**Describe in detail how the dependence of the dosimeter response on the axial separation between the vessel support beams and the dosimeters is included. Is the method used for including the effect of the support beams at Davis Besse also used for ANO-1 ?**

Response

**Set 1 - Question 12**

**Does the dissolution process used in the measurement of the powder fissionable dosimeters introduce more uncertainty than the process used to measure the wire dosimeters ? Is the C/M bias and standard deviation for the powder dosimeters different than for the dosimeter wires ?**

Response

The dissolution process used in the measurement of the four powder U-238 dosimeters (page B - 2) and the three powder Np-237 dosimeters (page B - 4) does not introduce

more uncertainty than the process used to measure the wire dosimeters. Page 7 – 18 shows the mean relative standard deviation for all sixteen U-238 dosimeters

Therefore, it appears that the powder and wire dosimeters have the same bias and standard deviation.

**Set 1 - Question 13**

**How does the NIOBIUM prediction compare with the analytic result of Equation (5.1) for the limiting geometry ?**

Response

**Set 1 - Question 14**

**The photo-fission corrections for the U-238(n,f) and the Np-237(n,f) dosimeters appear low compared to the results of other investigators. Have the predictions used to determine these corrections been compared to calculations made with the BUGLE-93 library ? Also, what photo-fission cross sections were used for U-238 and Np-237 and what is the basis for these values ?**

**Response**

With respect to the results of other investigators, one reason for a disparity can be explained by the fact that the neutron to gamma flux ratio differs

This point is illustrated by the following comparison of photo-fission factors (as defined above); the same photo-fission cross sections were used in each analysis.

- Davis Besse, Cycle 6: In-vessel U-238 PF correction factor = 1.050
- W reactor: In-vessel U-238 PF correction factor = 1.186

These photo-fission factors vary by 13.0 percent.

Regarding the question: “have comparisons been made to photo-fission corrections using BUGLE-93 data ?” Yes, for example, the ONS2 Cycles 9 – 14 fluence analysis used the Caldwell photo-fission cross sections<sup>D5,D6,D7</sup> with the BUGLE-93 material cross sections (for cavity dosimeters only).

**Set 1 - Question 15**

**What is the effect on the dosimeter response of Pu build-up, U-235 content and impurities ? Why aren't dosimeter response corrections required for these effects ?**

Response

U-235 Content in U-238 Dosimeters

Corrections were made to account for the effect of U-235 content in the U-238 dosimeters. The capsule dosimeters and a few of the cavity dosimeters had large U-235 concentrations (about 350 ppm), however the majority of the U-238 dosimeters had small U-235 concentrations (12 ppm). (See page 5 - 6 of the Topical Report).

Pu Build-up in the U-238 Dosimeters

The effect of plutonium build-in was analyzed and found to be negligible. For Davis Besse, Cycle 6, the operational time was 380.25 EFPD. The fraction of the total



**FTI Non-Proprietary**

Cs-137 produced from Pu fissions in the U-238 dosimeters during 380.25 EFPDs of operation is estimated to be less than 1.0 percent (see Figure D4).

Other Corrections for Impurities

**Set 1 - Question 16**

**Do the dosimeter response measurements conform to the applicable ASTM standards ? If no, justify any differences.**

Response

The dosimeter measurements conform to the applicable ASTM standards. The discussion of the “Measurement Methodology” in Section 5.0, and the discussions of the “Measurement Techniques” for (1) fissionable and activation radiometric dosimeters in Sections 5.1.1 and 5.1.2 respectively, (2) solid state track recorders in Section 5.2.1, and (3) helium accumulation fluence monitors in Section 5.3.1, indicate that the techniques and procedures agree with the ASTM standards. The ASTM standards refer to additional ASTM standards for “Spectrum Adjustment Methods”, “Application for Reactor Vessel Surveillance”, et cetera. These additional standards refer to techniques that differ from those explained in the “Semi-Analytical (Calculational) Methodology”, in Section 3.0, and the “Uncertainty Methodology”, in Section 7.0. These additional standards refer to the application of the measurements, to infer measured fluences, and are neither applicable to the measurements themselves, nor to vessel fluence predictions. The ASTM standards also refer to precision, bias and uncertainty in terms that are conflicting and inconsistent with mathematical statistics and the National Institute of Standards and Technology (NIST). Section 7.0 of the topical, “Uncertainty Methodology”, explains the treatment of the measurement

uncertainties. Section 7.0 also notes the validation of the measurement uncertainties in a NIST reference field.

**Set 1 - Question 17**

**Why isn't a NIOBIUM calculation required for determining geometry and self-absorption corrections for the non-fissionable dosimeters ?**

**Response**

The measured activity of each dosimeter was determined by the B & W radiochemistry laboratory, using QA - approved and certified procedures, data, and equipment.

The results produced by the present methods for determining geometry and self-absorption corrections have been shown to be reliable and accurate by the QA validation of the B & W laboratory during the Benchmark Experiment uncertainty analyses.

**Set 1 – Question 18**

**Provide Table B-2.2-1 including the SSTR measurement results.**

Response

The use of SSTRs was evaluated for the B&WOG cavity dosimetry program. However, as discussed on page 7 – 9 of the Topical, the standards for fissionable mass deposits and fission product track counts are still being developed. Therefore, SSTRs have not been validated for implementation to support the B&WOG vessel and material monitoring program with the methodologies presented in the Topical. The reference to SSTR measurements was inadvertent and will be changed (please see below).

**5.2.2 Measured Results**

Numerous SSTR fission-rate measurements were evaluated for the Davis Besse Benchmark Experiment. The initial set of SSTR C/M ratios evaluated for the experiment were in poor agreement with other dosimetry C/M ratios and M/M ratios. Several iterations were required before SSTR measurements were obtained that were consistent with the other dosimetry C/M and M/M ratios. While the final set of C/M ratios for the SSTRs were excellent, the only parameter that changed during the iterations was the SSTR measured results. It has been concluded that, while SSTRs do have some potential advantages over other dosimeter types, the state of development of SSTR technology is insufficiently advanced to justify their use as standard dosimeters in the B&WOG fluence analyses methodologies.

## D.2 Question Set 2

Question Set 2 will be addressed in a different format from Question Set 1. The format for Question Set 1 was straightforward in that the NRC sent FTI, and the B & W Owners a set of questions.<sup>D1</sup> FTI and the B & W Owners responded as shown in the previous 26 pages, (D - 1 through D - 26). To reduce costs, and have a better understanding of the questions and explanations on the second set, FTI and the B & W Owners met with the NRC and their contractor in a working meeting on August the fifth and sixth, 1998. This working meeting accomplished the goals of reducing the costs and improving communications. All of the NRC's 19 requests for additional information (RAIs) were satisfactorily addressed. In addition, very detailed discussions on the application of statistical methods were reviewed. Following the meeting, the NRC and their contractor requested that the statistical methods outlined during the review be briefly documented in the response to the second set of RAIs. They also requested that five additional points that they raised during the discussion be documented, and the complete explanations included.

The "Statistical Methods" section, D.2.1, provides a brief outline of the statistical methods used in the topical and explained during the August fifth and sixth NRC meeting. Section D.2.2, "RAI Set 2 Responses", refers to the Statistical Methods, and includes a few brief statements summarizing the discussion during the meeting on each of the 19 requests for additional information. The section following the RAI responses, D.2.3, discusses the "Statistical Processing of Table A-1 Data". The last section,

**Framatome Technologies Inc.**

D.2.4, "Additional Explanations", lists the five additional questions that the NRC raised during the meeting, and provides the requested explanations.

#### **D.2.1 Statistical Methods**

A predominant theme throughout the second set of RAIs, concerned the fundamental expressions of mathematical statistics. Therefore, the meeting on the fifth of August began with a review of the expressions which are the bases for the equations in the "Uncertainty Methodology" section (7.0) of the topical. Since nearly all references on statistical evaluations of uncertainty are based on the concept that the mean value of a predicted parameter is unbiased, the review began with the concept that uncertainty includes the possibility of multiple biases (systematic deviations), in addition to the usual random deviations.

It was noted that the definition of the best-estimate fluence implied that the calculational methodology was unbiased

Also noted, was the fact that it is not possible to use the methods of mathematical statistics to estimate the unbiased uncertainty in the vessel fluence, if the biases in the calculational methodology have not been uniquely identified and removed.

The area that incurred the most discussion and explanation, concerned the combination of uncertainties in the independent random variables (that may be functionally related, or correlated) to estimate the variance in the dependent variable. The discussions centered on topical Equation 7.6.

Equation D.5

can be derived from a Taylor series, which represents dependent random variable  $y$  in terms of independent random variables  $x_i$ . During the meeting discussion, concerning the development of Equation 7.6 from Equation D.5, there were several issues

**Framatome Technologies Inc.**

regarding (a) the truncation of the Taylor series, and (b) subsequent cross product dependencies between the random variables. To ensure that responses to the RAIs and "Additional Explanations" are clear, this discussion of statistical methods begins with the Taylor series relating two random variables,  $x$  and  $y$ , as shown by Equation D.1.

$$y = g(x) = \sum_{n=0}^{\infty} \frac{\frac{\partial^n g(\bar{x})}{\partial x^n} (x - \bar{x})^n}{n!} \quad (\text{D.1})$$

Independent of which specific parameters the variables  $x$  and  $y$  represent in Equation D.1, dependent variable  $y$  is a function of independent variable  $x$ . Thus,  $y$  cannot be determined without a value for  $x$ , and the uncertainty in the value of  $y$  cannot be determined without the uncertainty in the value of  $x$ .

$$\left( K_y \sigma_y \right)^2 = \quad (\text{D.2})$$

The uncertainty in the value of  $y$  is represented by the product of a confidence factor ( $K$ ) and the standard deviation ( $\sigma$ ) as shown by the left side of Equation D.2. The confidence factor for the dependent variable  $y$  is directly related to the confidence level for the independent variables.



When Equation D.1 is expanded into multiple  $x$  variables ( $x_i$ ), and substituted into Equation D.2, the resulting uncertainty expression for the dependent random variable  $y$  is represented by Equation D.3.

$$\left( K_y \sigma_y \right)^2 = \left( \sum_{n=1}^{\infty} \frac{\left[ \sum_i K_{x_i} \sigma_{x_i} \frac{\partial}{\partial x_i} \right]^n y(x_1, x_2, \dots, x_i)}{n!} \right)^2 \quad (\text{D.3})$$

During the meeting, Equation D.3 was the focus of considerable discussions, questions, and explanations. To provide clarity in the following discussion, Equation D.3 has been modified as expressed by Equation D.4.

$$\begin{aligned} \left( K_y \sigma_y \right)^2 = & \left( \left( K_{x_1} \sigma_{x_1} \right) \frac{\partial y}{\partial x_1} + \left( K_{x_2} \sigma_{x_2} \right) \frac{\partial y}{\partial x_2} + \right. \\ & \frac{1}{2} \left( K_{x_1} \sigma_{x_1} \right)^2 \frac{\partial^2 y}{\partial x_1^2} + \frac{1}{2} \left( K_{x_2} \sigma_{x_2} \right)^2 \frac{\partial^2 y}{\partial x_2^2} + \\ & \left. \frac{2}{2} \left( K_{x_1} \sigma_{x_1} K_{x_2} \sigma_{x_2} \right) \frac{\partial^2 y}{\partial x_1 \partial x_2} + \right. \\ & \left. \sum_{n=3}^{\infty} \frac{\left[ K_{x_1} \sigma_{x_1} \frac{\partial}{\partial x_1} + K_{x_2} \sigma_{x_2} \frac{\partial}{\partial x_2} \right]^n y(x_1, x_2)}{n!} \right)^2 \quad (\text{D.4}) \end{aligned}$$

**FTI Non-Proprietary**

In Equation D.4, the first and second order terms in the Taylor series have been explicitly included, and the independent variables have been reduced to  $x_1$ , and  $x_2$ .

The cross product dependencies between the independent variables, are included in the second and higher order derivatives.

While there are statistical applications where the second, and higher order derivatives are used, the discussions during the meeting focused on the fundamentals of  
**Framatome Technologies Inc.**

mathematical statistics. The mathematical statistics expression for the variance in  $y$  due to the propagation of uncertainties in the variables  $x_i$ , is based on a covariance matrix of  $x_i$  uncertainties. The expression for the covariance matrix, can be derived by truncating the Taylor series after the first derivative in Equations D.3 and D.4.

$$\sigma_y^2 = \tag{D.5}$$

Equation D.5 provides the form of the fundamental expression for uncertainty propagation in mathematical statistics. During the meeting, there was some confusion regarding the derivation of the covariances and response functions using the first order Taylor series terms. The appropriateness of using first and second order terms, as expressed by the first three lines in Equation D.4, was questioned.

References discussing the propagation of uncertainties generally divide Equation D.5 into two arrays, or matrices as shown by Equations D.6 and D.7. The first array (Equation D.6) is usually termed the response function matrix, or the sensitivity array, or the response surface.

**Response Function Matrix**

$$\sum_i \sum_j \frac{\partial y}{\partial x_i} \frac{\partial y}{\partial x_j} \tag{D.6}$$

This array is formed by squaring the derivatives on the right side of Equation D.5. The  $i$  index is the same as in Equation D.5, and the  $j$  index simply repeats the  $i$  values. If the indices in Equation D.6 were to represent the Equation D.4 variables, the values would be 1 and 2. It is understood that the product of the response function matrix (Equation D.6) and the covariance matrix (Equation D.7) produces Equation D.5.

**Covariance Matrix**

$$\tag{D.7}$$

The covariance matrix includes the products and cross products of the uncertainties (standard deviations with consistent levels of confidence),

$$\tag{D.8}$$

(D.9)

Equation D.10 is the same as Equation D.5 with the independent variables reduced to  $x_1$ , and  $x_2$ . As explained above when discussing Equation D.7, the variance in the dependent variable can be defined in terms of a unique covariance matrix of the independent variables.

$$\sigma_y^2 = \tag{D.10}$$

The covariance matrix for Equation D.10 is expressed below using matrix notation.

Covariance Matrix

$$\begin{vmatrix} \sigma_{11} & \sigma_{12} \\ \sigma_{21} & \sigma_{22} \end{vmatrix}$$

Equation 11 provides the expansion of the covariance matrix terms above into the product of standard deviations and correlation coefficients.

Covariance Matrix Expansion  
Using Correlation Coefficients

$$\begin{aligned} \sigma_{11} &= \sigma_{x_1} \sigma_{x_1} \rho_{x_1 x_1} \\ \sigma_{12} &= \sigma_{x_1} \sigma_{x_2} \rho_{x_1 x_2} \\ \sigma_{21} &= \sigma_{x_2} \sigma_{x_1} \rho_{x_2 x_1} \\ \sigma_{22} &= \sigma_{x_2} \sigma_{x_2} \rho_{x_2 x_2} \end{aligned} \tag{D.11}$$

The covariance is derived from the integral of the bivariate distribution in Equation 8 and related to the correlation coefficient in the bivariate form of Gauss' distribution function. Again, the expression in Equation 8<sup>D8</sup> is the same as Equation D.11 in this appendix.

Equation 1 represents the covariance matrix as expressed by Equation D.7 (in this appendix). Since the coefficient for each independent random variable in Equation 1<sup>D8</sup> is unity, the response function matrix (Equation D.6) in this appendix would be unity. Therefore, the covariance matrix represents Equation D.5. Equation 2 is the same as Equation 1,<sup>D8</sup> except that the coefficient for each independent variable ( $x_i$ ) is a constant term ( $a_i$ ). Thus, the products and cross products of the "a" terms represent the response function matrix (Equation D.6) in this appendix. Consequently, Equations 1 and 2 from Reference D8 are equivalent to Equations D.5, D.6 and D.7 in this appendix.

Equations 1

and 2 provide a linear relation between a dependent variable and a number of independent random variables that are functionally or correlatively related with correlation coefficients of unity. The coefficient of each expected independent variable is expressed using the symbol ( $k$ ). The response function matrix would thereby be noted by an array of  $k_i k_j$  symbols. The combination of the response function and covariance matrices is represented by Equation 3

In

Equation 6,<sup>D8</sup> the expression for the dependent variable standard deviation includes the square of the first derivative of the dependent variable with respect to the independent variables. There are no second or higher order derivatives. With the square of the first derivative, Equation 6<sup>D8</sup> is the same as Equation D.5 in this appendix, when there is no dependency between the independent variables.



Equation D.5 appears to be the fundamental expression for uncertainty propagation in applications of mathematical statistics. Equation D.5 can be derived by truncating the Equation D.3 Taylor series after the first order terms

If the set of "*i*" - dimensional variables in Equation D.5 is reduced to two ( $x_1$ , and  $x_2$ ), then Equation D.5 is reduced to Equation D.10. The two-dimensional Taylor series is expressed by Equation D.4, which includes explicit representation of first and second order derivatives. If the two-dimensional variables in Equation D.10 are reduced to one-dimension ( $x_1$ ), Equation D.10 is reduced to Equation D.12.

$$\sigma_y^2 = \left( \frac{\partial y}{\partial x_1} \sigma_{x_1} \right)^2 \quad (\text{D.12})$$

If Equation D.4 is reduced to one-dimension ( $x_1$ ), it would continue to include second order, and third order terms, et cetera. If the derivation of Equations D.5, D.10 and D.12 included the approximation of truncating the Taylor series after second, or higher order terms, then Equation D.12 would include the square of the standard deviation, squared,  $(\sigma^2)^2$ , as well as the square of the second derivative as shown by Equation D.4.

During the meeting, the explanations for several of the RAIs included applying Equation D.5 to Equations 7.3, 7.4 and 7.6. The following discussion outlines the application of Equation D.5 to these equations as presented during the meeting. The application involves defining the functional relation between the dependent and independent random variables. This functional relation is then applied to Equation D.5.

Uncertainty in Foil Dosimeter  
Self-Absorption Correction

$$I(s) = I(d) e^{\mu x} \quad (D.13)$$

The self-absorption of gamma-rays, or other radiation, in a dosimeter, reduces the radiation intensity ( $I$ ) from the dosimeter source ( $s$ ). When the source intensity is measured with a detector ( $d$ ), the measurements must be increased by the self-absorption loss to obtain an accurate intensity  $\{I(s)\}$ . The loss is a direct function of

the attenuation coefficient ( $\mu$ ) and the dosimeter thickness ( $x$ ). The integral of Equation D.13 provides a sufficient expression for determining the self-absorption.

(D.14)

Equation D.13 is also sufficient to substitute into Equation D.5 for estimating the effects of dosimeter thickness uncertainties on the self-absorption uncertainty as shown by Equation D.14.

Weight Uncertainty

$$\text{SpA} = \frac{\text{A}}{\text{gm}} \quad (\text{D.15})$$

The results of the dosimeter measurements are defined in terms of specific activity (SpA). The units are micro-Curies (A) from the product isotope per gram (gm) of the dosimeter parent isotope.

(D.16)

When the specific activity functional relation from Equation D.15 is substituted into Equation D.5, the effects of uncertainties in the dosimeter mass on the specific activity can be estimated as shown by Equation D.16.

**Framatome Technologies Inc.**

When Equations D.14 and D.16 were derived and discussed during the meeting, it was clear that the uncertainties in the independent random variables were functionally unrelated and therefore independent of one another.

The equations are thereby reduced to the square root of the sum of the squares. The familiar form of Equations D.14 and D.16 cleared up the questions concerning the uncertainties in the dosimetry measurements related to Equations 7.3 and 7.4.

There were four generally obscure areas related to Equation 7.6. The discussions in these areas included : (1) (2) the response function sensitivity terms, (3) the measured value associated with the measurement uncertainty, and the need to have the degrees of freedom represented by a set, and (4) the relation of the Equation 7.6 measurement uncertainty to the total dosimetry database of measurement uncertainties. The following discussion relates Equations D.5, D.7, D.9 and D.11 to clarify the obscurity in the four areas associated with Equation 7.6.

(D.17)

$$\frac{\partial M}{\partial m_d} = w_d \quad (\text{D.18})$$

While the dosimeter uncertainties are not dependent on one another, they are dependent on the same set of constants. Consequently, the appropriate treatment of the correlation coefficients should reflect a direct relationship. This treatment means that the values in the set of correlation coefficients, is unity.

As suggested by Equation D.5, the propagation of uncertainties with response functions determined from the Equation D.18 functional relation, should represent the appropriate material and dosimeter weights for evaluation of the measurement uncertainty, as shown by Equation 7.6.

As noted during the meeting, the values in the set of material dependent correlation coefficients were assessed to be unity. This assessment was based on the same type of evaluation used to determine the appropriate values for the set of dosimeter correlation coefficients. With different weights for the materials and the dosimeters associated with each material, and the values in the material and dosimeter sets of correlation coefficients being unity, Equation 7.6 represents a covariance matrix of material dependent dosimeter uncertainties nested within a covariance matrix of material uncertainties.

FTI and the B & W Owners have interpreted ASTM E 185 requirements, that are referenced in Appendix H, of 10 CFR 50, to be appropriately satisfied with four dosimeter material types.

the maximum value for the denominator counter is determined by sets of at least four dosimeters, each of a different material type. In the B & W Owners Group Cavity Dosimetry Experiment referenced in the topical, it is

**Framatome Technologies Inc.**

noted that there are twenty-four dosimeter - material sets. In most B & W Owners' capsules, there are four sets. In many other FTI analyses, there is just one set.

Appendix A of the topical, Tables A-1 and A-2 list 39 capsules and cavities in the dosimetry database (*DD*). Thus, the results from Equation 7.6 are evaluated for each capsule and cavity in the database. The measurement uncertainty ( $\sigma_M$ ) for the entire dosimetry database (*DD*) is evaluated using Equation D.19 to appropriately combine the capsule and cavity uncertainties ( $\sigma_{M(i)}^2$ ).

$$\sigma_{M(DD)}^2 = \sum_i^{DD} w_i \sigma_{M(i)}^2 \quad (D.19)$$

The value of the database variance in Equation D.19 is estimated to be less than, or equal to 49 percent. This gives a measurement uncertainty of 7 percent or less.



### D.2.2 RAI Set 2 Responses

This section provides the responses to the set of requests for additional information (RAIs) that were transmitted to the B&WOG in reference D2. The responses to each of the 19 RAIs are based on the discussions during the FTI, B & W Owners Group - NRC meeting. They also refer to the Statistical Methods section, which summarizes explanations discussed during the meeting. The responses include a few brief statements referencing the meeting.

#### Set 2 - Question 1

**Equations (7.4) and (7.5) appear to incorrectly combine (%) relative errors and absolute errors (e.g., measured in cm or mg). Please explain this apparent inconsistency.**

Response

Table 7-1, on page 7 – 1 2 of the topical, shows some measurement errors as absolute values, and some as relative values. As shown by Equations D.14 and D.16 in Section D.2.1, on page D - 41, all errors were converted to relative values for the propagation of uncertainties in Equations 7.1 through 7.5.

#### Set 2 - Question 2

**Why is the helium concentration of samples DB-BEC, 9/26, 9/27, 4/10 and 4/12, and DB-Li-5A and 5B (Tables B-4.2-1 and B-4.2-2) a factor of ~ 10 less than the other samples ? Are these samples shielded ?**

Response

The helium concentrations in the HAFM dosimeter samples noted in the question are approximately an order of magnitude less than other samples because these dosimeters

**Framatome Technologies Inc.**

are located in the nozzle and seal plate elevations as shown in Figure 4.2, on page 4 - 16. They are not shielded dosimeters.

**Set 2 - Question 3**

**Provide the values and basis for the measurement errors assumed in determining the dosimeter uncertainties of Tables 7-2 and 7-3.**

Response

Two of the four volumes from the "Uncertainty Assessment and Results of Niobium Analysis for Davis Besse Cavity Dosimetry Benchmark Experiment" were provided during the meeting. The information included (a) the values, and (b) the basis for the measurement errors assumed in determining the dosimeter uncertainties. "Meeting Question 1", under the heading of "Additional Explanations", Section D.2.4, addresses the other two volumes.

**Set 2 - Question 4**

**Why are the dosimeter measurement uncertainties of Tables 7-2 and 7-4 different ?  
Which values are used in the FTI analysis ?**

Response

**Set 2 - Question 5**

**Using a conservatively large or bounding value for the measurement uncertainty with Equation (7.9) results in a nonconservative estimate for the calculation uncertainty. A conservative calculation uncertainty should be determined using a minimum value for the measurement uncertainty.**

Response

based on the values which experimentalist assign to cross section measurements using the same activation techniques, the value of 7.0 percent is estimated as an appropriate measurement uncertainty as explained during the meeting.

**Set 2 - Question 6**

**The form of Equation (7.6) appears to be incorrect. Also, provide the values and basis for  $w_{mat}$ ,  $\rho_{mat}$ ,  $w_d$ ,  $\rho_d$ ,  $\sigma_{mat,d}$  and  $N_{\{mat,d|\geq 4\}}$  in Equation (7.6).**

Response

The “Statistical Methods” presented in Section D.2.1, summarizes the derivation of Equation 7.6, and explains the basis for its form on pages D - 42 through D - 46. During the meeting discussion, the correlation coefficients for  $\rho_{mat}$  and  $\rho_d$  were explained to have values of unity.

The standard deviations come from Table 7-4, on page 7 – 18, and include the covariance matrix with the combined set of correlation coefficients.

**Set 2 - Question 7**

**In the application of Equation (3.17), what irradiation period was used in determining the effect of the power history on the dosimeter response? If the power history used in Equation (3.17) was averaged over an irradiation interval larger than one month, provide an estimate of the effect of this approximation on the dosimeter response.**

Response

The total irradiation period was from December 5, 1988, to January 26, 1990, which constituted the operation of Davis Besse Cycle 6. While the duration of the time steps used to calculate the fraction of saturation varied, none of them were greater than 1 day.

**Set 2 - Question 8**

**Equations (7.1)-(7.5) assume that the contribution to the measurement error from a given error source is equal to the error in the source. For example, the error in the measurement due to dimensional errors is taken to be the same as the error in the dimensions. Since this is not generally valid, standard uncertainty analyses relate the error source and resulting measurement error using sensitivity factors which express the sensitivity of the measurement to errors in the source variable. These sensitivity factors can be significantly different than unity when the**

**Framatome Technologies Inc.**

measurement has a weak nonlinear dependence on the source variable (e.g., in the case of the exponential dependence of the absorption correction on the dosimeter thickness). These sensitivity factors should be included in the uncertainty equations.

Response

Equations 7.1 through 7.5 do appear to assume that the contribution to the measurement error from a given error source is equal to the error in the source. However, as explained during the meeting, and shown in Equation D.14 on page D - 41, Section D.2.1, the non-linear sensitivity factors, or response functions, are appropriately included in the respective uncertainty terms.

**Set 2 - Question 9**

**Provide the value and basis for the weighting  $\rho_{\text{mat}}$  used in Equation (7.13). Is the value the same as used in Equation (7.6) ?**

Response

The value and basis for the weighting  $\rho_{\text{mat}}$  used in Equation 7.13, results from the fact that the material dependent  $C/M$  benchmarks for any capsule or cavity come from a single calculational process. Thus, all material dependent  $C/M$  results are related. Consequently, the correlation coefficients are unity. The material correlation coefficients used in Equation 7.6 are also unity.

**Set 2 - Question 10**

**Please define the denominator in Equation (7. 10).**

Framatome Technologies Inc.

Response

The total number of independent capsule and cavity data sets in the dosimetry database (DD) is thirty-nine as described on page 7 - 28 of the topical.

**Set 2 - Question 11**

**Because of the strong fluence attenuation between the core and vessel, the dosimeter response is very sensitive to the methods and data used in these calculations. As a result, typical pressure vessel fluence calculations are expected to provide an accuracy of ~ 15% when predicting (> 1-MeV) dosimeter response. The major contributors to this uncertainty are the (1) relative core/vessel/dosimeter geometry (2) nuclear cross sections and fission spectra (3) determination of the core neutron source (4) methods and modeling approximations and (5) the Equation (3.17) adjustment for irradiation and decay times. In view of the fact that the observed M/C uncertainty is substantially less than 15 %, provide an explanation for this reduced M/C uncertainty. Have any adjustments (other than those explicitly identified in the report) been made to improve the M/C agreement ?**

Response

The  $C/M$  benchmark uncertainty in the topical is      percent. While the question suggests that the industry uncertainty is around 15.0 percent, draft regulatory guide DG-1053, dated June, 1996, and Table 2-1 (page 2 - 3) in the topical, indicate that the industry uncertainty is generally considered to be more than 20.0 percent, and nearly 30.0 percent when FTI predictions are not included to lower the average. FTI's high degree of precision is also noted in the PCA blind test, where the FTI predictions are

**Framatome Technologies Inc.**

## FTI Non-Proprietary

within the measurement uncertainty, while those of others have deviations of twice the uncertainty (NUREG/CR-1861 discusses the PCA results, Reference 37 in the topical).

The reasons for the outstanding accuracy and precision in the FTI predictions are generally costs and expertise. The FTI analyses are performed by senior analysts, who have developed very detailed models for the calculations, including pin by pin fission rates, et cetera. The analyses are therefore more costly than others in the industry.

The measurements are performed by an independent laboratory, and the results independently reported. For the Cavity Dosimetry Experiment, the experimental methods, results, and uncertainties were also checked by independent consultants. The calculations come from standard computer codes, and the FTI procedures are described in topical Section 3.0. The results of the calculations and measurements are shown in Table A-1. The NRC has confirmed the reduced value of the  $C/M$  uncertainty by statistically processing the Table A-1 data.

### Set 2 - Question 12

**In the third column of Table A-2, the value of 1 - C/M is provided instead of  $\sigma_{C/M}$ . Provide the plant dependent value of  $\sigma_{C/M}$ .**

**Framatome Technologies Inc.**

Response

The third column in Table A-2 will be removed. Since the value of  $\overline{\sigma_{C/M}}$  is defined by Equation 7.15, there is no value for each individual capsule and cavity.

**Set 2 - Question 14** (Due to formatting difficulties, Question 13 follows Question 15)

**The BAW-2241-P fluence methodology does not include the analytic determination (based on numerical sensitivities) of the fluence calculation uncertainty as described in DG-1053. Please identify any other calculation or measurement differences between the proposed methodology and the guidance of DG-1053.**

Response

The first statement, that the BAW-2241-P fluence methodology does not include the analytic determination (based on numerical sensitivities) of the fluence calculation uncertainty as described in DG-1053, is not accurate. It is not possible to infer the vessel fluence uncertainty from either benchmark uncertainties of calculations to measurements, or from measurement uncertainties. Therefore, as stated on page 1 - 2 of the topical, analytical vessel fluence uncertainties were integrated with capsule and cavity benchmark uncertainties.

In addition, the draft guide requirement that the measurement uncertainty include a reference field validation, is in progress. The Owners have agreed to send the NRC a copy of the report (for information only) after it is completed in 1999.

**Framatome Technologies Inc.**



Whether the topical meets all of the requirements of DG-1053, or whether there may be differences, the NRC agrees that the topical includes the most advanced fluence technology and most comprehensive uncertainty methodology developed to date, to meet the requirements of the draft guide.

**Set 2 - Question 15**

**The calculational perturbation factors of Appendix-C were determined using the BUGLE-80 fluence methodology rather than the most recent BUGLE 93 Semi Analytic approach. What is the effect on the M/C data-base and associated biases and uncertainties of using this earlier methodology ?**

Response

As discussed in the meeting, the effect of using the BUGLE-80 results on the  $C/M$  database, and thus on the bias and uncertainty, is negligible.

**Set 2 - Question 13**

**Were the benchmark data-base capsule and cavity measurements of Table A-1 which are identified by plant actually made at the assigned plant, or were the dosimeters/capsules from the assigned plant irradiated in a different (or surrogate) plant ? Please identify any measurements that were not actually installed and measured at the indicated plant.**

Response

As discussed in the meeting, and described in the "Integrated Reactor Vessel Material Surveillance Program" topical (BAW-1543A<sup>10</sup>), most B & W plant capsules were irradiated at a host (surrogate) plant. All cavity measurements were actually made at the indicated plant.

**Framatome Technologies Inc.**

**FTI Non-Proprietary**

**Framatome Technologies Inc.**

**Set 2 - Question 16**

**The standard deviation of the M/Cs (from the overall average M/C) in the Appendix-A data-base appears to be almost a factor of two larger than the value given in the text (on p. 7-33). Please provide an explanation for this difference.**

Response

The difference is a result of the energy dependent bias removal function for neutron energies above 0.1 MeV. Section D.2.4, "Additional Explanations" discusses the bias removal function in "Meeting Question 3". The evaluation of the NRC standard deviation, and the FTI value is discussed in the "Statistical Processing of Table A-1 Data" section (D.2.3) that follows.

**Set 2 - Question 17**

**The calculation uncertainty is determined by combining the measurement uncertainty,  $\sigma_M$ , and the standard deviation,  $\sigma_{C/M}$ , of Equation (7.16). However, it is not evident that these two quantities refer to the determination of the same response (as required). For example, it appears that  $\sigma_M$  refers to the uncertainty in the measurement of a specific nuclide (e.g., Ni-58(n,p)) while  $\sigma_{C/M}$  refers to the C/M deviation for the average of all nuclides of a given capsule. Please explain this apparent discrepancy and justify any differences in the response being used in the definitions of  $\sigma_M$  and  $\sigma_{C/M}$ .**

Response

The statement that the calculational uncertainty is determined by combining the measurement uncertainty,  $\sigma_M$ , and the benchmark standard deviation,  $\overline{\sigma_{C/M}}$  of

Framatome Technologies Inc.

Equation 7.16, is not accurate.

**Set 2 - Question 18**

**BAW 2241-P states that the BUGLE-93 calculations of one of the dosimeter responses is erroneous (p. 7-29) and that the BUGLE-93 calculated C/Ms for this type of dosimeter have been removed from the analysis (p. 7-31). In addition, it is stated (p. 6-4) that this dosimeter has "special problems." What is the C/M bias for this type of dosimeter and is this improved by the use of a BUGLE-93 (rather than CASK) photo-fission correction ?**

Response

**Set 2 - Question 19**

**Recent calculations described in NUREG/CR-6453 suggest that the BUGLE-93 cross section library results in an underprediction (relative to BUGLE-96 and SAILOR-95) of the Fe-54, Ni-58, U-238 and Np-237 cavity dosimeter reaction rates of 1%, 2%, 4%, and 10%, respectively. (The prediction of the in-vessel dosimeter reaction rates for the three libraries agree to within 1% .) In view of the difference between these libraries, please review and update the FTI M/C data-base and methodology, as necessary. Will this update allow the inclusion of the threshold dosimeter measurements that were excluded ?**

**Response**

In 1980, the BUGLE-80 library was considered to be the best in the industry for fluence analyses. By 1988, the NRC had convinced FTI and the B & W Owners that the fluence technology using the CASK library was too outdated. Therefore, in concert with the B & W Owners Group Cavity Dosimetry Experiment, FTI performed the analysis using both the CASK and BUGLE-80 libraries.

While the BUGLE-80 results showed a bias in the cavity dosimetry benchmark, the CASK results did not. In the capsule dosimetry benchmark results, neither library showed any statistically significant bias. Furthermore, the uncertainty in the capsule results from both libraries was statistically the same with greater than a 95 percent level of confidence.

Due to the BUGLE-80 bias, the NRC stopped recommending that library and began recommending the BUGLE-93 one. The B & W Owners again paid for a

**Framatome Technologies Inc.**

## **FTI Non-Proprietary**

comprehensive analysis and uncertainty evaluation of the Cavity Dosimetry Experiment. The reanalysis of the results showed no biases in either the capsule or the cavity. However, the Np-237 dosimeter results indicated a bias in that dosimeters cross sections. This was particularly evident in the capsule compared to both the BUGLE-80 and CASK results.

Now, the NRC is recommending another update, from the BUGLE-93 library to the BUGLE-96 one. It appears that the BUGLE-93 results could possibly be biased and under-predict the fluences relative to BUGLE-96.

Technically, FTI agrees that the Np-237 is probably biased, and the calculations under-predict the reactions (see Table 6-1, on page 6 - 3, and Table 6-2, on page 6 - 5 of the topical). Furthermore, updating the library to the best available one, is technically better than any other option. However, from economical considerations, updating the library is the least cost effective option. The topical already notes that Np-237 appears to have biased cross sections that cause the calculations to under-predict the measurements. The B & W Owners have funded a program, that will be completed by 1999, to evaluate the cause of the Np-237 bias. As noted in the "Meeting Question 3" discussion for "Additional Explanations" (Section D.2.4), FTI utilizes an energy dependent bias removal function to treat the effects of calculational biases in the Fe-54, Ni-58 and U-238 dosimeters.

Since the FTI calculational methodology, using the BUGLE-93 library, is not biased, and the deviations in the Fe-54, Ni-58 and U-238 reaction rates between the BUGLE-93 and BUGLE-96 calculations are well within the uncertainties of the FTI, methodology,

**Framatome Technologies Inc.**

FTI and the B & W Owners believe that a BUGLE-96 update is neither technically warranted, nor economically cost effective. Thus, in the future, only the Np-237 bias will be evaluated and corrected.

### **D.2.3 Statistical Processing of Table A-1 Data**

During the August the fifth and sixth meeting between FTI, the B & W Owners, and the NRC, the NRC explained that they had statistically processed the Table A-1 data in the topical. The processing included the creation of a dosimeter by dosimeter benchmark of  $M/C$  ratios for the specific activities. The  $M/C$  ratios for the 728 dosimeters in the dosimetry database were averaged to determine a mean value of 0.9940. The dosimeters were assumed to have independent uncertainties. Therefore, a benchmark uncertainty for the database was estimated by appropriately evaluating the standard deviation. The statistical procedures for the evaluation included assuming a bias,

The differences in each of the 728 benchmark ratios were squared, summed, and divided by 727 degrees of freedom. This gave a relative standard deviation

The NRC's conclusion from this evaluation was that the FTI methodology had no statistically significant bias

However, the uncertainty of      percent was considerably larger than FTI value of      percent, noted on page 7 - 33, and calculated with Equations 7-12, 7-13, and 7-15 from the Table A-2 data. Consequently, the NRC wanted an explanation

## FTI Non-Proprietary

concerning the validity of the FTI benchmark uncertainty, particularly explaining why a value closer to      percent would not more appropriately represent the methodology.

In the past, when the  $M/C$  ratio was used to convert calculations to measurements, the measurement bias and the conversion process, or unfolding uncertainty, were related to this ratio. However, when the NRC suggested in DG-1053, that vessel fluence predictions would not have an appropriate uncertainty, unless they were based on calculations, the  $M/C$  ratio lost its physical significance. In the topical and meeting discussion, the  $C/M$  ratio is referenced as the appropriate term for determining the bias and standard deviation

When the Table A-1 data was processed to determine the mean  $C/M$  ratio for the 728 dosimeters, the resulting value was 1.0310. Assuming that the mean value represents a bias, the standard deviation was computed to be      percent. This computation of the standard deviation assumes that all dosimeter benchmarks are independent of one another. Thus, the cross product dependency parameters in the covariance matrix are represented by a null set.

**Framatome Technologies Inc.**



The value of            percent is based on the assumption that all dosimeter benchmarks are independent of one another. However, as discussed in the "Statistical Methods" section (D.2.1, page D - 43, below Equation D.18, through page D - 45), and in the "Addition Explanations" section (D.2.4), on "Meeting Question 4", the dosimeter uncertainties for each capsule and cavity analyses in Table A-1 are not independent. The uncertainties are directly related to the five constant parameters in Table 7-1, on page 7 - 12 of the topical. Therefore, the appropriate treatment of the correlation coefficients, representing the cross product dependency between dosimeters, should reflect a direct relationship. This treatment means that the values in the set of correlation coefficients are unity.

The explanation and evaluation of the benchmark standard deviation, is focused on the  $C/M$  ratio, correlation coefficients of unity, the bias, and the standard deviation difference between a value of            percent, estimated in the topical (page 7 - 34, just

**Framatome Technologies Inc.**

## FTI Non-Proprietary

below Equation 7.19) and a value of      percent or greater, estimated from the above discussions. The difference between  $C/M$  and  $M/C$  ratios demonstrates why relative standard deviations are frequently closer to a natural logarithm normal distribution than a standard normal distribution. However, the topical discusses the fact that the database of benchmark deviations fits within Student's central "t" distribution with a probability greater than 95 percent. Thus, the  $C/M$  ratio is not a parameter that causes the standard deviation difference.

A set of null values for the correlation coefficient, will generally produce a lower standard deviation than a set with values of unity.

The correlation coefficients used in the topical are determined from the physics of the functional relations. Consequently, the correlation coefficient values in Equations 7.12, 7.13 and 7.15 are uniquely determined and do not represent a statistical approximation.

The bias evaluation is the key to understanding the difference between the standard deviation values greater than      percent, and the topical estimate      or the Equation 7.15 benchmark result of      percent. As discussed in the topical, and demonstrated by the mean  $M/C$  and  $C/M$  ratios, the fluence calculation, integrated over the energy range greater than 0.1 MeV, shows no indication of a bias.

**Framatome Technologies Inc.**

The discussions addressing "Meeting Question 5" in the "Additional Explanations" section (D.2.4), explain that each capsule and cavity analysis does not represent independent calculations of the dosimeters. There is generally a spatial and spectral fluence function at the dosimetry location. The fluence is multiplied by constant cross section - response functions to obtain the saturated asymptotic specific activity. This activity is multiplied by the analytical expression representing the fraction of saturation to obtain the specific activity for benchmark comparisons to the measurements (pages 3 - 30 through 3 - 32 in the topical). Thus, even though there may be four or more dosimeter materials, the benchmark evaluation uses correlation coefficients with values of one in Equations 7.12 and 7.13.

To evaluate the effects of removing the bias with Equation 7.13, the form of Equations 7.12 and 7.13 was modified to process systematic and random deviations. The processing of the systematic deviations used Equation 7.10 (page 7 - 28) to define biases

**Framatome Technologies Inc.**

**FTI Non-Proprietary**

**Framatome Technologies Inc.**

The 39 capsule and cavity standard deviations are combined as the root mean square, of the sum of the standard deviations, squared. The modified form of Equation 7.15 continues to have 38 degrees of freedom. The resulting benchmark standard deviation is      percent. The fact that this value is statistically within 3.01 percent of the benchmark standard deviation estimated with Equations 7.12, 7.13 and 7.15 in the topical, and is less than the topical value of      percent, provides confidence that the topical "Uncertainty Methodology" is appropriate.

The fact that the benchmark standard deviation in the database may be estimated to be greater than      percent, appears to be a function of (a) the      bias, and (b) the sets of unity correlation coefficients

The value of the mean bias affecting the database is estimated by combining the      biases in Table D-1.

The mean effective bias, estimated from the above evaluation is      percent. With the correlation coefficient values in the covariance matrix of dosimeter uncertainties represented by sets of unity, combining the bias, as if it represented a standard deviation, with the unbiased benchmark standard deviation, is simply additive. Consequently, the covariance matrix combination of the mean effective material bias, and the benchmark standard deviation, gives a biased standard deviation of      percent. This is comparable to the      percent biased standard deviation initially estimated by processing the  $C/M$  dosimetry benchmark ratios in Table A-1.

The summary of the evaluation is that differences between estimates of a benchmark uncertainty greater than      percent, versus the topical value of      percent, is due

**Framatome Technologies Inc.**

to the fact that the values greater than percent contain an energy dependent bias. The effects of the bias are furthermore accentuated by the fact that the dosimetry uncertainties for each capsule or cavity analysis are not independent. The dependency between the standard deviations in the covariance matrix, result in the energy dependent bias, directly increasing the unbiased benchmark standard deviation as an additive term.

#### **D.2.4 Additional Explanations**

As FTI was addressing the second set of RAI's during the August the fifth and sixth meeting between FTI, the B & W Owners, and the NRC, the NRC questioned five areas that needed in-depth additional explanations. These questions could not be addressed during the meeting, because of time constraints. This section of the appendix lists the five meeting questions, and provides more of an in-depth response than provided at the meeting.

##### **Meeting Question 1**

**Send the measured data and "Uncertainty Assessment..." documents from the B & W Owners Group Cavity Dosimetry Experiment to the NRC.**

##### **Discussion**

FTI and the B & W Owners have received the NRC's letter stating that there is no problem with the data being proprietary (from Joseph L. Birmingham, Office of Nuclear Reactor Regulation, U.S. Nuclear Regulatory Commission, dated, October 13, 1998). The documents are in the process of being copied, and will be forwarded to Dr. Lambros Lois when they are ready.

**Framatome Technologies Inc.**

**Meeting Question 2**

**The benchmark uncertainty includes results from CASK, BUGLE-80, and BUGLE-93. The NRC questions: how these three different cross section sets provide a consistent benchmark uncertainty ? It would appear to be necessary to update all capsule and cavity calculations with one consistent cross section set, preferably based on BUGLE-96. Why is this not necessary ?**

**Discussion**

The draft Regulatory Guide, DG-1053, and RAI 19 (Set 2), suggest that updating the technology for fluence analyses, including the latest cross section library, is advisable to ensure sufficiently accurate predictions of vessel fluence values. Technically, this suggestion is appropriate. However, as noted in the response to RAI 19, it is not cost-effective to routinely update the technology, if the current technology is accurate (representing a best-estimate, with no observable biases or errors), and has a well-defined uncertainty. Moreover, when it is warranted from both technical and economical considerations, to update the fluence technology, the most cost-effective option would not be to completely reanalyze all capsules, cavities, and dosimetry in the database. The incremental safety, licensing, operational, et cetera, benefits of such a reanalysis would have to be enormous to adequately offset the commensurate costs.

While reanalyzing all capsules, cavities, and dosimetry in the database would not generally be warranted economically, reanalyzing only one capsule or cavity would not be technically justifiable. As discussed in Section 7.0 of the topical and in this appendix, the B & W Owners Cavity Dosimetry Experiment, which also includes a comprehensive capsule analysis, represents just two degrees of freedom in the statistical evaluation of the benchmark data. Therefore, updating the technology with two

**Framatome Technologies Inc.**



## **FTI Non-Proprietary**

benchmarks would not provide a sufficient level of confidence in the results to ensure consistency with the safety evaluations.

FTI and the B & W Owners were faced with the situation of developing an economical, but technically valid program for updating the fluence technology for the Cavity Dosimetry Experiment. (See pages 1 - 1 and 2 - 11 in the topical, which discuss (1) updating the cross section libraries from CASK to BUGLE-80, and then to BUGLE-93, (2) updating the predictive methodology from measurement based to calculation based, and (3) updating the uncertainty methodology.) Updating the technology, with changes in both the predictive methods and the cross section libraries, would have been excessively costly if the entire database were reanalyzed. Nonetheless, the incremental gains in safety and licensing margins were considered to be technically important. Therefore, to be cost-effective and technically justifiable, the proposed improvement in the technology included benchmarks of the Cavity Dosimetry Experiment with the CASK, BUGLE-80, and BUGLE-93 libraries.

The measurement database was updated to exclude any effects of the analytical analyses. Thus, there is no dependence on any of the dosimeter measurements from the three libraries. As discussed in the topical, the update of the measurement uncertainties demonstrated that the estimated values were valid for all the previous dosimetry measurements.

The benchmarks to the Cavity Dosimetry Experiment, with calculations based on the CASK, BUGLE-80, and BUGLE-93 libraries, provided a means of assessing the uncertainty in the calculations with respect to each library.

**Framatome Technologies Inc.**

The bias removal function was found to be independent of the libraries, although there were some differences in the energy dependent factors. The calculations using the BUGLE-80 library were clearly biased by the vessel. Therefore, no cavity benchmark results were included in the BUGLE-80 comparisons to the other libraries. The Np-237 cross section in the BUGLE-93 library, was clearly biased in comparison to the CASK and BUGLE-80 results. Therefore, no Np-237 dosimetry was included in the BUGLE-93 comparisons to the results from other libraries. With the biases appropriately treated for each library, the benchmark standard deviations were evaluated. In addition, the benchmark results between libraries were compared and the standard deviations evaluated.

The unbiased uncertainty evaluation indicated that each library had an uncertainty that was statistically indistinguishable from the uncertainties in the other libraries. Furthermore, the evaluation indicated that the standard deviations between libraries were statistically insignificant compared to the standard deviations of each library.

The additional benchmark comparisons of the results from one library, to those of the other libraries, established a cross-reference relating the uncertainties between libraries. Thus, it is possible to estimate the differences in the results between calculations of capsule or cavity

**Framatome Technologies Inc.**

## **FTI Non-Proprietary**

dosimetry using the BUGLE-93 library, relative to calculations using CASK. The probability that the BUGLE-93 results will bound the CASK results is well-defined, with a high level of confidence.

If calculations using the CASK library are benchmarked to a set of measurements, and a benchmark uncertainty is estimated, then the BUGLE-93 benchmark uncertainty may be estimated without performing the calculations. The common benchmark of calculations using BUGLE-93 and CASK provides the means of combining the two benchmarks to estimate the standard deviation in the BUGLE-93 benchmark.

In conclusion, calculations using the CASK, BUGLE-80, and BUGLE-93 cross section libraries to estimate a benchmark uncertainty, provide consistency by including a cross-reference where the libraries are appropriately benchmarked to one another. The cross comparison of benchmark results, and the statistical assessment of the significance of any differences, provides the means of estimating an uncertainty with the appropriate level of confidence.

### **Meeting Question 3**

**The bias removal function within the energy range greater than 1.0 MeV, needs to be explained.**

#### **Discussion**

As discussed during the meeting between FTI, the B & W Owners, and the NRC, the FTI calculational methodology has a bias as a function of energy. The bias, the bias removal function that is used to eliminate the bias, and the application of the bias

**Framatome Technologies Inc.**

removal function to obtain best-estimate fluences, was previously presented to the NRC. The presentation was in a letter dated March 4, 1997, from Arkansas Nuclear One, Unit 1. This letter was in response to a set of Request for Additional Information regarding the RCS Pressure and Temperature Limit Technical Specification Change Request. The information discussed below is an update of that previously presented.

Before explaining the development of the bias removal function, the definition of the key terms is presented.

### **Definitions**

- (A) The bias removal function can be expressed as either a continuous function ( $f$ ) of energy ( $E$ ),

$$h = f(E),$$

or a discrete constant by energy group ( $g$ ),

$$h_g = \text{Constant}_g.$$

The discrete form is used in practice.

- (B) The  $h_g$ 's were determined during the evaluations and analyses of the Cavity Dosimetry Experiment, as discussed below. The numerical values of the  $h_g$ 's are given in Table D-2.
- (C) The  $h_g$  is independent of (1) any specific plant, (2) spatial locations throughout the core, reactor internals, vessel, and cavity, within the belt-line region, and (3) the dosimeter material type.

**Framatome Technologies Inc.**

- (D) Application of the bias removal function ( $h_g$ ) to the DORT - calculated fluence, produces the best-estimate (unbiased) fluence. Typically, this amounts to less than a 5 percent change in the magnitude of the calculated fluence. (The  $h_g$  is not applied to the measurements.)

## Development

### Introduction

One of the primary goals of the B & W Owners Cavity Dosimetry Program was to develop a calculational-based methodology that could be used to accurately determine the neutron fluence in the surveillance capsule, reactor vessel, and reactor vessel cavity structure. An accurate methodology already existed for the capsule and vessel, however, it was necessary to extend and modify the methodology to accurately calculate the energy-dependent dosimeter responses in the cavity. The measurement results from the Cavity Dosimetry Program were used in a statistical analysis to identify, and quantify an energy dependent bias in the calculated fluence. This calculational bias is a function of the methodology. As such, it is general, not specific to the Cavity Dosimetry Experiment, and therefore applies to all analyses that use the Semi - Analytical methodology described in the topical. The discrete form of the bias removal function, is applied on a group-by-group basis, using a set of constant "bias factors" ( $h_g$ ) which remove the bias in the calculated fluence in each specific energy group.

### The Concept of the Bias Removal Function

This section describes the general concept associated with the bias removal function. The true value of some arbitrary physical quantity,  $Q$ , is defined as  $Q^{\text{TRUE}}$ . The value

## FTI Non-Proprietary

of the same quantity, determined by some analytical process, is defined as C. Likewise, the value of the same quantity, determined by some experimental process, is defined as M. In general,

$$\begin{aligned} C &\neq Q^{\text{TRUE}}, \\ M &\neq Q^{\text{TRUE}}, \text{ and} \\ M &\neq C. \end{aligned}$$

The goal is to determine the best-estimate of the true value,  $Q^{\text{BEST}}$ , which in a calculational-based methodology is defined by:

$$Q^{\text{BEST}} = C_{\text{UNBIASED}} \quad (\text{D.20})$$

$$(\text{D.21})$$

$$(\text{D.22})$$

$$C_{\text{UNBIASED}} = C (h^{-1}) \quad (\text{D.23})$$

$$\text{where } h = \quad (\text{D.24})$$

$Q^{\text{BEST}}$  will of course differ from  $Q^{\text{TRUE}}$ , however,  $Q^{\text{TRUE}}$  is bracketed by  $Q^{\text{BEST}}$  over a range that is defined by either, the sum of  $Q^{\text{BEST}}$  and the uncertainty in  $Q^{\text{BEST}}$ , such as,

**Framatome Technologies Inc.**

$$\left[ Q^{\text{BEST}} - U(Q^{\text{BEST}}) \right] \leq Q^{\text{TRUE}} \leq \left[ Q^{\text{BEST}} + U(Q^{\text{BEST}}) \right] \quad (\text{D.25})$$

or, by the product.

$$\left[ C_{\text{UNBIASED}} (1 - U) \right] \leq Q^{\text{TRUE}} \leq \left[ C_{\text{UNBIASED}} (1 + U) \right] \quad (\text{D.26})$$

Combining Equations D.23 and D.26 yields

$$\left[ C (h^{-1}) (1 - U) \right] \leq Q^{\text{TRUE}} \leq \left[ C (h^{-1}) (1 + U) \right] \quad (\text{D.27})$$

(D.28)

### The Bias Removal Factor

The preceding generalized discussion expresses the theory upon which the determination of the bias in the fluence is based. In moving from the general to the

**Framatome Technologies Inc.**

specific, however, there are a number of significant differences, which will now be discussed.

The neutron fluence, which is the quantity of interest, is not (and cannot be) measured directly. Instead, a quantity that is related to the flux in a known way, - the dosimeter response - is measured. Consequently,  $M$ ,  $C$ , and  $C/M$  would not have the same relationship to the neutron flux ( $\phi$ ) that they would have had in the previous theoretical discussion, but the fundamental idea still applies.

The flux of interest is integrated over the energy range,  $E > 1.0$  MeV. The measured quantity is a dosimeter response. This response is related to the flux through energy dependent cross section - response functions. The dosimeter measurement represents an integration over the energy range of the dosimeter response. With four or more dosimeter measurements, each representing an integration over different energy ranges, a bias, which is a function of energy, can be uniquely identified. Since the energy dependent bias can be uniquely identified, an energy-dependent bias removal function can be derived to remove the bias from the calculated flux. While the bias removal is a function of energy, it is a constant related to the calculational methodology. It is not related to a plant-specific calculation, but rather to all calculations for every plant. Expressed discretely, the bias removal function would have the following form,

$$h_g = \quad (D.29)$$

and it would be used to determine the best-estimate flux as follows:

$$\phi^{BEST} = \sum_g (\phi_g^{calc}) (h_g^{-1}) \quad (D.30)$$



where  $g$  = energy index  
 $\phi_g^{calc}$  = calculated neutron flux in group "g"  
 $h_g$  = bias removal factor for group "g"

The bias removal methodology must be able to determine the fluence at numerous locations in the reactor vessel. Given the fact that the geometrical configuration of the core, and internals structure is very complex, it would be reasonable to think that the bias would be spatially dependent as well as energy dependent. If the energy-dependent bias was also a function of space, the best-estimate fluence at the vessel inside surface would have to be obtained using multiple sets of bias removal factors.

The possibility of a spatially dependent bias in the calculational methodology was one of the fundamental issues that the Cavity Dosimetry Experiment was designed to address.

Table D-2 Bias Removal Factors (E > 1 MeV)

Energy Group	Upper Energy, MeV	$h_g$
1	17.33	
2	14.19	
3	12.21	
4	10.00	
5	8.607	
6	7.108	
7	6.065	
8	4.966	
9	3.679	
10	3.012	
11	2.725	
12	2.466	
13	2.365	
14	2.346	
15	2.231	
16	1.921	
17	1.653	
18	1.353	
19	1.003	

Framatome Technologies Inc.

**Meeting Question 4**

**The measurement uncertainty computed with Equation 7.6, does not clearly represent the sensitivity of the response function relation between the database, and each of the 728 dosimeter measurements listed in Table A-1. The NRC would like an explanation describing the consistency between the individual dosimeter measurement uncertainties and the overall measurement uncertainty for the dosimetry database.**

Discussion

RAIs 1, 6 and 17 from Set 2, illustrate the range of meeting discussions that concerned the uncertainties in the measurements. The range varied from discussions concerning, (a) what is actually being evaluated in the benchmark of calculations to measurements, and consequently, what specifically is related to the benchmark uncertainty, to (b) what is the meaning of the correlation coefficients

## **FTI Non-Proprietary**

The NRC processed the dosimetry database in Table A-1 and confirmed that there was no bias in the FTI calculational methodology, for neutron reactions with energies above 0.1 MeV. From this result, a reasonable conclusion was that the benchmark uncertainty could be determined by statistically processing the individual dosimeters as outlined above in Section D.2.3, discussing the “Statistical Processing of Table A-1 Data”.

As the discussions during the meeting provided the additional information and explanations for the RAIs, it became clear that individual dosimeter benchmarks of calculated activities to measured values did not provide a sufficient benchmark for the calculational methodology, and thereby did not provide a sufficient benchmark uncertainty. Thus, even though the NRC processing of Table A-1 confirmed that FTI’s calculations of greater than 0.1 MeV fluences and activities have no bias, the conclusion that the statistical processing of the individual dosimeters provides an estimate of the benchmark uncertainty is not valid.

When the dosimetry is sufficient to provide two or more energy - dependent responses in the range above 0.1 MeV, the measurements are combined by weighting the respective materials. The measurement of the specific activity from neutron reactions with energies greater than 0.1 MeV is unbiased. Corresponding to the measured specific activity, there is a single calculation of the fluence as a function of space, energy, and the integrated time period for the dosimetry exposure. The dosimetry specific activities are calculated from the fluence spectral results, with energy group constants for the cross section - activity - response functions, and time dependent decay and operational effects represented analytically. The dosimetry in the capsules and cavity show negligible spatial - spectral effects (with the exception of the Owners Cavity Dosimetry Experiment) because they are in such close proximity to one another.

**Framatome Technologies Inc.**

The overall objective of the "Uncertainty Methodology" in Section 7.0 of the topical is to be able to have an appropriately high degree of confidence that the results of the calculated fluence, plus or minus an estimated uncertainty, have a known probability of bounding the true fluence. The fluence of interest has neutron energies greater than 1.0 MeV. The true fluence is defined in terms of measured specific activities, and the measurement techniques are calibrated to National Institute of Standards and Technology certified standards.

While the measurements are unbiased, they have an uncertainty associated with them due to random deviations. Consequently, in using the measurements as a reference for the benchmark of the calculations, it is necessary to know an estimate of the standard deviation and confidence level in the experimental methodology. The estimate of the standard deviation in the measured specific activity begins with Table 7-1 (page 7 - 12) in the topical. The random deviations in the table are combined in Equations 7.1 through 7.5 with examples of

**Framatome Technologies Inc.**

details shown in Equations D.14 and D.16. The result is a relative standard deviation for each dosimeter.

On page D - 42, in the paragraph above Equation D.17, the combination of dosimeter measurements for a single capsule or cavity evaluation is discussed in relation to the uncertainty determined with Equation 7.6. The calculations, and the calculational uncertainty evaluations, indicate that the capsule or cavity dosimetry have the same fluence. Therefore, all dosimeters of the same material type, such as Fe-54 foils, should have the same specific activity. Since the measurements have no biases (Section 7.1.1 of the topical, pages 7 - 9 and 7 - 10), a single mean measured specific activity is obtained by averaging the measured results.

The standard deviation in the mean specific activity for all dosimeters of the same material type could be estimated from the deviations in specific activity between pairs of the individual dosimeters. The individual deviations would be independent of one another. Accordingly, the cross terms in the covariance matrix would be zero, and the standard deviation would be estimated by the root mean square of the sum of the individual deviations, squared. This would include the statistical approximation that the degrees of freedom in the denominator, would be the total number of dosimeters of the respective material type, minus one.

While the above procedure would be acceptable, the preferable procedure (a) recommended by the draft regulatory guide, DG-1053, and (b) the one historically used in the fluence arena, is to use the components of the experimental methodology as

**Framatome Technologies Inc.**

discussed in the topical and represented by Equations 7.1 and 7.5. The standard deviation in the mean specific activity for all dosimeters of the same material type, would be estimated as the root mean square of the covariance matrix, as expressed by Equation 7.6.

The resulting response function is represented by Equation D.18, modified by the statistical approximation for the degrees of freedom. If the correlation coefficients for cross product dependency represent a null set, then the mean measurement uncertainty for all dosimeters of the same material, is the square root of the sum of the individual standard deviations, squared. However, as explained on page D - 43, following Equation D.18, the individual standard deviation for each dosimeter is dependent on a set of constant parameters. Accordingly, the values in the set of correlation coefficients are unity. Thus, the mean measurement uncertainty is the square root of the sum of the products and cross products of the individual dosimeter standard deviations.

The uncertainty that has been estimated in the above discussion is related to one material type in a single capsule or cavity evaluation. While this is an interesting value, and is suitable for benchmark comparisons of the calculated dosimeter material specific activity, the objective is to determine the uncertainty in the specific activities resulting from neutron reactions greater than 1.0 MeV. The uncertainty in a single material type of dosimeter measurements that principally respond to a unique portion of the energy range above 1.0 MeV, does not represent the uncertainty in the measurement of the entire range. Consequently, the uncertainties in several material types of dosimeters

that are sensitive to different ranges of the neutron spectrum above 1.0 MeV, are required.

In capsule or cavity evaluations of the greater than 1.0 MeV fluence, the dosimetry consists of several material types, with several dosimeters of each type. The measurements of the specific activity resulting from neutron reactions with energies greater than 0.1 MeV show no functional relation to the neutron energy. Thus, the Cu-63 reaction to produce Co-60 in the energy range above 5.0 MeV, and the Co-59 reaction to produce Co-60 in the energy range below 10.0 KeV, show no significant differences. Accordingly, the uncertainty in the combined measurements of the specific activity, incorporates a response function that provides each material uncertainty with an equal weight. Thus, in Equation 7.6, each of the four or more materials that are combined to represent the uncertainty in the greater than 0.1 MeV specific activity, has an equal weight (usually one-fourth). In addition, each dosimeter of that material in the capsule or cavity, has an equal weight relative to the inverse of the total number of dosimeters of that material type.

It has been explained above, and in the "Statistical Methods" section, that the correlation coefficients are represented by two sets

The result is the uncertainty in a capsule or cavity measurement of the specific activities greater than 0.1 MeV. The example of using Equation 7.6 in the topical, is associated with the B & W Owners Cavity Dosimetry Experiment. The topical discussion of measurement uncertainty (page 7 - 21, below Equation 7.7, and page 7 - 22) states that the standard deviation from Equation 7.6 is percent. "While this is a reasonable estimate for the

**Framatome Technologies Inc.**



## **FTI Non-Proprietary**

dosimeters in the cavity benchmark experiment, FTI considers a reasonable estimate for the entire database to be 7.0 percent or less".

The discussion in the topical continues, and explains how the database uncertainty is estimated to be 7.0 percent or less. While there are additional explanations of the statistical process, which include such pertinent details as the fact that at least 4 dosimeter - materials are grouped per set, which means that there are 143 sets in the database (with the Cavity Dosimetry Experiment consisting of 24 sets), there are no further developments of statistical equations showing the combination of the Cavity Dosimetry Experiment uncertainty with the rest of the capsule and cavity uncertainties in the database. During the meeting, it became clear that ending the development of statistical equations with Equation 7.6 in the topical caused confusion. The explanations in the topical which explained that there are 143 sets of measurements, with at least 4 dosimeter - materials per set, seemed to fit the format of Equation 7.6. Consequently, it appeared that all capsule and cavity dosimetry in the database was combined with Equation 7.6.

As noted in the discussion beginning with the second paragraph on page D - 45 in this appendix, and continuing through Equation D.19 on page D - 46, the measurement uncertainties for the capsules and cavities in the database are combined using Equation D.19. The weighting in Equation D.19 follows the same type of relations as expressed by Equations D.17 and D.18. Accordingly, the weight represents the response function. The correlation coefficient in the covariance matrix for cross product dependency parameters is represented by a null set. Thus, the uncertainty in the measurements for the entire FTI dosimetry database is determined by the square root, of the sum of the squares, of the uncertainties in each capsule and cavity measurement.

**Framatome Technologies Inc.**

To summarize, the sensitivity of the response function relations, between the database uncertainty and each of the 728 dosimeter measurement uncertainties, are grouped into three weighting functions. The reason for the three response function weights is that the measured specific activity for neutron reactions above 0.1 MeV is determined by a combination of dosimeter - materials. The dosimeters of the same materials in a capsule or cavity are grouped into individual material uncertainties by equally weighting each dosimeter. The various dosimeter materials within a capsule or cavity are grouped into sets of four dosimeter - materials to estimate the measurement uncertainty. Each dosimeter - material set uncertainty is combined using equal material - set weighting to estimate the uncertainty in a capsule or cavity analysis. The measurement uncertainty for the entire database is estimated by combining each capsule and cavity analysis. However, if one analysis represents 24 sets of measurements of the greater than 0.1 MeV specific activity, and another analysis represents just one set, then an appropriate weighting by set is needed. Therefore, each capsule and cavity is weighted by the respective sets of dosimeter - materials that provide measurements of the greater than 0.1 MeV specific activities.

**Meeting Question 5**

**The measurement uncertainty computed with Equation 7.6, and the benchmark uncertainty computed with Equation 7.15, do not appear to be consistent. This is particularly apparent considering that the benchmark uncertainty from Table A-1 is percent, when all dosimeters are treated independently. Explain how the statistical processing to determine the uncertainties is consistent.**

Discussion

RAIs 6, 11 and 14 from Set 2, along with “Meeting Question 4” from this section (D.2.4), illustrate the range of discussions during the meeting that focused on estimating the uncertainty in the calculational methodology. As noted in the response to RAI 14 (Set 2), it is not possible to infer a vessel fluence uncertainty (including an appropriate level of confidence) without performing an analytical uncertainty evaluation. Therefore, the uncertainties in the calculations are analytically determined with a series of sensitivity evaluations that propagate design, operational and fabrication uncertainties into fluence uncertainties. The fluence uncertainties are relative values representing the deviations in the fluence relative to the unbiased nominal fluence. The unbiased nominal fluence is determined assuming a reference design, with nominal operating conditions, and fabrication values for the various parameters.

The problem with the analytically estimated uncertainties, is assessing what confidence level and probability distribution that the root mean square deviations represent. The design, operational, and fabrication uncertainties are frequently defined as limiting or bounding values, and the confirmation of their validity rarely involves more than one measurement. Consequently, while it is possible to estimate a bounding uncertainty for the fluence at the vessel, and throughout the internals, and vessel-cavity structure, it is generally not possible to specifically define the level of confidence in the bounding uncertainty, or the probability that the combination of calculated results and uncertainties bound the truth.

The fact that it is not possible to infer a vessel fluence uncertainty without an analytical uncertainty evaluation, and the fact that it is not possible for the analytical fluence uncertainty to have a well defined level of confidence, means that there must be a second statistical technique to define the level of confidence in the calculational

**Framatome Technologies Inc.**

uncertainty.

While the meeting question referred to Equation 7.6, and it is now apparent that Equation D.19 represents the database measurement uncertainty, this does not change the point of the question. Equations D.19 and 7.15 should be consistent, but it is not apparent that they are consistent.

A large part of the questionable consistency between the measurement uncertainty (Equations 7.6 and D.19) and the benchmark uncertainty (Equation 7.15) was related to Equation 7.6. It was not clear what the measurement, and measurement uncertainty, actually represented. In addition, the cross product dependency between the individual dosimeter uncertainties being represented by a set of unity correlation coefficients, increased the ambiguity of what the uncertainty represented. The previous explanations in the sections on "Statistical Methods" (D.2.1) and "Additional Explanations" (D.2.4) for "Meeting Question 4", have described how the measurement uncertainty represents the standard deviation (7.0 percent) in the measurement of specific activities from neutron reactions with energies greater than 0.1 MeV. The topical included discussions explaining that the distribution of deviations could be represented by Student's central "t" with 142 degrees of freedom.

The previous explanations in this appendix, have cleared up quite a bit of the confusion related to Equation 7.6, and the measurement uncertainty. Thus, some of the apparent inconsistency between the measurement uncertainty and benchmark uncertainty (Equation 7.15) has also been cleared up. However, there are two important areas of

consistency that need to be explained. The first is the combination of  $C/M$  values represented by Equations 7.12 and 7.13. The second is that Equation 7.9 implies that the confidence factor and distribution of deviations are the same.

Concerning the combination of  $C/M$  values,

The product of energy dependent fluences, and constant energy group response function - cross sections, provide the specific activities for the benchmark comparison to the measurements. To obtain the measured values, at least four different dosimeter materials are combined. For the capsule or cavity dosimetry analyses, the dosimeter  $C/M$  values for each material are combined as expressed by Equation 7.12. Since the calculation represents one unique fluence analysis, and the calculated activity for each dosimeter of the same material is generally represented by one value, (even though there may be multiple dosimeters of that material), the material  $C/M$  is represented by one value.

The  $C/M$  values for each material in a capsule or cavity fluence analyses are combined as expressed by Equation 7.13. The weight, and cross product dependency for the different materials, could reflect the fluence spectrum that affects each material, and the amount of spectral overlap between the reactions in each material. However, the evaluation of the energy dependent bias function is based on the results of Equation 7.13.

Consequently, the calculated material activities are dependent on one fluence result, and are thereby dependent on one another. Likewise, with the energy dependent bias function evaluated from the results of Equation 7.13,

**Framatome Technologies Inc.**

each material uncertainty is not unique in relation to the total uncertainty. Thus, one equal weight combines the material dependent  $C/M$  results.

While Equations 7.12, 7.13 and 7.15 represent a reasonable statistical technique for propagating errors, the benchmark standard deviation of percent, as shown by Equation 7.16, on page 7 - 33 of the topical, and computed from Equation 7.15, causes concerns. The concerns are related to the fact that the standard deviation in  $M/C$  from the combination of 728 statistically independent dosimeters is percent. Consequently, during the meeting, the NRC raised the question whether the difference is not a result of inconsistency in the statistical techniques in Equations 7.12 and 7.13.

Removing the bias from the standard deviations in the reformulated form of Equations 7.12 and 7.13, and computing the benchmark uncertainty for the database using Equation 7.15, results in an unbiased uncertainty of percent. Therefore, the form of Equations 7.12, 7.13 and 7.15 appear to be appropriate for estimating the benchmark uncertainty in the Table A-1 database of greater than 0.1 MeV specific activities.

The second area of consistency that needs to be explained concerning Equations 7.6 and D.19, and Equation 7.15, is the confidence factor and distribution of deviations. In Equation 7.15, the denominator represents 38 degrees of freedom. (This is also true of the reformulated expression discussed above in the evaluation of an percent uncertainty.) In Equation D.19, the weight function denominator represents 142 degrees of freedom. The topical suggests that both the measurement and benchmark uncertainties can be represented by Student's central "t" distribution. Accordingly, the two different degrees of freedom are inconsistent with the formulation of Equation 7.9. However, the confidence factor differences for the 38 and 142 degrees of freedom, at a 95 percent confidence level, were applied to lower the measurement uncertainty when Equation 7.9 was used



**FTI Non-Proprietary**

Therefore, there is consistency between the

uncertainties

**Framatome Technologies Inc.**

References for *Appendix D*

- D1. United States Nuclear Regulatory Commission letter to J.J. Kelly, Manager, B & W Owners Group Services, **Request for Additional Information for Topical BAW-2241P**, from Joseph L. Birmingham, Project Manager, Office of Nuclear Reactor Regulation, January 30, 1998.
- D2. United States Nuclear Regulatory Commission letter to J.J. Kelly, Manager, B & W Owners Group Services, **Request for Additional Information for Topical BAW-2241P**, from Joseph L. Birmingham, Project Manager, Office of Nuclear Reactor Regulation, April 8, 1998.
- D3. Office of Nuclear Regulatory Research, **“Calculational and Dosimetry Methods for Determining Pressure Vessel Neutron Fluence”**, Draft Regulatory Guide, DG-1053, (page 1) United States Nuclear Regulatory Commission, June, 1996.
- D4. Office of Nuclear Regulatory Research, **“Calculational and Dosimetry Methods for Determining Pressure Vessel Neutron Fluence”**, Draft Regulatory Guide, DG-1053, (page 4) United States Nuclear Regulatory Commission, June, 1996.
- D5. T. G. Williamson, “Evaluation of the Photofission Effect in Pressure Vessel Dosimetry”, UVA/532886/NEEP88/101CN, University of Virginia School of Engineering and Applied Science, Charlottesville, Va., 22901, 1988.
- D6. J. T. Caldwell, et al, “Photonuclear Measurements on Fissionable Isotopes using Monoenergetic Photons”, LA-UR 76-161J, Los Alamos Scientific Laboratory, 1976.
- D7. L. Petrusa, “Photofission Effects in B&W 177 FA Reactor Vessel Surveillance Capsule Dosimeters”, *Proceedings of the Seventh ASTM-EURATOM Symposium on Reactor Dosimetry*, Kluwer Academic Publishers, P. O. Box 17, 3300 AA Dordrecht, the Netherlands.

**FTI Non-Proprietary**

- D8. Karel Rektorys, Editor, *Survey of Applicable Mathematics*, The M.I.T. Press, Massachusetts Institute of Technology, Cambridge, Massachusetts, 1969.
  
- D9. Paul L. Meyer, *Introductory Probability And Statistical Applications*, Second Edition, Addison-Wesley Publishing Company, Reading, Massachusetts, 1970.



***Appendix E* Generic PWR Uncertainties**

The purpose of this appendix is to update the uncertainties in this topical, BAW-2241P-A, "Fluence and Uncertainty Methodologies", that are associated with Westinghouse and Combustion Engineering (CE) fluence calculations. The update consists of reevaluating the benchmarks in FTI's dosimetry database. Equal weights are applied to each Pressurized Water Reactor (PWR) type: Westinghouse, CE, PCA test - reactor, and B & W.

This update was developed after the safety evaluation to the original publication of the topical was issued. The updated documentation is therefore presented as Revision 1 to the topical. The format for this revision is the original publication (now Volume 1, Revision 1) followed by this volume (2). The updates to the original publication only include the "Title" page, "Record of Revisions" page, and the pages with the "Table of Contents". Because the document is quite lengthy, the topical has been published in two volumes. Volume 1 contains the documentation from the original topical. This volume (2) is focused on responses to the NRC questions and contains the generic PWR update to the uncertainties. The two volumes together represent Revision 1 to the topical.

The reason for Revision 1 is to extend the application of uncertainties to all reactors of the pressurized water type. When the United States Nuclear Regulatory Commission (NRC) published the safety evaluation for the original version of this topical, they noted that the application of the methodology was limited to B & W (a McDermott company) designed reactors. As explained in the following section (Introduction and Background), the focus of the NRC's limitation was a concern with the industry's

## FTI Non-Proprietary

database of benchmark uncertainties from non - B & W designed PWRs, such as those designed by Westinghouse and CE.

The NRC explained that, if fluence analysts expect to apply their results to Westinghouse, CE, and B & W designed PWRs, then they need to have an adequate database for each respective reactor type. The adequate database consists of multiple benchmark comparisons of the results from the calculational methodology to appropriate dosimetry results from the measurement methodology. FTI agrees with the concept that analysts need multiple benchmark comparisons to each PWR type that they intend to analyze for fluence - embrittlement evaluations. The FTI database in this topical consists of 728 dosimeters responding to neutron reactions above 0.1 MeV. These 728 dosimeters come from 39 capsules and cavities. These 39 capsules and cavities are from 5 Westinghouse, 5 CE, 2 PCA, and 23 B & W capsule evaluations and 4 B & W cavity evaluations.

The uncertainty evaluation of the calculational methodology has indicated that the functional and correlated dependencies of the biases have been appropriately assessed. The result of the evaluation is that the best-estimate fluence from FTI's calculational methodology is unbiased throughout the beltline region, including the reactor internals, vessel, and vessel cavity structure. The uncertainty evaluation of the calculational methodology has also indicated that the precision in the best-estimate fluences is consistent with the embrittlement "Margin" terms from (a) the Pressurized Thermal Shock (PTS) Safety Analyses,<sup>3,4,5</sup> and (b) Regulatory Guide 1.99, Revision 2.<sup>17</sup> Statistical evaluations of the fluence uncertainties ensure that there is a 95 percent probability that the embrittlement "Margin" term will appropriately bound the vessel embrittlement evaluations with a value of  $\pm 2.000$  for the confidence factor. Table 7-6,

**Framatome Technologies Inc.**

on page 7 - 39 of this topical, gives the respective fluence uncertainties. This table is repeated below and noted as Table E-1.

Table E-1  
 Calculational Fluence Uncertainties  
 For B & W Designed PWRs

Type of Calculation	Uncertainty %	
	Standard Deviation	95 % / 95 % Confidence
Dosimetry (Capsule)	7.00	
Pressure Vessel		
Pressure Vessel (Extrapolated in Time)		

Sections E.1 through E.3.2 explain that the data set samples from Westinghouse and CE plants can be represented by the population of the FTI benchmark database. Thus, Table E-1 above would provide appropriate uncertainties for all PWRs.

In Section E.4 however, it is noted that even though the evaluations clearly indicate that (a) the Table E-1 uncertainties are applicable to Westinghouse and CE reactors, and (b) the benchmark standard deviation is percent for any PWR, there is the possibility that the uncertainties in the calculations are mostly dependent on plant uncertainties

The plant data may be too sparse for statistical evaluations to adequately detect this possibility. Therefore, the margin of safety for generic PWR fluence uncertainties has been reevaluated on a plant basis. The statistical results are shown in Table E-2. These fluence uncertainties are applicable to any PWR.

Table E-2  
 Calculational Fluence Uncertainties  
 For All PWRs

Type of Calculation	Uncertainty %	
	Standard Deviation	95 % / 95 % Confidence
Dosimetry (Capsule)		
Pressure Vessel		
Pressure Vessel (Extrapolated in Time)		



## **E.1 Introduction and Background**

In February of 1999, the NRC staff published the safety evaluation for the original version of this topical. The “Summary and Limitations” section of the safety evaluation concluded that the methodology is acceptable for determining the pressure vessel fluence of B & W designed reactors. Also noted, was the specific limitation that the methodology is applicable only to B & W designed reactors.

The topical presents two methodologies, one for determining the fluence and the other for estimating the uncertainty in the methodology for determining the fluence. The fluence and the uncertainty methodologies developed in the topical are fundamentally theoretical methods, combined with procedural and modeling approximations. The theoretical methods are generic, and the procedures and models are generic to PWR designs. Thus, the methodologies are applicable to any PWR. Consequently, the limitation of the methodology to B & W reactors in the “Summary and Limitations” section was confusing.

To clarify the confusion, discussions were held with the NRC staff. The discussions began by reviewing the methodologies that the NRC contractors and the industry have used for fluence and uncertainty evaluations. The methodologies fall into one of two categories; (1) those based on unfolding a measured fluence with a measurement-based uncertainty, and (2) those based on calculating the fluence with a calculational-based uncertainty. FTI used a measurement-based methodology for 20 years, and the other industry vendors continue to use it today. This methodology provides excellent techniques for determining the fluence values at capsule and cavity dosimetry locations. However, in 1993 the NRC held a meeting with the industry that focused on the

## FTI Non-Proprietary

consistency between vessel fluence uncertainties and the fluence uncertainties associated with the PTS rule, 10 CFR 50.61.<sup>6</sup> When the PTS safety analyses<sup>3,4,5</sup> are reviewed, it is clear that the fluence uncertainty must be consistent with a 95 percent probability that the vessel fluence value bounds the true value. In the months following the meeting, the NRC published draft regulatory guide DG-1025<sup>8</sup> (updated in 1996 to DG-1053<sup>19</sup>) describing “Calculational And Dosimetry Methods For Determining Pressure Vessel Neutron Fluence”. The draft regulatory guide notes that measurement-based fluence predictions are not consistent with the PTS safety analyses; only calculational-based fluence predictions are consistent.

FTI has explained to numerous utilities that without vessel dosimetry measurements, it is very difficult to show that there is a 95 percent probability that the “measured” vessel fluence bounds the true value. Consequently, FTI tailored the fluence and uncertainty methodologies in this topical to closely follow the draft regulatory guide.<sup>19</sup> Thus, the topical presents a calculational-based methodology that is consistent with the uncertainty “Margin” assumed in the PTS safety analyses.<sup>3,4,5</sup>

FTI has utility customers with Westinghouse designed reactors, and with Combustion Engineering (CE) designed reactors. These utilities have agreed that when evaluating vessel embrittlement for either the PTS rule (10 CFR 50.61),<sup>6</sup> or the (Regulatory Guide 1.99, Revision 2)<sup>17</sup> technical specification limits for pressure - temperature values during heat-ups and cool-downs, it is important for the fluence to be consistent with the embrittlement “Margin” term uncertainties.

The NRC staff has agreed that it would be preferable to utilize the BAW-2241P-A calculational-based methodologies on all PWRs, including those designed by Westinghouse and CE. However, they have noted that while FTI’s “Fluence and

**Framatome Technologies Inc.**

## **FTI Non-Proprietary**

Uncertainty Methodologies” are applicable to any PWR, there are technical issues associated with industry analyses of plant-specific uncertainties that need to be addressed. One company, that performs a significant number of non - B & W fluence analyses using a measurement-based methodology, consistently produces biases, with uncertainties between 10 and 25 percent. The FTI best-estimate fluence methodology produces unbiased results with an uncertainty of 9.9 percent as explained in the topical. Therefore, the NRC staff requested that the Westinghouse and CE analyses, that are part of the FTI dosimetry database, be specifically evaluated as a function of plant type to determine if consistent biases or large random uncertainties are evident. The staff noted that the FTI database is weighted with more B & W plants (27 capsules and cavities out of 39, or 69 percent B & W analyses). Furthermore, the B & W plants are weighted with more Crystal River, Unit-3, and Davis Besse, Unit-1 analyses (20 out of 27, or 74 percent). Thus, they requested that the statistical evaluation of the database be reviewed to verify that the data set samples from Westinghouse and CE plants are appropriately represented by the population of 728 dosimetry benchmarks in 39 capsules and cavities.

As part of the verification process, the NRC staff requested that the review of the data by plant type include:

- 1 - A description of the important physical parameters and characteristics affecting the uncertainties, with discussions explaining why differences between plant types do not result in the data representing different populations.
- 2 - An evaluation of the data, with discussions explaining why it represents an adequate set for estimating statistical properties.
- 3 - An evaluation substantiating that the statistical treatment of the data with the uncertainty methodology is appropriate to estimate the uncertainties.

**Framatome Technologies Inc.**

The focus of the NRC's question concerning the application of Table E-1 to Westinghouse, CE, and other non - B & W PWRs, is associated with the benchmark uncertainties of calculations ( $C$ ) to measurements ( $M$ ). Thus, the focus of this appendix is the reevaluation of the benchmark uncertainties from Table A-2 (page A - 25 in this topical). As shown by Equations 7.8 and 7.9 on page 7 - 26, the benchmark bias ( $B_{C/M}$ ) and relative variance ( $\sigma_{C/M}^2$ ) are determined from the

The reevaluation of the measurement and benchmark, biases and standard deviations, is based on the Table A-2 database. As previously noted, this database includes 5 capsules from 5 Westinghouse plants, and 5 capsules from 4 CE plants. The data samples from Westinghouse and CE plants have been independently evaluated. This independent evaluation addresses the crux of the NRC's concern with the uncertainties in Table E-1 being applied to other PWRs. In conversations with the

staff, they noted that there is a large inconsistency between Westinghouse benchmark uncertainties and FTI benchmark uncertainties for Westinghouse designed reactors.

## **E.2 Measurement Uncertainties**

Westinghouse uses a measurement-based unfolding methodology to evaluate capsule fluences. In 1994, they updated the benchmark evaluation of their entire capsule dosimetry database.<sup>E1</sup> Their reported overall uncertainty is 22.4 percent, with 12.1 percent in the form of a mean bias, and 10.3 percent in the form of a mean standard deviation. Several of the plants reported in the reference<sup>E1</sup> are also in the FTI dosimetry database. The overall FTI benchmark uncertainty is 9.9 percent, with no bias, and the total uncertainty in the form of a root mean square standard deviation. The large difference in uncertainties could be the result of the weighting of B & W plants in the FTI database. This section examines the measurement uncertainties for Westinghouse and CE plants, and discusses the three issues in the verification process that the NRC requested (page E - 7).

The measurement-based methodology that Westinghouse uses includes dosimeter activities in the same manner as CE and FTI. The activities measure the fluence - dosimeter reaction rate effects that are related to the fluence, but there is no measure of the fluence. Westinghouse, CE and FTI use the same techniques to evaluate biases in the measured activities (see pages 7 - 9 and 7 - 10 in this topical). While CE and FTI use the combination of unbiased activities and cross sections to assess any biased measurements of the fluence, Westinghouse includes unfolding techniques to actually evaluate the fluence. As noted in the FTI paper on "Biased Fluences In The Charpy Embrittlement Database" (given at the same conference as the Westinghouse update of capsule fluence evaluations<sup>E1</sup>), unfolding methodologies, such as FERRET-SAND,

**Framatome Technologies Inc.**

have previously introduced biases into the measured fluences. The following discussion reviews FTI's evaluation of "Measurement Biases".

### **E.2.1 Measurement Biases**

When FTI developed the calculational-based uncertainty methodology, an important step in the development was the evaluation of the uncertainty differences between the measurement-based methodology and the new calculational-based methodology. The reason for the evaluation is that the correlations of embrittlement are from a database that is based on measured specimen fluences. While it was clear that calculated vessel fluences would be a significant improvement over "measured" vessel fluences, it was not clear how the new calculational methodology would be consistent with the measured fluences in the existing capsule embrittlement database.

Since embrittlement evaluations (PTS<sup>6</sup> and Regulatory Guide 1.99, Revision 2<sup>17</sup>) are based on correlations of the change in the material specimen properties to the specimen measured fluences, it is apparent that calculated fluences must be equivalent to the measured ones as expressed below.

Capsule Embrittlement Database Criterion –

$$\begin{aligned} \textit{Measured Fluence} - \sigma_M(\textit{Fluence}) &\leq \\ \textit{Calculated Fluence} &\leq \textit{Measured Fluence} + \sigma_M(\textit{Fluence}) \end{aligned} \tag{E.1}$$

where

$\sigma_M$  is the standard deviation of the uncertainties (random deviations) in the measurements.

Calculations of capsule specimen fluences, using a methodology consistent with the draft regulatory guide,<sup>19</sup> must equal the measured specimen fluences determined for the embrittlement database (in the 1970's), within an uncertainty range that is equal or less than the uncertainty in the measurements. From Equation E.1, the standard deviation ( $\sigma$ ) in the capsule fluences predicted by calculations ( $C$ ) must be equal or less than the standard deviation of the measurement ( $M$ ) predictions as expressed by Equation E.2 .

$$\sigma_C \leq \sigma_M \quad (\text{E.2})$$

In the 1970's, FTI (then Babcock & Wilcox {B & W}) provided embrittlement and fluence measurements from capsule specimens to NRC contractors Simons<sup>15</sup> and Guthrie.<sup>16</sup> This data help establish the database for correlations of embrittlement to fluence. Guthrie performed the correlations of embrittlement properties, and Simons used FERRET-SAND to adjust the fluence values from Westinghouse, CE, and B & W capsules to provide Guthrie with fluences that were consistent with one another. Therefore, when FTI performed evaluations to determine if the new calculational methodology would provide fluence values equal to those of the 1970's, it was Simons' values that were used for the measured fluence comparisons.

The comparisons of the calculated fluences to Simons' measured ones gave very disappointing results. The differences between the values were much larger than anticipated, and consistently outside the range of the appropriate uncertainty. As indicated by Equation E.3, if the calculated fluence values were increased by a multiplicative bias factor (of approximately 12 percent), the differences were reduced and were within the acceptable range of the measurement uncertainty ( $\sigma_M$ ).

$$\text{Calculated Fluence} \left( 1 + \text{Bias} \right) = \text{Measured Fluence} \pm \sigma_M(\text{Fluence}) \quad (\text{E.3})$$

To better understand the calculational bias, the calculated and measured activities were compared. Surprisingly, the calculated and measured activities compared very well, with no evidence of a bias, as shown by Equation E.4 .

$$\text{Calculated Activities} = \text{Measured Activities} \pm \sigma_M(\text{Activities}) \quad (\text{E.4})$$

Pursuing the explanation for the bias, the calculated and original FTI measured fluence values were found to be in agreement and showed no bias. Reviewing Simons' FERRET-SAND adjusted fluence results as shown below, the adjustments were found to produce biases relative to the original predictions from all capsules {Westinghouse, CE, and B & W}.<sup>15</sup>

	Capsules	Database
<i>FERRET - SAND Fluence Biases</i>	$\left\{ \begin{array}{l} 1.35 \text{ Westinghouse} \\ 1.23 \text{ CE} \\ 1.12 \text{ B \& W} \end{array} \right\}$	= 1.30 <i>Average</i>

(E.5)

The B & W calculated and measured capsule fluence values for the embrittlement database had a 12 percent bias compared to Simons' measurement predictions. In addition to the B & W bias, it was found that the ABB-CE capsules had a 23 percent bias, the Westinghouse ones had a 35 percent bias, and the weighting of the biases produced an overall 30 percent increase in the fluence values that Guthrie used for the embrittlement correlation. FTI found that the biases in the embrittlement database fluences were caused by the FERRET-SAND adjustment techniques. These biases are



not real with respect to the theoretical models that are the bases for the calculations, nor are they real with respect to the experimental techniques that are the bases for the measured dosimeter activities. They are simply associated with biased unfolding methods and procedures in FERRET-SAND.

If the FERRET-SAND results are biased, there should be others who have also observed the biases. Reference 37 (in Section 8 of this topical) provides a comparison of the “PCA Blind Test” results from FERRET-SAND with those from the LSL-M2 predecessor. As indicated by Equation E.5, the FERRET-SAND fluence results should have been, and were higher than those determined by the LSL-M2 unfolding methods and procedures. The FERRET-SAND bias was confirmed by the Hanford laboratory, three years after the publication of Reference 37, when they revised the FERRET-SAND fluences to agree with the Oak Ridge laboratory LSL-M2 values.

In Reference E2, three senior scientists from Germany presented a paper that evaluates “Neutron Fluence Determination at Reactor Filters by  $^3\text{He}$  Proportional Counters: Comparison of Unfolding”. They stated that an unknown neutron spectrum in an iron filtered reactor beam was unfolded using the SAND-II iteration algorithm, and the appropriate response functions and covariance matrix. However, the scientists noted that as a consequence of the solution technique, the results reached by the SAND-II iteration may not be unique. Biases (systematic uncertainties) may arise in the spectrum. If the solution is not unique, then the SAND-II solution process is not valid. There is only one unique and valid flux spectrum at the reactor beam detector location.

These three unrelated incidences:

- (1) the FTI review of the FERRET-SAND adjustments to the industry fluences,

(2) the comparison of PCA results between Hanford using FERRET-SAND, and Oak Ridge using LSL-M2, and

(3) the German scientists finding that the SAND-II iteration may not be unique;

indicate that measured fluence results are frequently biased due to unfolding methods and procedures. As noted by Equation E.5, FERRET-SAND increases the measured fluence. Consequently, when calculated fluences are compared to measured values, the resulting mean  $C/M$  benchmark value would be less than unity. The  $C/M$  benchmark values in Reference E1 are noted to be less than unity.

When FTI processes Westinghouse and CE dosimeters to measure the activities, the experimental methodology is the same as that used for the B & W dosimetry, the NIST reference field dosimetry,<sup>E3</sup> and any other dosimetry. There are 141 dosimeters from Westinghouse and CE reactor capsules in the FTI database (Table A-1, pages A - 3 through A - 19). The five components of the measurement uncertainties listed in Table 7-1 on page 7 - 12 are exactly the same, regardless of where the dosimeters were irradiated. The evaluation of measurement biases uses the same National Institute of Standards and Technology (NIST) traceable standards and laboratory calibration procedures for all dosimetry, as described on pages 7 - 9 and 7 - 10. Consequently, neither the Westinghouse, nor CE, nor any dosimetry measurements of the specific activities are biased. No measured fluence values are evaluated in the topical database.

Concerning the three issues that the NRC requested be reviewed:

1. The important physical parameters and characteristics affecting the measurement biases are the NIST traceable calibration standards and the experimental

## **FTI Non-Proprietary**

procedures. As discussed above, Westinghouse measures the fluence with dosimeter reaction rates and unfolding techniques. CE measures the fluence with dosimeter activities and a normalization of calculations to the mean measured specific activity. FTI does not measure the fluence, only the dosimeter specific activities are measured.

The “measurement” of the fluence requires processing measured dosimetry results with an analytical technique. Due to differences in the operational, fabrication, and design characteristics of each type of plant, the analytical technique to determine measured fluences can be a function of the plant type. The NRC's draft regulatory guide<sup>19</sup> recommends testing the fluence measurement methodology with a reference field standard. However, in 1994, when scientists and engineers from Westinghouse, CE, FTI, and the industry met to discuss the implications of the draft guide, no one had used reference field fluence standards for calibrating their fluence measurements. Consequently, the fluence measurements from Westinghouse, CE, FTI, and the industry may be biased.

As noted in the original version of this topical, the basis for evaluating uncertainties must be benchmark comparisons of the results from the experimental methodology to a reference standard that is known to be unbiased. The principal technique used by experimentalist to ensure that their measured results have no biases, is calibrating the methodology to certified standards referable to NIST. Without a NIST reference field fluence standard, the industry's measured fluences cannot be certified to be unbiased.

**Framatome Technologies Inc.**

## FTI Non-Proprietary

Unlike fluence measurements, which can be dependent on plant type, and for which there are no calibrations to NIST standards, dosimetry measurements have no functional dependency on reactor plant type, and there are dosimeter activity standards directly referable to NIST. The topical explains how these standards are used in the experimental calibration process to ensure that the specific activities from each dosimeter measurement are not biased. The FTI database of dosimeter activities from Westinghouse and CE plants is part of a population of unbiased measurements.

2. The evaluations of 141 dosimeters from Westinghouse and CE plants that are used to determine the measurement biases, represents a sufficiently adequate data set. As noted above, the physical parameters and characteristics of the dosimeters, the irradiation source, and the experimental process have no related dependencies. Therefore, the data represents an independent set of 141 samples. Such a set is adequate for estimating the biases and standard deviations in the data, and is adequate as an independent sample for estimating the FTI dosimetry database population biases and standard deviations.
3. The experimental methodology that is used to evaluate the dosimetry measurements in the FTI database has been validated by NIST.<sup>E3</sup> This validation substantiated the statistical treatment of the bias with the calibration procedures. The experimental methodology is generic and is not dependent on the dosimetry parameters or characteristics. Thus, there are no measurement biases in the dosimetry database, and the Westinghouse and CE data represent samples from the FTI database population.

Framatome Technologies Inc.

### **E.2.2 Measurement Standard Deviation**

As discussed in the “Uncertainty Methodology” section in this topical, the uncertainties in the measurements (and calculations) arise from two types of deviations, systematic and random. The systematic deviations are caused by some fundamental problem with the predictive methodology and are thereby functionally related to some variable or parameter. If there is a single functional relation between the systematic deviations and some variable, then there is a single bias. If there are two or more functional relations, then there may be two biases, or multiple biases. If there are two or more biases associated with the data, then it is not appropriate to use the techniques of mathematical statistics to estimate the standard deviation in the data. If there are no biases, or only one bias, then the techniques of mathematical statistics are appropriate.

Since there are no biases in the dosimetry measurements of the FTI database, the random deviations in the experimental process are determined from the component uncertainties listed in Table 7-1 on page 7 - 12 of the topical. These deviations are only dependent on the random variables in the experimental process and are therefore independent of where the dosimeters were irradiated. Consequently, Westinghouse and CE data samples from the FTI dosimeter database have the same standard deviation as the general population, 7.0 percent.

Concerning the three issues that the NRC requested be reviewed:

- 1 - The physical parameters and characteristics affecting the measurement standard deviation are the five parameters and experimental procedures listed in Table 7-1 on page 7 - 12 of the topical. The experimental procedures and parameters are independent of the plant where the dosimeters were irradiated.

## FTI Non-Proprietary

Therefore, the standard deviation estimated for each dosimeter measurement is independent of the sample and is based on the database population.

2 -

The standard deviations estimated for the 141 dosimeters have no unique properties that distinguish them from any other sampling of dosimetry in the FTI database population. Consequently, the Westinghouse and CE dosimeter measurements represent an adequate data set for statistically estimating the standard deviation.

3 - The measurement uncertainty methodology that is used to statistically evaluate the dosimetry data from Westinghouse and CE plants is the same as that used for any dosimeter measurement. This methodology has been validated by NIST.<sup>E3</sup> NIST concluded that the accuracy and precision that the B & W laboratory has estimated for the measurement uncertainties are valid values. Thus, the measurements have no statistically significant biases, and the methodology for estimating the standard deviation from the component uncertainties in the experimental process is valid. The NIST validation thereby substantiates the statistical treatment of the Westinghouse and CE dosimeter measurements.

**Framatome Technologies Inc.**

### E.3 Benchmark Uncertainties

As discussed previously, the crux of the NRC's concern with the uncertainties in Table E-1 being applied to PWRs, other than ones designed by B & W, is that Westinghouse has reported benchmark uncertainties with biases of 25.2 percent, a mean bias of 12.1 percent, and a mean standard deviation of 10.3 percent.<sup>E1</sup> However, 5 of the plants that are in the Westinghouse benchmarks of Westinghouse designed plants, are also in the FTI benchmark database. While the Westinghouse benchmark suggests that the Prairie Island plant has a  $C/M$  bias of 25.2 percent, the FTI benchmark indicates no bias. Furthermore, the FTI benchmark database indicates that all FTI fluence analyses of Westinghouse plant capsules have no bias, and have an uncertainty represented by a root mean square standard deviation

## **FTI Non-Proprietary**

It would be expected that the biases and standard deviations in the benchmark comparison of calculations and measurements would be similar between Westinghouse, CE, and FTI. However, as noted in the discussion above, the Westinghouse mean benchmark bias of 12.1 percent, indicates an inconsistency with the FTI calculational and measurement methodology, which has no bias in the benchmark database. The bias inconsistency accentuates the inconsistency in the overall uncertainty estimated by Westinghouse and FTI. FTI's overall benchmark uncertainty is just the root mean square standard deviation from the capsule and cavity analyses, percent. Since Westinghouse uses the calculated fluence spectrum as the “a priori” spectrum for unfolding the measured fluence, and they do not incorporate a bias removal function, the overall uncertainty is the statistical combination of the bias (12.1 percent<sup>E1</sup>) and the standard deviation (10.3 percent<sup>E1</sup>) with correlation coefficients of unity. Thus, the overall uncertainty from the Westinghouse capsule benchmark database is 22.4 percent.

The NRC would like FTI to isolate the Westinghouse and CE plants, and statistically process the FTI benchmark data by plant type. The statistical processing is to ensure that no biases are associated with Westinghouse or CE plants, and that the fluence uncertainty can be appropriately represented by a root mean square standard deviation. As explained in the “Introduction and Background” section, with 69 percent of the FTI benchmark database weighted with B & W plants, the NRC wants to know whether the large B & W weighting disguises differences in the Westinghouse and CE plant uncertainties? In statistical terms, the question is whether the Westinghouse and CE data is unique or does it represent samples from the same population? There is a corollary to the question: If the uncertainties are plant dependent, does the statistical evaluation associated with the uncertainty methodology sufficiently estimate the standard deviation? The following discussions address the benchmark biases and

**Framatome Technologies Inc.**



standard deviations associated with Westinghouse and CE plants in relation to the FTI benchmark database.

### **E.3.1 Benchmark Biases**

The benchmark biases for the FTI database are discussed in Section 7.2.1 on pages 7 - 27 and 7 - 28. The expression used to estimate the bias is Equation 7.10. To determine the benchmark  $C/M$  value for each PWR plant type, the  $C/M$  value is determined for each dosimeter within a capsule.

Table E-3 gives the  $C/M$  values for the 5 Westinghouse plants in the FTI dosimetry database, and Table E-4 gives the values for the 4 CE plants. Using Equation 7.10 to compute the respective biases for the Westinghouse and CE plants, and statistically estimating the values, shows that there are no statistically significant biases associated with either the Westinghouse plant samples or the CE plant samples.

Concerning the three issues that the NRC requested be reviewed:

- 1 - The physical parameters and characteristics that affect the benchmark bias are those associated with the calculations since the measurements have previously been reviewed in Section E.2.1. The calculational methodology is discussed in Section 3 of the topical. There is nothing associated with the BUGLE-93 cross

## FTI Non-Proprietary

sections, or the DORT model that would bias the results with respect to plant type. The methods and procedures used in the modeling of the various plant types are not unique or sensitive to any physical parameter or characteristic that differentiates one plant from another. Therefore, as noted in Tables E-3 and E-4, the mean  $C/M$  benchmark values for Westinghouse and CE plants show the same statistical traits as the mean  $C/M$  benchmark value for the FTI database. The relation between (a) the unbiased standard deviation in the data, and (b) the difference between the mean  $C/M$  values and unity, indicates that the benchmark deviations are of a random nature. No statistically significant biases are evident.

The  $C/M$  benchmark results reported in Reference E1 show large biases. The 12.1 percent mean bias<sup>E1</sup> is inconsistent with the FTI results in Table E-3, which have a 0.0 mean bias.

As the NRC staff knows, the Virginia Power Corporation has an expert in the field of fluence analyses. Virginia Power developed their own independent analytical methodologies for discrete ordinates, and Monte Carlo modeling of the North Anna (Units 1 and 2) and Surry (Units 1 and 2) reactors. To help

**Framatome Technologies Inc.**

## FTI Non-Proprietary

substantiate the fact that calculations of Westinghouse reactors are not inherently biased, FTI requested Virginia Power send their discrete ordinates dosimetry calculations and the measurements. (The measurements only involved the activation of the dosimetry, no measured fluences were predicted from unfolding techniques.)

It was also requested that FTI be allowed to statistically process the dosimetry  $C/M$  benchmarks using the uncertainty methodology in the topical. The Virginia Power benchmark comparisons of dosimetry calculations to measurements consisted of 42 dosimeters in 9 capsules from both North Anna units, and both Surry units. The evaluation of the mean bias and standard deviation are shown in Table E-5 (page E - 28). The Virginia Power benchmark results are consistent with those from FTI. They indicate that no statistically significant bias can be observed in the benchmark data. This of course is inconsistent with the Westinghouse results in Reference E1.

- 2 - The benchmark data for the Westinghouse and CE plants includes a combination of 141 dosimeter comparisons. The Westinghouse data consists of 63 dosimeters, and the CE data, 78 dosimeters. For the data to represent adequate sets for estimating the biases, it must be sufficiently normal.

The distribution of deviations in the FTI dosimetry benchmark database were shown to adequately fit within William Sealy Gosset's (Student's) central "t" distribution (pages 7 - 33 and 7 - 34). The key criterion was that 95 percent of

**Framatome Technologies Inc.**

Thus, the CE plant  $C/M$  benchmark deviations appropriately fit within the central “t” distribution.

Thus, the Westinghouse  $C/M$  benchmark deviations appropriately fit within the central “t” distribution.

the data needs to be separated by physical parameters and characteristics to evaluate the functional and correlative dependencies on the respective variables.

3 -

The fact substantiates the conclusion that neither data sample has a statistically significant bias.

**Framatome Technologies Inc.**

Table E-3

Westinghouse Plant Benchmarks

Plant	$C/M$
Prairie Island, Unit 1	
North Anna, Unit 1	
North Anna, Unit 2	
Shearon Harris, Unit 1	
Zion, Unit 1	

Sample Statistics

Parameter	Value
Mean $C/M$	
Bias	0.0
$\overline{\sigma}_{C/M}$ (Sample)	
$\overline{\sigma}_{C/M}$ (Population)	

Table E-4

CE Plant Benchmarks

Plant	$C/M$
Calvert Cliffs, Unit 2	
Millstone, Unit 2	
St. Lucie, Unit 2	
Waterford, Unit 3	

Sample Statistics

Parameter	Value
Mean $C/M$	
Bias	0.0
$\overline{\sigma}_{C/M}$ (Sample)	
$\overline{\sigma}_{C/M}$ (Population)	

Table E-5

Virginia Power Combined Statistics  
 From North Anna, Units 1 & 2  
 And Surry, Units 1 & 2

Parameter	Value
Mean $C/M$	
Bias	0.0
$\sigma_{C/M}$	7.46 %

**E.3.2 Benchmark Standard Deviations**

The benchmark standard deviation for the FTI database is discussed in Section 7.2.2 on pages 7 - 32 and 7 - 33. One expression that is used to estimate the standard deviation is Equation 7.15. Without any biases in the data, this expression is appropriate for estimating the standard deviation in the database population listed in Table A-2 (pages A - 25 and A - 26). It is also appropriate for estimating the standard deviation in the isolated samples from Westinghouse and CE plants. Table E-3 (page E - 26) and Table E-4 (page E - 27) provide the respective sample statistics for the Westinghouse and CE plants.



## **FTI Non-Proprietary**

The weighting of the capsule benchmark data by plant significantly reduces the number of data points by plant type. The 63 Westinghouse dosimeter benchmarks are reduced to 5 independent plants as shown in Table E-3. Thus, the estimate of the benchmark standard deviation is based on 4 degrees of freedom (DF).

The 78 CE dosimeter benchmarks are reduced to 4 independent plants as shown in Table E-4. Thus, the estimate of the benchmark standard deviation is based on 3 degrees of freedom (DF).

$$\chi^2 = \sum_i^k \frac{\left( \textit{Observed}_i - \textit{Expected}_i \right)^2}{\textit{Expected}_i} \quad (\text{E.6})$$

$$\frac{\sigma_w}{\chi_{\{9|4\}}} \leq \sigma_{DD} \leq \frac{\sigma_w}{\chi_{\{1|4\}}} \quad (\text{E.7})$$

Concerning the three issues that the NRC requested be reviewed:

- 1 - The physical parameters and characteristics that affect the benchmark standard deviations are those associated with the calculations. The measurements used by FTI have no biases and the standard deviations have been validated by NIST as noted in Section E.2.2. The calculational modeling of Westinghouse, CE, B & W, and other PWRs is affected by the uncertainties associated with (1) the fuel rod fission sources, (2) the design and fabrication tolerances for the fuel, internals, and vessel, and (3) the operational characteristics of the reactor. These uncertainties could increase the calculational uncertainties in one plant type versus another. If the calculational uncertainties are increased, the calculation to measurement benchmark uncertainties will be increased in direct proportion.

FTI is the fabricator of many Westinghouse vessels. Deviations in fabrication specifications are thereby very consistent. The significant operational characteristics that affect fluence predictions are the downcomer inlet temperatures and the former region temperatures. FTI has performed the conversion work on several Westinghouse plants for former region flow. In addition, the sensitivities of the control system with respect to inlet temperatures in the Westinghouse plants for which FTI is responsible for the reload licensing have been reviewed.

- 2 - Evaluations of the Westinghouse and CE plant data, which show that it represents adequate sets for estimating standard deviations, was discussed in Section E.3.1 for the benchmark bias evaluation. As noted in that discussion, both the Westinghouse and CE plant deviations in the benchmark data appropriately fit within the central “t” distribution. The discussion above, concerning the Westinghouse and CE standard deviations being representative of a sampling from the FTI benchmark database population, also indicates that the plant data represents adequate sets for estimating statistical properties.

Thus, the statistical and physical evidence substantiates the treatment of Westinghouse and CE uncertainties with the statistical properties that have been estimated for the FTI database.

#### **E.4 Plant Dependent Benchmark Uncertainties**

The above assessment in Sections E.1 through E.3.2, is sufficient to present the conclusion to this appendix. The uncertainty methodology and statistical evaluation of the benchmark database have been reviewed. The review verifies that data set samples from Westinghouse and CE plants can be represented by the population of the FTI benchmark database. The large inconsistency between Westinghouse dosimetry benchmark uncertainties, and FTI benchmark uncertainties for Westinghouse designed reactors, has been explained. The key difference is the biased results that Westinghouse shows in the “measured” fluences in Reference E1. Biases in unfolding techniques, such as FERRET-SAND, have been observed by (1) Oak Ridge unfolding with LSL-M2, (2) German scientist finding that the SAND-II iteration process may not be unique, and (3) Virginia Power benchmark uncertainties. However a NIST reference field was used to validate that the FTI measurement uncertainties are unbiased. Consequently, the unbiased FTI uncertainties in Table E-1 are applicable to Westinghouse, CE, and B & W reactor plants, and any similar PWR or test - reactor.

The problem with the above conclusion is the combination of statistical inference and safety analyses. Even though the evaluations clearly indicate that, (a) the Table E-1 uncertainties are applicable to Westinghouse and CE reactors, and (b) the benchmark standard deviation is percent for any plant, there is the possibility that the uncertainties in the calculations, and thereby the benchmark uncertainties, are mostly dependent on plant uncertainties associated with the fuel, internals, vessel, and operation. If the uncertainties are unbiased random variables, but are plant dependent, then the statistical properties need to be evaluated on a plant basis.

The fluence uncertainties in Table E-1 are associated with the Table A-2 benchmark database of capsule and cavity uncertainties. To increase the margin of safety associated with any PWR fluence calculation, FTI has reevaluated the benchmark database uncertainties using a plant basis. The statistical results are shown in Table E-6 on page E - 35.

Table E-6

Statistical Combination of Plants

Plants	$C/M$	$\sigma_{C/M}$
Westinghouse		
CE		
PCA		
B & W		

Combined Statistics

Parameter	Value
Mean $C/M$	
Bias	0.0
$\sigma_{C/M}$	

$$B_c(\text{Fluence}) = 0.0$$

(E.8)

$$\sigma_c(\text{Dosimetry Fluence}) \leq$$

(E.9)

$$\overline{\sigma_{c/M}} (\text{Plant Benchmark Database}) \leq$$

(E.10)



These confidence factors are appropriate for a 95 percent confidence level.

$$\sigma_c (\text{Vessel Fluence}) \leq \quad (\text{E.11})$$

Section 7.2 on pages 7 – 36 through 7 – 41 explains that there are additional sets of analytical uncertainties associated with the vessel fluence. The first set is related to the analytical evaluations of the source, design, fabrication, and operational uncertainties. Combining these uncertainties with Equation E.9, gives the vessel fluence uncertainty as shown by Equation E.11. The second set of additional uncertainties is associated with the source uncertainties when extrapolated over time. Combining these source - time related uncertainties with Equation E.11, gives the EOL vessel fluence uncertainty as shown by Equation E.12. While Equation E.12 defines an EOL uncertainty, this value is only valid with appropriate fluence monitoring evaluations.

$$\sigma_c (\text{EOL Vessel Fluence}) \leq \quad (\text{E.12})$$

These results are summarized in Table E-2 on page E – 4.

*Appendix E* References

- E1. E.P. Lippincott and S.L. Anderson, "Systematic Evaluation of Surveillance Capsule Data", Proceedings of the 9'th International Symposium on *Reactor Dosimetry*, Czech Republic, September, 1996, World Scientific Publishing Co., River Edge, NJ.
- E2. M. Matzke, W.G. Alberts, and E. Dietz, "Neutron Fluence Determination at Reactor Filters by <sup>3</sup>He Proportional Counters: Comparison of Unfolding Algorithms", *Reactor Dosimetry*, ASTM STP 1228, Harry Farrar IV, et alia, editors, American Society for Testing and Materials, Philadelphia, 1994.
- E3. J.R. Worsham III, "Standard and Reference Field Validation", FTI document # 51-5003585-00, released, 4/26/99.
- E4. R.E. Maerker, "LEPRICON Analysis of Pressure Vessel Surveillance Dosimetry Inserted into H.B. Robinson-2 During Cycle 9", *Nuclear Science And Engineering*, # 96, (pages 263-289), 1987.

*Appendix F* FTI Responses to the -

**Request for Additional Information \* on  
Topical BAW-2241P, Revision 1  
*Fluence and Uncertainty Methodologies***

**Question 1**

Were the calculations and measurements (including the processing required to convert the measured activities to reaction rates) used in determining the Westinghouse Power Company (W) and Combustion Engineering (CE) data base of calculated to measured ratios (C/Ms) performed by FTI using the methods described in the topical report? If not, provide justification for assuming this data constitutes a single population and can be combined to determine an overall C/M bias and calculational uncertainty.

**Response**

The calculations and measurements used in determining the Westinghouse Power Company (W) and Combustion Engineering (CE) data-base of calculated to measured ratios (C/Ms) were performed using the methods described in the topical (BAW-2241P, Revision 1). The measured activities for the 141 Westinghouse and CE dosimeters came from the B & W Nuclear Environmental Services laboratory (a McDermott Company) as described in Reference 33, Section 8. Since the measurements were performed using the B & W laboratory procedures, there were no

---

\* This *Appendix* contains its own Reference section. Reference F1 refers to the NRC requests for additional information.

## FTI Non-Proprietary

conversions to other forms. The calculated activities of the radioactive product isotopes in the dosimeters came from the calculated reaction rates in the target isotopes. As shown in Table A-1, on pages A - 3 through A - 19, the measured and calculated activities from Westinghouse and CE dosimetry are treated the same as dosimetry from B & W reactors and the PCA test reactor.

Since the measured and calculated evaluations of the Westinghouse and CE dosimetry are the same as that for all the dosimetry in the FTI data-base, the measurement ( $M$ ) and benchmark ( $C/M$ ) uncertainties should not be unique. For this reason, and others discussed in *Appendix E*, the Westinghouse and CE dosimetry data appear to represent a sample from the same population, which is the FTI dosimetry data-base.

### Question 2

Were any FTI evaluations of W or CE dosimetry excluded from the BAW-2241P data base and, if so, provide justification for excluding this data.

### Response

No evaluations of W or CE dosimetry were excluded from the BAW-2241P data-base. The original release of the topical occurred in April of 1997. The processing of the data-base was completed by December of 1996. At that time, the 5 Westinghouse and 5 CE capsules represented all of those in the FTI data-base. The last Westinghouse capsule analysis was from the Prairie Island plant; it was completed in June of 1996 (Reference A14, *Appendix A*). The last CE capsule analyses was from the Calvert Cliffs plant, it was completed in February of 1994 (Reference A4, *Appendix A*). Since 1996, there have been other Westinghouse capsule analyses. (They will be included in the FTI data-base when it is updated.)

Framatome Technologies Inc.

**Question 3**

Provide the method and basis used for determining the values of  $\sigma_{C/M}$  (Population | DF = 38) in Tables E-3 and E-4. What is the basis for assuming the W data is one sample out of the 39 plants in the FTI data base ?

**Response**

The method and basis used for determining the values of the benchmark standard deviation ( $\sigma_{C/M}$ ) in Tables E-3 (page E - 26) and E-4 (page E - 27), follows the same concepts of mathematical statistics as those discussed on pages D - 30 through D - 33 (*Appendix D*). To explain the method and basis, the following discussion reviews examples of estimating the standard deviation with the probability distribution function defined to be either Gauss's, or (Student's) William Sealy Gosset's central "t".

Equation 7.15 on page 7 - 32 of the topical is appropriate for estimating the benchmark standard deviation for a set of *C/M* data. If one set of central "t" data has a total of four deviations  $\{\sigma_{C/M}(DF = 3)\}$  (where DF is the degrees of freedom), and another set has essentially an infinite number  $\{\sigma_{C/M}(DF = \infty)\}$ , then the comparison, or combination of the statistical properties is somewhat complex.

$$\begin{aligned}
 P \left\{ \pm 1.0 \sigma_{C/M} (DF = 3) \right\} &= 61 \% \\
 & \neq 68 \% = P \left\{ \pm 1.0 \sigma_{C/M} (DF = \infty) \right\}
 \end{aligned}
 \tag{F.1}$$

Equation F.1 shows that  $\pm 1.0$  standard deviation, with 3 degrees of freedom (DF = 3), gives a 61 % probability (*P*) of representing the deviations in the data set,



The example assumes a complete data-base population of random deviations that are known to exactly fit Gauss's probability distribution function. The sum of (the first moment of) all the deviations is 0.0. The mean value of the sum of the square of (the second moment of) all the deviations (the variance,  $\overline{\sigma^2}$ ) is 2.0. This gives a standard deviation of  $\sqrt{2.0}$ , or 1.414. A sample of 4 deviations is taken from the population. If the sample is a statistically valid one, it will have the same properties as the population. This means that the sum of the first moment of sample deviations is 0.0, and the mean value of the variance is 2.0.

$$\begin{aligned}
 \text{Mean} \\
 \text{Variance} \\
 \text{Estimate}
 \end{aligned}
 &= \left( \begin{array}{c} \text{Variance For A} \\ \text{Statistically Known} \\ \text{Data - Base} \end{array} \right)_{\text{Gauss}} \times \left\{ \begin{array}{c} \text{Central "t" Statistical} \\ \text{Function For Estimating} \\ \text{A Finite Data - Base} \end{array} \right\}_{\text{Gosset}}
 \end{aligned}
 \tag{F.3}$$

$$\overline{\sigma^2} =$$

For most evaluations, Gauss's distribution of the data is not attainable.

Thus, the degrees of freedom (DF) is  $N' - 1$ , or  $DF = 3$ .

As noted in the worded expression for Equation F.3, the estimate of the mean variance ( $\overline{\sigma^2}$ ) may be defined by the product of the two terms. The term in parenthesis ( ) is the expression for Gauss's data-base population. This means that the deviations ( $\Delta X_n$ ) fit a Gaussian probability distribution function. The term in braces { } is the expression for estimating the mean variance assuming that, due to the finite number of data points, there is some uncertainty associated with the sample of data being part of the Gaussian population.

When the Westinghouse and CE benchmark data samples were selected from the FTI data-base population to independently evaluate the statistical properties, two methods of estimating the (standard deviation) variance were used. These methods are the ones just described, based on Equation F.3. Thus, Tables E-3 and E-4 in *Appendix E* have two values for the estimated standard deviation for the samples. Reviewing the



Westinghouse plant benchmarks in Table E-3, the first value of the root mean square standard deviation is based on Equation F.3 with the number of plants ( $N$ ) being 5, The second value of the root mean square standard deviation is also based on Equation F.3, with  $N$  equal 5.

The assumption for the above evaluation is not that the Westinghouse data is one sample out of 39 plants, it is that the 5 capsules from the Westinghouse plants are not unique relative to the 39 capsules in the FTI data-base. The basis for assuming that the Westinghouse capsules are not unique comes from the NRC request that the review of the measured and calculated data by plant type include (page E - 7):

- 1 - A description of the important physical parameters and characteristics affecting the uncertainties, with discussions explaining why differences between plant types do not result in the data representing different populations.

There is no difference in the dosimetry measurements for Westinghouse plants, nor is there a difference in the analytical methods to calculate the dosimetry activities. Therefore, the sample of Westinghouse deviations should have the same central "t" probability distribution function as the deviations from the data-base population.

**Question 4**

How do the *C/M* values of the five selected W plants compare with the *C/M* values for the other plants in the W data base of Reference-1 in the submittal? In view of the *C/M* difference between the five selected plants and the W data base average, provide justification for using the *C/M* value based on the five plants.

**Response**

Table F-1 compares the *C/M* values from the five Westinghouse (W) plants analyzed by FTI, with the values that Westinghouse notes in Reference E1 from their data-base.

Plant	<u>W</u> <sup>E1</sup>	FTI
Prairie Island Unit 1	.748	
North Anna, Unit 1	1.017	
North Anna, Unit 2	1.017	
Shearon Harris, Unit 1	.927	
Zion, Unit 1	.780	
<b>Mean <i>C/M</i></b>	<b>.898</b>	<b>1.039</b>
<b>FTI Data-Base Mean <i>C/M</i> (39 Capsules &amp; Cavities)</b>		<b>1.026</b>

Table F-1 also includes the mean *C/M* value from the FTI benchmark data-base,

## FTI Non-Proprietary

which is 1.026 This data-base value is very close to the 1.039 value for the Westinghouse plant sample. The 0.898 mean  $C/M$  value for the Westinghouse analyses is close to the 0.879 value in their data-base (Reference E1).

The mean  $C/M$  value for the Westinghouse analyses is 10.2 percent less than unity (.898), while the mean value for the FTI analyses is 3.9 percent greater than unity. The differences between the Westinghouse mean  $C/M$  value and the FTI one (-10.2 and +3.9 percent) result in a 14.1 percent absolute difference. These differences are not a concern because they have been previously explained. The explanation is discussed on pages E - 11 through E - 13, and the first paragraph on page E - 14 of *Appendix E*. The FTI  $C/M$  comparison is the actual measured specific activity, while the Westinghouse comparison is the unfolded flux (fluence rate). On page E - 12, in Equations E.3 through E.5, it is explained that the FERRET-SAND methods have caused a 12.0 percent bias in the  $C/M$  comparisons of unfolded fluence values relative to FTI results. Subtracting the 12.0 percent expected difference, from the 14.1 percent difference, gives a 2.1 percent residual.

### Question 5

What is the effect on the bias and uncertainty calculation of eliminating the seven (of twenty-seven) B & W capsule /cavity measurements from the FTI uncertainty analysis (p. E-34, paragraph-3)? How is this effect accommodated in the methodology?

### Response

The effect on the calculation to measurement benchmark bias and

**Framatome Technologies Inc.**

the (unbiased) uncertainty ( $\overline{\sigma_{C/M}}$ ) caused by eliminating seven of the twenty-seven B & W capsule - cavity measurements from the FTI uncertainty analysis (page E - 34, paragraph 3) is shown below in Table F-2.

Table F-2		Uncertainty Comparison	
Number of B & W Plants	Bias	$\overline{\sigma_{C/M}}$	
20			
27			

Tables E-6 and F-2 also show that the mean standard deviation for 20 B & W capsules and cavities is %. If the other 7 capsules and cavities from the B & W plants were to be added to the 20, the mean standard deviation for the 27 capsules and cavities would decrease to %. Thus, the effect on the standard deviation caused by eliminating the 7 capsules and cavities is to increase the estimated value.

The effect of these increases on the methodology is related to (1) the overall bias for all Pressurized Water Reaction (PWR) plants, (2) the overall standard deviation for all PWR plants, and (3) the confidence factor for all PWR plants.

the overall bias for all PWR plants in the data-base continues to be statistically insignificant, as shown in Table E-6.

The standard deviation increase in the B & W data, for 20 capsules and cavities, produces an increase in the overall PWR standard deviation. The combination of 39 capsule and cavity benchmarks in the FTI data-base (including the 27 B & W capsules and cavities) produced a standard deviation of % (page 7 - 33, Equation 7.16). Eliminating the 7 B & W capsules and cavities, and combining the benchmarks in the FTI data-base with equal plant weights, increases the standard deviation from % to % (assuming 38 degrees of freedom). Thus, the eight percent increase shown in Table F-2, results in a five percent increase in the overall standard deviation for all PWR plants.

The elimination of the 7 B & W capsules and cavities from the data-base allowed the methodology for estimating the standard deviation to include response function weights of the data by plant type. The assumption of plant dependent response functions reduced the degrees of freedom to eleven. With eleven degrees of freedom, versus thirty-eight, the confidence factor to achieve a 95 percent confidence level increased from [redacted]. An increased confidence factor results in an increase in the uncertainties in the benchmarks and the calculations.

**Question 6**

Was the energy-dependent bias used in the FTI methodology applied to the Virginia Power calculations of Table E-5 and, if not, discuss the applicability of these results to the FTI methodology.

**Response**

The energy dependent bias used in the FTI methodology manifests itself as

The energy dependant bias, observed in the FTI methodology, was evident in the Virginia Power benchmark of calculations to measurements shown in Table E-5 (page E - 28). However, the Virginia Power analyst did not use the FTI bias removal function described on page D - 80. Nor did the analyst develop an energy dependant bias. The application of the energy dependent bias removal to the benchmark of the Virginia Power calculations, shown in Table E-5, was through the combination of uncertainties with Equation 7.13.

Thus, both the Virginia Power and FTI methodology have no bias in the greater than 1.0 MeV dosimeter reactions. The fact that the Virginia Power methodology for the calculations shows no bias, supports the fact that the FTI methodology can produce unbiased calculations of Westinghouse plants. This is in contrast with the fact that the Westinghouse methodology produces biased calculations of their plants.

**Question 7**

In view of the substantially reduced calculational uncertainty associated with the CE plants, provide justification for including this data in the FTI data base.

## FTI Non-Proprietary

How is it assured that the inclusion of the CE plants in the FTI data base does not result in a reduction in the calculational uncertainty applied to the W and B&W plants ?

### Response

The benchmarks of the calculational to measurement uncertainty for the CE plants is %, as shown in Table E-6, (page E - 35). This is substantially less than the FTI data-base uncertainty for plant benchmarks, which results in a root mean square standard deviation of %, as shown by Equation E.10 (page E - 36). With the CE plant standard deviations combined with Westinghouse and B & W plants, the data-base standard deviation is reduced from % to % with eleven degrees of freedom. The assurance that the CE plants may be included with the population of the twelve plants in the data-base, comes from testing the population with (Student's) William Sealy Gosset's central "t" probability distribution function.

Reviewing Table E-3 (page E - 26) for Westinghouse plants, and Tables E-6 and A-2 (page A - 25) for the B & W plants, shows that indeed, no plant has a mean deviation greater than

## FTI Non-Proprietary

The fact that the following three conditions are true, is assurance that the CE plant deviations are not biasing the uncertainty for Westinghouse and B&W plants. (1) The deviations from Westinghouse, CE, PCA, and B & W plants fit within (Student's) William Sealy Gosset's central "t" distribution. (2) The fit is based on the conditional probabilities related to twelve plants. (3) The product of the central "t" confidence factors, for the appropriate conditional probabilities, and the standard deviation of %, bounds the plant deviations. Thus, the CE plant data appears to be an appropriate part of the FTI plant data-base population. The low CE plant standard deviation is merely a fortuitous random occurrence.

### Question 8

Why are the  $\sigma_{C/M}$  values for the W and CE plants of Tables E-3 and E-4 different than the values given in Table E-6?

### Response

The  $\sigma_{C/M}$  (standard deviation) values for the Westinghouse and CE plants in Tables E-3 (page E - 26) and E-4 (page E - 27) are different than the values given in Table E-6 (page E - 35) because

This concept was explained when addressing Question 3, on pages F - 3 through F - 7. Rather than list the mean deviations of each of the twelve plants in Table E-6, to define the plant weighted standard deviation ( %) of the FTI benchmark data-base, the mean deviation for each grouping of plant types is given. The reason for giving the mean deviation by plant type is to address the possibility that the uncertainties in the



## FTI Non-Proprietary

calculations, and thereby the benchmarks, are dependant on plant type. As discussed in topical Section E.4, “Plant Dependent Benchmark Uncertainties”, on pages E – 33 and E – 34, the statistical evaluation of the data set samples from the Westinghouse and CE plants could be represented by the statistical properties of the FTI data-base population. However, it was noted that this conclusion could be simply due to a fortuitous combination of the estimated properties. Thereby, the statistical inference of the conclusion would not be appropriate to ensure safe conditions.

Equation F.3 (page F - 5) was used to define a root mean square standard deviation for each plant type in Table E-6. Using the Westinghouse plant data in Table E-3 as an example,

If the mean deviation ( $\overline{\Delta X}$ ) is unbiased, then its value is zero. Squaring the mean deviations from the five Westinghouse plants, with  $N$  equal 5, gives a root mean square standard deviation of %, as shown in Table E-6.

the standard deviations can be useful when evaluating the differences between data sets that are not statistically equivalent. As the NRC noted in the previous question (Question 7 on page F - 12), the CE plant data appears questionable relative to the comparable mean standard deviations for the Westinghouse, PCA, and B & W plants. The reason that the CE data appears questionable is due to the estimates of the mean standard deviations by plant type. Each plant type mean standard deviation is based on its unique degrees of freedom ( $N$ ).

**Question 9**

There are certain plant features (e.g., vessel thickness, presence of a thermal shield and capsule location) that can have a unique effect on the  $C/M$  ratios and require a separate uncertainty analysis. Provide justification for concluding that plants with these types of features do not have to be analyzed separately.

**Response**

There are various plant features, including the ones that the NRC specifically noted in the above question, that may effect the  $C/M$  ratios, and be outside the bounds of the uncertainty analysis presented in this topical. There is no justification for concluding that plants that have features that were not part of the overall uncertainty evaluations may be included under the uncertainty results of this topical. In fact, for each plant-specific fluence analysis, there must be an evaluation of (1) the dosimetry measurements, (2) the  $C/M$  ratios, and (3) the analytical uncertainties, to justify the application of the uncertainties in Tables E-1 and E-2 (on pages E - 3 and E - 4 respectively).

In the topical, on pages 7 - 16 and 7 - 17, in Tables 7-2 and 7-3, there are lists of all the dosimeter types that were qualified, or requalified, to be used in conjunction with fluence monitoring. The qualification assessment focused on each laboratory's experimental methodology, to ensure an uncertainty methodology that was appropriately associated with the experimental results. The uncertainty methodology demonstrated that the experimental methodology produced unbiased measurements, or statistically insignificant biases. Moreover, the measurements were determined to have well-defined statistical uncertainties. The statistical uncertainties were defined in terms of (a) standard deviations, (b) levels of confidence consistent with embrittlement

## **FTI Non-Proprietary**

uncertainties, and (c) the central “t” probability distribution function. Any plant-specific fluence evaluation may only use the dosimeter types qualified in the topical. Furthermore, the results of the plant-specific measurements must include an uncertainty evaluation for every dosimeter. The mean standard deviation in the dosimeter activation - reaction measurements must be consistent with the dosimetry qualification outlined in the topical.

The measurement qualification in the topical evaluated more dosimeter types than listed in Tables 7-2 and 7-3. However, the unlisted dosimeter types, such as the Solid State Track Recorders (SSTRs), were disqualified because they could not meet the qualification requirements. For example, as discussed on page 7 - 9, the SSTRs do not have a sufficient mass standard for determining biases in the thin-film deposits.

No new dosimeter types, or new locations of the dosimetry, may be implemented in plant-specific fluence evaluations without a comprehensive measurement uncertainty evaluation, such as that discussed in the topical.

In addition to the disqualified dosimeter types noted in the topical, two of the types that are qualified for measurement uncertainties in Tables 7-2 and 7-3 are disqualified later. As noted on page 7 - 18, in Table 7-4, the dosimeters are disqualified when assessing the uncertainties in the greater than 0.1 MeV activation - reactions and fluence values. The type of dosimeter is sufficient for the spectrum that it covers. However, this dosimeter type has statistical properties that are inconsistent with the other dosimeters covering other portions of the greater than 0.1 MeV spectrum. Thus, it is insufficient for dosimeters to be combined with other dosimeters to estimate the statistical uncertainties in the greater than 0.1 MeV fluence. (At a later date, the dosimeters could be qualified to have consistent statistical properties, and thereby be incorporated into the list of qualified dosimetry.)

**Framatome Technologies Inc.**

The other dosimeter type that is disqualified is . As noted on page 7 - 29, when discussing the application of Equation 7.12, the dosimeters are disqualified for evaluating fluence uncertainties because the reactions are inconsistent with previous calculational benchmark uncertainties. This inconsistent behavior is observed when benchmark ratios of calculations to measurements are compared for the various qualified dosimetry. Since the dosimetry is disqualified for  $C/M$  benchmark evaluations, it would be inconsistent to have the statistical properties of the measurements partially based on this dosimeter type. Thus, it is disqualified from evaluations where it would be combined with other dosimeters to estimate the statistical uncertainties in the greater than 0.1 MeV fluence. (Like the dosimetry, the dosimetry could be qualified to have consistent statistical properties at a later date.)

Once the plant-specific dosimetry measurements have been shown to be consistent with the FTI dosimetry measurement data-base, the plant-specific dosimetry benchmark ratio ( $C/M$ ) must also be shown to be consistent. On page 7 - 34, following the Equation 7.19 estimate of the standard deviation in the calculations of dosimetry activation - reactions,

produces a benchmark uncertainty of percent.

Each plant-specific  $C/M$  ratio must be statistically consistent with the FTI benchmark data-base. This does not imply that each  $C/M$  ratio must be within percent of unity. Rather, when the plant-specific evaluation becomes part of the data-base (at a later time, during a data-base update) the distribution of deviations must fit within William Sealy Gosset's central "t" (Student's "t"). For example, three of the data-base plants, and a plant-specific evaluation, could have a  $C/M$  deviation as large as

percent. However, if a plant has a feature that is unique to the data-base, then the plant-specific deviation must be within the percent standard deviation of the data-base. Thus, if a plant has a unique feature, the only justification for applying the FTI data-base calculational uncertainty to the plant, is if there is a high probability that the uncertainty is applicable. The means of achieving the high probability is to reduce the acceptable  $C/M$  deviation.

The third evaluation that must be performed for a plant-specific evaluation, is the verification that the analytical uncertainties remain valid. There are two parts of the analytical uncertainty verification. The first is associated with the  $C/M$  verification discussed above. The second is associated with verification of the uncertainties in the parameters and variables that are part of the analytical modeling and computational procedures (Section 7.2, "Dosimetry Calculational Biases and Standard Deviations", pages 7 - 23 through 7 - 27).

The  $C/M$  verification discussed above is based on the assumption that the unique feature associated with a specific plant has been evaluated with respect to the physical parameters and characteristics. The basis for the physical evaluation is the same as that noted by the NRC in item 1, on page E - 7. If the evaluation indicates that the calculational methodology has sensitivities to the uncertainties associated with the unique feature that are similar to other uncertainties, then the  $C/M$  evaluation is adequate. However, if the evaluation indicates that the calculational methodology has greater uncertainty sensitivities, then an additional analytical uncertainty must be evaluated, and the result added to the existing FTI calculational uncertainties.

The second part of the analytical uncertainty verification is reviewing the uncertainties in the parameters and variables that comprise the uncertainties in the analytical

## FTI Non-Proprietary

modeling and computational procedures. The unique feature in a specific plant evaluation may be such that the  $C/M$  results are not sufficient to validate the uncertainty. An example of such a situation occurred in the FTI evaluation of the Virginia Power, Surry plant, Unit 1, Capsule X analyses.<sup>F2</sup>

The Surry, Capsule X analyses included partial length poison rods, of two different lengths, in two peripheral fuel assemblies. Moreover, the three-dimensional neutron source distribution originated from Virginia Power calculations. The unique features of the Surry, plant-specific analyses, were partial length rods, of two different lengths, and the Virginia Power source calculation. While Virginia Power source calculations are part of the FTI benchmark data-base (North Anna, Unit 1, Capsule V, and North Anna, Unit 2, also Capsule V, page A - 25), the depressed peripheral powers created a second degree of uniqueness. The locations and operational history of Capsule X could provide only a marginal verification that the FTI calculational uncertainties would be applicable.

To verify that the FTI calculational uncertainties from the data-base would be applicable to the Surry fluence analysis, the analytical source uncertainty evaluated for the topical, needed to be revalidated. In addition, the three-dimensional, multi-channel synthesis needed to be validated. The benchmark calculations in the data-base incorporated a function over the axial length of the problem (Section 3.3.1, "Three-dimensional Synthesis of Results", on pages 3 - 24 through 3 - 29 in the topical).

To validate the Virginia Power three-dimensional source distribution, with particular emphasis on the depressed peripheral powers, the statistical properties of the FTI analytical uncertainty evaluation for the source were reviewed. Virginia Power evaluated their (true) three-dimensional results (no synthesis) with respect to their in-

## **FTI Non-Proprietary**

core instrumentation. The statistical properties were shown to be consistent with the bases for the FTI uncertainties. Thus, the uncertainties in the source distribution for the partial length poison rods were validated.

To validate the three-dimensional, multi-channel syntheses

The evaluation reviewed the deviations in the relative fluence distribution between the FTI synthesis and the Virginia Power benchmarked results. The deviations should be consistent with the FTI uncertainties. If they were, then no additional uncertainty would be needed for the calculations. The uncertainties in the multi-channel synthesis analysis of the partial length poison rods were consistent with the FTI uncertainties for single channel synthesis. Thus, the uncertainties in the calculations were validated for the unique feature of partial length poison rods.

The above discussion notes that there is no general justification for assuming that specific plants, with unique features, that were not a part of the FTI benchmark data-base, would have calculational uncertainties associated with the data-base. The data-base uncertainties include: (1) the dosimetry measurements, (2) the ratio relating the comparison of the calculations to measurements,  $C/M$ , and (3) the components of the analytical modeling and computational procedures

If a plant-specific feature is found, that is unique in relation to the three types of uncertainties evaluated in the topical, then the validity of the uncertainties must be verified. If the uncertainties associated with a unique feature in a specific plant cannot be shown to be statistically consistent with the FTI uncertainty data-base, then the calculated fluence uncertainty must be appropriately increased.

*Appendix F* References

- F1. United States Nuclear Regulatory Commission letter to J.J. Kelly, Manager, B & W Owners Group Services, **Request for Additional Information - Framatome Topical Report BAW-2241P, Revision 1**, from Stewart Bailey, Project Manager, Office of Nuclear Reactor Regulation, October 26, 1999.
  
- F2. M.J. DeVan and S.Q. King, **Analysis of Capsule X, Virginia Power Surry Unit No. 1, Reactor Vessel Material Surveillance Program**, BAW-2324, Framatome Technologies Inc., April, 1998.



## ***Appendix G* BWR Benchmarks & Uncertainties**

### **G.1 Introduction**

The purpose of this appendix is to update the uncertainties in the AREVA NP benchmark database to include boiling water reactor (BWR) fluence calculations. In previous revisions to this topical, AREVA NP showed that its fluence and uncertainty methodologies applied to all pressurized water reactors (PWR). The benchmarks in this revision show that the AREVA NP neutron physics methodology that was accepted for PWR licensing applications in Revision 1 can be appropriately modified for BWRs. The benchmarks of the BWR methodology described in this appendix constitute Revision 2 to BAW-2241P.

Before developing this appendix, AREVA NP held discussions with the Nuclear Regulatory Commission (NRC) concerning the required content for its acceptance. It was agreed that the basic methodology for the (a) fluence calculations, (b) dosimetry measurements, and (c) uncertainty evaluations would be the same for PWRs and BWRs. However, a set of BWR benchmarks was necessary to show consistency between the uncertainty in the BWR fluence methodology and uncertainties and the AREVA NP database.

The basis of the theoretical methodology for calculating the fluence in a BWR is the same as that for a PWR. The DORT<sup>G1</sup> computer code is used in the same manner for both, and both use the BUGLE-93<sup>7</sup> cross section library. The source term for PWRs

and BWRs is developed from core-follow data that matches the in-core operational measurements of the three dimensional power. Since the theoretical methodology for BWRs is the same as that for PWRs, the uncertainty methodology would also be the same. However, the complexity associated with varying water densities in the axial segments of BWR fuel assemblies introduces an additional uncertainty into the analytical modeling.

The key consideration with respect to BWR fluence methods is the varying water densities. Because of the variation in the water densities, there are additional components to the calculational uncertainties. These components must be included in the mathematical statistics for determining the biases and level of confidence in the mean standard deviation. Using the updated BWR methods, the uncertainties in the calculations have been validated with an updated benchmark database. The estimated values of the analytical uncertainties for BWR and PWR results are the same with the exception of the additional ones for water density effects. The combined uncertainties for the BWR calculations are presented in Section G.4.2, "Calculational Uncertainties." The additional contribution due to water density effects is presented in Section G.4.2.4, "Analytic Sensitivity."

This appendix presents the calculational methodology that has been updated for BWR fluence evaluations. It also presents the BWR benchmarks and calculational uncertainty.

## G.2 Background

As explained in Revision 1 of this topical, the AREVA NP dosimetry database has measurements ( $M$ ) with certified uncertainties from reference field validation by the National Institute of Standards and Technology. Thus, the AREVA NP benchmarks include a certified uncertainty for the calculated ( $C$ ) results as well as the benchmark  $C/M$  uncertainties.

The NRC noted that confirmatory benchmarks are necessary to have a valid estimate of BWR uncertainties. The NRC indicated that sufficient benchmarks would be (1) the PCA results,<sup>G4</sup> (2) the comparison to the NRC BWR benchmark problem in NUREG/CR-6115,<sup>G5</sup> and (3) a capsule comparison from an operating plant.<sup>G6</sup>

To confirm that the BWR uncertainties estimated in this appendix have the appropriate level of confidence, the results from the benchmark comparisons noted above must be consistent with the existing AREVA NP database. For the PCA, the comparison needs to review the consistency with the BWR geometry. For the NRC BWR benchmark problem, the deviations between the Brookhaven National Laboratory (BNL) and AREVA NP results must be consistent with the deviations that were associated with the PCA results. Finally, for the operating plant capsule comparison, the deviations must be consistent with the AREVA NP database.

The accuracy of the BWR fluence calculations is like that PWRs, there is no bias. The BWR benchmark comparisons provide confidence that the random uncertainties are within the population of the AREVA NP benchmark database.

### G.3 Extension of Fluence Methods

Revision 1 of the topical report presents two methodologies, one for determining the fluence and the other for estimating the uncertainty in the methodology for determining the fluence. This section focuses on extending the methodology for determining the fluence throughout the BWR “beltline” region. The following section (G.4) focuses on the “Uncertainty Update”.

There are two major parts of AREVA NP’s methodology for determining the fluence. The first part is the evaluation of dosimetry measurements. The second is the calculation of the fluence throughout the reactor internal structures, vessel, and reactor shield-support structure within the “beltline” region.

The theoretical and experimental methods used to determine the calculated and measured results for the fluence and dosimetry activities are not dependent on the reactor design. Thus, the theoretical and experimental methods (DORT, BUGLE-93, etc.) for BWRs are the same as those for PWRs. While the approximations used to obtain solutions to the theoretical methods for PWRs need to be extended when applied to BWRs, the measurement process requires no extension of the techniques or procedures. Consequently, the experimental methodology is not discussed in this section. The BWR experimental methods are the same as those discussed in Section 5 of this topical report. This section addresses the BWR calculational models and procedures used in the solution of the theoretical methods.

### G.3.1 Solution of BWR Fluence Methods

The fluence methodology presented in this report describes theoretical methods, with procedural and modeling approximations that provide accurate and reliable predictions of the greater than 0.1 MeV fluence values. These methods were originally developed for PWRs but they are generic to any water-moderated reactor. Consequently, the PWR calculational models and procedures are utilized as the basis for calculating the fluence throughout the internal components and vessel of BWRs. While the PWR approximations are generic to any water moderated reactor, there are three areas where the approximations must be expanded to provide accurate and reliable predictions of the greater than 0.1 MeV fluence values for BWRs. The following discussion explains the development process that led to the identification of the three areas. The discussion continues by explaining that the development of the expanded models and procedures ensured the same accuracy, with unbiased results, as previously shown with the benchmark database.

In 2001, AREVA NP formed a joint venture with Siemens. Siemens had developed the technology for modeling BWRs and this technology had been approved by the NRC for licensing applications. The joint venture provided the essential expertise for applying PWR fluence methods to BWR designs. Three areas that were found to require an extension of the PWR models and procedures to analyze the BWR vessel fluence values were: (1) the transport of neutrons from the core through the internal structures associated with the jet pumps, (2) the integrated core leakage function from the fuel, and (3) the three-dimensional synthesis of the core leakage function. The details of the development in each of the three areas are described in Sections G.3.1.1, G.3.1.2, and G.3.1.3 respectively.

### G.3.2 Neutron Transport Through Jet Pumps

Neutron transport from the core region through the internals and other reactor structures can be formulated by dividing it into two parts for the purpose of this discussion. The first part involves the leakage of neutrons from the core. The second involves the transport of the neutrons through the internal components and vessel to the concrete shield and support structure. The AREVA NP models and procedures used to obtain a solution to the transport process in the second part are equally applicable to PWRs and BWRs. However, if BWR dosimetry is located within the radiation shadow area of the jet pumps, the modeling of the pump structures must include the same type of procedures for [ ] accuracy as those used in PWRs [ ]

Figure 3-2 on page 3 - 6 represents a schematic of the radial plane of a PWR. To model this geometry, a cylindrical coordinate system  $(r, \theta)$  is used. However, there is a problem [ ]

[ ]

]

[

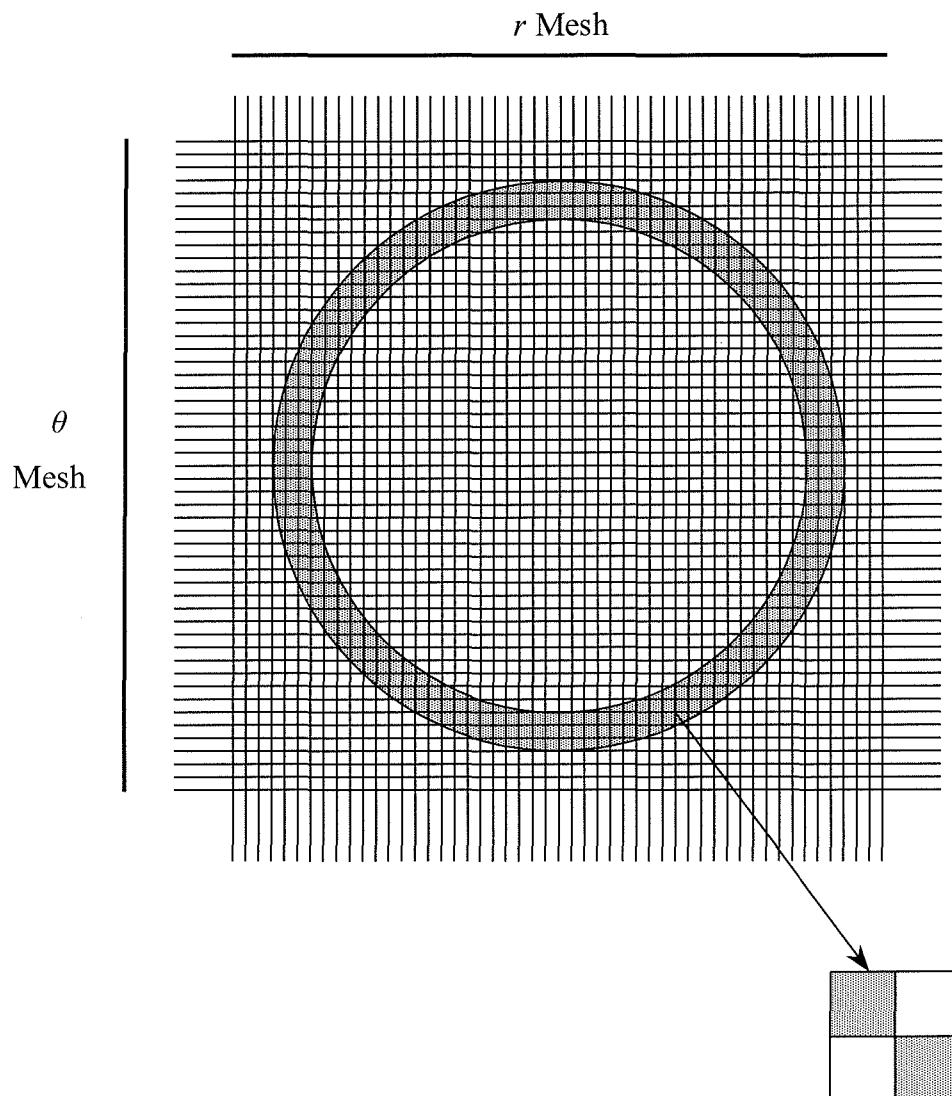
]

Figure G-1 on the following page represents a schematic of a cylindrical section of a jet pump component in the radial plane. The vessel flux is shielded from the neutrons leaking from the core by the internal structures, such as the jet pumps. Therefore, the maximum vessel flux does not occur in the shadow behind the jet pump structures. Consequently, the evaluation of the maximum flux does not need an accurate pump model. However, the evaluation of the dosimetry in the shadowed area behind the jet pump structures is affected by the pump modeling. [

] The following discussion reviews the models and procedures used to attain the needed accuracy in the flux calculations.

Reviewing Figure G-1, the jet pump structure is schematically shown in the radial plane as the “shaded” tubular region. The coordinates, noted by the square crosshatch of grid lines, are cylindrical.

Figure G-1  
Schematic of  $r, \theta$  Modeling  
For Jet Pump Tubular Structure





NON-PROPRIETARY

---

The abscissa (horizontal line) is noted as the radial ( $r$ ) coordinate, and the ordinate (vertical line) is noted as the angular ( $\theta$ ) coordinate. [

]

[

]

[

]

[

]

(G.1)

[

]

[

]

[ ] (G.2)

[

]

[ ] (G.3)

[

]

The extension of the AREVA NP models and procedures to BWR jet pumps provides a means of accurately evaluating dosimetry reactions near the pumps. [

]

### G.3.3 Core Leakage Function

An important consideration in the flux solution for vessel fluence evaluations is the leakage of neutrons from the core. The AREVA NP methods are based on the solution of the three dimensional ( $\mathbf{r}$ ) fission rates integrated over the energy (E) and angular variables ( $\mathbf{\Omega}$ ) of the velocity groups (g), and time ( $t$ ). The accuracy of the process begins with the core-follow simulation of the measured fission rates for power production. The core-follow results match the measurements within the uncertainty criteria for the magnitude of the core power and the nodal power distribution.

The measurements of core operation are taken at periodic intervals. The core-follow simulation of the operation utilizes the measured data from each period to follow the power production. Given the close relationship between the calculated three-dimensional power distribution and the comparable measurements of axial segments for each assembly, the core-follow time-steps provide a numerical means of integrating the fission rates over the operational cycles. The average time-weighted source parameters are those given in Equations 3.1 and 3.2 on pages 3 – 11 and 3 – 12. As shown by the equations, the neutron source terms are represented by three-dimensional ( $\mathbf{r}$ ) values for each fuel rod and axial rod segment. These sources are processed for the cylindrical coordinate system used in the DORT modeling.

Since the discrete source eigenfunctions represent a solution to the three-dimensional neutron transport equation, these source eigenfunctions may be returned to a three-dimensional neutron transport model to serve as a “fixed” source term. The neutron transport theory expression with a “fixed” source eigenfunction  $\{S(\mathbf{r}, E, \mathbf{\Omega})\}$  is represented by Equation G.4.

$$\boldsymbol{\Omega} \cdot \nabla \phi(\mathbf{r}, E, \boldsymbol{\Omega}) + \Sigma_T(\mathbf{r}, E) \phi(\mathbf{r}, E, \boldsymbol{\Omega}) = S(\mathbf{r}, E, \boldsymbol{\Omega}) \quad (\text{G.4})$$

The average time-weighted collision density parameters  $\{ \Sigma_T(\mathbf{r}, E) \phi(\mathbf{r}, E, \boldsymbol{\Omega}) \}$  from the three-dimensional core-follow calculations are evaluated using the same procedures as those used for the source parameters. Assuming that there is no average time-weighted effect on the leakage function  $\{ \boldsymbol{\Omega} \cdot \nabla \phi(\mathbf{r}, E, \boldsymbol{\Omega}) \}$ , the collision density parameters and source parameters in Equation G.4 produce the same flux values as those from the average time-weighted core-follow calculations.

[

]

Using the models and procedures discussed in Section 3 of this topical to compute BWR leakage rates from the core periphery indicates that the approximations in the modeling and procedures must be updated. The average time-weighted “fixed” source

NON-PROPRIETARY

---

eigenfunctions and collision density parameters do not produce accurate peripheral flux values. To understand the failure in the approximations, the solution of Equation G.4 needs to be reviewed. DORT provides a general numerical solution of Equation G.4, but it is not useful to evaluate the relationship between the leakage rate, collision density, and source density. [

[ ] (G.5)

[

]

The neutrons crossing the boundary between  $\mathbf{r}'$  and  $\mathbf{r}$  represent the leakage of source neutrons from  $\mathbf{r}'$ . If we consider a fuel region defined by an array of  $\mathbf{r}'$  mesh points, the leakage from the  $\mathbf{r}'$  region is evaluated by integrating the current density at the surface of the fuel, the boundary of  $\mathbf{r}'$ . The leakage of the greater than 0.1 MeV flux from the surface of the fuel region is expressed by the Equation G.6 integrals over

NON-PROPRIETARY

---

energy ( $E$ ), angle ( $\Omega$ ), and the surface area ( $A$ ) perpendicular ( $\perp$ ) to a unit of the vector “ $\mathbf{r}'_{\perp A}$ ” in the direction of the neutron current from the region.

$$Leakage(\bar{\mathbf{r}}, \bar{E}, \bar{\Omega}) = \int_A \int_E \int_{\Omega} \Omega \cdot \left( \frac{\mathbf{r}'_{\perp A}}{|\mathbf{r}'|} \right) \phi(\mathbf{r}', E, \Omega) dA dE d\Omega \quad (G.6)$$

[

]

Substituting the equivalent Equation G.5 solution into the integral part of Equation G.6 gives the leakage [ ] with energies greater than 0.1 MeV and an exponential integral function ( $f_{leakage}$ ). Since (a) the current density is determined by the angular integral of the vector flux density  $\{\Omega \phi(\mathbf{r}, E, \Omega)\}$ , and (b) the source density produces the flux from the leakage, and scattering reaction rate densities  $\{\Sigma_s(\mathbf{r}', E) \phi(\mathbf{r}', E, \Omega)\}$ , [ ]

[



]

During any one cycle of operation and for many successive reload cycles, the water density in an axial segment of a PWR fuel assembly is essentially constant. Therefore, the collision rate  $\{\Sigma_T(\mathbf{r}', g) \phi(\mathbf{r}, g, \Omega_n)\}$  in the fuel region is directly proportional to the source  $\{S(\mathbf{r}', g, \Omega_n)\}$  [

]

[

] These

approximations in the PWR models and procedures produce accurate flux results within the core region of the peripheral fuel assemblies, and for dosimetry reactions. However, in a BWR model, the core and dosimetry calculational accuracy is insufficient. The problem is that the water concentration ( $N^{\text{Water}}$ ) in an axial segment of a fuel assembly varies during a cycle, and may vary from cycle to cycle for the assemblies located in the same position on the periphery of the core. Consequently, the total cross section  $\{\Sigma_T(\mathbf{r}', g)\}$  varies with time during the operation of the various cycles.

[

] Equation G.7 gives the expression for extending the core leakage model to treat a variable water density.

[ ] (G.7)

In Equation G.7, the symbol “ $f_{leakage}^{-1}$ ” represents the inverse operation of the Equation G.6 leakage function,  $f_{leakage}$ . [

]

[

]

[

]

[

]

Using the models and procedures discussed in Section 3 of this topical report to compute BWR leakage rates from the core periphery indicates that the approximations in the models and procedures are insufficient. [

]

### G.3.4 Three-Dimensional Synthesis

The fluence calculational methodology discussed in the previous sections (3.1.2 and 3.3.1) of this topical report begins with “exact” three-dimensional ( $\mathbf{r}; x, y, z$ ) core-follow analyses (no synthesis approximation) for the core region. Reviewing the results from any PWR model shows that all cores that operate without control rods or non-uniform poison shields have only one unique axial ( $z$ ) power shape. Moreover, those cores that operate with axial power shaping rods (B & W plants) can be modeled using only one unique axial power shape for fluence (rate) calculations. Thus, collapsing the “exact” three dimensional model to two dimensional models ( $x, y$ ) or ( $r, \theta$ ) is a straightforward integral process. It is also straightforward to integrate the  $r, \theta$  model over the  $\theta$  direction and incorporate the  $z$  - source distribution when developing the  $r, z$  model.

When the peripheral fuel of a PWR core has axially segmented fuel assembly components to shield a critical weld location, multichannel - planar models, with piece-wise continuous axial shape functions, are necessary for calculating the three-dimensional effects. However, the models and procedures continue to be clear-cut. The number of discrete axial channels is generally no greater than four.

BWR fluence analyses, like the PWR analyses discussed in Sections 3.1.2 and 3.3.1, begin with “exact” three dimensional core-follow models in the core region. Reviewing the results from BWR analyses shows that there are many unique axial ( $z$ ) power shapes associated with normal operation. Not only does the inserted position of the control rods contribute to various distinctive axial shapes, but the degree of boiling also creates unique axial power shapes.

The degree of boiling is a function of the axially integrated power in the channel of each assembly. Each assembly in the core with a different “assembly” power will have a different axial power shape. Due to the many unique “assembly” powers and axial power shapes in the BWR core, collapsing the “exact” three-dimensional model to two-dimensional models for fluence analysis is more complex than discussed in Section 3.3.1. In addition, the coupling of the boiling water density and the axial power shape, along with the control rod position and the axial power shape does not provide an accurate means of axially integrating the water density and control rod effects for a  $r, \theta$  model. [

]

Due to the complexity of collapsing the “exact” three-dimensional model of the core to two-dimensional models for three-dimensional synthesis analysis of the vessel fluence,

the best method for calculating the three-dimensional flux would appear to be an “exact” three-dimensional model (*e.g.* TORT). However, the accuracy of three-dimensional models like TORT is very poor. The problem is not the calculational methods; it is the limitations associated with the computer are the governing factor. For each of the sixty-seven BUGLE energy groups, and each of the one-million mesh points used in the three-dimensional modeling, there are on the order of one-hundred directional flux values. This results in over six-billion, seven-hundred-million values for the flux (fluence rate) solution that must be iteratively evaluated. Therefore, the three-dimensional synthesis model discussed in Section 3.3.1 has been extended for BWR analyses.

[

]

The axial spacing of the planar regions is developed from the “exact” three-dimensional core-follow model. The core-follow model results are used to identify the axial shape functions that best represent the effects of the control rod positions and the degree of channel boiling. The axial spacing of the planar regions is not uniform since inflections in the shape functions do not generally occur in equal increments.

Figure G-2  
Schematic of Three Dimensional Synthesis  
For BWR Fuel Assemblies

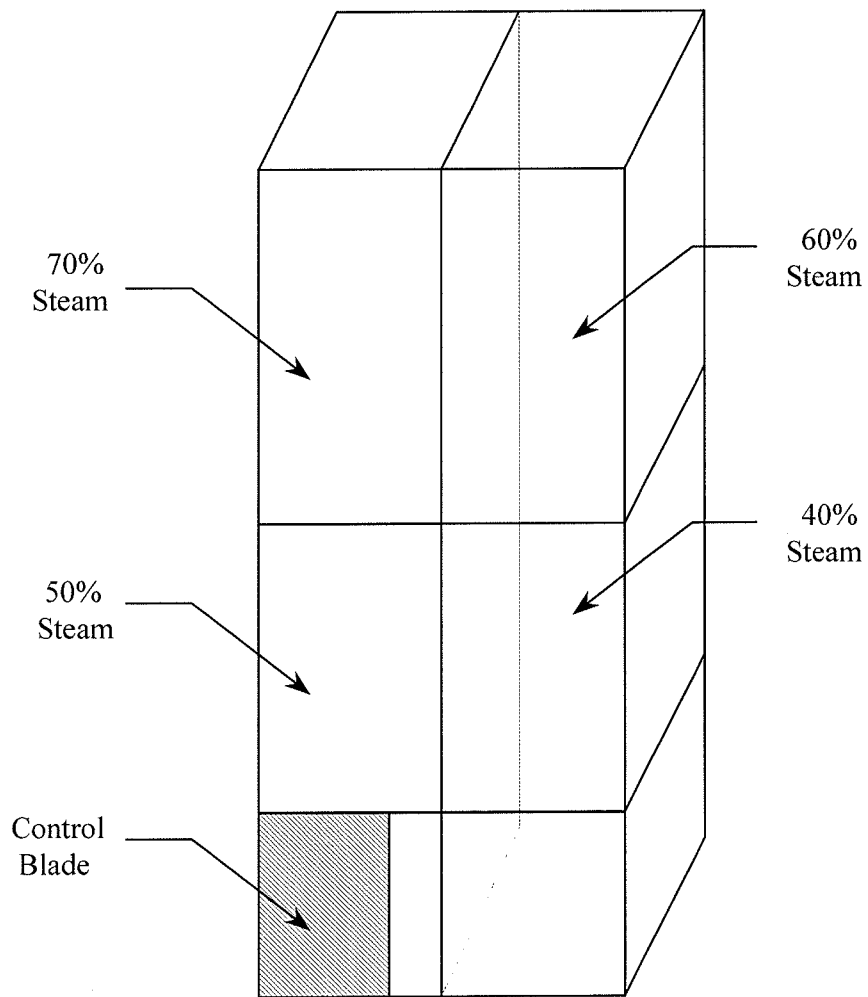


Figure G-2 on the previous page provides a schematic of two boiling water fuel assemblies. The purpose of the schematic is to help explain the extension of the synthesis methods. The schematic is not as detailed as the synthesis model. Instead, it represents three unequally spaced planar regions for the axial mesh spacing rather than seven or more. Each synthesis and schematic planar region represents a combination of  $x, y$  or  $r, \theta$  planar regions from the core-follow model. Viewed from the top of the figure, looking down, the  $x, y$  assembly pitch of the radial plane of the core region would be obvious. The combination of axial segments from two or more planar regions in the core-follow model would give one of the assembly segments that are shown in Figure G-2.

$$S^{3D}(x, y, \overline{\delta z}, \overline{E}, \overline{\Omega}) = \frac{\int_{\delta z} S^{3D}(x, y, z, \overline{E}, \overline{\Omega}) dz}{\int_{\delta z} dz} \quad (\text{G.8})$$

Equation G.8 expresses the integration of the three-dimensional (3D) source function ( $S^{3D}$ ) for each planar region segment of a fuel rod modeled in the synthesis calculation. In Figure G-2, the Equation G.8 source function  $S^{3D}$  is schematically associated with the axial segment of one assembly. To develop the source function for a two dimensional “ $R\theta$ ” synthesis calculation, a  $z$ -dependent multichannel source function ( $S_C^Z$ ) is used as shown by Equation G.9.

$$[ \quad \quad \quad ] \quad (\text{G.9})$$



NON-PROPRIETARY

---

The  $x, y$  or  $r, \theta$  planar regions in the “ $R\theta$ ” synthesis calculation not only include the Equation G.9 source functions in each axial segment, but the functional weighting of the collision reactions is also included. As discussed above, in Section G.3.1.2 for the “Core Leakage Function,” the core-follow time-steps provide a numerical means of integrating the source and collision parameters over the operational periods of interest for the fluence evaluations. [

]

[ (G.10)

[

]

To summarize, the AREVA NP synthesis models and procedures described previously in Section 3.3.1, are appropriate for BWR calculations. However, the multichannel-planar models used previously for PWRs needed to be expanded to accurately model BWRs. The reason for the modeling – procedure extension is the multiple time-dependent, non-separable, axial power shapes, which result from control rod insertion and the effects of channel boiling during operation. The shapes from each core-follow time-step are integrated into average time-weighted axial shapes for each assembly. These time-weighted, average assembly shapes provide the basis for the BWR multichannel modeling. The extension of AREVA NP’s models and procedures for BWR synthesis calculations involves more channels than previously evaluated and thereby more calculations to obtain the integrated coupling of the “ $R\theta$ ” planes with piece-wise axial shape functions.

[

]

The extended models and procedures for synthesis calculations of BWRs are validated in the same manner as the core leakage function and the transport of neutrons through the jet pumps. [

]

The methodology presented in Section 3 has been extended as explained above in Section G.3.1. The extension includes a more accurate treatment of (1) the transport of neutrons from the core through the internal structures associated with the jet pumps, (2) the integrated core leakage function from the fuel, and (3) the three-dimensional synthesis of the core flux function. With the more accurate treatment, the methodology presented in this appendix is appropriate for calculating the flux (fluence rate) throughout the internal structures and vessel of BWRs.

#### G.4 Uncertainty Update

This topical report presents two methodologies, one for determining the fluence and the other for estimating the uncertainty in the methodology for determining the fluence. The fluence and uncertainty methodologies are fundamentally theoretical methods that include procedural and modeling approximations. The theoretical methods are generic to all light water reactors (LWRs). While the models and procedures discussed in Section 7, the “Uncertainty Methodology” are generic, the results in *Appendix A*, “AREVA NP’s Dosimetry Database” are weighted with more B & W plants. The statistical evaluation of the models and procedures was expanded in *Appendix E* to equally weight all PWR plants. This section extends the discussion of the uncertainty evaluation to all LWR plants.

Uncertainties are evaluated for the (1) measurements, (2) calculations, and (3) benchmark comparisons of the calculations to the measurements. Two types of deviations, systematic and random, characterize these uncertainties. The systematic deviations are caused by inaccurate results with one or more unique biases producing the errors. The random deviations have no specific cause. However, the standard deviation from a “normal” distribution function, that is estimated using mathematical statistics, represents the precision of the overall random uncertainty. The mathematical statistics processing of the distribution of random deviations provides a level of confidence in the precision of the results. The level of confidence in the fluence uncertainty needs to be consistent with the level of confidence in the embrittlement uncertainty.

#### G.4.1 Measurement Uncertainties

One essential part of the uncertainty methodology is that all uncertainties must be defined in terms of reference standards that are known to be “true” values. As explained in the regulatory guide for determining the vessel fluence,<sup>G3</sup> the measured results are not “true” values unless they have been validated by a National Institute of Standards and Technology (NIST) reference field. The NIST reference field validation is more than the usual calibration standards for the experimental equipment. It is the validation of the measured dosimetry results by a NIST team. The NIST team independently performs the measurements and compares their results to those of the laboratory that AREVA NP uses for its measurements (B & W). Moreover, the NIST team reviews each part of the experimental process. By reviewing each part, they determine if any small biases exist and whether any biases essentially cancelled each other. As explained in AREVA NP’s “Standard and Reference Field Validation” document,<sup>E3</sup> NIST certified that the B & W laboratory has no statistically significant biases. Thus, the mean value of the measured results is accurate and only varies randomly about the “true” value. NIST also confirmed that the laboratory’s estimate of the standard deviation in the random uncertainties provided the appropriate level of confidence in the variation of the mean measurement about the “true” value.

The dosimeters associated with BWR specimen capsules are of the same type and form as those validated by NIST for the B & W laboratory measurements. Consequently, the AREVA NP evaluation of BWR dosimetry measurements is valid. In fact, AREVA NP has the only “reference field” validation of BWR dosimetry uncertainties.

The AREVA NP dosimetry measurements have no statistically identifiable bias and have a standard deviation that is not greater than 7.0 %.

$$\text{Mean Measurement Uncertainty} \leq 7.0 \%$$

(G.11)

#### G.4.2 Calculational Uncertainties

The uncertainties in the calculational methodology are determined from two evaluations, a computational sensitivity of the parameters affecting the calculations, and a benchmark of the calculated dosimetry results to the measurements. The parameters affecting the solution of Equation G.4 are evaluated using a set of sensitivity calculations of the neutron source, geometry, material composition, and modeling. The statistical combination of the fluence rate deviations from the sensitivity evaluations provides an estimate of the standard deviation in the dosimetry reactions and greater than 0.1 MeV vessel fluence values. The DORT results from Equation G.4 are compared to the AREVA NP dosimetry database to evaluate biases statistically, [

]

[

]

The benchmark of the dosimetry database provides the means of evaluating biases in the calculational methodology [

] The following discusses (1) the PCA benchmark results, (2) the AREVA NP comparison to the NRC BWR benchmark problem in NUREG/CR-6115, and (3) the comparison of AREVA NP capsule calculations for Browns Ferry Unit 2.

#### G.4.2.1 Pool Critical Assembly Benchmark

The Pool Critical Assembly (PCA) is a test reactor located at the Oak Ridge National Laboratory (ORNL). Between September the third of 1978 and January the fourteenth of 1981, the PCA was setup to simulate two different reactors; specifically the internals and vessel structure. The reactors are designated by the respective water region widths of the reflector and downcomer; 8/7 for the reflector/downcomer of one reactor, and 12/13 for the other. Reactor operation activated the dosimetry in seven locations along the axis as shown in Figures 1.1.2 and 1.1.3 of Reference G4 (pages 1.1-4 and 1.1-5). The importance of the measurements was to serve as a “blind test.” Each participant making fluence predictions for the utility industry would submit their results prior to knowing the results of the measurements. ORNL and the NRC judged the accuracy and precision of the participants. AREVA NP (participant “Y”) had the most accurate results.

As explained in Reference G4, on pages 2.4-2 through 2.4-8, the dosimetry measurements for locations “A1” and “A3M” are not as accurate as those for locations “A4” through “A6”. Consequently, the comparison of the dosimetry results is focused on these later three locations.

The key to these locations for the BWR benchmark is that, a calculational methodology that is accurate, and shows no correlation of the random deviations, will remain accurate, independent of the steel and water configurations of the internal and vessel structures. Therefore, when the AREVA NP calculations of the dosimetry in locations “A4” through “A6” are compared to the measurements for the reactor with an “8” centimeter reflector and a “7” centimeter downcomer (8/7), there should be no obvious



NON-PROPRIETARY

trend in the ratio of calculations to measurements,  $C/M$ . Moreover, when the calculations of the “A4” through “A6” dosimetry are compared to the measurements for the reactor with a “12” centimeter reflector and a “13” centimeter downcomer (12/13), there should be no obvious trend in the ratio of calculations to measurements either for the dosimetry locations or the two different reactor internal configurations. The following AREVA NP results have been taken from Reference G4 Tables 7.1.2 and 7.1.3 on pages 7.1-3 and 7.1-4.

<b>8/7 Configuration: <math>C/M</math> Comparison</b>			
	<b>Location</b>		
<b>Dosimetry</b>	<b>A4</b>	<b>A5</b>	<b>A6</b>
$^{237}\text{Np}(n,f)$	0.92	0.92	0.87
$^{58}\text{Ni}(n,p)$	0.92	0.88	0.88
$^{27}\text{Al}(n,\alpha)$	0.91	0.89	0.90
$^{238}\text{U}(n,f)$	0.85	0.83	0.79
<b>12/13 Configuration: <math>C/M</math> Comparison</b>			
$^{237}\text{Np}(n,f)$	0.98	0.98	0.96
$^{58}\text{Ni}(n,p)$	0.94	0.86	0.94
$^{27}\text{Al}(n,\alpha)$	0.96	0.93	0.94
$^{238}\text{U}(n,f)$	0.90	0.87	0.85

AREVA NP Inc.  
(An AREVA and Siemens Company)

The standard deviation for the dosimetry measurements varies. It was estimated that the  $^{238}\text{U}$  may be as high as 15 % due to  $^{235}\text{U}$  impurities and photofissions, the  $^{237}\text{Np}$  may be about 10 %, and the  $^{27}\text{Al}$  and  $^{58}\text{Ni}$  may be as low as 6 %. In addition to the dosimetry measurement uncertainties, there is an uncertainty of 4 % associated with the PCA absolute power. Using the AREVA NP database, the calculational uncertainty is [ ] As discussed in Reference G4, the overall ratio of calculational results to measurements for all participants was somewhat less than 1.0. This indicates that there is a bias in the PCA measured data. Independent of a possible measurement bias, the  $C/M$  comparisons for the dosimetry locations in both the 8/7 and 12/13 configurations indicate that the AREVA NP calculations have no bias as a function of spatial location or as a function of steel – water configurations. Moreover, the combined calculational and measurement standard deviation ( $\sigma$ ) for the  $C/M$  comparisons ( $\overline{\sigma_{C/M}}$ ) is 17.0 % for the  $^{238}\text{U}$  dosimeters, 12.8 % for  $^{237}\text{Np}$ , and 10.0 % for  $^{27}\text{Al}$  and  $^{58}\text{Ni}$ . Thus, the  $C/M$  benchmark comparison for the PCA indicates that the AREVA NP calculations are exceptionally accurate, with no bias and a small standard deviation of [ ] The AREVA NP calculations may be used for any LWR or other configurations of steel and water structures with an expected standard deviation [ ]

#### G.4.2.2 NUREG/CR-6115 BWR Benchmark

Even though the PCA “blind test” was supposed to resolve the problem that the NRC had with inaccurate calculations of fluence rates throughout the industry, only

AREVA NP had results that were accurate enough to have valid calculations of vessel fluence values. Therefore, the other fluence analysts throughout the industry continued to “unfold” “measured” fluence values even though there were no vessel measurements. As part of Regulatory Guide 1.190, “Calculational And Dosimetry Methods For Determining Pressure Vessel Neutron Fluence”,<sup>G3</sup> the NRC ended the concept of “unfolding” “measured” vessel fluence values. The regulatory guide required that vessel fluence predictions be based only on calculated results. Moreover, it was suggested that calculational benchmarks be performed for PWRs and a BWR. The benchmark calculations are described in NUREG/CR-6115 (6115).<sup>G5</sup> The following summarizes the comparison of the AREVA NP calculated results to the Brookhaven National Laboratory (BNL) results.

The key to making a comparison of  $\frac{AREVA\ NP}{BNL - 6115}$  is the criteria developed to determine acceptable versus unacceptable deviations. Since both AREVA NP and BNL analyzed the PCA, the criteria for acceptable deviations were developed from the PCA results. In view of the fact that the AREVA NP calculations were the most accurate and the AREVA NP database includes the PCA results, the AREVA NP uncertainties were extracted from *Appendix A*. The AREVA NP calculations have no statistically significant bias and a standard deviation of [        ]. The BNL results for the PCA were compared to the measurements and those from the AREVA NP calculations. From this comparison, it was estimated that the BNL results in 6115 had no statistically significant bias and the standard deviation is on the order of the mean experimental uncertainty for the dosimetry 10.7%. Statistically combining these standard deviations indicates that the standard deviation of the AREVA NP and 6115

comparison ( $\overline{\sigma_{AREVA NP/6115}}$ ) should be about [            ]. However, considering that most of the modeling deviations associated with the neutron source, geometry, material composition, and modeling methods have been eliminated, the actual mean deviation should be statistically insignificant. Since an insignificant deviation is defined as one-third of the standard deviation, the AREVA NP and 6115 comparison should agree to within [            ].

The following figures depict the comparison of the AREVA NP calculations and the 6115 results. The format of the figures follows that used in NUREG/CR-6115. The deviations are presented as a function of the azimuthal direction for a fixed radius and the axial location of the maximum fluence rate (306.605 centimeters).<sup>G5</sup> The table below summarizes the key deviations from the figures.

*AREVA NP* / *BNL - 6115* Comparison of Key Deviations

<b>Radial Location</b>	<b>Mean Deviation</b>	<b>Standard Deviation</b>	<b>Maximum Deviation (Location)</b>
Downcomer			
Vessel 0T			
Vessel ¼T			
Vessel ½T			
Vessel ¾T			
Vessel T			

NON-PROPRIETARY

---

Figure G-3

—

Figure G-4

Figure G-5

Figure G-6



Figure G-7

Figure G-8

NON-PROPRIETARY

---

]

On page 36 in the table “Comparison of Key Deviations,” the mean value of the first moment of the deviations is the “Mean Deviation” from the figures. In each of the six radial locations, from the downcomer to the outside surface of the vessel, the mean deviation is less than [ ]. Thus, as discussed above, the deviations between the AREVA NP calculations and the 6115 results are insignificant.

While the combined standard deviation of the  $\frac{AREVA\ NP}{6115}$  comparison would be expected to be [ ], the standard deviation in each of the six radial locations is much less, varying from [

] Thus, it would appear that AREVA NP calculations of BWRs are indeed accurate with a small mean random uncertainty.

Reviewing the figures, and the “Comparison of Key Deviations” table [

] Along the radial location of the downcomer, the standard deviation is [

] Likewise, along the vessel inside surface, the standard deviation is [

] While random deviations of [

NON-PROPRIETARY

---

]

[

] Again, to model

the cylindrical jet pump structures located at the various locations, [

] Therefore, the

$\frac{AREVA\ NP}{6115}$  comparison indicates that the AREVA NP calculational methodology is equally accurate for BWRs and other LWRs with similar core neutronic characteristics and steel – water configurations in the internal and vessel structures.

While there is nothing more that can be inferred about the accuracy and random uncertainty of the AREVA NP calculations from the 6115 benchmark comparison, there is an interesting comparison associated with the capsule results. The capsule in the BWR benchmark was located around the three degree azimuthal position. Around this position, there is a local bias as seen in Figures G-3 and G-4, and the table showing the “ $\frac{AREVA\ NP}{6115}$  Comparison of Key Deviations”. Thus, when the AREVA NP dosimeter reaction rate calculations are compared to the 6115 values, there is an overall bias of [            ]. This bias is the mean value from the table below which shows the dosimetry reaction rate comparison.

*AREVA NP* / *BNL - 6115* Dosimetry Reaction Rate Comparison

[

Detector Type	Axial Location (cm)	Radial Location 318 cm	Radial Location 319 cm	Radial Location 320 cm	Radial Location 321 cm
Ti-46	302.8				
Fe-54	302.8				
Ni-58	302.8				
Cu-63	302.8				
Np-237	306.6				
U-238	306.6				

]

If the “*AREVA NP* / *6115* Dosimetry Reaction Rate Comparison” table above were to be used to adjust the vessel inside surface fluence rate values, all vessel fluence values would be biased by [            ]. Whereas, the table providing the “*AREVA NP* / *6115* Comparison of Key Deviations” shows that the vessel fluence values are accurate with an insignificant bias. This substantiates the fact that “unfolding” the vessel fluence based on a limited set of dosimetry measurements can be invalid.

NON-PROPRIETARY

---

### G.4.2.3 Browns Ferry Unit 2 Benchmark

The Tennessee Valley Authority (TVA) provided AREVA NP with a contract to refuel Browns Ferry Units 2 and 3 with blended low enriched uranium (BLEU) fuel. BLEU fuel does not have the same neutronic characteristics as normal low enriched uranium fuel. Consequently, the issue of fluence rate differences between BLEU and normal low enriched uranium fuel needed to be addressed. TVA wanted to ensure that the existing pressure – temperature curves continued to be valid. Thus, AREVA NP performed an analysis of the flux in Browns Ferry Units 2 and 3 with BLEU fuel. The results were a comparison of the BLEU fuel flux compared to the normal low enriched uranium fuel flux.

To ensure a consistent evaluation between the AREVA NP and the GE Nuclear Energy (GENE) fluence rate, a benchmark of the Browns Ferry Unit 2 “30” Capsule was evaluated. In Reference G6, GENE discusses the capsule fluence evaluation. They note that the flux wire measurement for the Browns Ferry Unit 2 Capsule included iron, copper and nickel dosimeters. The capsule was removed at the end of Cycle 7 during the refueling outage, following the October first, 1994 shutdown. Spectrum unfolding techniques were utilized to “measure” the fluence rate with neutron energies above 1.0 MeV. The result in terms of neutrons per square centimeter – second was:

$$\boxed{\text{Measured Flux} = 5.9 \times 10^8} \quad (\text{G.12})$$

NON-PROPRIETARY

---

GENE reports that their calculated flux was  $9.5 \times 10^8$  giving a calculated to measured ratio of:

$$C/M \text{ (GENE)} = \frac{9.5 \times 10^8}{5.9 \times 10^8} = 1.61$$

The AREVA NP calculations of the greater than 1.0 MeV flux, at a 100 % rated power level of 3293 mega-Watts thermal, produced a result of  $6.6 \times 10^8$ . The  $C/M$  ratio is therefore:

$$\begin{aligned} C/M \left( \begin{array}{l} \text{Browns Ferry Unit 2} \\ \text{30 - Degree Capsule} \end{array} \right) \text{AREVA NP} &= \frac{6.6 \times 10^8}{5.9 \times 10^8} \quad (\text{G.13}) \\ &= 1.12 \end{aligned}$$

This benchmark of the Browns Ferry Unit 2 Capsule indicates that the AREVA NP calculations for BWRs are very accurate and within the random uncertainty of the AREVA NP database.

#### G.4.2.4 Analytic Sensitivity

The analytic sensitivity evaluation performed previously for the neutron source and geometry may be extended to the BWR modeling-procedure uncertainties. The BWR extensions for (1) the transport of neutrons from the core through the internal structures associated with the jet pumps, (2) the integrated core leakage function from the fuel, and (3) the three-dimensional synthesis of the core flux function, represent a subset of

NON-PROPRIETARY

---

the previous evaluations. The previous calculations have been updated and extended to treat the BWR modeling and procedures described in Sections G.3.2 through G.3.4. As noted with the previous analytical uncertainty evaluation, the results of the deviations have no well-defined level of confidence. [

]

[

]

$$\sigma_c (Analytic) = [ \quad ]$$

(G.14)

[

] a confidence factor of [ ] provides a 95 % level of confidence in the uncertainty with [ ] degrees of freedom.

[



]

$$\sigma_C (Dosimetry) = [ \quad ]$$

(G.15)

### G.4.3 Summary

Previous bias evaluations associated with the calculations are discussed in Section 7.2.1 (pages 7 – 27 through 7 - 31). It is noted that not only are the measurements unbiased and highly accurate, but the mean value of the calculated neutron fluence values is also unbiased. The benchmark comparisons of the calculations to the dosimetry measurements indicate that there are no statistically significant biases associated with the fluence reactions with energies greater than 0.1 MeV. [

$$B_C (Fluence) = 0.0$$

(G.16)



NON-PROPRIETARY

---

Section 7.3, beginning on page 7 – 36, explains how the standard deviations from the analytic sensitivity evaluation were estimated to be consistent with [ ] the vessel fluence standard deviation. Equation 7.22 forms part of the basis [ ] and Equation 7.23 gives the combined standard deviation for the vessel. The uncertainty in Equation G.15 is sufficient to represent the fluence uncertainty at dosimetry locations. Utilizing Equations 7.22 and 7.23, the vessel fluence uncertainty is that shown by Equation G.18.

$$\sigma_c(\text{BWR Vessel Fluence}) = [ ] \quad (\text{G.18})$$

The vessel fluence uncertainty, represented by the Equation G.18 standard deviation, is consistent with [ ] providing a 95 % level of confidence that vessel fluence - embrittlement predictions will be within the uncertainty of the embrittlement database.

The AREVA NP uncertainties associated with BWR dosimetry measurements and calculations are unbiased (Equation G.16) and have well-defined standard deviations for the appropriate levels of confidence. The AREVA NP results from the laboratory measurements appear to be the only ones for a BWR with NIST reference field validation. The measured standard deviation has been validated to be less than 7.0 %. The extended models and procedures (Sections G.3.2 through G.3.4) have an estimated uncertainty from analytic sensitivity evaluations that is not greater than [ ] for predictions of dosimetry results. The combination [ ]



**Appendix G References**

- G1. Mark A. Rutherford, et al, "DORT, Two Dimensional Discrete Ordinates Transport Code, (BWNT Version of RISC/ORNL Code DORT)," AREVA NP Document # BWNT-TM-107, May, 1995.
- G2. S. Sitaraman, et al, "Licensing Topical Report, General Electric Methodology for Reactor Pressure Vessel Fast Neutron Flux Evaluations," GE Nuclear Energy, Document # NEDO-32983-A, Revision 0, December, 2001.
- G3. Office of Nuclear Regulatory Research, "Calculational And Dosimetry Methods For Determining Pressure Vessel Neutron Fluence," U.S. Nuclear Regulatory Commission, Regulatory Guide 1.190, March, 2001.
- G4. W.N. McElroy "LWR Pressure Vessel Surveillance Dosimetry Improvement Program: PCA Experiments And Blind Test," Hanford Engineering Development Laboratory, NUREG/CR-1861 (HEDL-TME 80-87), July, 1981.
- G5. J.F. Carew, K. Hu, A. Aronson, A. Prince, G. Zamonsky, "PWR and BWR Pressure Vessel Fluence Calculation Benchmark Problems and Solutions," Brookhaven National Laboratory, NUREG/CR-6115 (BNL-NUREG-52395), September, 2001.
- G6. L.J. Tilly, B.D. Frew, B.J. Branlund, "Pressure – Temperature Curves for TVA Browns Ferry Unit 3," GE Nuclear Energy, GE-NE-0000-0013-3193-02a-R1, Revision 1, August, 2003.

NON-PROPRIETARY

---

*Appendix H* AREVA NP Responses to the:

**Request for Additional Information\*<sup>H1, H6</sup> (RAI) on  
*Appendix G* of BAW-2241P, Revision 2**

**Set 1, RAI 1**

On page G-2 it is stated that “The estimated value of the uncertainty for BWR (boiling water reactor) and PWR (pressurized water reactor) results is the same.” The same notion is also stated on page G-3 and elsewhere in the report. The NRC staff notes that Framatome ANP (FANP) {now AREVA NP} recognizes that the uncertainties associated with BWR axial void distributions are not negligible. Please articulate the concept of equal uncertainty for BWR and PWR plants including the void fraction.

Response

The concept of an equal random fluence uncertainty for BWR and PWR plants, when the BWR uncertainty includes additional random variables such as the void fractions, does call into question the validity of the concept. The following discussion reviews (1) the analytic sensitivity, (2) the void – power relationship, and (3) the benchmark uncertainty, and its analytic and measurement components. The response to RAI 6 discusses equal sensitivity evaluations for BWRs and PWRs.

To assess the uncertainty in the calculations an “analytic sensitivity” evaluation is performed. A component of the sensitivity evaluation for BWRs that is not part of the

---

\* This appendix contains its own Reference section. References H1 and H6 are the NRC RAIs.

NON-PROPRIETARY

---

sensitivity evaluation for PWRs is the boiling – void fraction effect on moderator density. When void fraction uncertainties are included in the BWR analytic sensitivity evaluation, the random uncertainty in the fluence rate (time-averaged flux) increases above that for PWRs. [

]

A component of the void fraction uncertainties includes power uncertainties. In the saturated boiling regime there is a direct “void fraction – power” relationship. Equation H.1 gives the thermodynamic relationship between the nodal power, and the product of the mass flow and the enthalpy change from the inlet to the outlet of the nodal channel.

$$Power \ (Btu/hr) = \left[ Enthalpy_{Outlet} - Enthalpy_{Inlet} \right] \left( \frac{Btu}{lb_m} \right) Mass \ Flow \ \left( \frac{lb_m}{hr} \right) \quad (H.1)$$

The relationship between the inlet, outlet, and nodal enthalpy is based on a linear model. Thus, the enthalpy of a node is just the average of the inlet and outlet enthalpies. Given that the fluid conditions of interest are saturated, the void fraction ( $\alpha$ ) is defined by the nodal enthalpy and the saturated liquid and vapor conditions. This is shown by Equation H.2.

$$\alpha = \frac{Enthalpy(node) - Enthalpy(liquid)}{Enthalpy(vapor) - Enthalpy(liquid)} \quad (H.2)$$

The definition of the void fraction is also expressed by Equation H.3.

$$\alpha = \frac{Volume_{Vapor}}{Volume_{(Vapor + Liquid)}} \quad (H.3)$$

NON-PROPRIETARY

---

The volume of vapor and liquid in Equation H.3 would be the same as the nodal moderator volume. Using the value of the void fraction from Equation H.2 and the definition in Equation H.3, the nodal moderator density of vapor and liquid is defined by Equation H.4.

$$\text{Density (node)} = \{ \alpha \} \text{Density (vapor)} + \{ 1 - \alpha \} \text{Density (liquid)} \quad (\text{H.4})$$

Equations H.1 through H.4 express the void – power relationship. While the functional relationship between void fraction and power shows a direct proportionality, it is not clear how much the void fraction uncertainty is functionally dependent on the power uncertainty. To quantitatively examine the uncertainty relationship, benchmark comparisons of power distributions would be useful. The benchmark comparisons would need to be in two unique sets. The first set would include the power – void relationship, such as BWR benchmarks, the second set would have no void relationship, such as PWR benchmarks.

[

]

These results suggest that a standard deviation of [ ] for the void fraction uncertainty would be consistent with the benchmark databases. Thus, in the analytical sensitivity evaluation of the fluence uncertainty for the BWR calculations, a standard deviation of



NON-PROPRIETARY

---

[ ] would be appropriate as a unique random variable. [

]

*Appendix G* shows the estimate of the “*BWR Dosimetry Benchmark*” uncertainty to be [ ]. Thus, the void fraction uncertainty is not the only one included in the additional BWR uncertainties.

Another reason that the estimated value of the BWR uncertainty is greater than the PWR value of [ ] is related to the confidence that is associated with the standard deviation. [

] To have a generically applicable uncertainty, such as for Westinghouse reactor designs, the confidence factor needed to be increased. In *Appendix E*, Revision 1 of this topical, the confidence factor was changed to reflect the [ ] degrees of freedom that would be generic to PWRs. Now by extending Revision 2 of this topical to BWR designs, the same concern exists. The benchmark database consists of three PWR types, one PCA, one NRC reference model, and the BWRs.

With the addition of BWRs to the database,[

] To appropriately treat the addition of the BWRs in the database the uncertainty is increased.

NON-PROPRIETARY

---

The statement that: “The estimated value of the uncertainty for BWR and PWR results is the same.” is indeed invalid. The uncertainty methodology for BWRs and PWRs is the same. Furthermore, [

] AREVA NP will revise *Appendix G* to replace the invalid statements.

**Set 1, RAI 2**

Figure G-2 represents a schematic of the 3-D synthesis for BWR fuel assemblies.

[

]

Response

[

]

[

](G.10)

[

]

NON-PROPRIETARY

---

[

]

The optimum number of cells would be based on the criteria outlined in Regulatory Guide 1.190.<sup>H4</sup> The criteria suggest that reducing the number of nodal cells would be acceptable as long as the accuracy in the solution is consistent with the uncertainty analyses.

[

]

[

] (G.7)

[

]

$$Leakage(\mathbf{r}', \bar{E}, \bar{\Omega}) = \int_A \int_E \int_{\Omega} \mathbf{\Omega} \cdot \left( \frac{\mathbf{r}'_{\perp A}}{|\mathbf{r}'|} \right) \phi(\mathbf{r}', E, \mathbf{\Omega}) dA dE d\Omega$$

(G.6)

[

]

[

NON-PROPRIETARY

---

[ ] (H.5)

[ ] (H.6)

[ ]

**Set 1, RAI 3**

In Section G.4.2 (page G-30) you stated that “The benchmark of the dosimetry database provides the means of evaluating biases in the calculation methodology

[ ]”

- a) Please describe [ ].
- b) While the NRC staff noted FANP's comments regarding the National Institute of Standards and Technology/FANP relationship, the absence of a bias should be concluded from the results rather than be declared a priori.

NON-PROPRIETARY

---

Response (b)

The response to this RAI addresses part (b) first, concerning the a priori dismissal of a bias. In Section G.4.1, FANP (now AREVA NP) discusses the “Measurement Uncertainties.” Any bias in the measurements is identified by the National Institute of Standards and Technology (NIST). As explained in AREVA NP’s “Standard and Reference Field Validation” document,<sup>E3</sup> NIST certified that AREVA NP has no statistically significant biases in the measurements.

In Section G.4.2, AREVA NP discusses the “Calculational Uncertainties.” Every bias in the calculations is identified by benchmark comparisons to the unbiased measurements. When making the statement that: “The benchmark of the dosimetry database provides the means of evaluating biases in the calculation methodology [

],”

it was not intended to mean that unbiased calculational results were declared a priori.

As discussed in Revision 1 of this topical, [

] the calculations produce exceptionally accurate, unbiased results.

The AREVA NP discussion in the initial paragraph of Section G.4.2 would be worded better if it stated that: “The DORT results from Equation G.4 are compared to the AREVA NP dosimetry database to (1) evaluate biases statistically,” [

NON-PROPRIETARY

---

]

Response (a)

Once the functional cause of biases in the calculations have been identified by benchmark comparisons to unbiased data, the uncertainty in the calculations, with the biases removed, needs to be quantified. AREVA NP uses the methods of mathematical statistics to quantify the unbiased uncertainty in the calculations. Mathematical statistics is based on the concept that there are only two types of deviations associated with any set of parameters: systematic and random.

In a calculational process, systematic deviations are related to inaccurate functional causes. They would be identified as either constant errors or biases. There are no errors in AREVA NP calculations that have been independently reviewed; [

] Using mathematical statistics, the random uncertainty is quantified in terms of a “normal” distribution of deviations, a level of confidence, the degrees of freedom, and the positive square root of the variance.

In Regulatory Guide 1.190 the NRC defines the random variables that produce the uncertainty in the fluence rate results. The distribution of deviations, level of confidence, degrees of freedom, and the positive square root of the variance are identified for each component of the random variables. Consequently, an analytic sensitivity evaluation

NON-PROPRIETARY

---

may be performed to estimate the uncertainty in the fluence rate throughout the internal structures, vessel, and vessel – biological shield structures.

The difficulty with the results from the analytic uncertainty is that [

] all components of the random variables are acting independently and simultaneously in a Monte Carlo simulation of the uncertainty propagation. However, as discussed in RAI 1, Set 1, the void uncertainty is partially dependent on the power uncertainty.

[

] There is neither a level of confidence that can be defined for the standard deviation in the calculations, nor is there a set of correlation coefficients that can be defined between each uncertainty component.

The general formulation for the propagation of random uncertainties is expressed by Equation D.5. [

]

[

] (D.5)

NON-PROPRIETARY

---

When this expression is simplified [

] the benchmark uncertainty representing  
the combination of calculated and measured uncertainties is expressed as

$$\sigma_{C/M}^2 = \sigma_C^2 + \sigma_M^2 \quad (\text{H.7})$$

[

] the square root of the mean variance ( $\sigma_{C,M}$ ) between the  
calculations and measurements is actually an integral combination of two random  
variables ( $C$  and  $M$ ) with unique deviations ( $\Delta$ ) for each respective one as expressed by  
Equation H.8.

$$\sigma_{C,M} = \int_{\Delta_C = -\infty}^{+\infty} \int_{\Delta_M = -\infty}^{+\infty} \frac{\Delta_C \Delta_M}{2 \pi \sigma_C \sigma_M \sqrt{1 - \rho^2}} \quad (\text{H.8})$$

$$\exp \left( -\frac{1}{2(1 - \rho^2)} \left[ \frac{\Delta_C^2}{\sigma_C^2} - 2\rho \frac{\Delta_C \Delta_M}{\sigma_C \sigma_M} + \frac{\Delta_M^2}{\sigma_M^2} \right] \right) d\Delta_C d\Delta_M$$

When Equation H.7 is formulated to represent the benchmark uncertainty, the  
approximations [ ] are typically not  
considered. Equation H.7 simply looks like an algebraic expression that can be  
rearranged to solve for the calculational uncertainty in terms of the standard deviation,  
 $\sigma_C$ .



NON-PROPRIETARY

---

$$\sigma_C = \sqrt{\sigma_{C/M}^2 - \sigma_M^2} \quad (\text{H.9})$$

However, Equation H.9 is not theoretically valid and it leads to meaningless results. Consequently, the only valid means of estimating the calculational uncertainty,  $\sigma_C$ , is by [ ]

If Equation H.9 were to be used with the AREVA NP measurement and benchmark database to attempt to estimate the calculational uncertainty,  $\sigma_C$ , the significance of the meaningless results would be obvious as demonstrated by the following discussion.

NIST has reviewed the AREVA NP measurements to quantify the uncertainties. The measurement database is completely accurate, containing no biases, and has a precision that can be represented by a standard deviation of 7.0% with a normal distribution ( $\sigma_M = 7.0\%$ ). Except for NIST, no dosimetry measurements have a higher degree of accuracy and precision.

The AREVA NP benchmark database has also been shown to be highly accurate and there is a high level of confidence in the statistical properties including the standard deviation of 8.64% for a normal distribution ( $\overline{\sigma_{C/M}} = 8.64\%$ ). If Equation H.9 were to be used to compute the standard deviation in the calculations, the results would be 5.06%. Thus, even though the calculations have been benchmarked to the measurements to estimate the uncertainties in the calculations, the calculations would now miraculously be more precise than the measurements.

NON-PROPRIETARY

---

The above result is of course meaningless. To quantify the uncertainty in the calculations, with the biases removed, the AREVA NP fluence uncertainty methodology employs [ ] a consistent set of analytic – calculational, benchmark, and measurement uncertainties.

**Set 1, RAI 4**

In the application of the PCA benchmark, eyeballing the results listed in the Table on page G-32 for the C/M comparisons there seems to be a bias. Any comments?

Response

AREVA NP would agree that the table of  $C/M$  comparisons for the PCA benchmarks does indicate a bias. However, it does not indicate a bias in the AREVA NP calculations.

If the  $C/M$  comparisons in the table on page G – 33 were unique to AREVA NP, then a PCA benchmark bias would be of concern. However, the AREVA NP comparisons are not unique. Nine of the ten participants in the reaction rate “blind test” from 1981 had biases like those in the table on page G – 33. As explained by McElroy, NIST (McGarry) and CEN/SCK (Fabry) in Reference G4, there were inaccuracies in the dosimetry measurements. The PCA operation involved four independent periods at various power levels. Thus, not only did the dosimetry decay need to be adjusted, but the absolute power of the PCA needed to be accurate. Unfortunately, the PCA power was based on two measurements that were not within the instrumentation uncertainty of one another.

AREVA NP Inc.  
An AREVA and Siemens Company

NON-PROPRIETARY

---

While the power uncertainty was defined by a  $\pm 4\%$  standard deviation, it is not certain that during any one period of operation, or for each specific power level, that the power was not biased by 4%. There are not enough independent periods of operation with sufficient measurements to confirm that the measurements represented a normal distribution of uncertainties.

Based on the calculational results from the nine participants, the measurements are probably biased. However, given a small bias in the measurements, the AREVA NP results show no bias in the steel – water regions. Consequently, the PCA benchmark indicates that the BWR modeling of the internal structures, vessel, and vessel – biological shield structures should be unbiased and within the random uncertainty of the AREVA NP benchmark database.

**Set 1, RAI 5**

Regarding the FANP/BNL-6115 comparisons on Figures G-3 to G-8, shouldn't the biases mentioned for Figures G-3 and G-4, be in Figures G-5 through G-8?

Response

The biases that are discussed on pages G - 43 and G - 44 for Figures G-3 and G-4 should also be in Figures G-5 through G-8. The cause of the biases has been identified to be the differences in the mesh increments used by BNL and FANP (now AREVA NP), and the perturbations caused by the jet pumps and core periphery. Thus, the maximum biases at 3.6° and 6.7° in Figures G-3 and G-4 will also appear in Figures G-5 through G-8. However, the maximum biases at 3.6° and 6.7° in Figures G-3 and G-4 are not the maximum ones in Figures G-5 through G-8. In Figures G-5 through G-8, the maximum biases are at 38.5° and 45.0°. Except for 45.0°, the biases in Figures G-5 through G-8

NON-PROPRIETARY

---

also occur in Figures G-3 and G-4. The bias at 45.0° in Figure G-3 does not occur because the figure shows the downcomer region in front of the jet pumps. It is the combination of the finer jet pump mesh and the perturbation in the flux caused by the jet pump material that results in the bias. Thus, expect for 45.0° in Figure G-3, each bias noted in Figures G-3 through G-8 also occurs in all the figures.

### **Set 1, RAI 6**

This is an extension of comments 1, 2 and 3. In Section G.4.2.4 “Analytic Sensitivity,” FANP seems to suggest that the analytic uncertainty from Appendix E should be extended to the BWRs. Given that the axial void fraction is a major uncertainly contributor, please comment on the proposed extension.

### Response

In the response to RAI 1 Set 1, FANP (now AREVA NP) noted that the *Appendix G* statement that: “The estimated value of the uncertainty for BWR and PWR results is the same.” is not valid. The uncertainty methodology for BWRs and PWRs is the same, but the specific values are not. When the simultaneous combination of all random variables affecting the fluence rate is considered, a unique [ ] void fraction uncertainty should increase the PWR benchmark uncertainty from a value of [ ] to a BWR value of [ ]. *Appendix G* shows the estimate of the “*BWR Dosimetry Benchmark*” uncertainty to be [ ]. Thus, there are additional uncertainties which affect the overall BWR uncertainty.

In RAI 2, Set 1, the NRC wanted AREVA NP to further explain the collapsing of the core nodal solution, which incorporates multiple axial (*z*) nodal cells, to a model with

NON-PROPRIETARY

---

fewer ( $z$ ) nodal cells. The key issue with respect to this RAI is the optimum number of collapsed cells without affecting the uncertainty. AREVA NP explained that the optimum collapsing is based on the criteria outlined in Regulatory Guide 1.190.<sup>H4</sup> Nodal cells could be combined until the accuracy in the solution becomes inconsistent with the uncertainty analyses. [

]

In the response to RAI 3, Set 1, AREVA NP explained that the benchmark of the dosimetry database provides [

] The difficulty with the sensitivity evaluation is that there is neither a level of confidence that can be defined for the standard deviation in the calculations, nor is there a set of correlation coefficients that can be defined between each uncertainty component.

[

]

When discussing the “Analytic Sensitivity” in Section G.4.2.4, AREVA NP states that the BWR benchmarks are consistent with (1) the dosimetry database, and (2) the benchmark database referenced in *Appendix E*. Moreover, based on the consistency between the analytic uncertainty and the benchmark database, a 95 % level of confidence

NON-PROPRIETARY

---

in the calculational uncertainty is established with [ ] degrees of freedom. As the NRC notes, the analytic uncertainty from *Appendix E* is extended to BWRs.

The analytical uncertainty associated with BWR calculations is dependent on [

] Statistical evaluations of the fluence uncertainties must ensure consistency with the level of confidence and degrees of freedom in the embrittlement database which has a confidence factor of  $\pm 2.000$  for the embrittlement “Margin” term.<sup>H5</sup>

As the NRC staff noted in their discussion of the additional information presented in *Appendix E*, it is important to explain that the differences between the plant types do not create differences between the physical parameters and characteristics affecting the uncertainties. If there are no differences affecting the uncertainties, then the uncertainties are representative of the same population. As AREVA NP notes in the beginning paragraph (page G - 47) of the “Analytic Sensitivity” evaluation, the *Appendix E* uncertainty values are the same for PWRs and BWRs [

]

As the NRC staff suggested in their discussion of the additional information presented in *Appendix E*, [

NON-PROPRIETARY

---

]

For example, the benchmark standard deviation in *Appendix E* is [ ] while that in *Appendix G* is [

] there are additional uncertainties affecting the BWR data in *Appendix G* that are not associated with the PWR data in *Appendix E*. These additional uncertainties represent a combined uncertainty of [ ]. Thus, there is an increased uncertainty in the analytic – calculational standard deviation that is associated with BWR benchmark comparisons.

For the analytic – calculational standard deviation that is associated with the BWR vessel, the combined value represents an even higher increase. The *Appendix E* vessel standard deviation is [ ] while that in *Appendix G* is [

] increase in the analytic – calculational uncertainty associated with BWR vessels.

Thus, the extension of *Appendix E* uncertainties and statistical properties to *Appendix G* does result in an increase in the uncertainties associated with BWR s.

### **Set 2, RAI 1**

In view of the increased void fraction (relative to PWRs) in the regions above the core and in the upper core and downcomer, justify the use of the [

NON-PROPRIETARY

---

] in BWR applications. Are the BWR models more likely to have negative fluxes (as experienced in Model C of the Davis Besse PWR evaluation) and, if so, how will this be treated? How are the void fractions in these upper regions determined and what fluence uncertainty is introduced by this determination?

Response

RAI 1, Set 2 has four parts: [ ] negative fluxes, void fractions, and the upper region uncertainty. While the additional information that is provided is somewhat related, each part also involves information that is separate and unique from the other parts. Consequently, each part is addressed separately in a paragraph specifically concerning that part.

[



NON-PROPRIETARY

---

]

The negative fluxes encountered in the  $r, z$  Model C DORT calculation of the Davis Besse benchmark evaluation occurred in the upper nozzle and seal plate regions, above the top of the beltline, in the air cavity between the vessel and the concrete. These flux values were determined to be the result of computer-memory-related inabilities to specify a large enough angular quadrature and/or small enough spatial mesh intervals. If the mesh and quadrature intervals are too large in either the PWR or BWR models, then negative fluxes and other indications of inaccurate results would be expected. However, the computer technology continues to advance with greater and greater capabilities in processing calculations like those found in DORT models. Today, neither PWR nor BWR models would be expected to have negative fluxes. Calculations of the nozzle and seal plate regions following the Davis Besse benchmark evaluation have not had negative flux values and none would be expected in the future.

The void fractions in the upper regions, beyond the top of the fuel, are determined from the volumetric weighting of the void fractions exiting each fuel assembly. The model for the void fraction is a three-dimensional core-follow calculation. The key to the core-follow calculation is that it is a time-dependent benchmark of the actual operation of the core throughout each cycle. The inputs to the core-follow calculations are the measured core parameters, such as the control rod positions, system flow, etc. The outputs from the core-follow calculations are power distributions that may be directly compared to measurements. The accuracy of the void fractions and power distributions is represented by a standard deviation of [ ] in the power.<sup>H3</sup> The void fraction – power uncertainty is discussed in the additional information provided in the response to RAI 1, Set 1.

NON-PROPRIETARY

---

The upper shroud, dome-head region contains the homogenized void fraction from the assembly weighted void fractions. In this region [

] Calculations of this region have shown no negative flux values.

The fluence uncertainty from the top of the active fuel to the shroud dome-head varies from a value of [ ]. The [ ] value is representative of the core-follow benchmark comparison, while the [ ] value is representative of dosimetry benchmark comparisons combined with analytic uncertainties. The development of the components of the [ ] value is presented in *Appendix G* on pages G - 50 and G - 51. The development is further discussed on page H - 18 in the additional information provided for RAI 6, Set 1. [

] the fluence uncertainty in the region above the top of the active fuel is defined as being representative of [ ].

### **Set 2, RAI 2**

How will core/vessel/dosimetry configurations that do not have sufficient symmetry to allow a 45-degree sector representation be treated?

Response

The AREVA NP modeling of the core, vessel and dosimetry is explicit. As discussed in *Appendix G*, Section G.3.2, "Neutron Transport Through Jet Pumps", if there is some

NON-PROPRIETARY

---

complexity resulting from the geometrical shape of an object and the model coordinates, then [

] Consequently, if the core/vessel/dosimetry configurations do not have sufficient symmetry to allow a 45-degree sector representation, then the model will be expanded to a 90-degree treatment or whatever angular mesh representation would be appropriate.

### **Set 2, RAI 3**

Describe the differences between the BWR and PWR in-vessel and cavity dosimetry (dosimetry wires/foils, holder tubes, encapsulation, etc.) and how these differences will be accounted for in the BWR models. For example, how will the dosimetry perturbation and correction factors of Appendix B be determined in the case of BWRs? Is additional uncertainty introduced by these differences?

#### Response

There are various differences between the BWR and PWR in-vessel and cavity dosimetry, *i.e.*, dosimetry wires/foils, holder tubes, encapsulation, etc. Moreover, there are various differences between the various PWRs with respect to the in-vessel and cavity dosimetry. However, as discussed in the response to RAI 2, Set 2 above, AREVA NP does not use modeling approximations to treat the dosimetry wires/foils, holder tubes, encapsulation, etc. AREVA NP uses explicit modeling. Therefore, every different characteristic of the BWR in-vessel and cavity dosimetry is accounted for in AREVA NP's modeling.

The *Appendix C* dosimetry perturbation factors are a good example of the explicit modeling that AREVA NP uses in its fluence analysis. The Davis Besse benchmark

NON-PROPRIETARY

---

evaluation included dosimetry measurements of the reactor support beams, the inlet and outlet nozzles, and the seal plate. (Pages 3 - 16 and 4 - 16 through 4 - 18 illustrate the locations of the beams and nozzles, and the dosimetry.) The modeling of the beltline dosimetry only required single channel synthesis. However, the modeling of the beams and nozzles required multi-channel [

] As explained in Section 3.2, “DORT Perturbation Calculations”, the beams and other cavity structures were explicitly modeled as were the dosimetry wires/foils, holder tubes, encapsulation, etc. The *Appendix C* dosimetry perturbation factors represented the ratio of the DORT results from the multi-channel synthesis model above the beltline to the DORT results from the single channel synthesis model below the beltline.

The *Appendix B* correction factors treat effects such as photofissions, impurities, dosimetry self absorption, etc. The treatment of these effects will be independent of whether the dosimetry is associated with PWRs or BWRs.

In general, the reason for using multi-channel [ ] synthesis rather than a single channel model is due to the non-separable complexities that are part of the fluence evaluation. In BWR models these complexities include channel voiding and control rods that result in a non-separable flux function. In the PWR model for Davis Besse these complexities included nozzles and support beams. As discussed in *Appendix G*, Section G.4.2, “Calculational Uncertainties”, and specifically the “Analytical Sensitivity” in Section G.4.2.4, there are uncertainties introduced by differences in the BWR design that are not part of PWR designs. Moreover, as noted in the additional information provided in the response to RAIs 1 and 6, Set 1, the benchmark to PWR dosimetry is represented by a standard deviation of [ ] while the benchmark to BWR dosimetry

NON-PROPRIETARY

---

is represented by [      ]. Clearly differences between the BWR and PWR designs and operation result in additional uncertainties in the calculations of in-vessel and cavity dosimetry.

**Set 2, RAI 4**

Provide justification for any differences between the proposed dosimetry response methods and those described in the corresponding ASTM standards.

Response

The dosimeter measurements conform to the applicable ASTM standards. The discussion of the “Measurement Methodology” in Section 5.0, and the discussions of the “Measurement Techniques” for (1) fissionable and activation radiometric dosimeters in Sections 5.1.1 and 5.1.2 respectively, and (2) helium accumulation fluence monitors in Section 5.3.1, describe how the techniques and procedures comply with the ASTM standards. The ASTM standards include additional standards for “Spectrum Adjustment Methods”, “Application for Reactor Vessel Surveillance”, etc. These additional standards refer to techniques that differ from those explained in (a) the “Semi-Analytical (Calculational) Methodology”, in Section 3.0, (b) the “Extension of Fluence Methods” for BWRs in Section G.3, (c) the “Uncertainty Methodology”, in Section 7.0, and (d) the “Uncertainty Update” for BWRs in Section G.4. These additional ASTM standards refer to pseudo-measured fluence values, and to precision, bias, and uncertainty in terms that are conflicting. ASTM standards that deviate from experimental practice as noted above are not used.

NON-PROPRIETARY

---

**Set 2, RAI 5**

Because of the strong exponential fluence attenuation, the calculation of the fluence is sensitive to both the distance separating the core and the vessel and the barrel thickness. What quality assurance procedures will be used to insure that these dimensions are accurate and within the uncertainty assumed in the Section G.4.2 fluence calculation uncertainty analysis?

Response

It was found that the ASME standards prescribed the acceptable tolerances when determining what was appropriate for the reactor pressure vessels and vessel internal structures, such as the shroud (barrel). Subsequently, it was found that manufacturing organizations met the prescribed ASME standards and that the tolerances were either noted on the respective drawings for the shroud, vessel, etc, or the drawings noted conformance with the ASME standards. When AREVA NP develops a fluence model for a particular reactor, the drawings are reviewed and a quality assurance check performed. Not only are the nominal, best-estimate cylindrical dimensions obtained for each component's inside and outside diameter, but the tolerances are also obtained. These tolerances include inner and outer diameters as well as eccentricity, concentricity, ellipticity and parallelism. Thus, the complete three-dimensional tolerance characteristics of the diameters are known for each shroud and vessel. This ensures that the sensitivity of the fluence calculations to the strong exponential fluence attenuation in the distance between the core and shroud (barrel), and shroud and vessel is appropriately treated with the fluence uncertainty.

NON-PROPRIETARY

---

**Set 2, RAI 6**

The PWR analysis included in Equation 7.25 provides an additional uncertainty for the temporal extrapolation to End-of-Life (EOL). Provide the corresponding EOL extrapolation uncertainty for the Appendix G BWR analysis.

Response

In 1961, when the ASTM established a standard for reactor vessel surveillance, ASTM E 185-61, “Standard Practice for Conducting Surveillance Tests for Light-Water Cooled Nuclear Power Reactor Vessels”, AREVA NP (formerly Babcock & Wilcox) developed an integrated program to monitor vessel material test specimens (Reference 14, Section 8). Each of the 11 reactors would monitor the vessel only twice during the operational lifetime of 40 years. Vessel material characteristics at EOL would be determined through the combined characteristics of all test specimens.

When the NRC implemented 10 CFR 50, Appendix H, “Reactor Vessel Material Surveillance Program Requirements” in 1973, the monitoring of vessel materials continued to reflect combinations of multiple cycles with predictions of EOL vessel characteristics. However, there was the requirement to define an EOL fluence value and a comparable uncertainty (Reference 12, Section 8). It was evident that test specimen uncertainties and extrapolated vessel fluence uncertainties would not be the same.

The problem with defining an EOL fluence value was that there were no restrictions on reactor operation and core fuel management with respect to fluence – embrittlement damage to the vessel. Therefore, a hypothetical equilibrium cycle was defined to have the identical neutronic characteristics as the last group of monitored cycles. The

NON-PROPRIETARY

---

uncertainty in the fluence extrapolated to EOL would then be the uncertainty in the last group of monitored cycles combined with the power uncertainties in the equilibrium cycle. Equation 7.25 includes the estimation of the power uncertainties in the equilibrium cycle combined with the standard vessel fluence uncertainty from DORT monitoring calculations based on core-follow measurements.

AREVA NP supported 5 of the first 7 reactors that were granted a renewed license for 60 years of operation. Part of the 60 year licensing requirements was to update the EOL vessel fluence and to estimate the uncertainty in this extrapolated fluence. Based on more than 20 years of operation, in more than 50 reactors, it is obvious that the equilibrium cycle represents a hypothetical concept with no quantitative validity. However, to address license renewal RAIs, the propagation of uncertainties from “perturbed” equilibrium cycles was estimated. This uncertainty propagation provided the vessel fluence uncertainty in “un-monitored” cycles that were slightly perturbed from the monitored reference cycle. See Table D – 2, “Vessel Fluence Uncertainty Propagation” on page D - 20 of Reference H7.

AREVA NP no longer supports the estimated uncertainty in un-monitored cycles. Consequently, the results from Equation 7.25 are not significant with respect to fluence uncertainties. AREVA NP has developed a cycle-by-cycle monitoring program that bounds the estimate of the vessel fluence and has a precisely defined uncertainty. Nonetheless, to address this RAI, the EOL uncertainty has been calculated using Equations G.18 and 7.25. The standard deviation is 18.99%.



NON-PROPRIETARY

---

**Set 2, RAI 7**

Operation with MELLLA+ can affect the conditions in the downcomer. How will these changes be accounted for in the fluence evaluation?

Response

The downcomer water properties are explicitly modeled in the core-follow simulation of each BWR's operating cycle. The downcomer water properties are the initial conditions for the water entering each fuel assembly. If the water properties are not accurate, the void – power relationship in each nodal volume will be inaccurate. Any such inaccuracies would be obvious in the core-follow benchmark comparison of calculated powers to measured values.

To replicate the core-follow benchmark to measurements and maintain the same degree of accuracy in the void – power relationship, the downcomer water properties as well as the nodal water properties are exactly duplicated in the DORT model for the fluence calculations. To exactly duplicate the core-follow downcomer water properties in the DORT model requires the integration of the core-follow time-steps. Thus, with each change in the conditions in the downcomer due to operation with MELLLA+, the water properties are explicitly represented. The time-step to time-step changes in the core-follow model are directly integrated over the time period to obtain time-averaged water properties for the DORT fluence model.

As the NRC noted in RAI 5, Set 2, there is a strong exponential attenuation in the fluence rate that is sensitive to the downcomer geometry between the shroud (barrel) and vessel. This strong exponential attenuation is also sensitive to the downcomer water properties.

NON-PROPRIETARY

---

[

] This concept is further explained in the additional information provided in the response to RAI 9, Set 2.

### **Set 2, RAI 8**

Recognizing that  $v/\kappa$  (ratio of neutron production rate to power) depends on fuel isotopics and burnup, how will this dependence be included in the BWR core neutron source? Describe how the effect of increased Pu in the high burnup fuel is included. Does this treatment allow for the cycle-specific variations? In view of the large variation in fuel burnup between fuel bundles and the dependence of the number of neutrons produced per fission ( $\nu$ ) on fuel burnup, what uncertainty is introduced by neglecting this dependence in Equation (4.1)?

### Response

In the explicit three-dimensional core-follow model of reactor operation each assembly is represented, generally with one-quarter core symmetry. Moreover, each assembly is divided into nodal sections along the axial length of the fuel. The axial length of each node is 6 inches or less. Thus, for a fuel stack height of 150 inches, there would be 25 nodes representing each assembly. The core-follow model explicitly treats the neutron production rate and power production within each nodal volume. Consequently, the burnup of the fuel is explicitly modeled as are the resulting isotopic transmutations.

[ ] the ratio of the neutron production rate to power production is explicitly modeled. This includes

NON-PROPRIETARY

---

the nodal burnup and the related isotopic effects on the neutron and power production. As noted above in the response to RAI 7, Set 2, the explicit modeling of the ratio of the neutron production rate to power production in the core-follow model involves discrete time-steps. To replicate the explicit core-follow modeling in the DORT calculation, the neutron and power production rates are integrated over the core-follow time-steps. A time-averaged ratio of the neutron production rate to power production is thereby modeled in the DORT calculation.

The effect of the increased Pu on the neutron source calculation is a time-dependent effect that increases with higher and higher fuel burnups. The time dependence of the macroscopic cross sections (isotopics) and the neutron source eigenfunction (neutron emission rates by isotope) are treated with the integral of the macroscopic cross sections and source function over the time periods of interest.

The time dependence of the DORT isotopics, including the plutonium, is based on a quasi-static, core-follow calculation of the plant operation. The quasi-static calculational results, such as the Pu fission rates, are determined for each time-step. The results within each time step are considered static (independent of time), but the results, such as the Pu concentrations, vary from time step to time step. The Pu fission - neutron emission rates are determined within the three-dimensional nodal volume for each time step.

The integral over time is not specifically identified in Equation 3.2, but the process of determining the plutonium isotopic sources from the fission – emission rate includes time-average weighting of the ratio of neutron emission rates to power production. Thus, the Pu isotopes as a function of burnup (time at power) are directly included in the calculations of the neutron source for each node. Since the Pu isotopics and reaction rates are determined as a quasi-static function of time, using discrete time steps which

NON-PROPRIETARY

---

explicitly follow the core operation from cycle-to-cycle, the multi-cycle variations of Pu effects on the source are explicitly included in the calculations.

The variation in fuel burnup between nodes and thereby between assemblies is modeled explicitly. This modeling includes, core-follow calculations which match the measured operational data, quasi-static time steps to appropriately treat time dependent behavior, explicit representation of the isotopics within the each node, and three-dimensional representation of the fuel pin nodal segments. Thus, the dependence on the changing isotopics as a function of burnup, and the corresponding changes in the number of neutrons produced per fission in the fuel volume are not neglected. The burnup dependence of the neutrons produced per fission within a node is included in the neutron source calculation. However, Equations 4.1 and 4.2 (now Equations 3.1 and 3.2) on pages 3 - 11 and 3 - 12 respectively, have consolidated the expressions for the ratio of neutron production rates to fission power such that it is not clear how the neutron source in each node of the assembly is represented.

The ratio of neutron production rates to fission power is a weight applied to the nodal emission spectra. It is also combined with the normalized spatial power density and renormalized to represent a relative spatial source density. Finally, the absolute (not-normalized) source density for the core is determined from the integral of the spatial source density over the volume of the fuel.

While the burnup dependence of the number of neutrons produced per fission is “not neglected” in the calculations of the neutron source, there are combinations of source term components, expressed by Equation 4.1 (now Equation 3.1), that represent approximations. If the effect of neutron production per fission in the fuel is treated as an

NON-PROPRIETARY

---

isolated component of the uncertainty, it would be directly related to the uncertainties in fuel isotopics.

The uncertainty in the neutron production per fission can be bounded by the isotopes producing the most neutrons per fission and the least neutrons per fission. This uncertainty was modeled in the analytic sensitivity evaluation and represents a relative deviation of nearly 20% with a 99% degree of confidence.

The uncertainty in neutron production due to the uncertainty in the nodal burnup of the fuel can be modeled with the uncertainty in the power distribution. The uncertainty in the power distribution is represented by a normal distribution when it is defined on the basis of an absolute deviation in the relative power distribution. Using an upper bounding deviation with a 95% confidence level in the analytic sensitivity indicates that the local uncertainty would be about 18% with a relative peripheral power of 0.50, and about 30% with a relative peripheral power of 0.30.

**Set 2, RAI 9**

The method of Section G.3 [ ] assumes a simple correlation, based on core-follow calculations, [ ]

provide planar comparisons of [ ]]. The comparisons should be made for typical planes in the upper region of the core where there is substantial voiding. Comparisons should be provided for a range of BWR conditions including (a) power distribution and (b) cycle fuel burnup. In addition

NON-PROPRIETARY

---

to the bundle-wise comparisons, provide the percent mean and standard deviation [ ] for bundles in the outer three rows of the core.

Since the treatment of boundary conditions and core leakage has a substantial dependence on (a) the core boundary geometry (e.g., number of bundles with two faces to the reflector) and (b) the specific core-follow code used to determine the correlation, comparisons should also be provided for various core boundary shapes and the core-follow codes which will be used to determine the correlation

#### Response

RAIs 9, 10, 11 and 13 in Set 2 are all related. Moreover, as discussed in a telephone conference call with the NRC, [ ]. Consequently, there is a misunderstanding of the information presented in the topical. The NRC has subsequently requested additional information based on the misunderstanding. AREVA NP however cannot provide the additional information requested in RAIs 9, 10, 11 and 13 from Set 2 because analyses were not performed as the NRC assumed. Therefore, the NRC agreed that it would be appropriate to send the additional information that clarified the misunderstanding without providing the specific data that was requested.

The explanation that follows therefore provides additional details concerning the explanation of the leakage function. It also explains how the [ ] The explanations in response to this RAI (9, Set 2) are also part of the response to RAIs 10, 11 and 13 in Set 2. Thus, the response to RAIs 10, 11 and 13 will entail much less information and will use this RAI's explanations as a reference.

NON-PROPRIETARY

---

[ ]

[ ] (G.7)

[ ] Therefore, the NRC wanted data that would confirm that the Equation G.7 relationship was valid.

[ ]

[ ] the water density in each nodal and downcomer region, at each time-step, is determined from core-follow calculations as suggested by the NRC and as explained in the response to RAI 7, Set 2: The water properties are explicitly modeled in the core-follow simulation of each BWR's operating cycle. Moreover, if the water properties were inaccurate, the void – power relationship in each nodal volume would be inaccurate. Inaccurate powers would be obvious in the core-follow benchmark comparison of calculations to

NON-PROPRIETARY

---

measurements. [

] As noted in Section G.3.3,  
if the DORT results with average time-weighted parameters are not the same as the time-averaged results from the core-follow calculations, then the approximations associated with the DORT models and procedures are insufficient.

[

]

[

] (G.5)

[



NON-PROPRIETARY

---

]

[

]

Equation G.4, on page G - 14 of *Appendix G*, represents the “steady state” neutron transport equation. Its solution provides “steady state” simulations of reactor operation in that it provides a flux solution for time periods that are long compared to the neutron precursor half-life and short compared to isotopic depletion and thermal - hydraulic

NON-PROPRIETARY

---

feedback effects. The time-eigenvalue for this quasi-static state is hypothetically included in the source eigenfunction. If fluence analyses were to be based on the quasi-static form of Equation G.4 there would be no issue [

] Quasi-static - core-follow analyses based on Equation G.4, with the source eigenfunction appropriately expanded to include the time-eigenvalue, can determine the flux [ ] This flux value however is only valid for the appropriate time-step. To consider a complete operating cycle, or multiple cycles of operation, multiple time-steps are required. [

]

Utilizing multiple time-steps in a fluence analysis is not an effective utilization of resources. Moreover, with the appropriate neutron physics methods there is no technological benefit to employing multiple time-steps to develop the flux solution. By expanding the Equation G.4 solution to represent long time periods, the effects of isotopic depletion and thermal – hydraulic changes may be appropriately treated. [

]

Equation H.10 below is Equation G.4 expanded to include the time-dependent integral for multiple operational periods with variable isotopic concentrations.

$$\int_t \boldsymbol{\Omega} \cdot \nabla \phi(\mathbf{r}, E, \boldsymbol{\Omega}, t) dt + \int_t \Sigma_T(\mathbf{r}, E, t) \phi(\mathbf{r}, E, \boldsymbol{\Omega}, t) dt = \int_t S(\mathbf{r}, E, \boldsymbol{\Omega}, t) dt \quad (\text{H.10})$$

Average time-weighted terms may be defined to represent the integration of the second term on the left side of Equation H.10 and the term on the right side. In RAI 8 the NRC

NON-PROPRIETARY

---

requested additional information to ensure that the time-averaged source term had included all the variables that are represented by the core-follow burnup calculations. AREVA NP responded that every variable and parameter in the core-follow analysis is precisely represented in the DORT fluence analysis. Thus, a time-averaged source term,  $S(\mathbf{r}, E, \boldsymbol{\Omega}, \bar{t})$ , may be defined to represent the integration over multiple operational periods.

The time-averaged source term is used in Equation G.4 to determine the time-averaged flux { fluence rate,  $\phi(\mathbf{r}, E, \boldsymbol{\Omega}, \bar{t})$  }. Moreover, the time-averaged collision rate,  $\Sigma_T(\mathbf{r}, E, \bar{t}) \phi(\mathbf{r}, E, \boldsymbol{\Omega}, \bar{t})$ , may be defined to represent the integration of the second term on the left side of Equation H.10. The total macroscopic cross section  $\Sigma_T(\mathbf{r}, E, \bar{t})$  includes the integrated isotopic concentration changes due to depletion and thermal – hydraulic effects. In addition to the time-averaged source term, the time-averaged collision rate is used in Equation G.4 to determine the fluence rate.

The last time-integrated term that would provide the means of using Equation G.4 to determine the fluence rate is the leakage function. This is the first term on the left side of Equation H.10. [

] Thus, the leakage rate is expressed by the function  $\boldsymbol{\Omega} \cdot \nabla \phi(\mathbf{r}, E, \boldsymbol{\Omega}, \bar{t})$  when using Equation G.4 to solve for the fluence rate.

[

NON-PROPRIETARY

---

]

[

]

To resolve the issue of whether the time-averaged leakage function  $\mathbf{\Omega} \cdot \nabla \phi(\mathbf{r}, E, \mathbf{\Omega}, \bar{t})$  is an appropriate expression to be used in Equation G.4 to represent the solution of the fluence rate  $\phi(\mathbf{r}, E, \mathbf{\Omega}, \bar{t})$ , [

NON-PROPRIETARY

---

[ ]

[

]

[ ]

[ ] (H.11)

[

] There are two clear implications from the results of Equation H.11. The first is that the approximation of the time-averaged leakage function  $\mathbf{\Omega} \cdot \nabla \phi(\mathbf{r}, E, \mathbf{\Omega}, \bar{t})$  would not be

NON-PROPRIETARY

---

adequate if the [ ] The second is that the right side of Equation H.11 is only an appropriate solution to the left side if some technique can be used to provide a solution to the integral. There is no mathematical technique for determining [ ] independent of the integral on the left side. Nonetheless, if [ ] can be determined, then the right side of Equation H.11 is an appropriate solution to the left side.

As the NRC noted in the second paragraph to RAI 9, - the treatment of the boundary conditions for the leakage function has a substantial dependence on (a) the core boundary geometry (*e.g.*, the number and geometry of the surfaces) and (b) the specific code used to determine the calculation. To solve the left side of Equation H.11, AREVA NP uses the [ ]

]

[ ] for fluence rate analyses, it is not appropriate to represent the complete method that is applied to the DORT model. The expression for the leakage function needs to be expanded to include the coupled variables of space, energy and solid angle. Equation G.6 is the expansion of the [ ] leakage function to include the appropriate variables. Equation G.6 also shows that

NON-PROPRIETARY

---

whether we are considering an exponential integral function or a Bickley-Naylor function for cylindrical coordinates, the solution will continue to be dependent on the

[

]

[

]

[

NON-PROPRIETARY

---

]

**Set 2, RAI 10**

In order to determine the effect of using [ ], provide a comparison of the DORT calculated fluence for (a) the case in which the [ ] determined by the core-follow code calculation are input and (b) the case in which the [ ] are input. The comparisons should be made for the azimuthal inner-wall > 1-MeV fluence for a typical plane in an upper region of the core where there is substantial voiding. Provide a comparison of the [ ] together with the fluence [ ] mean and standard deviation. [ ]

]



NON-PROPRIETARY

---

Response

[

] The discussion from  
Section G.3.3, “Core Leakage Function” provides an explanation of the procedures used to ensure that the DORT calculational methods are accurate: The accuracy of the fluence evaluation process begins with the core-follow simulation of the measured fission rates for power production. The core-follow results match the measurements within the uncertainty criteria for the magnitude of the core power and nodal power distribution.

Assuming that there is no average time-weighted effect on the leakage function  $\{ \mathbf{\Omega} \cdot \nabla \phi(\mathbf{r}, E, \mathbf{\Omega}) \}$ , the collision density parameters and source parameters in DORT will produce the same flux values as those from the average time-weighted core-follow calculations.

[

NON-PROPRIETARY

---

]

Using the PWR models and procedures developed in Section 3 of this topical to compute BWR leakage rates from the core periphery indicates that the approximations in the modeling and procedures must be updated. The average time-weighted “fixed” source eigenfunctions and collision density parameters do not produce accurate peripheral flux values. The average time-weighted effect of the leakage function  $\{ \mathbf{\Omega} \cdot \nabla \phi(\mathbf{r}, E, \mathbf{\Omega}, t) \}$  needs to be modified [ ]

**Set 2, RAI 11**

Recognizing the complex dependence of the fluence ( $\phi$ ), source (S) and total cross section ( $\Sigma_T$ ) [

]?

**Response**

A unique and real value of the water density from the core-follow simulation of reactor operation is used [

NON-PROPRIETARY

---

]

**Set 2, RAI 12**

Provide the energy for which the FANP/BNL-6115 flux comparisons of Section G.4.2.2 have been made.

Response

The flux comparisons between FANP (now AREVA NP) and BNL-6115 in Section G.4.2.2 were for neutron energies greater than 1.0 MeV (million electron volts, megavolts). This includes Figures G-3 through G-8 and the table, “*FANP/BNL-6115* Comparison of Key Deviations”.

**Set 2, RAI 13**

Describe the application of the Section G.3.2 jet-pump/riser modeling procedure and the [ ] in the Browns Ferry-2 (BF-2) dosimetry analysis. Provide a comparison of the BF-2 bundle-wise [ ]

NON-PROPRIETARY

---

]. What

is the effect of this difference on the calculated fluence?

#### Response

This request contains five parts, describing the application of the procedures in Sections G.3.2, G.3.3 and G.3.4, providing a comparison of the differences between core-follow data and Equations G.7 and G.10, and discussing the effect of Equations G.7 and G.10 on the calculated fluence. To help ensure clarity, each response will be discussed independently in a paragraph.

The Section G.3.2 procedure, “Neutron Transport Through Jet Pumps” addresses one of the issues that the NRC has discussed previously. Other analysts have frequently found greater inaccuracies in the calculations of reactions that are shadowed by the jet pumps than those calculations that have no shadowing effect from neutrons leaking from the core. In BNL-6115, “PWR and BWR Pressure Vessel Fluence Calculation Benchmark Problems and Solutions” Carew of Brookhaven and the NRC compare the results of MCNP and DORT calculations in Figure 5.4.6. One of the issues that Figure 5.4.6 addresses is the explicit modeling of the jet pumps with the MCNP geometry and the approximation required in DORT. Comparing Figure 5.4.6 and Figure G-4 in the AREVA NP topical, some of the same biased deviations are evident. Based on the MCNP results and those in the AREVA NP DORT analyses, the BNL-6115 DORT could probably be improved with a finer jet pump mesh. The resolution to the issue of the jet pumps possibly causing biased deviations in their shadow is addressed by the Section G.3.2 procedure. To accurately model the jet pumps, the non-uniform attenuation that they cause must be appropriately treated. Equations G.1 through G.3 provide a means of demonstrating that the DORT modeling represents the proper non-uniform attenuation. The Browns Ferry-2 DORT model that AREVA NP developed

NON-PROPRIETARY

---

included the appropriate treatment of the jet pumps. The criteria represented by Equations G.1 through G.3 were satisfied.

The application of the Section G.3.3 modeling procedure is discussed in the response to RAI 9, Set 2. [

] The Browns Ferry-2 DORT model that  
AREVA NP developed included the appropriate treatment of [  
]

The application of the Section G.3.4 modeling procedure is discussed in the response to RAI 2, Set 1. The issue that is addressed is the appropriate treatment of [

] The Browns  
Ferry-2 DORT model that AREVA NP developed included the appropriate treatment of  
[  
]

As noted in the response to RAI 2, Set 1, the AREVA NP evaluation of axially homogenizing several nodes concluded that, - even with the appropriate treatment of [ ] there would be too much detail lost. For example the shroud cracking seems to be around the jet pump supports.  
[



NON-PROPRIETARY

---

**Set 2, RAI 15**

The [ ] bias removal function of Appendix D can result in a (non- conservative) reduction in the vessel fluence prediction. Is this bias removal function applied in BWR applications? If so, provide justification.

Response

The [ ] bias removal function is applied to BWR calculations of the “best-estimate” fluence values. The cause of the [ ] bias in the DORT calculated fluence values is most probably the method of treating the source eigenfunction. While the reactor core is operating with [ ] the fluence rate – time-integrated form of Equation G.4 is not represented. Consequently, there is no mathematical function for producing [ ] The bias caused by this approximation in the methods is not related to a PWR, BWR or any other core model. Thus, the bias removal function should be applied to the results of all DORT models that lack the mathematical function [ ]

The NRC request for additional information includes the statement that the [ ] bias removal function can result in a non-conservative reduction in the vessel fluence. While the bias removal function contains [ ]

[ ] In fact as AREVA NP noted and the NRC confirmed in *Appendix D*, pages D - 57, Set 2 – Question 16, and D - 61 through D - 68, in the section on the “Statistical Processing of Table A-1 Data”, AREVA NP has no statistically significant

NON-PROPRIETARY

---

bias in the greater than 1.0 MeV fluence rate. That is, calculating the  $M/C$  ratio before the application of the bias removal function, the NRC obtained a value of .9940. This shows a statistically insignificant bias. When AREVA NP applied the bias removal function to the calculations, the bias continued to be statistically insignificant. The [ ] in the DORT methods and results in the best-estimate of the fluence throughout the internal structures, within the vessel, and throughout the reactor cavity structure.

**Set 2, RAI 16**

Were the calculation/modeling and measurement methods described in the topical report used in the analysis of the PCA dosimetry experiment, the Browns Ferry Unit 2 (BF-2) capsule measurement and the BNL-6115 benchmark? If not, describe any differences and their effect on the comparisons. For example, were the jet pump [ ] procedures of Section G.3 used in the BF-2 analysis?

Response

The calculational modeling and methods described in this topical report were used in the analysis of the PCA dosimetry experiment, the Browns Ferry Unit 2 capsule, and the BNL-6115 benchmark. Thus, these benchmark comparisons appropriately represent samples from the benchmark database. Moreover, they provide additional confirmation of the uncertainty values noted in Section G.4 of the topical. As noted in the response to RAI 13, Set 2 above, [

]



NON-PROPRIETARY

---

The measurement methods described in this topical report were not used in the development of the data from the PCA dosimetry experiment, the Browns Ferry Unit 2 capsule, and the BNL-6115 benchmark. The PCA experiment contained measurements from the Oak Ridge National Laboratory (ORNL). While ORNL and other national laboratory contributors to the PCA experiment described methods that were consistent with AREVA NP standards, which are consistent with ASTM standards, there are measurements of reactor power and power distributions that have different methods from those associated with power reactors. This is discussed further in the response to RAI 4, Set 1. In addition, the measurement uncertainties associated with the BNL-6115 benchmark are those from the PCA experiment. Since the uncertainties associated with the BNL-6115 benchmark are equivalent to the PCA experiment, these uncertainties are not included in the benchmark database. Including them would be equivalent to weighting the benchmark to the PCA experiment twice.

The Browns Ferry Unit 2 capsule measurement was performed by GE Nuclear Energy. While GE discusses measurement methods for the iron, copper, and nickel dosimeters that are consistent with AREVA NP standards, which are consistent with ASTM standards, there is no evidence that the GE laboratory has been benchmarked to a reference field. Thus, it would be expected that the GE laboratory results lack the confirmation that is required by Regulatory Guide 1.190<sup>H4</sup> and that is part of the AREVA NP quality. Nonetheless, the calculated benchmark comparison to the Browns Ferry Unit 2 capsule measurement indicates that the benchmark uncertainty is consistent with the AREVA NP database.

NON-PROPRIETARY

---

*Appendix H* References

- H1. M.C. Honcharik (NRC), "Request for Additional Information, Issues Related to BAW-2241, *Appendix G*, 'Fluence and Uncertainty Methodologies,' Framatome ANP, Project Number 728," facsimile to G.F. Elliott (Framatome ANP), June 17, 2005.
- H2. H.A. Hassan, *et alia*, "Power Peaking Nuclear Reliability Factors", AREVA NP Document # BAW-10119P-A, February, 1979.
- H3. H. Moon, "Siemens Power Corporation Methodology for Boiling Water Reactors: Evaluation and Validation of CASMO-4 / MICROBURN-B2", AREVA NP Document # [EMF-2158(P)], December, 1998.
- H4. Office of Nuclear Regulatory Research, "Calculational And Dosimetry Methods For Determining Pressure Vessel Neutron Fluence", Regulatory Guide 1.190, U.S. Nuclear Regulatory Commission, March, 2001
- H5. Office of Nuclear Regulatory Research, "Radiation Embrittlement Of Reactor Vessel Materials", Regulatory Guide 1.99, Revision 2, U.S. Nuclear Regulatory Commission, May, 1988.
- H6. M.C. Honcharik (NRC), "Request (Round Two) for Additional Information on BAW-2241, *Appendix G*, 'Fluence and Uncertainty Methodologies,'" e-mail to G.F. Elliott (Framatome ANP), September 8, 2005.
- H7. M.A. Rinckel, J.R. Worsham III, *et alia*, "Demonstration of the Management of Aging Effects for the Reactor Vessel", BAW-2251-A, August, 1999.